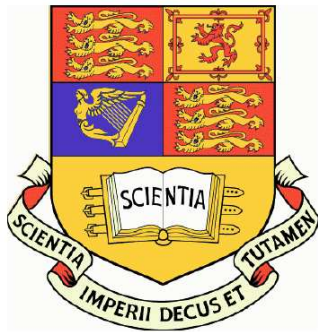


An information-theoretic study of neuronal spike correlations in the mammalian cerebral cortex



Fernando Montani

Department of Bioengineering

Supervisor: Simon R. Schultz, Department of Bioengineering

A report submitted in partial fulfillment of the requirements for the PhD, The University
of London

January 2008

Short Abstract

We have used information theory to examine whether stimulus-dependent correlation could contribute to the neural coding of orientation and contrast by pairs of V1 cells. To this end, we have used a modified version of the method of information components. This analysis revealed that although synchrony is prevalent and informative, the additional information it provides is frequently offset by the redundancy arising from the similar tuning properties of the two cells. Thus, coding is roughly independent with weak synergy or redundancy arising depending on the similarity in tuning and the temporal precision of the analysis. Our findings suggest that this would allow cortical circuits to enjoy the stability provided by having similarly tuned neurons without suffering the penalty of redundancy as the associated information transmission deficit is compensated by stimulus dependent synchrony.

The underlying origins of synchronized firing between cortical neurons are still under discussion. GABAergic inhibitory neurons may be involved in the generation of oscillatory activity in the cortex and its synchronization. Specifically, reduction of GABAergic inhibition may favour cortical plasticity producing functional recovery following focal brain lesions. We present a computational and analytical model of a topographically mapped population code which includes a focal lesion as well as a process for receptive field enlargement. Our finding shows that by tuning the receptive field plasticity to a certain value, the information transfer through the cortex after stroke can be optimized.

A widespread distribution of neuronal activity can generate higher-order stochastic interactions. In this case, pair-wise correlations do not uniquely determine synchronizing spiking in a population of neurons, and higher order interactions across neurons cannot be disregarded. We present a new statistical approach, using the information geometry framework, for analyzing the probability distribution function (PDF) of spike firing patterns by considering higher order correlations in a neuronal pool. We have studied the limit of a large population of neurons and associated a deformation parameter to the higher order correlations in the PDF. We have also performed an analytical estimation of the Fisher information in order to evaluate the implications of higher order correlations between spikes on information transmission. This leads to a new procedure to study higher order stochastic interactions. The overall findings of this thesis warn about making any extensive statement about the role of neuronal spike correlations without considering the case of higher order correlations.

Long Abstract

In chapter I of this thesis we present a review of the historical background of the previous spike correlation studies and current state of the problem. In the chapters II, III and IV of this thesis we have applied an information theoretic approach to study the role of correlations in the neuronal code, using the responses of pairs of neurons to drifting sinusoidal gratings of different orientations and contrasts recorded in the primary visual cortex of anesthetized macaque monkeys. In chapter V we investigate the effects of a focal stroke in a population of neurons on information transmission using a computational and analytical approach to the problem. Finally, in chapter VI we use a novel analytical approach to study effects of higher order correlations in a population of neurons.

It has been proposed in neuroscientific literature that pooling can lead to a significant improvement in signal reliability, provided that the neurons being pooled are at most weakly cross-correlated. We have computed mutual information, and compared the information available from pairs of cells with the sum of the single cell information values. This allowed us to assess the degree of synergy (or conversely, redundancy) in the coding. In chapter II of this thesis, we show that due to a loss of information encoded in the neuronal identity of the cells, pooling spikes across neurons leads to a loss of a large fraction of the information present in their spike trains.

We have used information theory to examine whether stimulus-dependent correlation could contribute to the neural coding of orientation and contrast by pairs of V1 cells. To this end, in chapter III, we have used a modified version of the method of information components. This analysis revealed that although synchrony is prevalent and informative, the additional information it provides is frequently offset by the redundancy arising from the similar tuning properties of the two cells. Thus, coding is roughly independent with weak synergy or redundancy arising depending on the similarity in tuning and the temporal precision of the analysis. Our findings suggest that this would allow cortical circuits to enjoy the stability provided by having similarly tuned neurons without suffering the penalty of redundancy as the associated information transmission deficit is compensated by stimulus dependent synchrony.

In chapter IV, we present a discussion about different measures of correlations and in particular we propose the Jensen-Shannon Divergence as a measure of the distance between the

corresponding probability distribution functions associated with each spikes fired observed patterns. We applied this Divergence for fixed stimuli as a measure of discrimination between correlated and independent firing of pairs of cells in the primary visual cortex. This provides a new, information-theoretic measure of the strength of correlation. We found that the relative Jensen-Shannon Divergence (measured in relation to the case in which all cells fired completely independently) decreases with respect to the difference in orientation preference between the receptive field from each pair of cells. Our finding indicates that the Jensen-Shannon Divergence can be used for characterizing the effective circuitry network in a population of neurons.

The underlying origins of synchronized firing between cortical neurons are still under discussion. Inter-cellular communication through chemically mediated synaptic transmission is considered a major contributor to the formation of neuronal synchrony. GABAergic inhibitory neurons may be involved in the generation of oscillatory activity in the cortex and its synchronization. Specifically, reduction of GABAergic inhibition may favour cortical plasticity producing functional recovery following focal brain lesions. Research into neurotransmitter systems is therefore of paramount importance to understand the origins of synchronized spiking. However, it is necessary to understand first how simple focal abnormalities in GABAergic modulators can affect the information transmission in an impaired brain tissue. In chapter V, we present a computational and analytical model of a topographically mapped population code which includes a focal lesion as well as a process for receptive field enlargement (plasticity). The model simulates the recovery processes in the brain, and allows us to investigate mechanisms which increase the ability of the cortex to restore lost brain functions. We have estimated the Fisher Information carried by the topographic map before and after the stroke. Our finding shows that by tuning the receptive field plasticity to a certain value, the information transfer through the cortex after stroke can be optimized.

A widespread distribution of neuronal activity can generate higher-order stochastic interactions. In this case, pair-wise correlations do not uniquely determine synchronizing spiking in a population of neurons, and higher order interactions across neurons cannot be disregarded. We present a new statistical approach, using the information geometry framework, for analyzing the probability distribution function (PDF) of spike firing patterns by considering higher order correlations in a neuronal pool. In chapter VI, we have studied the limit of a large population of neurons and associated a deformation parameter to the higher order

correlations in the PDF. We have also performed an analytical estimation of the Fisher information in order to evaluate the implications of higher order correlations between spikes on information transmission. This leads to a new procedure to study higher order stochastic interactions.

The overall findings of this thesis warn about making any extensive statement about the role of neuronal spike correlations without considering the general case inclusive of higher order correlations, and suggest a need to reshape the current debate about the role of spike correlations across neurons.

To Chiara Montani, my baby daughter

Acknowledgements

I am very thankful to my supervisor Simon R. Schultz for giving me the opportunity to work in his Laboratory and for his experienced advice, encouragement and support in the development of this research. I would like to thank especially Stefano Panzeri for helping and supervising me in the development of chapter VI of the thesis. I also thank him for a pleasant and fruitful collaboration.

I would like to thank Mauricio Barahona for his invaluable advice and support during these three years of research. This thesis would not have been achieved without the support of Adam Kohn who helped me understand the basic methodologies in neuroscience. His criticism was invaluable for the development of Chapter II and III of this thesis. I also thank Matt Smith for giving me the opportunity to collaborate with him.

During my staying in London I very much appreciated the collaborations and discussions with Aman Saleem, Hildur Einarsdóttir, Naveed Ejaz and Kit Logden. I enjoyed the very nice atmosphere they created when we ran the Journals Clubs with the support of Holger Krapp and Simon Schultz. I thank especially Elias August, both for his friendship and for carefully reading this thesis.

I would like to thank O. A. Rosso (The University of Newcastle, Australia) both for his friendship and for his help towards the development of chapter IV of this thesis. I am very thankful to Ilya Nemenman (Los Alamos National Laboratory) who helped me through discussions on the implementation of his NSB method. I wish to thank Ana Lopez (Oxford University), one of the sharpest scientific minds I have known with a fine sense of humor, for the wonderful discussions. I would like to thank Ines Samengo (Centro Atomico Bariloche, Argentina) and Marcelo A. Montemurro (Manchester University) for their support, scientific and non-scientific advice. I would like to thank E. V Albano, A. Vulpiani, H. Wio, C. Tsallis and F.A. Tamarit for interesting and helpful discussions, when I met them during my stay in Spain.

Finally, I would especially like to thank my wife, Araceli, who gave me her full support and love during the development of this thesis. Without her emotional and financial support it would have been impossible to complete this research, particularly living in London.

CONTENTS

1. <i>Introduction</i>	2
1.1 Synchronized spike activity	2
1.1.1 Historical review	2
1.2 The current state of the problem	9
1.2.1 A topic of intense debate in the neuroscience community	9
1.3 From Signal Detection Theory to Information Theory	15
1.3.1 Signal Detection Theory	15
1.3.2 Information Theory	19
1.4 A Guide to the Thesis	25
2. <i>Is the Pooling of sensory information across neurons an efficient mechanism for de-coding?</i>	28
2.1 Introduction	28
2.2 Methods	33
2.3 Experimental Procedures	34
2.3.1 Visual stimuli	34
2.4 Theoretical Procedures	35
2.4.1 Entropy estimators	36
2.4.2 Example: Information available for a single pair of neurons	42

2.4.3	Numerical Implementation	42
2.5	Direction Coding	43
2.5.1	Spike train cross-correlograms (CCGs)	43
2.5.2	Mutual Information	44
2.6	Contrast Coding	46
2.7	Pooling	48
2.8	Discussion	50
3.	<i>The role of correlations in orientation and contrast coding in the primary visual cortex</i>	54
3.1	Introduction	55
3.2	Methods	58
3.3	Experimental Procedures	67
3.3.1	Visual Stimuli	68
3.3.2	Response characterisation	69
3.4	Results	69
3.4.1	Direction coding: information adds linearly across cells	70
3.4.2	The role of correlations in direction coding: a balance of redundant and synergistic effects	74
3.4.3	Greater separation in direction preference leads to synergy	80
3.4.4	Contrast coding is redundant	82
3.4.5	Transfer and autocorrelation functions	85
3.4.6	Information rate	92
3.5	Discussion	94
3.5.1	An useful Mechanism for surviving	97

3.5.2	Hypercolumns and the physiological origin of synchronization	98
4.	<i>Towards an alternative measure of spike correlations</i>	101
4.1	Introduction	101
4.2	Methods	103
4.3	Results	107
4.4	Discussion	111
5.	<i>The accuracy of a neural population code after focal ischaemia</i>	113
5.1	Introduction	113
5.2	Topographic mapping of the cortex	118
5.3	Methods: A mathematical model of functional reorganization	120
5.3.1	The disinhibition model of post-lesion plasticity	123
5.3.2	A simulation of nonlinear neuronal responses	124
5.4	Results	127
5.4.1	Fisher topographic information	127
5.4.2	Fisher information for a lesioned retinotopic code	128
5.5	Discussion	134
6.	<i>An analytical approach to the PDF and Fisher Information considering higher-order correlations in a population of neurons</i>	136
6.1	Introduction	136
6.2	Methods	138
6.3	Results	142
6.3.1	Pooling across neurons:	142
6.4	Discussion	150

7. <i>Conclusions</i>	152
<i>Appendix</i>	158
.1 Publications	159

LIST OF FIGURES

1.1	d' measures the distance between two normal distributions of equal variance. . .	18
1.2	Percentage of correct detections for an ideal observer in a detection task as a function of SNR.	20
2.1	Tuning curves for two V1 neurons. B-F, Scatter plots of responses of V1 pair to 100 presentations of each stimulus show independence of spike count correlation and orientation (modified Figure from Kohn and Smith 2005)	30
2.2	Relationship between firing rate and spike count correlation r_{sc} for stimuli of different orientations (contrast). There are not significant differences between the Population histograms at different orientations (contrast). Modified Figure from Kohn and Smith 2005	31
2.3	Schematic illustration of the determination of the preferred orientation (contrast) by using five full contrast grating stimuli, and for a given pair of cells in V1. For simplicity the tuning curves of this pairs of cells are represented in this illustration by the two Gaussian functions. The two highest responses would correspond to the preferred orientation of each cell.	33
2.4	Relative performance of several information estimators. Two different time windows were chosen for counting spikes: A 5ms, resulting in cardinality $K = 10$ from the ensemble responses. B 40 ms, cardinality $K = 76$	41
2.5	Cross-correlograms for each of five different stimulus directions, for the same pair as shown in the previous figures.	44

2.6	Comparison of the information available from the pair of neurons ($I_{ensemble}$) in a time window T , with the sum of the informations obtained from each constituent neuron (I_{sum}) and the information from a pooled code in which the identity of the cell firing each action potential is ignored (I_{pooled}).	45
2.7	Information adds approximately linearly across cells. A The total (ensemble) information available for each pair is plotted against the sum of the information available from each cell constituting the pair (n=102 pairs). Redundant points lie below the diagonal. The black diamond indicates the pair shown in Figures 1-3. B Histogram of the total (ensemble) information available for each pair divided by the sum of the information from each cell.	47
2.8	Coding of contrast by a stereotypical pair of V1 neurons. A Cross-correlograms for each of 4 contrast values. B Information analysis results.	48
2.9	Coding of contrast is substantially redundant across the entire dataset. A Comparison of pair and linear summation information values. The black diamond shows the pair considered in the previous figure. B Histogram showing the degree of redundancy across the dataset.	49
2.10	The effect of pooling (ignoring the identity of the cell which fired each spike train) is a substantial loss of information. A Direction coding. B Contrast coding. . . .	51
3.1	Information component breakdown. The ensemble mutual information can be broken down into a linear component, the reduction of information due to the redundancy caused by overlap in tuning curves, and the contribution of correlated firing (I_{cor}). The noise correlation term can be further broken down to separate out the effect of the average level of correlation over all stimuli, and the stimulus-dependence of correlation – the latter term captures any effects due to coding by explicit modulation of correlation/synchronization.	60
3.2	The effect of Δ (at $T = 40$ ms for 102 pairs of neurons). $I_{cordep0}$ correspond to $\Delta = 0$	66

3.3	Direction coding by two pairs of neurons. <i>A, B</i> Direction tuning curves for two pairs of neurons the first pair are both direction-selective, the second only slightly directionally biased (fitted using von Mises functions). <i>C, D</i> Cross-correlograms for each of the pairs above show that fine-timescale synchronization is induced for stimulus directions that drive both cells relatively well. The cross-correlation was measured for the five stimuli indicated by the filled circles in <i>A, B</i> . <i>E, F</i> Information analysis: the total information available from each pair of neurons ($I_{ensemble}$) is compared for different integration time windows T to the sum of the information values obtained from each constituent neuron alone (I_{sum}) and to the information from a pooled code in which the identity of the cell firing each action potential is ignored (I_{pooled}).	71
3.4	Information adds relatively linearly across cells. <i>A</i> The total (ensemble) information available for each pair is plotted against the sum of the information available individually from each cell constituting the pair. The time window used for counting spikes was 5 ms. Pairs marked A and B correspond to the pairs illustrated in Figure 2 <i>A, B</i> . <i>B</i> The synergy fraction (defined as $1 - I_{sum}/I_{ensemble}$ and indicating the fraction of information beyond that expected if the cells are independent) is plotted against the time window used for counting spikes. The lines show the average (+/- s.e.m.) over the entire dataset, and over only those pairs showing ensemble information lower than 1 bit (this latter curve excluding potential artefactual redundancy effects). <i>C</i> Pooling spikes across cells destroys a substantial amount of information in almost all cases indicating that the pattern of spikes across cells is informative.	73
3.5	Information component analysis for the example pairs, showing how the balance between a synergistic contribution due to orientation dependent synchronization ($I_{cor-dep}$), and redundant contributions from tuning overlap ($I_{sigstim}$) and the average level of correlation ($I_{cor-ind}$), give rise to the overall level of synergy or redundancy. The information components I_{lin} , $I_{sigstim}$ and I_{cor} add together to give the total information $I_{ensemble}$. Panels <i>A, B</i> correspond to the same pairs of cells described in Figure 3.3 <i>A, B</i>	76

3.6	<p>Information components across the entire population of 102 pairs (direction coding). <i>A</i> Histogram of the relative contribution of I_{cordep} to the total information for a time window of 5 ms. <i>B</i> $I_{sigstim}$, reflecting the redundant contribution due to the overlap in tuning curves, is generally non-zero but is not strongly correlated with the overall amount of synergy or redundancy. <i>C</i> Correlational effects captured by I_{cor} are more strongly related to the extent of synergy in the coding. <i>D</i> The stimulus-dependent correlational component is strongly related to the extent of synergistic coding, whereas (<i>E</i>) the average level of correlation is unrelated. <i>F</i> A bar chart capturing the average value of each information component (expressed as a fraction of the total information, $I_{ensemble}$) over the entire dataset. Error bars indicate standard error of the mean (N=102).</p>	77
3.7	<p>A The relative effects of the information component are timescale-dependent. Bar charts show the average fraction of the information accounted for by the different components for time windows ranging from 2 to 80 ms: while the redundant contribution of $I_{cor-ind}$ grows with time window, the effects of the other components follow a ‘U’ or inverted ‘U’ curve. B Wide separation in direction preference leads to synergy. Time windows $T = 5ms$. Direction coding is redundant for pairs of neurons with similar tuning (negative synergy fraction).</p>	79
3.8	<p>Contrast coding. <i>A</i> Contrast tuning for a typical pair of cells (normalized to the maximal response of one of the cells). <i>B</i> Cross-correlograms show a decrease in the precision of spiking synchrony as contrast decreases. <i>C</i> The ensemble information is lower than the sum of that available from each individual cell contrast is coded redundantly by this pair of neurons. <i>D</i> Information components – the overall effect of I_{cor} is for this example minimal; the redundant effect can be seen to stem from $I_{sigstim}$, reflecting the strong overlap in contrast tuning.</p>	81

3.9	Contrast coding across the population of 71 pairs of cells for which contrast data were available. <i>A</i> Histogram of the relative contribution of I_{cordep} to the total information for a time window of 5 ms. <i>B</i> The relationship between $I_{sigstim}$, the component reflecting the contribution due to the overlap in tuning curves, and the extent of redundancy as indicated by the negative synergy fraction. <i>C, D, E</i> The relationship between the magnitude of each of the correlation components of the information, and the overall extent of synergy, on a pair by pair basis across the entire dataset. <i>F</i> A histogram showing the average fraction of information captured by each component across the dataset.	84
3.10	Redundancy is observed across the entire dataset for contrast coding. <i>A</i> Even at $T = 5$ ms, redundancy was observed (points below diagonal). The pair marked ‘C’ is that referred to in Figure 3.8. <i>B</i> The degree of redundancy in the coding of contrast quickly becomes substantial as the time window is increased. The results for contrast coding are indicated by squares and a black line; the results for direction coding (from Figure 3.4 b) by the grey line and circles.	86
3.11	<i>A, B</i> , Transfer function between pair of cells for two different stimuli orientation. <i>C, D</i> Autocorrelation functions for cell 1 for the two different preferred orientation. <i>E, F</i> Autocorrelation functions for cell 2 for two different preferred orientation (Pair A, time window fixed at 160 ms).	88
3.12	<i>A</i> , Transfer function between pair of cells for the minimum, and <i>B</i> for the maximum firing rate (pair of cells with the smallest I_{cordep} value which can be found in Figure 3.6D, time window fixed at 160 ms).	90
3.13	<i>A, B</i> Autocorrelation functions for two different preferred orientation (pair of cells with the smallest I_{cordep} value which can be found in Figure 3.6D , time window fixed at 160 ms)	91
3.14	Calculating asymptotic information rates. <i>A, B</i> . Information rate estimates at different word lengths for Pair A and for individual neurons, with bin widths $t=5$ ms. The information rate is the limit of these curves as L approaches infinity.	93
3.15	Detecting changes in the orientation of tiger stripes (“orientation stimuli”) is vital for the surviving of a primate.	98

4.1	For a typical pair of cells in V1 the JSD was calculated taken into account the full stimuli orientation dependency at seven different time windows (named as JSD Full).	107
4.2	$T = 5$ ms, The relative Jensen-Shannon Divergence as a discrimination measure of correlations normalized with respect to its maximum value for this data set. In the upper part of this Figure the Synergy-Fraction is also plotted as function of Difference in Orientation Preference. Notice that cells with similar preferred orientation are more likely to share a higher quantity of common inputs than those that present less similarities.	110
5.1	Illustration of the mechanism for receptive field enlargement following a lesion. A The overall receptive field is formed from the sum of separate excitatory and inhibitory contributions - this is crucial for the mechanism to work. B With a lesion at the position indicated, the inhibitory component is reduced by a factor $1 - \exp(-d^\alpha/\gamma)$, where d is the distance from the lesion. This leads to disinhibition on one side of the receptive field, and consequently enlargement towards the lesion of the overall receptive field. For the example shown, $\gamma = 10$ and $\alpha = 4$	121
5.2	A contour plot of the mapped receptive field of a single neuron, in the population before the a stroke lesion is induced The x- and y- coordinates represent degrees of visual field (Montani 2007d ; Einarsdottir and Montani and Schultz)	125
5.3	Receptive field adaptation following stroke-like lesion of different sizes, obtained by computer simulation. The damage is represented with black dotted lines. The intact neuron responds to the lesion by expanding its receptive field towards the damaged area (Montani 2007d ; Einarsdottir and Montani and Schultz).	126
5.4	Expansion in the receptive field versus the distance between the damage and the neurons is shown for different values of plasticity γ , which are dependent on the size of the damage. The blue line refers to $\gamma = 0.02$, green line to $\gamma = 0.1$ and the red line to $\gamma = 0.81$. Expansion is defined as the change in percentage between the base width of the receptive field pre- and post lesion (Montani 2007d ; Einarsdottir and Montani and Schultz).	127

5.5	Fisher Information components in the 2-D topographic map before the stroke. The different values of the Fisher information are displayed as a color map for different values of x and y . Notice that the changes in colors, inside each individual neuron, are due to the finite size effect of the lattice. For the example shown, $\gamma = 0, \sigma_n = 1, \sigma_{ex} = 2$ and $\sigma_{in} = 1$	130
5.6	Fisher Information components in the 2-D topographic map before the stroke. The different values of the Fisher information are displayed as a color map for different values of x and y . Notice that the changes in colors, inside each individual neuron, are due to the finite size effect of the lattice. For the example shown, $\gamma = 10, \sigma_n = 1, \sigma_{ex} = 2$ and $\sigma_{in} = 1$. Following stroke-like damage the information surrounding the damaged area is increased mostly due to an increase in the excitatory component I_{ex} .	131
5.7	Analytical results for Fisher Information as a function of the degree of plasticity γ . Solid black line indicates coding accuracy when the damage covers 3 % of the neurons in the population, the dotted line refers to 30 % damage and the dashed refers to 50 % damage. The population includes 64 neurons with a side length of visual space, i.e. distance before it starts repeating, equal to 40 and $\sigma_{ex} = 2$ and $\sigma_{in} = 1$).	132
5.8	Fisher Information as a function of the degree of plasticity γ using our simulation of nonlinear neuronal responses on the analytical expression (eq. 5.15). The black solid line indicates coding accuracy when the damage covers 10 % of the neurons in the population, the dashed line refers to 30 % damage and the dotted line refers to 70 % damage. The population includes 225 neurons with original receptive field spread $\sigma = 2$. The curves are normalised to the Fisher information prior to the stroke. The left asymptote corresponds to the performance after stroke, but prior to functional recovery.	133
6.1	Widespread probability distribution, $P(r)$, accounting for higher order correlations .	144

Notation

CCG cross-correlogram

ECG electrocardiogram

EEG electro-encephalogram

JSD Jensen-Shannon Divergence

KLD Kullback-Leibler Divergence

LFP local field potential

LGN lateral geniculate nucleus

MUA multi-unit activity

NSB Nemenman, Steveninck, Bialek, entropy estimator

PDF probability distribution function

RF receptive field

ROC Receiver operating characteristic

SD standard deviation

SDT Signal Detection Theory

SNR Signal Noise Rate

V1 primary visual cortex

1. INTRODUCTION

1.1 *Synchronized spike activity*

1.1.1 *Historical review*

In 1926 Adrian and Zotterman, using the afferent nerve of stretch receptor in the frog muscle, showed that it was possible by amplification to record the impulse in single nerve fibers. They summarized their results in this single sentence: "The impulses set up by a single end-organ occur with a regular rhythm at a frequency which increases with the load on the muscle and decreases with the length of time for which the load has been applied". Ever since Adrian and Zotterman observed that the firing rate of peripheral touch receptors coded for the pressure applied to a patch of skin, neuroscientists have been trying to understand the neural code.

However, understanding brain functions requires interdisciplinary approaches involving many levels of study: from the molecular level through the cellular level (individual neurons), to the level of relatively small assemblies of neurons (for example cortical columns); to the case of larger subsystems as the one which subserves visual perception, and up to the level of large systems including the cerebral cortex, the cerebellum, and to nervous system as a whole. Neuroscience encompasses approaches ranging from molecular and cellular studies to human psychophysics and psychology. Moreover, theoretical analysis of physiological data and computational modelling are important tools for characterizing what nervous systems do, determining how they function, and understanding why they operate in particular ways.

Unfortunately, it is extremely difficult to understand exactly how sensory information is processed in the mammalian brain. For example, the influx of sensory information to a single mammalian superior retina is detected by an array of millions of receptors, each

capable of detecting the difference between hundreds of gray levels. They have integration times which allow them to detect new signals in just a few seconds. These inputs are then processed by hundreds of millions of other neurons, and many of them interact with each other in complex ways. Moreover, depending on stimulus conditions a different sort of inputs is generated which will eventually modify these interactions dynamically. With this huge level of complexity, the experimental tools which have been available during the last thirty years were insufficient to account for all the involved variables.

One of the main experimental challenges in neuroscience during the last thirty years was to demonstrate that distributed neural populations in the visual cortex process information in a cooperative way. The visual cortex is composed of a large number of areas, which contain neurons that are tuned to different visual features. Temporally correlated activity of individual neuronal pairs within the visual cortex has been investigated in many laboratories since the early 1980s (Toyama et. al. 1981a; Michalski et. al. 1983 ; Toyama et. al. 1981b; Ts'o et. al. 1986; Volgushev 1998; Aiple and Krueger 1998; Ts'o and Gilbert 1988, Gochin et. al. 1991; Hata et. al. 1998; Alonso et. al. 1998; Molotchnikoff et. al. 1998), most often with a motivation to reveal structural coupling between cells. This approach to functional anatomy had been methodologically and conceptually outlined by (Perkel et. al. 1967; Gerstein and Perkel 1969; Moore et. al. 1970; Kirkwood 1979; Aersten et. al. 1989, Surmier and Weinberg 1985), and successfully applied to the invertebrate nervous system (Bryant et. al. 1973). The results of these different studies showed the presence of temporally precise synchronization within the cat and macaque visual cortex. But, these correlations occurred between cells showing the same feature preference. Because the peaks in the correlograms were centered around zero the obtained correlations were attributed to common inputs and no attempts were made at this stage to determine whether response synchronization might depend on the stimulus configuration.

Evidence has indeed been obtained that many neurons within a column of cat visual cortex can engage in a state of highly synchronous activity in response to an optimally oriented moving light bar (Gray-Singer 1989; Gray et. al. 1989). Oscillatory activity in the gamma frequency range was observed in both multi-unit activity (MUA), these are spike sequences elicited by clusters of neighboring cells which are not further subdivided into contributions of individuals cells, and local field potential (LFP) signals, which may be thought of as a local EEG (electro-encephalogram) signal of a cortical column. LFP oscillations can only

be observed when many neurons fire in synchrony, since otherwise the individual neurons electric fields would simply cancel out. Furthermore, the occurrence of high frequencies demonstrates that local synchrony is generated with high temporal precision, which is also indicated by the MUA responses. The idea that whole groups of neighboring neurons could discharge synchronously in response to the same visual object has been attracting neuroscientists attention for many years (Kreiter and Singer 1996a; Kreiter and Singer 1996b). Furthermore, this idea is in general agreement with the hypothesis that neighboring cells with similar functional properties are tightly coupled to form what is called a neural group (Edelman 1987).

The parietal and the motor cortex hold similar organizational principles as the visual cortex, and also consist of numerous areas. Any cerebral activity involves large numbers of areas. Coordinate activity between neurons can be present in these areas. This coordination has been investigated by studying the correlations between field potentials, which reflect the average activity of large groups of neurons in the vicinity of a recording electrode (Mitzdorf 1985). The strength of coupling between transcortically recorded field potentials in different cortical areas changes dynamically during the performance of a behavioral task. Synchronization has been found between areas of the visual and parietal cortex, and between areas of the parietal and motor cortex, in cats that are awake (Roelfsema 1997). Therefore, synchronization on a fine temporal scale may be also a natural mechanism for the integration and coordination of neuronal activity between different brain regions.

But, what is exactly synchronization for? Interpretations were disparate. It has been proposed that correlations might act as an extra channel for information, carrying messages about the outside world not carried by other aspects of spike trains such as the overall firing rate (Gray 1999; Richmond and Gawne 1998; Abbott and Dayan 1999; Panzeri et. al. 1999). Others have proposed that correlation interferes with decoding the information represented by the firing rate of a population of neurons (Zohary et. al. 1994; Shadlen and Newsome 1998, Mazurek et al 2002). On the other hand, Von der Malsburg 1981 proposed that the temporal correlations between neurons could help to avoid a potentially combinatorial problem in neural coding. Theories that propose the creation of "cardinal" cells to represent particular combinations of signals from lower-order neurons are implausible because the number of combinations to be coded exceeds the number of neurons available. In Von der Malsburg theory, which constitutes the original formulation of the binding theory, the activity of low-

order neurons would be combined only when their spike activity was synchronized to within a few milliseconds to create a synchronously active cell assembly. Synchronization would be dynamically modulated, so that a particular cell could belong to one cell assembly at one moment and to a second at another; in this way, the combinatorial problem can be avoided and arbitrarily large numbers of states can be coded with a reasonable number of neurons.

It has been thought that synchronous activity within the millisecond time range may be the signature of neuronal assembly formation. If correlated activity can be the signature of neuronal assemblies, it may be essential in the context of multiple object encoding (Von der Malsburg 1981; Von der Malsburg and Schneider 1986; Singer 1990a; Singer 1993). According to the temporal binding hypothesis of von der Malsburg, cells belonging to the same assembly fire action potentials synchronously with a precision of a few milliseconds, and cells belonging to different assemblies fire asynchronously. The temporal binding hypothesis requires cortical neurons to act as coincidence detectors (Abeles 1982; Softky 1994; Koenig et. al. 1994). Neuroscientists have been trying to find evidence for this proposal in the nineties (Alonso et. al. 1996; Matsumara et. al. 1996; Castelo-Branco 1998, Mangulis and Tang 1998; Prut et. al. 1998; Stevens and Zador 1998; Christiakova 1998, Azouz and Gray 1999; Larkum et. al. 1999).

Two studies (Kreiter and Singer 1992; Kreiter and Singer 1996b) in which coherent high frequency oscillations and long-range synchronization were investigated in the motion-sensitive area MT of awake fixating macaque monkey, yield several important findings. First, they demonstrated the existence of synchronization of local and distant cell groups and also oscillatory activity in the gamma frequency range in the cortical area outside primary visual cortex in the awake animal, indicating that these phenomena might be of general importance for visual information processing. Second, synchronization was shown to be stimulus dependent: a given pair of neurons or neuronal groups which synchronized their responses when activated with a single contour, fired independently when stimulated with two different contours (but see Roelfsema et. al. 2004). Third, while differences in synchronization were significantly different in these two stimulus conditions, firing rates did not change in a systematic way. Thus, some information about the stimulus is conveyed by the relative timing of spikes, which is unavailable from firing rates alone. Fourth, they found synchronization to be independent of the detailed characteristic of orientation and motion of the coherent stimulus (but see Kohn and Smith 2005; Samonds and Bonds 2005).

De Charms et al. (1996) demonstrated that the relative timing of cortical action potentials can signal stimulus features themselves, a function even more basic than feature grouping. They found that populations of neurons in the primary auditory cortex can coordinate the relative timing of their action potentials such that spikes occur closer together in the time during continuous stimuli and in this way cortical neurons can signal stimuli even when their firing rates do not change. Different alternative solutions to the binding problem have been suggested by (Singer 1990b; Singer and Gray 1995; Kreiter and Singer 1996a; Engel et. al. 1997; Roelfsema 1998). In this framework, neurons may belong to the same assembly in one stimulus condition and belong to separate assemblies in yet another stimulus condition. The temporal binding hypothesis predicts the existence of particular stimulus-dependent changes of synchrony. The occurrence of synchrony seems to be therefore more an attribute of the dynamic state of the neuronal network than a mere side effect of anatomical coupling.

However, theoretical achievements which may account for visual feature integration, using the temporal correlation hypothesis such as binding theory, are usually based on suggestive evidence found by Kreiter and Singer in the visual cortex (Kreiter and Singer 1996a; Kreiter and Singer 1996b). Over the last ten years there has been no conclusive evidence about the binding theory. Several critics have indeed suggested that the theory does not hold up (Shadlen and Movshon 1999; Palanca and DeAngelis 2005). According to the alternative binding by rate enhancement hypothesis, features of single perceptual object are bound instead if the neurons encoding them jointly enhance their response (Roelfsema et. al. 2004). On the other hand, the influential Feature Integration Theory developed by Anne Treisman (Treisman and Gelade 1980) suggested instead that attention is responsible for binding different features into consciously experienced wholes. That is, the neurological literature supports the idea that binding is a high level process. But, conceptual problems arise when the binding is considered as strictly intra-cortical (Eckhorn et. al. 1988; Gray-Singer 1989). Intra-cortical binding through oscillation essentially solves the problem using circular logic. The cortex binds object features to identify the object, but to bind the features the cortex needs to know in advance that they are part of the same object. If we consider synchrony to be informative to perceptual events, some representation of that information must also be available in the retina. The object-binding problem therefore can not be completely solved in primary visual cortex, and the computation involved cannot be completed until a fairly

high level in the cortical hierarchy. Hence, a natural question is why synchrony should be present in the primary visual cortex if binding is not computed there?

Neurons in cortex receive 3,000-10,000 synaptic inputs, 85 % of which are excitatory. Nearly half of the excitatory input to any one neuron comes from nearby neurons that fall within a cylinder of 100-200 μ m radius, arranged as a column, sometimes termed a mini-column (Desimone 1991; Andersen 1995; Churchland et. al 1994; Cobb et. al. 1995). This suggests that cortical neurons receive abundant excitatory input and are embedded in a network of highly convergent signals. The networks have a recurrent nature, it is likely therefore that those most excitatory neurons receive similar inputs and emits spikes under similar conditions. This means that the conditions that lead to a response of any of one neuron in mini-column are likely to involve considerable activity from a large number of its inputs and its outputs. It is therefore reasonable to expect that many spikes inputs will arrive in synchrony within a very small time window.

As we pointed out before there are several experiments, which show that the timing of visual events on a millisecond scale can influence perception. These experiments have demonstrated that the visual system can group features on the basis of similarity of time course, a natural extension of the Gestalt concept (Leonards et. al. 1996; Alais 1998; Usher and Donnelly 1998; Lee and Blake 1999; Samonds and Bonds 2005). In this sense the experiments support in some way the original conjecture von der Malsburg's. Von der Malsburg's (1981) original conjecture support indeed the idea that temporal synchrony could be created by visual input. However, one should keep in mind that even if temporally precise activity is a necessary condition for binding, it might not be a sufficient condition. This kind of statement was supported by (Golledge et. al. 2003) who found that firing rates, rather than correlations, are the main element of the population for feature binding in the primary visual cortex. They did not find that neuronal groups systematically synchronized their responses when they were activated with a single contour, and they found that cells fired independently when stimulated with two different contours. The ultimate role of synchronization in the primary visual cortex in the object group features recognition remains still unclear.

The integration of features into gestalt entities is one the most important challenges in cognition. In order to get a better understanding of how the brain can possibly know that features belong to the same objects it is reasonable to expect that cortical synchrony starts

with visual stimulus and the retinal inputs. Spatial and temporal correlations in the visual scene cause synchronous activation of populations of retinal cells. This leads to matching cortical latencies, triggering synchronization. Transient synchrony occurs with either dynamic or novel stimuli (Kruse and Eckhorn 1996) propagating from retina to LGN (lateral geniculate nucleus) to the cortex (Castelo-Branco 1998; Neuenschwander et. al. 2002).

Transient visual inputs are in particular capable of eliciting burst of cortical activity whose onset is reliable to within a few milliseconds, and whose duration can be as brief a few milliseconds (Kohn and Smith 2005; Shadlen and Newsome 1994; Bair and Koch 1996 Bair 1997; Buracas et. al. 1998). This supports the idea that it is not really clear how to distinguish visually elicited synchrony and hypothetical synchrony due to binding. If we suppose that many inputs spikes can arrive in synchrony within a very small time window while the cortical column is active, this would imply that cortical neurons can respond selectively to synchronous input with a few milliseconds.

But, these are not the only issues that remain unsolved. The underlying origins of synchronized firing between cortical neurons are also still under discussion. It has been thought for instance that inter-celular communication through chemically mediated synaptic transmission was the major contributor for in the formation of synchronized spikes firing. This is, the network of GABAergic interneurons connected by chemical synapses was a candidate for the generator of synchronized oscillations in the hippocampus (Fukuda et. al. 2000). On the other hand, electrical coupling by gap junctions between neurons were only thought as a key element of neuron to neuron communication in early brain development. However, there are growing morphological and physiological evidence which indicates that the electrical synapse can also play an important role in the juvenile and adult brain (Venance et. al. 2000), and remarkably, electrical synapses in the cortex are frequently found to connect GABAergic interneurons. This is the case for instance in the striatum (Kita et. al. 1990) the hippocampus (Venance et. al. 2000), the cerebellum (Mann-Metzer 1999), the reticular thalamic nucleus (Landisman et al. 2002), and the neocortex (Gibson et. al. 1999, Galarreta and Hestrin 1999 Fukuda et. al. 2000). Recent experiments have shown that electrical synapses can be involved in synchronizing neural activity. Blocking of inhibition and excitation does not reduce the synchronization of interneurons in the molecular layer of the cerebellum between which electrical synapses have been identified (Mann-Metzer 1999). Neuronal synchrony of neurons interacting via electrical and/or inhibitory synapses is still being highly

debated (Venance et. al. 2000; Lewis et. al. 2003; Pfeuty et. al. 2003; Pfeuty et. al. 2005; Bennett et. al. 2004).

It is still not clear how intrinsic cellular properties would exactly affect synchrony of neurons coupled via inhibitory or electrical synapses, or what is the real significance of the combination of electrical and inhibitory couplings for neuronal dynamics. The electrical coupling between neurons might define synchronized domains. Synaptic interactions might also have some influence in synchronization. The cerebral cortex and hippocampus can indeed show synchronized bursts of activity underlying strong recurrent excitatory connections, the presence of intrinsically burst-generating neurons, ephaptic (non-synaptic) interactions among closely spaced neurons (Buzsaki et. al. 1996), and synaptic plasticity.

If we consider the information coding is based on dynamics and synchronization of neural activity then the idea of considering the information coding as a multi-level process several hierarchical levels can be very attractive (Borisjuk et. al. 1997). In this framework dynamical model can be helpful to understand the basic properties of information processing in the brain. However, it is yet not even well known how single cell coupled with other cells display nonlinear dynamic properties and its role in the rhythmic synchronization of electrically coupled neurons (Makarenko and Llinas 1998). This high level of complexity makes it very difficult to account for all the underlying involved physical phenomena which might be involved in the origins of synchronized firing.

1.2 *The current state of the problem*

1.2.1 *A topic of intense debate in the neuroscience community*

The nature of the neural code is a topic of intense debate within the neuroscience community. One of the central issues in neural coding is whether individual action potentials and individual neurons encode independently from each other, or whether correlations between different spikes and different neurons carry a significant amount of information. Independent-spikes codes are much simpler to analyze than correlation codes, and thus if correlations were not important for information decoding then this would strongly affect our strategies in the study of the neural code. So, if we want to study the neural code, we must consider whether

individual neurons act independently, or not.

If they act independently, then the relative timing of spikes contains no additional information about the stimulus. In contrast, if correlations between the spiking of different neurons provide additional information about a stimulus that cannot be obtained by considering all their firing patterns individually we have a correlation code. An independent neuronal code assumes that neurons act independently, and means that one does not need to take correlations into account. Influential models of population coding have assumed independence of the cell firing rate (Georgopoulos 1990). They are based on the idea that the nervous system can take population average over neurons in order to achieve reliable stimulus coding, in the same way that an experimenter with a single electrode can determine the single neurons response properties by averaging over trials of stimulus representation.

Within this framework, if we considered a pair of correlated neurons with overlapping tuning curves and without any stimulus correlation dependence, the covariance of neuronal firing would be conceived as a limiting factor for a population of neurons to convey information due to the introduction of redundancies (Zohary et. al. 1994). Contrary to models which assume independence, synchronous firing of two or more neurons is one possible mechanism for conveying extra information compared to an independent neuron code. Rhythmic oscillation of population activity provides another possible mechanism. Both synchronous firing and oscillations are common features of the activity of neuronal populations. However, the existence of these features is not sufficient for establishing a correlation code, because it is essential to show that a significant amount of information is carried by the resulting correlations.

Neurons in the retina, LGN, and primary visual cortex respond to light stimuli in restricted regions of the visual field called their receptive fields. Retinal ganglion cells in the same vicinity have long been known to have receptive fields that overlap extensively. This means that the retinal code at the level of the ganglion cells intrinsically uses populations of neurons to represent even the sharpest spatial features within a visual image. In addition, natural visual scenes have strong spatial correlations (Field 1987; Van der Schaaf A. and van Hateren 1996), which may cause an even wider group of ganglion cells to participate in encoding any single feature within a natural image. A central issue in studying the retina, LGN, and primary visual cortex is to understand how information is represented collectively by the activity of

a population of neurons. It is well known that the visual information reaches the brain by way of a fine cable, the optic nerve. In the traditional view of retinal function, each ganglion cell axon represents an independent channel of the information the eye conveys to the brain. The bundle of such axons comprising the optic nerve forms a set of labelled lines, each conveying the presence of a specific feature. Given the limited capacity of the optic nerve, the idea that each of these features should be nearly unique has been attractive for a long time (review by Barlow 2001).

Information theory (Shannon 1948) allows us to address how much the neuronal responses tell us about the stimulus. We can use it to ask what forms of neuronal response are optimal for conveying information about the stimuli. The relevance of information theory for neuroscience ultimately derives from the fact that the brain possesses many subsystems that acquire, process and transmit information. Therefore many brain structures can be considered as communication channels, and the appropriate mathematical framework for the analysis would be the Information Theory. Mutual Information (Shannon 1948) quantifies how well an ideal observer can discriminate between all members of the stimulus set based on the neuronal responses of a single trial.

To understand the neural code means to know how information about the outside world is carried in neuronal spike trains. It has been known for many years that neuronal spike trains fired by adjacent cortical neurons exhibit correlations - the probability of one cell firing may depend upon whether another cell fires an action potential (Zohary et. al. 1994; Kreiter and Singer 1996a; Kreiter and Singer 1996b; Gawne 1993; De Oliveira et. al. 1997; Lebedev et al. 2000; Mastronarde 1983). Whether (and how) such correlations contribute to the coding of sensory information remains highly debated. Some experimental and theoretical findings support the usefulness of temporal correlations among a population of neurons. Information theoretical considerations have shown that correlations of neuronal firing can enhance the accuracy of populations responses, increase the information rates and allow for increased stimuli discriminability (Snippe and Koenderink 1992; Richmond and Gawne 1998; Abbott and Dayan 1999, Panzeri et. al. 1999).

Synchronous spikes in a neuronal ensemble can carry extra information not available from individual spikes elicited by the neurons independently. It is usually referred as synergy (redundancy) when the information conveyed by an ensemble of neurons is larger (smaller)

than the sum information conveyed by each neuron independently (Panzeri et. al. 1999). Retinal ganglion cells have been found to encode synergistically (Meister 1996), roughly independently (Nirenberg et. al. 2001), or redundantly (Puchalla et. al. 2005). In the lateral geniculate nucleus, Dan et al (1998) reported synergistic effects. In the cortex, most studies have concluded that neurons provide roughly independent information, with some evidence for weak synergy in V1 (Reich et. al. 2001; Golledge et. al. 2003; Kayser et. al. 2004), the motor cortex (Averbeck and Lee 2003; Oram et. al. 2001), and the somatosensory cortex (Petersen 2001).

It is important to point out that the mentioned studies, the authors used different metrics. For instance, Meister associate an information measure with individual occurrences of events. In this framework correlations can act as an extra channel of information and removing them would lead to a loss of information rather than a gain. Puchalla et. al. 2005 estimated synergy/redundancy ($\Delta_{Synergy} > 0$ and < 0 , respectively), where this measure is the total information that neuronal responses provide about a set of stimuli minus the information provided by the individual responses taken separately. However, this measure can be positive, negative, or zero both when correlations are not important for decoding (Nirenberg and Latham 2003). On the other hand, Nirenberg et. al. 2001 uses the conditional relative entropy, or average KullbackLeibler distance (ΔI), between the "correlated dictionary", $P(\mathbf{s}|\mathbf{r})$, and the "independent dictionary" $P_{ind}(\mathbf{s}|\mathbf{r})$. ΔI can be used to assess the importance of correlation for decoding, and is equal to $I_{cor-dep}$ obtained using the Information breakdown method (Pola et. al. 2003). One would expect the approach used by Meister would capture the effects of only one kind of correlations, synchronous spikes across neurons and not the correlations which could be captured by the use of ΔI (or $I_{cor-dep}$). Hence, the use of different metrics would eventually lead to different conclusions.

In the visual, auditory, motor and premotor cortex and the hippocampus, changes of synchronization in relation to external or internal events have been observed without significant changes of firing rates (Vaadia et. al. 1995; De Charms et. al. 1996; Kreiter and Singer 1996b; Riehle et. al. 1997; Sakurai 1999). These findings show that information about these events was available to the nervous system by relative timing of spikes. Many behavioral responses are completed too quickly for the underlying sensory process to rely on estimation of neural firing rates. Hence, the fine temporal structure of spike trains should play an important role and the temporal pattern of activity should carries information about the stim-

ulus (Mainen and Sejnowski 1995). But, which features of the pattern are important? It has been hypothesized that stimulus-driven oscillatory activity in a neuron is a code of significant stimulus (Borisjuk et. al. 1990; Borisjuk et. al. 2000b). Recent studies in the somatosensory cortex show that the complexity of the response of biological neuronal populations is potentially contained in precise spike timing. Information about stimuli in the striate cortex could be encoded in the precise spike timing, rather than neuronal firing rate (Panzeri et. al. 2001b). Cortical neurons with similar stimulus selectivities are found in close proximity to each other (Hubel et. al. 1962; Mountcastle 1957; De Angelis et. al. 1999).

It is highly debated how neurons in the cerebral cortex represent a stimulus when the response variability is correlated (Zohary et. al. 1994; Lampl et. al. 1999, Shadlen and Newsome 1998). At another level when these correlations are present they may have significant effect on the population coding of sensory information. Several pieces of evidence point to correlations between V1 neurons being orientation and contrast dependent (Kohn and Smith 2005; Samonds and Bonds 2005). Recently, Samonds and Bonds 2005 have proposed that cortical synchrony originates from coherent spatiotemporal stimulus structure, whereas bursts and oscillations maintain and modulate synchrony by preserving its coordination across cell populations. Oscillation occurs more often for drifting as opposed to stationary gratings (Engel et. al. 1990), and thus, one would expect that they are only relevant for motion processing. Synchronization and oscillation may therefore play a key role in propagating information reliably. Oscillations can help to maintain transient synchronization. This allows the possibility that synchronization could be used in higher cognitive processing in the cortex. This higher order spatial and temporal properties of visual stimuli are progressively extracted in the pathway from the retina through the cortex. Therefore, at the level of the striate cortex correlations become progressively harder to detect (Purpura et al. 1994) as the stimuli encoding become more and more abstract.

Hence, it is not straightforward to use the appropriate stimuli to identify the representation of the visual information at this higher level of the visual system (Usrey and Reid 1999). Neurons interact through different dynamical pathways in the complex architecture of visual processing in the cortex of primates. It may not be preposterous therefore to think of synchrony as a mechanism for reliable signal transmission that extracts higher-order correlations as a gestalt rather than as an active binding mechanism that represents a secondary code to link a system of simple feature extraction.

This is, higher order correlations might well be a necessary feature to transmit information between different parts of the brain, and also they could help to decode information about the stimuli through the pathway from the retina to the cortex. However, to test all these hypothesis it would be necessary to design an experiment where complex or natural stimuli could activate higher order correlations in a population of neurons. But, at the same time, it would be important to avoid all the possible unwished effects of anesthetics. This is a huge challenge, since nowadays it seems more reliable to perform experiments using just basic stimuli, because one would expect that they will not affect the responses if the animal is awake or under the effect of anesthetics. Once again, this is a limitation if we want to achieve a much better understanding of what the role of higher correlations is as a gestalt in the processing of information.

Neurons could learn in each level of processing to extract relevant information about the stimuli using a biologically unsupervised learning strategy (Thorpe 2005). Information about spatial and temporal properties of visual stimuli can be progressively extracted in the pathway from the retina through the cortex as if we were considering a non-linear network. Higher-order features extraction could be interpreted as the binding of lower-order local features, but the importance of the distinction between an active intra-cortical binding mechanism versus higher-order filtering is that the latter process will not run into a circular logic contradiction. However, it might still not pass every possible test of feature binding (for a discussion review see Shadlen and Movshon 1999).

Just by gathering the above mentioned experimental and theoretical evidences, we can guess that to investigate the role of temporal correlated neuronal activity is a key element for the understanding of the neuronal coding. To get a better understanding of the role of correlations can have widespread implications, not only for our basic understanding of how the brain operates, but also in our understanding of neuronal dysfunctions (Uhlhaas and Singer 2006).

However, the matter of how the coding of sensory information is affected by spike correlations across neurons has been fraught with dissension, and the debate has become polarized into two different postures that co-exist in the neuroscientific community. One of the postures, supported by many authors (Eckhorn et. al. 1988; Gray-Singer 1989; Gray et. al. 1989; Meister et. al. 1995; Vaadia et. al. 1995; De Charms et. al. 1996; Dan et. al. 1998, Steinmetz et. al. 2000) is that correlations are important in the coding of sensory infor-

mation, whereas others have proposed that they are not important (Nirenberg et. al. 2001; Oram et. al. 1998, Petersen 2001; Levine et. al. 2002; Panzeri et. al. 2002a; Panzeri et. al. 2002b, Averbeck et. al. 2003; Averbeck and Lee 2003; Averbeck and Lee 2004; Golledge et. al. 2003).

This dissension can be traced to different methods used to assess the role of synchronized spike firing. For instance, one of the most used methods consisted in looking for stimulus-dependent changes in cross-correlograms (Eckhorn et. al. 1988; Gray-Singer 1989, Gray et. al. 1989; Vaadia et. al. 1995; De Charms et. al. 1996). However, the firing rate can alter the shape of cross-correlograms making it difficult to separate information carried by firing rates from information carried by correlations. Moreover, cross-correlograms account only for near synchronous spikes. This is, they do not account for correlations which occur on a longer time scales and among patterns of spikes.

1.3 From Signal Detection Theory to Information Theory

1.3.1 Signal Detection Theory

One of the early objectives of psychophysics research was to measure the sensitivity of our sensory systems. This research has led to the development of the idea of a threshold, the least intense amount of stimulation needed for a person to be able to see, hear, feel, or detect a stimulus. But, one of the problems with this concept was that even though the level of stimulation remained constant, people were inconsistent in detecting the stimulus. Factors other than the sensitivity of sense receptors influence the signal detection process. There is no single, fixed value below which a person never detects the stimulus and above which the person always detects it. In general, psychophysics researchers define a threshold (or attitude) as that intensity of stimulation at which a person can detect some percentage of all times, for example, fifty percent.

An approach to solving this problem was provided by Signal Detection Theory. This theory deals with the detection of the stimulus as a decision-making process, which is determined by the nature of the stimulus, by how sensitive a person is to the stimulus, and by cognitive factors. In other words, a person will be able to detect more intense sounds or lights more easily than less intense stimuli. But, a more sensitive person requires a weaker stimulus

intensity than a less sensitive person would. According to the theory, there are a number of psychological determiners of how we will detect a signal, and where our threshold levels will be. Experience, expectations, physiological state (e.g. fatigue) and other factors affect thresholds (attitudes).

Signal Detection Theory provides a precise language and graphical notation for analyzing decision making in the presence of uncertainty. The general approach of signal detection theory has direct application in terms of sensory experiments, and also offers a way to analyze many different kinds of decision problems. If a person is quite uncertain as to whether the stimulus was present, the individual will decide based on what kind of mistake in judgment is worse: to say that no stimulus was present when there actually was one or to say that there was a stimulus when, in reality, there was none.

Let's illustrate this with an example from everyday life. Suppose a person is expecting an important visitor, someone that it would be unfortunate to miss. As time goes by, the person begins to hear the visitor and may open the door, only to find that nobody is there. This person is detecting a stimulus, or signal, that is not there because it would be worse to miss the person than to check to see if the individual is there, only to find that the visitor has not yet arrived.

In a typical sensory experiment that involves a large number of trials, an observer must try to detect a very faint sound or light that varies in intensity from clearly below normal detection levels to clearly above. The person responds positively (i.e., there is a stimulus) or negatively (i.e., there is no stimulus). There are two possible responses, Yes and No. There are also two different possibilities for the stimulus, either present or absent.

Psychophysics research has established that when stimuli are difficult to detect, cognitive factors are critical in the decision an observer makes. If a person participates in an experiment and receives one dollar for each Hit and there is no penalty for a False Alarm, then it is in the person's best interest to say that the stimulus was present whenever there is uncertainty. On the other hand, if the person loses two dollars for each False Alarm, then it is better for the observer to be cautious in saying that a stimulus occurred. This combination of rewards and penalties for correct and incorrect decisions is referred to as the Payoff Matrix. If the Payoff Matrix changes, then the person's pattern of responses will also change. This alteration in responses is called a criterion shift.

There is always a trade-off between the number of Hits and False Alarms. When a person is very willing to say that the signal was present, that individual will show more Hits, but will also have more False Alarms. Fewer Hits will be associated with fewer False Alarms. As such, the number of Hits is not a very revealing indicator of how sensitive a person is; if the person claims to have heard the stimulus on every single trial, then the person will have said Yes in every instance in which the stimulus was actually there. This is not very impressive, however, because the person will also have said Yes on every trial on which there was no stimulus. Mathematical approaches have been used to determine the sensitivity of an individual for any given pattern of Hits and False Alarms; this index of sensitivity is called d' (d-prime) and is equal to the square-root of the signal-to-noise ratio. A large value of d' reflects greater sensitivity.

Signal Detection Theory is an intent to quantify the ability to discern between signal and noise. It constitutes one of the first attempts to model the processes involved in elementary perceptual recognition tasks. It is based on the assumption that nearly all reasoning and decision making takes place in the presence of some uncertainty. It could be used to evaluate performances and can also help to solve problems in psychophysics.

To develop a measure of sensitivity, it is necessary to go beyond a simple description of the data. A measure that describes the detectability of a signal must be based on the idea of how the detection process work as a whole. The basis is constructed from statistical decision theory and is similar to the idea that are used in statistical testing to make decision between two hypothesis. To make predictions of the signal detection model the form of the signal and noise distribution must be assumed. The simplest and most natural approach is the normal distribution. However, this can also constitute a limitation.

Receiver operating characteristic (ROC) analysis was originally developed for using with radar technology to separate observer variability from the innate detectability of the signal. Sensitivity, or recall rate, is a statistical measure of how well a binary classification test correctly identifies a condition. The specificity is a statistical measure of how well a binary classification test correctly identifies the negative cases, or those cases that do not meet the condition under study. The Receiver Operating Characteristics (ROC) of a classifier shows its performance as a trade off between selectivity and sensitivity. In signal detection theory, a receiver operating characteristic (ROC), or simply ROC curve, is a graphical plot of the

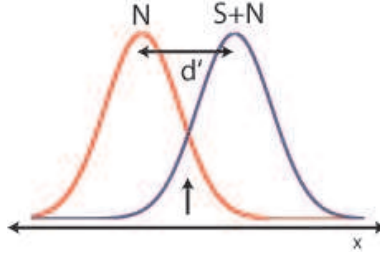


Fig. 1.1: d' measures the distance between two normal distributions of equal variance.

sensitivity vs. $[1 - \text{specificity}]$ for a binary classifier system as its discrimination threshold is varied. Measurement of ROC curves provides an objective tool for describing the ability of an observer to detect an object structure in any particular imaging situation, independent of the attitude or threshold which the observer assumes.

In simple idealized detection situations ROC curves exhibit certain symmetric properties and performance ranking of imaging systems is unambiguous. ROC analysis is related in a direct and natural way to cost/benefit analysis of diagnostic decision making. ROC analysis provides tools to select possibly optimal models and to discard suboptimal ones independently from (and prior to specifying) the cost context or the class distribution. But, ROC curves determined in actual visual detection experiments are characteristically asymmetric and a generally meaningful measure for comparing such curves has not been identified so far.

The basic idea behind signal detection theory is that neurons are constantly sending information to the brain, even when no stimuli are present. This is called in this framework neural noise. The level of neural noise fluctuates constantly. When a faint stimulus, or signal, occurs, it creates a neural response. The brain must decide whether the neural activity reflects noise alone, or whether there is also a signal.

For very intense signals, there is no problem in deciding if there was a stimulus because the neural effect of the signal far outweighs the neural effect of the noise. Similarly, when there is no signal, the nervous system does not respond as it does when an outside signal is present, so decisions are easy. On the other hand, for near-threshold signals, it can be difficult to know whether neural activity results from noise alone or from a signal plus noise. At this point, the observer makes a decision based on the payoff matrix (Green and Swets 1966; Wickens 2001).

1.3.2 *Information Theory*

In order to get a better understanding on how we see, hear and think, we need to learn how the activity of neurons relates to the state of the perceived world. Neurons use spikes of membrane potential, known as action potentials, to convey information. As these are unitary events, the set of individual time points of each action potential completely describes a neuron response to sensory stimulation.

How to characterize the neuronal responses by a given stimuli is indeed very difficult, because of the complexity and variability of the neuronal responses. Neurons typically respond by producing complex spike sequences that reflect both the intrinsic dynamics of the neuron and the temporal characteristics of the stimulus. Isolating features of the response that encode changes in the stimulus can be difficult, especially if the time scale for these changes is of the same order as the average interval between spikes. Neuronal responses can vary from trial to trial even when the same stimulus is presented repeatedly. A potential source is the randomness associated with various biophysical processes taking place during a trial. The complexity and trial-to-trial variability of action potential sequences make it unlikely that we can describe and predict the timing of each spike deterministically. But, a complete description of the stochastic relationship between a stimulus and a response would require us to know the probabilities corresponding to every sequence of spikes that can be evoked by the stimulus. That is, the neural responses and their relation to the stimulus, are completely characterized by the probability distribution of spikes (time) as function of the stimulus. The independent-spikes code would correspond to the case in which the generation of each spike is independent of all other spikes in the train. In contrast, if the individual spikes do not encode independently of each other, we call the code a correlation code, because correlations between spikes may carry additional information. In reality, information is likely to be carried by both the individual spikes and through correlations, and some arbitrary dividing line must be established to characterize the code.

In 1948 Shannon published *A Mathematical Theory of Communication* in two different volumes of the *Bell System Technical Journal*. His work was focused on the problem of how to best encode the information a sender wants to transmit. Shannon developed Information Theory, as a measure for the uncertainty in a message while essentially inventing what became known as the dominant form of "information theory". He invented information theory as a

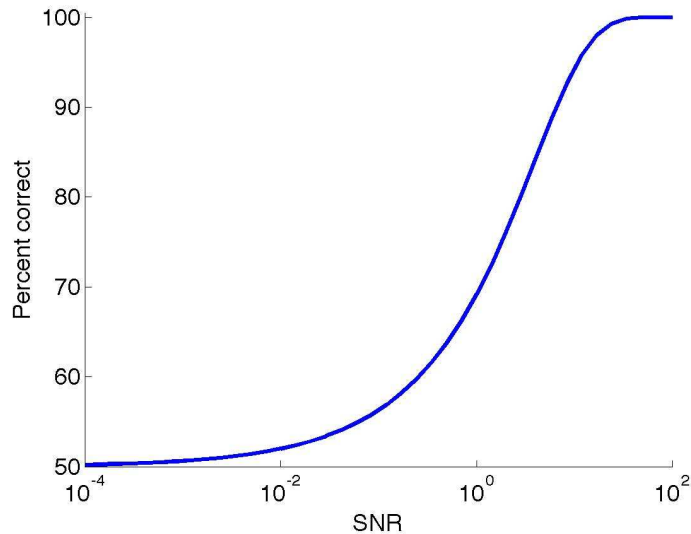


Fig. 1.2: Percentage of correct detections for an ideal observer in a detection task as a function of SNR.

general framework for quantifying the ability of a coding scheme or a communication channel (such an optic nerve) to convey information. It is assumed that the code involves a number of symbols (such as different neuronal responses), and that the coding and transmission process are stochastic and noisy. Communication channels, if they are noisy, have only limited capacities to convey information. The techniques of information theory are used to evaluate these limits and find coding schemes that saturate them. Moreover, information theory allows us to address how much the neuronal responses tell us about the stimulus. We can use them to ask what forms of neuronal response are optimal for conveying information about the neuronal stimuli. Therefore many brain structures can be considered as communication channels, and an appropriate mathematical framework is the information theory.

This basic approach was introduced quite some time ago (Werner and Mountcastle 1965), but the state of the art in single cell information analysis has advanced considerably in recent years. This is, the understanding of the principles which could lead the processing of sensory information, was considerable boosted by the use of Shannon Information Theory (Strong et. al. 1998b; Tolhurst 1989; Rolls et. al. 1997a; Rolls 1997b; Panzeri et. al. 1999; Panzeri et. al. 2001b; Nirenberg and Latham 2003; Averbek et. al. 2006). This approach has been quite successful in studying the sensory processing properties of single neurons,

just by estimating the mutual information that neuronal responses convey about a set of controlled sensory stimuli.

The mutual information measures the amount of information that the knowledge of a given random variable (y) conveys about another random variable (x). Mutual information can also be expressed as a Kullback-Leibler divergence, of the product $p(x)p(y)$ of the marginal distributions of the two random variables X and Y , from $p(x,y)$ the random variables joint distribution:

$$\begin{aligned}
 I(X, Y) &= D_{KL}(p(x, y)|p(x)p(y)) \\
 &= \sum_{x \in X} \sum_{y \in Y} p(x, y) \log_2 \frac{p(x, y)}{p(x)p(y)} \\
 &= H(X) + H(Y) - H(X, Y),
 \end{aligned} \tag{1.1}$$

where $H(X) = \sum_{x \in X} p(x) \log p(x)$, $H(Y) = \sum_{y \in Y} p(y) \log p(y)$ are the Shannon marginal entropies, and $H(X, Y) = \sum_{y \in Y} p(x, y) \log_2 p(x, y)$ is the joint Shannon entropy of X and Y . This quantity can be evaluated for different coding schemes, and used to make conclusions about the nature of the representation of the sensory information by neuronal spike trains.

However, the problem with real measures of entropy is that they depend on a limited number of samples provided by the experiment. It is therefore important to use a theoretical approach that can remove sample size dependent bias from the entropy estimations. On the other hand, it is well known that approaches usually performed to estimate the entropy tend to underestimate it since they are biased, and this effect can be avoided by the use of a perturbative expansion in the asymptotic regime. The idea of calculating entropy by counting coincidences was proposed a long time ago by Ma for physical systems in the micro-canonical ensemble, where a uniform distribution of entropy corresponds to states of fixed energy. The Bayesian prior proposed by Nemenman et. al. 2004 extends this idea to an arbitrarily complex distribution. The goal of this method (which in the following will be denoted by NSB) is to construct a Bayesian prior, which generates a nearly uniform distribution of entropies in order to correct sample size dependent bias at its source.

Let's go back for a moment to the Signal Detection Theory framework. An interesting measure is the signal-to-noise ratio (SNR). SNR allows us to quantify the size of the applied or controlled signal relative to fluctuations that are outside experimental control. It has gen-

eral applicability to the analysis of sensory discrimination, or to evaluate the performance of neuronal networks. A common use of SNR is to compare the quality of electrophysiological recordings containing events, action potentials or local field potentials, recorded in the presence of noise. This measure can be used to characterise the reliability of neural information transmission (Schultz S.R 2006). The signal-to-noise ratio is defined as the ratio between a signal and the background noise

$$SNR = \frac{P_{signal(\nu)}}{P_{noise(\nu)}}, \quad (1.2)$$

where ν is the frequency. In a signal detection scenario where a signal shifts between two values 0 and Δr , assuming an additive Gaussian noise of variance σ_N^2 , the SNR can be expressed as

$$SNR = \frac{\Delta r^2}{\sigma_N^2} = d'^2, \quad (1.3)$$

where $d' = \sqrt{SNR}$ (see Figure 1.1) is the discriminability between signals and a commonly used measure in psychophysics (Green and Swets 1966). Figure 1.2 shows the probability finding a correct detection in this framework, which can be obtained by integrating over the Gaussian noise (Green and Swets 1966; Reike et. al. 1998; Schultz S.R 2006). If SNR becomes large, performance approaches 100 % correct, at $SNR = 1$, the percentage of correct discriminations is 69 % which is a common definition of the threshold for detection in the psychophysics literature.

SNR can be also interpreted as an information quantity, in the sense of Shannon mutual information. This is, considering that signal and noise follow Gaussian distributions and for the case of a discrete time channel with additive Gaussian noise (Cover and Thomas 1991), the mutual information reads

$$I = \frac{1}{2} \log_2(1 + SNR). \quad (1.4)$$

In the continuous channel with Gaussian noise it can be expressed as (Shannon, 1949)

$$I = \int_0^\infty \frac{1}{2} \log_2(1 + SNR(\nu)) d\nu \quad (1.5)$$

This information capacity provides an upper bound on the mutual information. The power spectrum of a Gaussian process can be seen as an ordered list of the variances of frequency

components. Each of these frequencies can be viewed as a "symbol", and the information carried follows the form of the information per symbol. Then the total information is obtained by summing over all independent symbols, and normalizing to express it as an information rate. These steps can be accomplished by integrating over frequencies.

The discussion presented above brings to light some of the basic connections between Signal Detection Theory and Information Theory. However, it does not tell us yet how it can be possible to encode information about a given stimuli when complex spikes occur only about once per second.

Shannon's Information Theory formalizes the relationship between events, such as stimulus and response events, strictly based on their probabilities of occurrence (e.g., $P(s_i|r_j)$, the probability that stimulus s_i occurred given the response r_j). Information Theory allows us to address how much the neuronal responses tell us about the stimulus independently of any mechanism or model.

Information theory tells us how much information about a set of stimuli is encoded in a set of responses, which is a measure of how accurately we can know what stimulus was presented, given the response. This measure can also be defined as the reduction in uncertainty about which stimulus was presented before and after analyzing the response.

Hence, the first factor that determines the information is the a priori uncertainty in the stimulus set. To quantify this uncertainty, Shannon defined a measure $H(S)$ called entropy, which is in many regards analogous to the entropy (disorder) defined in thermodynamics. Once we analyze the response to the stimulus we will typically still be somewhat uncertain about which stimulus was presented; this residual uncertainty, called equivocation, can be quantified by $H(S|R)$, i.e., the entropy about the stimulus given the response.

Two factors contribute to equivocation: first, because of noise, two presentations of the same stimulus may evoke different responses. Second, the difference between the responses to different stimuli might be small. $H(S|R)$ is thus a function of the overlap between the responses to one stimulus and the responses to the other stimuli. The difference between $H(S)$ and $H(S|R)$ is the average reduction in uncertainty about the stimulus given the response, called the mutual information.

The real advantage of the Shannon mutual information measure is that it is independent

of any mechanism or model of how the stimulus and response are related. This can be particularly useful when the firing pattern of the neuron is known, but when the cause of this response is not known. Calculating information content requires only the stimuli and the responses to be represented by a code. Information theory does not specify which code to use, but simply says, for a given code, how much information is present. The key to applying this method in neurophysiology is to define an appropriate stimulus set code and a response set code.

Information theory is concerned with how efficiently information sources can be compressed and transmitted. Neurons communicate with each other with a series of pulses, each of which we call an action potential or spike. The rate at which spikes occur for a given neuron changes with stimulus variations. More subtle changes, like in the probability distribution of the inter-spike intervals, can also occur. This is, the stimulus is encoded in the pattern of action potentials but the same stimulus does not result in exactly the same pattern.

Spikes are about a millisecond long. However, neuroscientists have found very low discharge rates (less than 1 spike/sec and even zero) and rates as high as several thousand spikes/sec. For cortical neurons, for example, typical range are between zero and 100 spikes/s. Spikes typically have the same waveform and amplitude, and it is usually assumed that when spikes occur they encode information. But, in general spike timing can deviate much from the Poisson behavior.

It is also necessary to know how neurons process their inputs. Each neuron usually receives input from many neurons. When each input produces a spike, whether a spike is excitatory or inhibitory, and on how the neuron integrates these inputs determines the neuron's information processing function. The neuron will produce a spike only when the timing and strength of these inputs is correct. Excitatory inputs tend to cause spikes; inhibitory inputs tend to suppress them. If a time interval that spans several spikes occurring in a neuron's inputs is considered, neural computation amounts to each neuron producing spikes based on the timing of its inputs. Moreover there are many neurons and how they are connected to each other is also extremely complex.

Several inputs are processed. Potentially those inputs could be expressing information together rather than individually. This is a population or an ensemble code working together to represent information. One neuron is just too noisy to represent the stimulus. The idea

of a simple averaging across neurons responding to the stimulus seems to be to very naive to be a real representation of the neural code. Moreover, the spike timings among neurons are correlated. An induced stimulus-correlation will occur when a common stimulus generates correlations between neurons, whereas a connection induced correlation will occur when interneuronal connections link spike timing.

In the following chapters of this thesis we will make clear the overwhelming importance of probabilities and statistics in neuroscience. In a broader framework, Information Geometry provides an essential tool for understanding stochastic process, higher order stochastic correlations, and for developing the investigation of previously unexplored possibilities in the Information Theory framework. Its general validity as an statistical approach would allow predictions to be made beyond the sensory periphery.

1.4 A Guide to the Thesis

In the following chapters of this thesis we revive the debate about neuronal spike correlations which we think has been jeopardized by very general and too ambitious statements like the one made around the binding theory.

In chapter I of this thesis we present a review of the historical background of the previous spike correlation studies and current state of the problem. In the chapters II, III and IV of this thesis we have applied an information theoretic approach to study the role of correlations in the neuronal code, using the responses of pairs of neurons to drifting sinusoidal gratings of different orientations and contrasts recorded in the primary visual cortex of anesthetized macaque monkeys. In chapter V we investigate the effects of a focalized stroke in a population of neurons on information transmission using a computational and analytical approach to the problem. Finally, in chapter VI we use a novel analytical approach to study effects of higher order correlations in a population of neurons. Extensive conclusions are presented in the last chapter of the report (chapter VII).

More specifically, it has been proposed in neuroscientific literature that pooling can lead to a significant improvement in signal reliability, provided that the neurons being pooled are at most weakly cross-correlated. We have computed mutual information using the NSB estimator, and compared the information available from pairs of cells with the sum of the

single cell information values. This allowed us to assess the degree of synergy (or conversely, redundancy) in the coding. In chapter II of this thesis, we show that due to a loss of information encoded in the neuronal identity of the cells, pooling spikes across neurons leads to a loss of large fraction of the information present in their spike trains.

We have used information theory to examine whether stimulus-dependent correlation could contribute to the neural coding of orientation and contrast by pairs of V1 cells. To this end, in chapter III, we have used a modified version of the method of information components. This analysis reveals that although synchrony is prevalent and informative, the additional information it provides is frequently offset by the redundancy arising from the similar tuning properties of the two cells. Thus, coding is roughly independent with weak synergy or redundancy arising depending on the similarity in tuning and the temporal precision of the analysis. Our findings suggest that this would allow cortical circuits to enjoy the stability provided by having similarly tuned neurons without suffering the penalty of redundancy as the associated information transmission deficit is compensated by stimulus dependent synchrony.

In chapter IV, we present a discussion about different measures of correlations and in particular we propose the Jensen-Shannon Divergence as a measure of the distance between the corresponding probability distribution functions associated with each spikes fired observed patterns. We applied this Divergence for fixed stimuli as a measure of discrimination between correlated and independent firing of pairs of cells in the primary visual cortex. We found that the relative Jensen-Shannon Divergence (measured in relation to the case in which all cells fired completely independently) decreases with respect to the difference in orientation preference between the receptive field from each pair of cells. Our finding indicates that the Jensen-Shannon Divergence can be used for characterize the effective circuitry network in a population of neurons.

The underlying origins of synchronized firing between cortical neurons are still under discussion. Inter-cellular communication through chemically mediated synaptic transmission is considered a major contributor to the formation of neuronal synchrony. GABAergic inhibitory neurons may be involved in the generation of oscillatory activity in the cortex and its synchronization. Specifically, reduction of GABAergic inhibition may favour cortical plasticity producing functional recovery following focal brain lesions. Research into neu-

rotransmitter systems is therefore of paramount importance to understand the origins of synchronized spiking. However, it is necessary to understand first how simple focal abnormalities in GABAergic modulators can affect the information transmission in an impaired brain tissue. In chapter V, we present a computational and analytical model of a topographically mapped population code which includes a focal lesion as well as a process for receptive field enlargement (plasticity). The model simulates the recovery processes in the brain, and allows us to investigate mechanisms which increase the ability of the cortex to restore lost brain functions. We have estimated the Fisher Information carried by the topographic map before and after the stroke. Our finding shows that by tuning the receptive field plasticity to a certain value, the information transfer through the cortex after stroke can be optimized.

A widespread distribution of neuronal activity can generate higher-order stochastic interactions. In this case, pair-wise correlations do not uniquely determine synchronizing spiking in a population of neurons, and higher order interactions across neurons cannot be disregarded. We present a new statistical approach, using the information geometry framework, for analyzing the probability density function (PDF) of spike firing patterns by considering higher order correlations in a neuronal pool. In chapter VI, we have studied the limit of a large population of neurons and associated a deformation parameter to the higher order correlations in the PDF. We have also performed an analytical estimation of the Fisher information in order to evaluate the implications of higher order correlations between spikes on information transmission. This leads to a new procedure to study higher order stochastic interactions.

The overall findings of this thesis warn about making any extensive statement about the role of neuronal spike correlations without considering the general case inclusive of higher order correlations, and suggest a need to reshape the current debate about the role of spike correlations across neurons.

2. IS THE POOLING OF SENSORY INFORMATION ACROSS NEURONS AN EFFICIENT MECHANISM FOR DECODING?

Pooling spikes across neurons constitute a simple solution to the decoding of neuronal activity in population of neurons. Nearby neurons in the visual cortex often partially synchronize their spiking activity. Despite the widespread observation of this phenomenon, its importance for visual coding and perception remains to be uncovered. In this chapter we took advantage of recent advances in entropy estimation techniques, using them in the context of the Information Theory to study the coding of the contrast and direction of motion of visual stimuli by pairs of simultaneously recorded neurons in the macaque primary visual cortex. Our findings show that destroying the identity of which neuron fired which action potential resulted in a substantial loss in information about stimulus direction. Nonlinear dendritic summation would appear to be a necessary feature of a decoder capable of making use of the additional information contribution, and thus circumventing the pooling limit.

2.1 Introduction

An important problem in neuroscience is to understand how psycho-physical performance can be related to the signaling of single sensory neurons. It has been thought for instance that combining signals across a pool of neurons can generate superior psychophysical sensitivity if the noise carried by individual members of the pool is averaged out. This eventual benefit of the pooling would be only achievable to the extent that the noise carried by individual neurons is independent.

The implications of accounting interneuronal correlations would place limits on the effectiveness of signal pooling (Johnson et. al. 1973; Johnson 1980; Parker and Newsome 1998). All the beneficial effects of the pooling would be diminished even by the presence of a very weak

correlation (Zohary et. al. 1994; Shadlen et. al. 1996).

Neuronal spike trains fired by adjacent cortical neurons exhibit correlations: the probability of one cell firing an action potential depends upon whether another cell fires (Mastrorade1983; Gawne 1993; Zohary et. al. 1994; Kreiter and Singer 1996b; De Oliveira et. al. 1997, Maldonado 2000). What would therefore be the ultimate role of interneuronal correlation in the processing of sensory information considering they might reduce the effectiveness of the signal pooling? Correlations would be a detrimental factor for perception. The beneficial effects of pooling would be curtailed, rendering to a more plausible mechanism the use of the sensitivity of single neurons to psychophysical decisions (Zohary et. al. 1994).

The spike count correlations are typically used to characterize correlations between repeatedly trial-to-trial fluctuations in response strength. They interfere with pooling as a strategy to overcome response variability in a population rate code (Zohary et. al. 1994; Shadlen and Newsome 1998). In the visual system, spike count correlation is either assumed (Gawne 1993; Gawne et. al. 1996; Reich et. al. 2001) or known to be stimulus independent (Zohary et. al. 1994; Bair et. al. 2001), suggesting that it arises from variations in the state of the cortical network unrelated to the input provided.

Correlations in response profiles of individual signal across different stimuli are called "signal correlation" because they are entirely attributable to stimulus selectivity. On the other hand, correlations which are manifested as covariation of the trial-by-trial fluctuation around the mean response to the stimulus are named "noise correlations". These covariations are observed at fixed stimulus, and they are not attributable to the stimulus (this will be discussed further in Chapter III, in the framework of the Information breakdown method).

Recently, (Kohn and Smith 2005) have measured the spike correlation count between single V1 neurons during spontaneous activity and for activity evoked by stimuli of different orientations and contrasts. Changing stimulus orientation will likely alter the pool of cortical neurons that provides input to the recorded pair, with the predicted effect on correlation depending on the architecture of V1. This is, if the dominant input to V1 cells is feed-forward, correlation should be orientation independent. But, if recurrent connections predominate, correlation could be sensitive to orientation (Ben-Yishai et. al. 1995).

Figure 2.1 shows the orientation tuning and range of orientations (thick line) used to measure correlation for an example pair. Figure 2.1 B-E shows how many standard deviations away

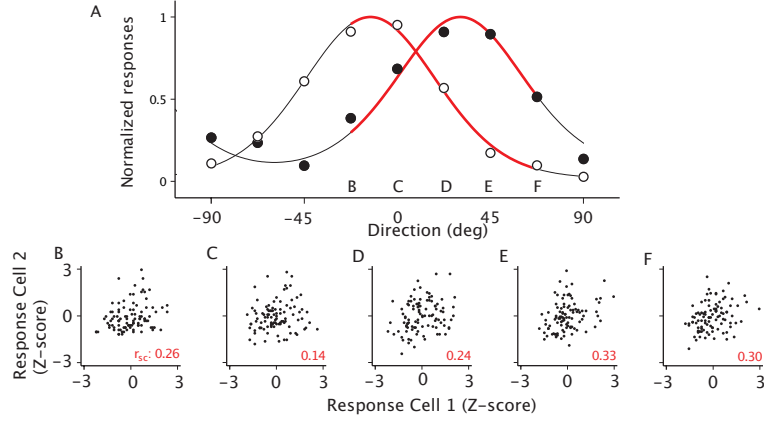


Fig. 2.1: Tuning curves for two V1 neurons. B-F, Scatter plots of responses of V1 pair to 100 presentations of each stimulus show independence of spike count correlation and orientation (modified Figure from Kohn and Smith 2005)

from the mean response for each stimulus are present for each of these observations. The the Pearson correlation coefficient of the evoked spikecounts of two cells to the repeated presentation of a particular stimulus, r_{sc} , is calculated as follows: $r_{sc} = \frac{E[N_1 N_2] - E[N_1] E[N_2]}{\sigma_{N_1} \sigma_{N_2}}$, where E is the expected value, σ is the SD (standard deviation) of the responses, and N_1 and N_2 are the spike counts of cell 1 and 2, respectively. Statistical evaluation is performed after converting r_{sc} to Z-scores using the Fisher transformation as follows: $z = \frac{1}{2} \ln\left(\frac{1+r_{sc}}{1-r_{sc}}\right)$. The values of the spike correlation count do not depend on the stimulus orientation or the evoked firing rate.

Figure 2.2 shows frequency histograms for spike count correlation in the population of pairs, arranged for each pair from the orientation (contrast) that was most effective at driving the two cells to which was least effective. The results suggests that the relationship between the efficacy of an oriented (contrast) stimulus and the correlation in trial-to-trial variability of evoked spike count is small, and therefore this variability arises from orientation-independent (contrast-independent) variations in trial-to-trial cortical excitability. According to von der Malsburg, binding of features belonging to one object is represented by synchronous neural discharges. These results show that spike count correlations do not merely reflect the fixed anatomical connectivity. Moreover, they do not show any kind of evidence against the original von der Malsburg's binding hypothesis (Von der Malsburg 1981).

Spike synchrony is usually identified as a peak centered on zero time lag in the cross cor-

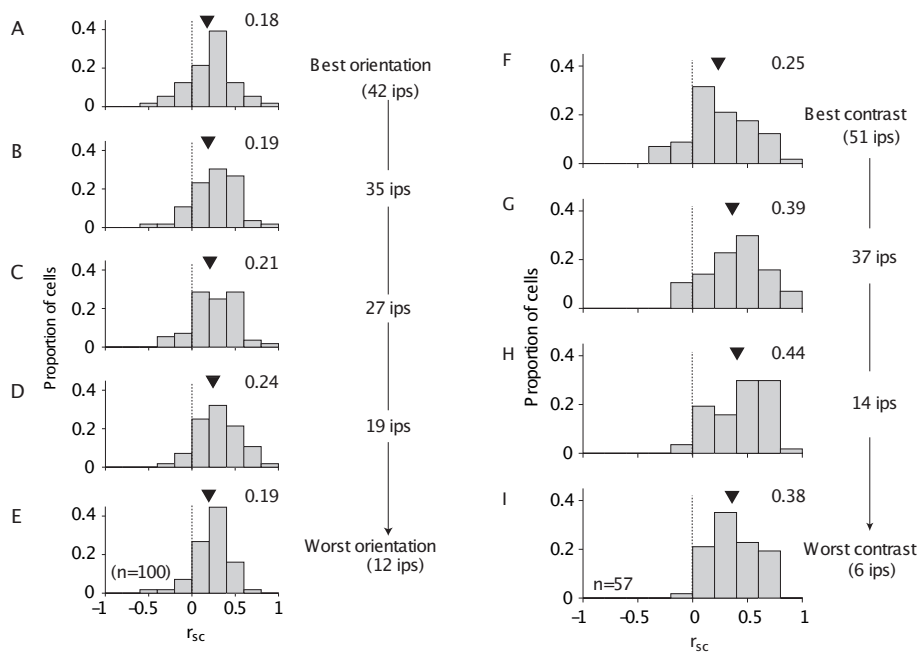


Fig. 2.2: Relationship between firing rate and spike count correlation r_{sc} for stimuli of different orientations (contrast). There are not significant differences between the Population histograms at different orientations (contrast). Modified Figure from Kohn and Smith 2005

relograms. Neurons can covary their discharge for many reasons, and the simplest of these is spike timing covariation. This is, a tendency unrelated to firing rate for the two neurons to discharge at the same time corresponds to the common understanding and to our use of the term synchrony. But factors other than synchrony can and do create peaks in cross-correlograms and many of these certainly contribute to many reported cases of correlated firing. Shuffle correction techniques are used to remove components from correlograms that are due to events that cause the same spike rate modulation on every repetition of an experiment, time-locked to some measurable event like the onset of a visual stimulus.

Indirect measures of synchrony also have been shown to depend on basic stimulus parameters such as orientation and speed (Gray et. al. 1997; Friedman-Hill et. al. 2000; Frien et. al. 2000). How would synchrony between single neurons in primary visual cortex (V1) be affected by such basic stimulus manipulations as orientation and contrast ? Changing stimulus in orientation and contrast will modify the magnitude of the response of the pool, allowing to compare the relative influence of sensory drive and ongoing cortical activity on correlation. This would allow us to test how correlations might possibly act as an extra channel for information (Gray 1999; De Charms et. al. 1996; Panzeri et. al. 1999). If there is not such dependency on the stimulus dependent synchronization, then pairs of cells with overlapping tuning properties will tend to interact redundantly (Panzeri et. al. 1999). This would limit the number of neurons which could be pooled together for perception and all the hypothetical beneficial effects of pooling would be curtailed (Zohary et. al. 1994).

Several pieces of evidence point to correlations between V1 neurons being direction and contrast dependent (Kohn and Smith 2005; Samonds and Bonds 2005). Kohn and Smith have found that correlated responsivity arises from mechanisms operating at two distinct timescales. The first mechanism is the orientation tuning, which determines the strength of temporally precise synchrony. The second is the contrast sensitivity: low-contrast stimuli results in stronger overall correlation but on a broad time scale, and high-contrast stimuli leads to sharper synchronization (Kohn and Smith 2005).

In this chapter we present in detail the first part of a reanalysis performed over Kohn and Smith experimental data set (Kohn and Smith 2005). This analysis form part of the first work conducted in collaboration with Kohn and Smith (Montani et. al. 2007a). The question we are focusing is whether or not the stimulus dependence of this correlation

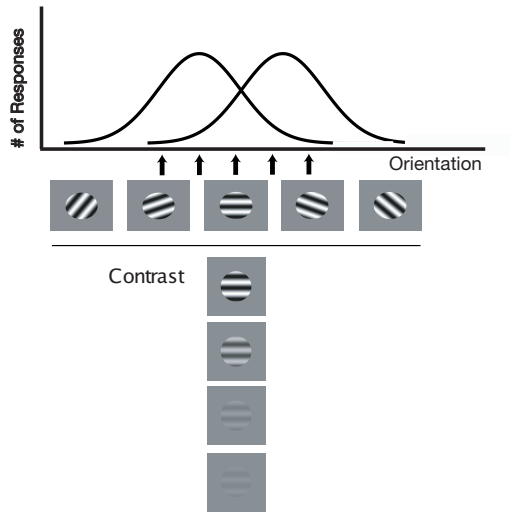


Fig. 2.3: Schematic illustration of the determination of the preferred orientation (contrast) by using five full contrast grating stimuli, and for a given pair of cells in V1. For simplicity the tuning curves of this pairs of cells are represented in this illustration by the two Gaussian functions. The two highest responses would correspond to the preferred orientation of each cell.

affects the limits correlation imposes upon information transmission (Zohary et. al. 1994; Panzeri et. al. 1999).

We used information theory in order to address this question (Montani et. al. 2007a). Mutual information was computed using the NSB estimator (Nemenman et. al. 2004), which will be presented below, and compared the information available from pairs of cells with the sum of the single cell information values. This allowed us to assess the degree of synergy (or conversely redundancy) in the coding. We have used information theory to examine whether stimulus-dependent correlation could contribute to the neural coding of orientation and contrast by pairs of V1 cells.

2.2 Methods

To evaluate the effect of correlation on the population coding of sensory information responses of pairs of single neurons in primary visual cortex (V1) of the anaesthetised macaque monkey were recorded (Kohn and Smith 2005). Stimuli were luminance-modulated, drifting sine-

wave gratings presented at a frame rate of 100 Hz. There were measured, in order, the direction, spatial and temporal frequency, and size tuning for drifting sine-wave gratings (Kohn and Smith 2005). After characterising the stimulus preference (see Figure 2.3) for each cell independently, the correlation for responses evoked by stimuli of different directions and contrasts was measured (Kohn and Smith 2005).

The spatial and temporal frequency of these test stimuli were set between the preferred values of the two cells or at the value of the cell that responded less vigorously. Stimuli were presented between the receptive field (RF) centers of the cells and covered both RFs (Kohn and Smith 2005).

2.3 *Experimental Procedures*

Recordings were made by Kohn and Smith (Kohn and Smith, 2005) in 10 cynomolgus (*Macaca fascicularis*), one bonnet (*Macaca radiata*), and one pig-tailed (*Macaca nemestrina*) adult male monkeys. All experimental procedures were approved by the New York University Animal Welfare Committee. A very precise description of the experimental methods can be found in the original paper (Kohn and Smith 2005).

2.3.1 *Visual stimuli*

After characterizing the stimulus preference of each cell independently, the correlation for spontaneous activity and for responses evoked by stimuli of different orientations and contrasts was measured (Kohn and Smith 2005). The spatial and temporal frequency of these test stimuli were set between the preferred values of the two cells or at the value of the cell that responded less vigorously. Stimuli were presented between the receptive field (RF) centers of the cells and covered both RFs. All measurements were made using stimuli presented in a circular aperture to the dominant eye of the less responsive cell. Stimuli were surrounded by a gray field of average luminance.

Receptive fields were initially mapped by hand on a tangent screen, the position and the dimensions of the receptive field being qualitatively determined by listening to the discharge

on the audio monitor (Kohn and Smith 2005). The nonpreferred eye was then occluded and a front-surface mirror was used to center the receptive field on the monitor. After a brief qualitative determination of the preferred orientation, spatial frequency, and temporal frequency, quantitative assessment of tuning characteristics commenced under computer control.

Direction and contrast experiments were performed in separate blocks of trials. Within most (90 %) of these experiments, the presentation order of each direction or contrast was block randomized. In the direction experiments, they presented full-contrast gratings drifting in five distinct directions, spanning the range between evoking a weak response and driving both cells strongly. In the contrast experiments, the direction was fixed to that most effective at driving the pair of cells, and the stimulus were presented at four contrasts, typically 1.56, 6.25, 25 and 100 % (Kohn and Smith 2005).

For cells with low contrast sensitivity, the range of contrasts was adjusted to extend it from 12.5 to 100 % in octave steps. Stimuli lasted for 2.56 sec with a 3 sec inter-stimulus interval, and were showed on an isoluminant gray screen. Each stimulus was presented 30-200 times. However, for the purposes of the information calculations (see below), these stimuli were broken into individual cycles of the drifting grating, and thus a much greater number of experimental trials (480 to 3200, mean 1300) were available for the purposes of information estimation.

2.4 Theoretical Procedures

Spike count covariance and fine timescale synchrony were previously found to depend on both stimulus orientation and contrast (Kohn and Smith 2005). To examine whether this stimulus-dependent correlation could contribute to the neural coding of stimulus parameters by pairs of V1 cells, we computed Shannon mutual information using the NSB estimator (Nemenman et. al. 2004), and compared the ensemble information available from the pair of cells ($I_{ensemble}$) with the sum of the single cell information values (I_{sum}). This allowed us to assess the degree of synergy (or conversely redundancy) in the coding. Responses were quantified by the number of spikes fired by each cell in the pair within a time window T ; for a pair of cells, this thus provides a multinomial response code with cardinality $K =$

$(n_{max,1} + 1)(n_{max,2} + 1)$ where $n_{max,i}$ is the maximum number of spikes fired by cell i of the pair for any trial or stimulus.

Our information theory analysis has been performed, by considering each cycle to be one experimental trial. Information was calculated from response bins with fixed time window lengths (which were integral fractions of the cycle length T , i.e. $T, T/2, T/4$ etc). The information in each such bin (relative to the start of the cycle) was calculated, collecting trials across stimulus cycles, and then finally the information results were averaged across the time windows within the cycle. Note that some (simple V1) cells were cycle-modulated; for such cells, the results should be taken to be average information estimates, which should not affect conclusions with regard to the relative effect of correlations.

2.4.1 Entropy estimators

In this section we will review some of the basic problems of entropy and mutual information estimations for discrete variables and give a brief classification of different approaches to the problem.

It is well known that the naive or “plugin” estimator of entropy tends to underestimate it (it is biased). This can be understood in the framework of the Jensen inequality (Cover and Thomas 1991). The entropy is a concave function and therefore a “plugin” estimator of entropy tends to underestimate the real value of the entropy (a rigorous proof of this statement can be found in Paninski 2003). The usual approach has been to attempt to avoid this by the use of a perturbative expansion in the asymptotic regime (Panzeri and Treves 1996). An alternative idea, that of calculating entropy by counting coincidences, was proposed a long time ago by Ma for physical systems in the micro-canonical ensemble, where a uniform distribution of entropy corresponds to states of fixed energy (Ma 1981). In a neuroscience context, this would correspond to the assumption that the probability distribution of response words at a fixed spike count is close to uniform (Strong et. al. 1998a; Schultz and Panzeri 2001). The Bayesian approach proposed by Nemenman, Shafee and Bialek (2002), building upon ideas formulated by (Wolpert and Wolf 1995) and (Samengo 2002), extends this idea to arbitrarily complex distributions. The goal of the NSB method is to construct a Bayesian prior which generates a nearly uniform distribution of entropies in order to correct sample size dependent bias at its source.

In the following we are going to review the basic ideas of the NSB entropy estimator method (Nemenman et. al. 2004), and we will compare the effectiveness of NSB in comparison with the computation of the entropy via the naive “plugin” approach, and by using a sophisticated analytical method for correcting bias (Panzeri and Treves 1996).

Consider the problem of estimating the Shannon entropy for a given probability distribution $\mathbf{p} = \{p_i\}$,

$$H = - \sum_{i=1}^K p_i \log_2 p_i \quad (2.1)$$

where the index i runs over K possibilities. For instance, \mathbf{p} might be the distribution of spike counts observed to be fired by a neuron – in which case i would represent “number of spikes + 1” (as zero spikes fired is also a possible response). Consider N samples (trials) which were obtained from a given experiment, where each possibility i occurred n_i times: if N is much bigger than K we can approximate $p_i \approx f_i = n_i/N$, and therefore the entropy can be expressed in terms of the observed frequencies as

$$H_{naive} = - \sum_{i=1}^K f_i \log f_i \quad (2.2)$$

The problem is that this “plugin” approach tends to underestimate the entropy. Several attempts to solve this problem were made by (Carlton 1969), who made asymptotic bias corrections by adding a term of order $O(K/N)$. This approach was developed further by (Panzeri and Treves 1996), and amounts to (in brief)

$$H = H_{naive} + Bias[H(R)] \quad (2.3)$$

where

$$Bias[H(R)] \approx - \frac{1}{2N \ln 2} \sum_s \hat{R}_s \quad (2.4)$$

and \hat{R}_s denotes the number of relevant bins for for a trial with stimulus s , i.e. the response bins in which the occupancy probability $p(i|s)$ (at given s) is non-zero. Note that if a bin is observed never to be occupied, it is ambiguous whether that is because it has a true zero occupancy probability, or because responses simply have not been observed for long enough. Choice of \hat{R}_s is a subtle issue, and is to some extent dependent upon data characteristics. (Panzeri and Treves 1996) made use of a Bayesian prior for the number of relevant bins, and iteratively re-estimated it. This procedure has been found to be effective for a number of types of single-unit electrophysiology data (e.g. Panzeri and Schultz 2001a; Rust et. al. 2002), but after much detailed analysis, we found its performance to be inadequate for the analysis of many of the pairs in the V1 dataset, despite the relatively large number of trials available (480-3200) compared to many other information theoretic analyses in the literature. This is, an adequate sampling was obtained with NSB at as low as 100 trials, but this was not the case with other entropy estimators.

Several approaches for estimating entropies without using such an asymptotic expansion approach have recently been presented (Nemenman et. al. 2004; Paninski 2003). We will follow the approach of Nemenman et al.

Recall our examination of the probability distribution \mathbf{p} from equation (2.2). Bayes' rule tells us that we can express the posterior probability of \mathbf{p} ($\equiv \{p_i\}$, $i = 1..K$ discrete random variable), given that we have just observed i to have occurred n_i times.

$$P(p|n_i) = \frac{P(n_i|p)P(p)}{P(n_i)} \quad (2.5)$$

Note that the number of times we observe each response value i to occur must add up to the total number of experimental trials N .

$$\sum_{i=1}^K n_i = N \quad (2.6)$$

In equation (2.5), the “prior” distribution is $P(\mathbf{p})$ – in principle, we could choose a prior such that our estimator of the entropy of $P(\mathbf{p})$ does not depend upon the number of trials. This is obviously a desirable quality! To do this, we can express $P(\mathbf{p})$ in terms of the Dirichlet

family of priors (Nemenman et. al. 2004). This should allow us to construct a prior which does not depend on inverse powers of N (which even the naive approximation does implicitly, as $f_i = n_i/N$). The Dirichlet family are characterised by a parameter β ; they can be written as

$$P_\beta(\mathbf{p}) = \frac{1}{Z} \delta(1 - \sum_{i=1}^K p_i) \prod_{i=1}^K p_i^{\beta-1} \quad (2.7)$$

where

$$Z = \frac{\Gamma^K(\beta)}{\Gamma(K\beta)} \quad (2.8)$$

δ and Z are functions which enforce the normalization of \mathbf{p} and P_β respectively (δ being the Dirac delta function, and Γ stands for Eulers Γ function). Maximum likelihood estimation corresponds to Bayesian estimation with this prior in the limit $\beta \rightarrow 0$, while a uniform prior is implemented by $\beta = 1$. (Nemenman et. al. 2002) observed that fixing a particular value of β (and thus fixing the prior) specifies the entropy almost exactly. For an ‘‘incorrect’’ prior, the estimate of entropy is thus dominated by the prior, rather than determined by our actual knowledge – that is to say, it is biased.

Ideally, we would like to compute the whole *a priori* distribution of entropies

$$P_\beta(H) = \int dp_1 dp_2 \dots dp_K P_\beta(\{p_i\}) \delta(H + \sum_{i=1}^K p_i \log_2 p_i) \quad (2.9)$$

But this is quite difficult to achieve. In order to get an entropy estimate with small bias one could simply fix a flat prior distribution of entropy $P(H)$. One way of doing so is by defining

$$P(H) = 1 = \int \delta(H - \xi) d\xi \quad (2.10)$$

where ξ is the expected entropy. If we could find a family of priors $P_\beta(\mathbf{p})$ which result in δ functions over H , and if by changing β we move the peak across the whole range of

entropies uniformly, then we will effectively be choosing the proper prior for each entropy. We will thus come close to the objective of removing bias at its source. Because the entropy of distributions chosen for P_β is sharply defined and monotonically dependent on the parameter β we can effect this goal by averaging over β . The main idea of the NSB approach is thus to construct a prior

$$P_\beta(p) = \frac{1}{Z} \delta(1 - \sum_{i=1}^K p_i) \prod_{i=1}^K p_i^{\beta-1} \frac{d\xi(\beta)}{d\beta} P(\beta) \quad (2.11)$$

which will perform this task even when N is small. In this equation Z is again a normalizing coefficient and $\frac{d\xi(\beta)}{d\beta}$ ensures the uniformity for *a priori* expected entropy ξ .

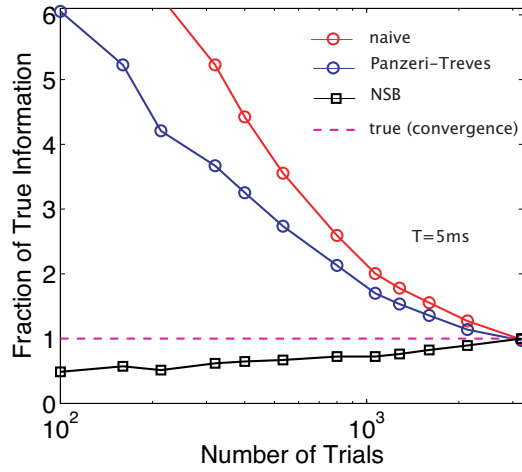
This Dirichlet priors allow all the K dimensional integrals to be calculated analytically (see Wolpert and Wolf 1995, giving for the moments of the entropy

$$(H^{NSB})^m = \frac{\int d\xi \rho(\xi, \mathbf{n}) \langle H^m(\mathbf{n}) \rangle_{\beta(\xi)}}{\int d\xi \rho(\xi, \mathbf{n})} \quad (2.12)$$

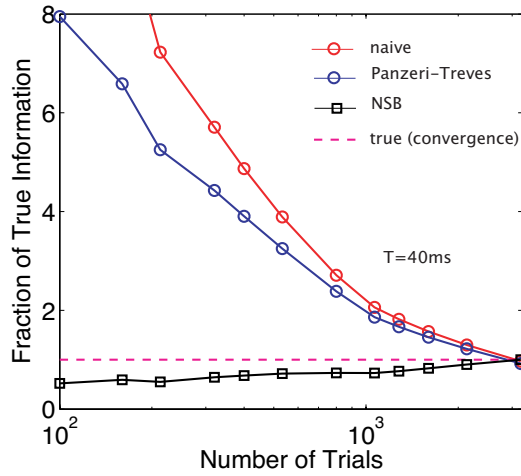
where $\mathbf{n}=\{n_i\}$, and $m=1,2$ correspond to the entropy and its second moment. $\langle H^m[n_i] \rangle_{\beta(\xi)}$ is the expectation value of the m^{th} entropy moment at a fixed β (Wolpert and Wolf 1995) and the posterior density is a function of the proposed Dirichlet prior,

$$\rho(\xi|\mathbf{n}) = P_\beta(\xi) \frac{\Gamma(\kappa(\xi))}{\Gamma(\beta(\xi))} \prod_{i=1}^K \frac{\Gamma(n_i + \beta(\xi))}{\Gamma(\beta(\xi))} \quad (2.13)$$

Summarizing, the main idea of NSB is to construct a Bayesian prior, which generates a nearly uniform distribution of entropies in order to avoid bias at its origin. These results were obtained by (Nemenman et. al. 2002; Nemenman et. al. 2004); we have tried here to give, in as simplistic terms as possible, an explanation of how the method works. We will now illustrate the performance of the method with an example.



A



B

Fig. 2.4: Relative performance of several information estimators. Two different time windows were chosen for counting spikes: **A** 5ms, resulting in cardinality $K = 10$ from the ensemble responses. **B** 40 ms, cardinality $K = 76$.

2.4.2 Example: Information available for a single pair of neurons

In order to test the effectiveness of the entropy estimator developed by (Nemenman et. al. 2004), we performed calculations of the total mutual information conveyed by a single pair of cells in V1 (Kohn and Smith 2005) using the naive estimator, using the Panzeri-Treves bias correction, and using the NSB method. Figure 2.4 shows the total information estimated through these different approaches. The ensemble (pair) mutual information was calculated using different subsets of the total available number of trials, which *in this case* was sufficient for all methods to converge to the same asymptote, which we can consider to be the true information. The results speak for themselves.

The NSB approach was the only one we found to be adequate across the entire dataset, despite the relatively large number of trials available (480-3200) compared to many other information theoretic analysis in the literature. Note that this was a particularly (although not entirely unusual) hard to sample pair of cells; for some other pairs, adequate sampling was obtained by NSB at as low as 100 trials.

2.4.3 Numerical Implementation

It can be found online two different implementations of the NSB method available from the authors <http://nsb-entropy.sourceforge.net/>. We have converted the Octave code to a MatLab compatible version. The source code of implementation are in C++ and MatLab/Octave.

NSB requires a substantial amount of numerical integration and function inversion. The Matlab version is pretty basic in its functionality, works cross-platform, but this version has the inability of MatLab to index discrete structures that can exist in a space with cardinality of more than 2^{32} . The C++ code is faster.

2.5 Direction Coding

2.5.1 Spike train cross-correlograms (CCGs)

The timing of action potentials between nearby neurons is often correlated or synchronized, as shown by a peak in the spike train cross-correlogram (CCG) (Figure 2.5). To compute the CCGs, the spike train of each cell is represented as a binary time series with 1 ms resolution such that:

$x_j^i(t) = 1$, if on trial i neuron j fired an action potential during the t^{th} millisecond

$x_j^i(t) = 0$, otherwise

The CCGs are computed as follows:

$$CCG(\tau) = \frac{\frac{1}{M} \sum_{i=1}^M \sum_{t=1}^N x_1^i(t) x_2^i(t + \tau)}{\theta(\tau) \sqrt{\lambda_1 \lambda_2}} \quad (2.14)$$

where M is the number of trials, N is the number of bins in the trial, x_1^i and x_2^i are the spike trains of neurons 1 and 2 on trial i , τ is the time lag, and λ_1 and λ_2 are the mean firing rates of the two cells. $\theta(\tau)$ is the following triangular function:

$$\theta(\tau) = T - |\tau|$$

where T is the trial duration in seconds. This function corrects for the degree of overlap of the two spike trains for each time lag (i.e., that there are T opportunities for simultaneous events in a trial of length T but only $T - 1$ opportunities for coincidences at time lags of 1 ms, etc).

All CCGs were corrected for correlation induced by the stimulus, subtracting a shift predictor calculated from trials 1 to $n - 1$, with an offset of one trial. Specifically, the shift predictor was calculated as,

$$SHIFT(\tau) = \frac{1}{M - 1} \sum_{i=1}^{M-1} \sum_{t=1}^N x_1^i(t) x_2^{i+1}(t + \tau) \quad (2.15)$$

It is used a shift predictor rather than an all-way shuffle correction, because the latter is

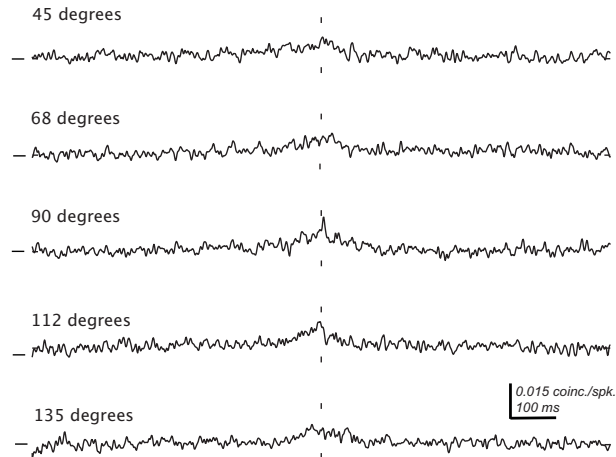


Fig. 2.5: Cross-correlograms for each of five different stimulus directions, for the same pair as shown in the previous figures.

affected more strongly by slow fluctuations in neuronal responsivity. In cells for which the firing rate displayed strong temporal modulation (i.e., simple cells), shuffle correction occasionally resulted in artifactual peaks in the CCG caused by bleed through this modulation. Shift correction effectively reduced the presence of these relatively rare artifactual peaks but otherwise resulted in CCGs that were essentially identical to those obtained with shuffle correction.

The CCGs are normalized by the geometric mean spike rate which is the most common used normalization, it facilitates therefore comparison with previous studies (Mastronarde1983; Bair et. al. 2001). This normalization provides also results which are most comparable with measures of spike count correlation (Kohn and Smith 2005).

Figure 2.5 shows a typical pair of V1 cells (the same pair used in Fig. 2.4) with substantial modulation in the height of the central peak of the cross-correlogram of the neurons spike trains: synchronization is maximised at a particular direction that drives the firing of both neurons, and falls off around this stimulus.

2.5.2 Mutual Information

We introduce in this section an Information Theoretical analysis of 102 pairs from the original dataset of (Kohn and Smith 2005). This is we have chosen a subset of 102 pairs of cells,

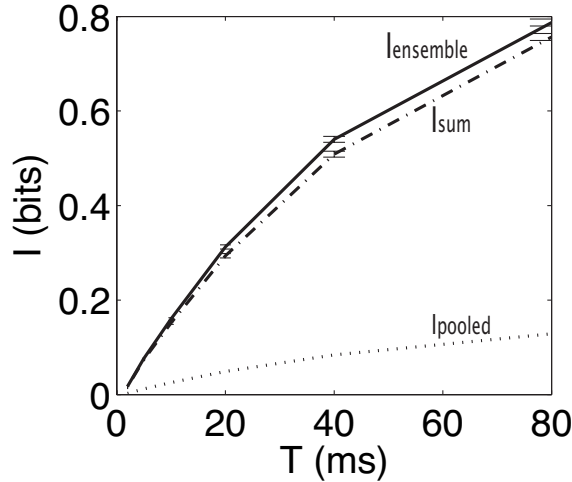


Fig. 2.6: Comparison of the information available from the pair of neurons ($I_{ensemble}$) in a time window T , with the sum of the informations obtained from each constituent neuron (I_{sum}) and the information from a pooled code in which the identity of the cell firing each action potential is ignored (I_{pooled}).

from the original data set with 104 pairs, with had the higher number of trials in order to make trustable our Information analysis. We will refer as "synergy" (redundancy) when the information conveyed by an ensemble of cells ($I_{ensemble}$) is bigger (smaller) than the sum information conveyed by each independently (I_{sum}). We will name I_{pooled} the information conveyed if spikes are pooled across cells, that is, when the identity of the cells is not taken into account.

What is the effect of this stimulus dependent correlation on the information transmitted by the pair of neurons? This is shown in Figure 2.6: the resulting interaction is very mildly synergistic: the ensemble mutual information ($I_{ensemble}$) grows more rapidly with the time window over which spikes are counted than the sum of the single cell information values (I_{sum}) does. Figure 2.6 also shows that pooling spikes across cells (I_{pooled}) leads to a drop in information (see Section 2.7).

We analyzed the degree of synergy (redundancy) of direction coding at a fixed time window of 40 ms, for 102 pairs of cells in V1. The fractional degree of synergy (defined as $1 - I_{sum}/I_{ensemble}$) was on average $to - 0.02352 \pm 0.005$ (s.e.m.).

An alternative measure is the redundancy index which based on information rates

(Reich et. al. 2001). The definition of synergy adopted here is essentially the same as the definition adopted by (Gawne 1993).

Our findings (Figure 2.7) lead to the conclusion that information about direction essentially summates across pairs of neurons as it would if the neurons were actually independent, although they are substantially correlated. This is an example of *informational independence*, even though there is substantial *response dependence* (Schneidman et. al. 2003) between these cells.

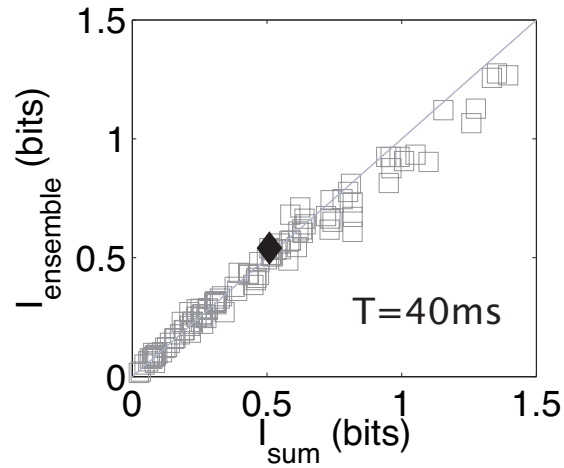
2.6 Contrast Coding

In the previous section we studied the coding of information about visual stimulus direction by pairs of neurons motivated by the directional dependence of response synchronization. However, the contrast of the stimulus can also modulate the synchronization between pairs of neurons (Kohn and Smith 2005). Cross correlograms (CCGs) provides insights into the temporal structure of responses by using different sinusoidal grating contrast stimuli, whereas Mutual Information estimations can provide insights not only into the the temporal structure of responses but also into the degree to which information about contrast stimuli is encoded at different time windows.

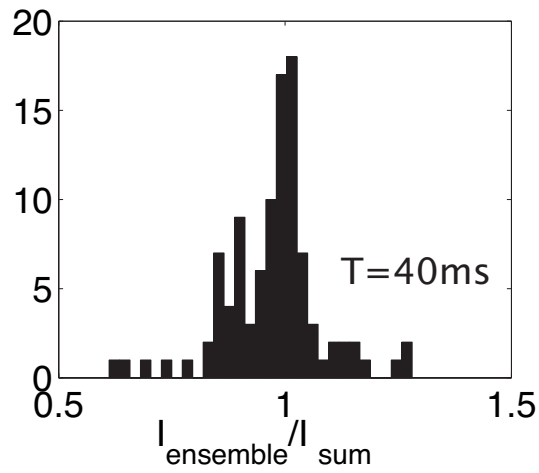
Figure 2.8 shows that reducing stimulus contrast reduces the temporal precision of synchronous firing, but enhances the correlated response variability on longer time scales. We analyse the degree of synergy (or rather redundancy) for the neural coding of contrast by a somewhat stereotypical V1 pair. Figure 2.9 shows the picture over the entire population of 71 pairs for which contrast data were available. In almost all cases ($17.24 \pm 0.2\%$) redundancy was observed.

Our findings indicate that the different stimuli responses convey redundant information about contrast, despite the presence of significant correlation as it is showed in Figure 2.8 . However, since nearby neurons in V1 are tuned to similar stimulus features, it is reasonable to expect significant redundancy in the contrast coding.

Sensory redundancy is important because knowledge of regularities in the environment is advantageous for many purposes, such as making predictions. Redundancy can be a measure



A



B

Fig. 2.7: Information adds approximately linearly across cells. **A** The total (ensemble) information available for each pair is plotted against the sum of the information available from each cell constituting the pair ($n=102$ pairs). Redundant points lie below the diagonal. The black diamond indicates the pair shown in Figures 1-3. **B** Histogram of the total (ensemble) information available for each pair divided by the sum of the information from each cell.

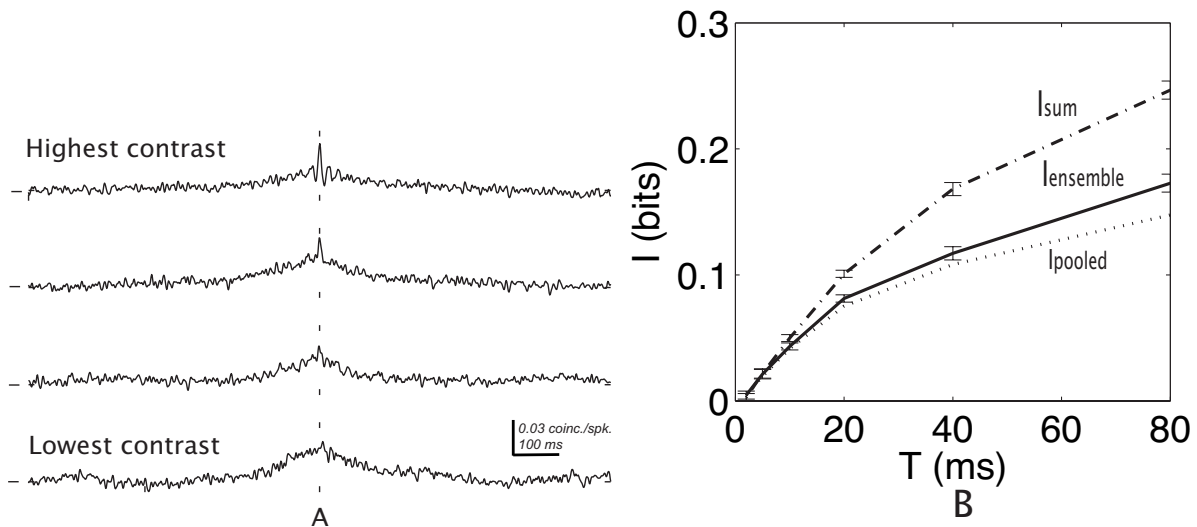


Fig. 2.8: Coding of contrast by a stereotypical pair of V1 neurons. **A** Cross-correlograms for each of 4 contrast values. **B** Information analysis results.

of any kind of statistical regularities. It can be important for learning, inductive inference, and the information-processing in the brain might help to survival by exploiting it.

2.7 Pooling

Most studies of neural coding have addressed the problem of how neurons encode sensory events. However, the brain also faces the complementary problem that of decoding: given the activity in a certain population of cells, what was the sensory event that evoked it? In practice, decoding must occur for the successful transmission of information from one group of neurons to a second group. Consider a target population which receives input from a set of neurons with widely disparate tuning properties. To conserve all sensory information during synaptic transmission, the target neuron must conserve the "label" of the spikes arriving from multiple input neurons at different places on its dendritic tree.

A simple solution to the decoding problem has been proposed, namely pooling (Darian-Smith et. al. 1973). Pooling (summing spikes together from a neuronal pool regardless of the cell which fires them) is a popular population decoding strategy (Shadlen et. al. 1996; Shadlen and Newsome 1998). The idea is that target neurons simply sum up, or pool, the

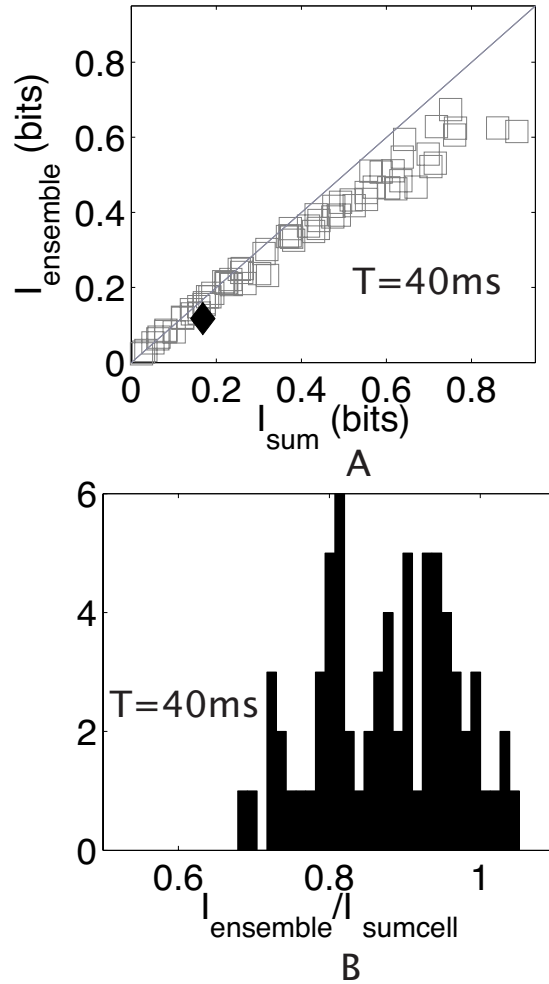


Fig. 2.9: Coding of contrast is substantially redundant across the entire dataset. **A** Comparison of pair and linear summation information values. The black diamond shows the pair considered in the previous figure. **B** Histogram showing the degree of redundancy across the dataset.

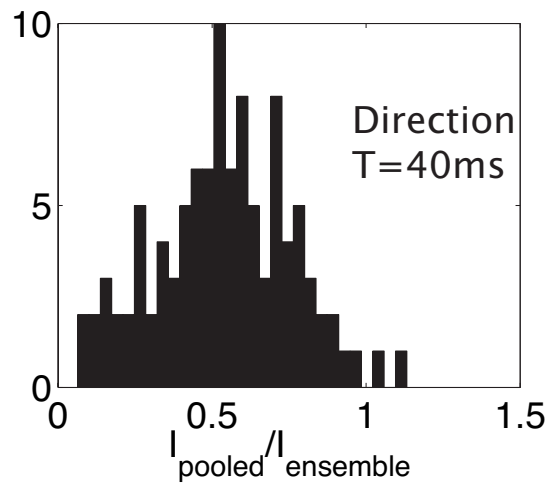
activity of the afferent population. It has been proposed that pooling can lead to a significant improvement in signal reliability, provided that the neurons being pooled are at most weakly cross-correlated (Darian-Smith et. al. 1973; Zohary et. al. 1994).

However, Figures 2.6 and 2.8 show a loss of information when the "pooled" code was used, although this was much greater for the example of direction coding. How general was this? Figure 2.10 shows that the loss of information due to pooling is generally much greater for direction than for contrast coding. Neural codes that pool spikes across neurons lose a large fraction of the information present in their spike trains. This is due to the loss of information encoded in the neuronal identity of the spikes.

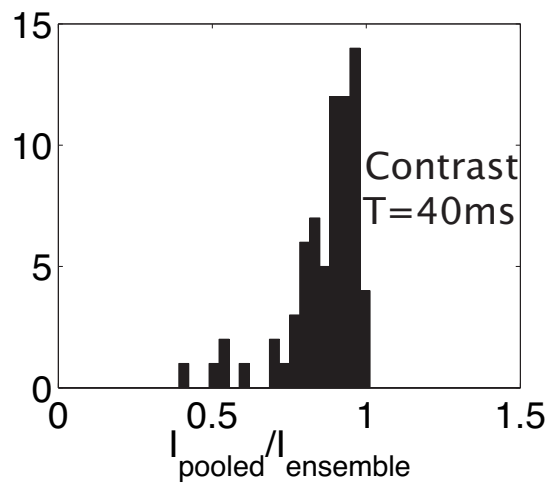
2.8 Discussion

We used information theory in order to understand how correlations between the spikes fired by pairs of V1 neurons contribute to the direction and contrast coding. Our main findings were that at timescales of the order of 40 ms, information about direction adds approximately linearly across pairs of cells, whereas information about contrast adds sub-linearly (redundantly). In both cases the responses covary (due to the synchronization), so the neurons are response-independent, but in the first case the neurons are informationally independent also (or approximately so), but in the second case the neurons code redundantly. What is the explanation for this?

The neurons generally (although not always) have a substantial overlap in their direction tuning curves (i.e. positive signal correlation), and also have positive noise correlation due to fine-timescale synchronization of their responses. Information-theoretic analysis predicts that in this regime, if the noise correlation is not stimulus-dependent, then the neurons will interact redundantly (Panzeri et. al. 1999; Panzeri and Schultz 2001a). If the synchronization is instead stimulus-dependent (as we see here), there is in addition an "extra channel" of information, which makes the stimuli easier to discriminate by an ideal decoder (which takes correlation into account) and makes up for the information lost due to redundancy. This effect can be further analysed in terms of an information component breakdown (Pola et. al. 2003; Montani et. al. 2007b), which is going to be presented in the next chapter.



A



B

Fig. 2.10: The effect of pooling (ignoring the identity of the cell which fired each spike train) is a substantial loss of information. **A** Direction coding. **B** Contrast coding.

The contrast dataset provides us with a natural control for the direction coding analysis. This is, in the contrast data set, the tuning curves of different neurons in a pair tend to be fairly similar, and synchronization is at lower contrasts less temporally precise. This resulted in a coding regime more similar to the traditional intuition, in which correlations tend to result in redundancy, and thus limit the number of neurons whose outputs could usefully be combined to represent the stimulus variable. The major factors driving the differences in contrast and orientation coding are thus the greater redundancy due to similarity in the tuning curves between pairs of cells for contrast coding, and a slightly lower degree of stimulus dependence in the correlation. The brain could take advantage of the robustness provided by the redundancy in contrast, and the accuracy due to the informational independency in the orientation code. These factors have been explored in more detail by performing an information component decomposition (Pola et. al. 2003) and will be presented in the next chapter.

Our results are roughly in line with previous information analyses that have found the existence of weak synergy or independent coding in V1 (Reich et. al. 2001; Kayser et. al. 2004). Their findings show that keeping track of which neurons fire preserves a considerable amount of information already present in the responses. This strategy is of help for removing redundancy across neurons with similar tunings, and prevent a greater information loss from summing responses information with different selectivities. This suggest that codes that use information available of the ensemble are more plausible.

One major difference between this investigation presented here and these previous studies were that we characterized the complete response characteristics of each neuron in the pair, and generated a set of stimuli which, as far as possible, drove both neurons across their dynamic range, and included stimuli which excited both neurons well. There are also substantial differences in the analyzes performed. In our study, we took advantage of recent advances in entropy estimation techniques (Nemenman et. al. 2004). This was crucial to the current study, as despite working well for the analysis of single cell recordings, other estimation techniques resulted in significant residual bias with this paired recordings dataset.

Destroying the identity of which neuron fired which action potential resulted in a substantial loss in information about stimulus direction. This provokes the question: how could down-

stream neurons decode / make use of the positive information contribution provided by the stimulus-dependent synchronization? Integrate-and-fire type neuronal operation would effectively pool input spikes regardless of origin, thus being subject to the (Zohary et. al. 1994) limitations on combining information from correlated input neurons. Nonlinear dendritic summation (Hausser and Mel 2003) would appear to be a necessary feature of a decoder capable of making use of the additional information contribution, and thus circumventing the pooling limit.

However, as complicated as a dendritic tree appears on the surface, it has long been considered that the whole cell functions as a simple one compartment summing unit, where as in an idealized democracy, all synapsis have an equal opportunity to influence neuronal output through the axon (Roddey et. al. 2000). This is, the rule for combining the effect of many synapses under this assumption is generally considered to be linear, and can therefore be expressed as a weighted sum of excitatory and inhibitory synaptic inputs. But, the integrative properties of the dendrites are determined by a complex of mixtures of factors, including their morphology, the spatio-temporal patterns of synaptic inputs, the balance of excitation and inhibition, and neuromodulatory influences, all of which interact with many voltage-gated conductances present in the dendritic membrane.

Linear models can often adequately describe the neural encoding process for weak (i.e., low intensity) sensory stimuli (Roddey et. al. 2000), but neurons are nonlinear (Chacron 2006). An optimal linear decoder for spatially localized stimuli will not capture all of the information in pyramidal cell spike trains, because it only has access to a fraction of the information transmitted by pyramidal cells. Hence, nonlinear decoders are necessary to fully access information in pyramidal cell spike trains. Neurons would perform nonlinear operations on incoming pyramidal cell spike trains to access all the information (Hausser and Mel 2003).

3. THE ROLE OF CORRELATIONS IN ORIENTATION AND CONTRAST CODING IN THE PRIMARY VISUAL CORTEX

The spiking activity of nearby cortical neurons is not independent. Numerous studies have explored the importance of this correlated responsivity for visual coding and perception, often by comparing the information conveyed by pairs of simultaneously recorded neurons with the sum of information provided by the respective individual cells. Pairwise responses typically provide slightly more information, so that encoding is weakly synergistic. The simple comparison between pairwise and summed individual responses conflates several forms of correlation, however, making it impossible to judge the relative importance of synchronous spiking, basic tuning properties, and stimulus (in)dependent correlation. In this chapter we have applied an information theoretic approach to this question, using the responses of pairs of neurons to drifting sinusoidal gratings of different orientations and contrasts, recorded in the primary visual cortex of anesthetized macaque monkeys. Our approach allows us to break down the information provided by pairs of neurons into a number of components. The results we present in this chapter are part of a second work we have carried out in collaboration with Kohn and Smith (Montani et. al. 2007b).

This analysis reveals that although synchrony is prevalent and informative, the additional information it provides is frequently offset by the redundancy arising from the similar tuning properties of the two cells. Thus, coding is roughly independent with weak synergy or redundancy arising depending on the similarity in tuning and the temporal precision of the analysis. We suggest that this would allow cortical circuits to enjoy the stability provided by having similarly tuned neurons without suffering the penalty of redundancy as the associated information transmission deficit is compensated for by stimulus dependent synchrony.

3.1 Introduction

The brain processes sensory information in multiple stages. Information is transmitted by trains of action potentials (spikes) or, less frequently by local field potentials (LFPs). Spikes are brief electrical impulses which travel along the membrane of a cell and are used by neurons to communicate the local output signals. This is, sensory signals from the external world are converted in the cortex into a series of spikes fired by a population of neurons. On the other hand, LFPs are low-frequency ($< 250Hz$) voltage fluctuations measured at the electrode, which account for the sum of dendritic synaptic activity within the volume of the tissue, and represent the local inputs.

The relationship between the spike activities of neurons and the state of the perceived world is of paramount importance for understanding the brain functions. The spiking activity of nearby cortical neurons is not independent, and we need to understand how neurons work together to represent sensory information. A central question in neuroscience is therefore understanding how information about the outside world is carried in neuronal spike trains. Information can be carried in spike rate (Werner and Mountcastle 1965; Tolhurst 1989) spike timing (Panzeri and Schultz 2001a), spike correlations across neurons (Kreiter and Singer 1992; Kreiter et. al. 1996; De Charms et. al. 1996; Roelfsema 1997, Gawne et. al. 1996), or a combination of these. Recently, a great deal of attention has been focused on correlated firing, this the probability of one cell spiking is related to whether other nearby cells fire (Zohary et. al. 1994; Engel et. al. 1990; Kreiter et. al. 1996; Gawne 1993; De Oliveira et. al. 1997; Lebedev et al. 2000; Mastronarde 1983; Ts'o and Gilbert 1988, Maldonado 2000; Bair et. al. 2001).

Whether such correlations affect the coding of sensory information is still highly debated. It has been proposed that correlations might act as an extra channel for information, carrying messages about the outside world not carried by other aspects of spike trains such as the overall firing rate (Gray 1999; Richmond and Gawne 1998; Abbott and Dayan 1999; Panzeri et. al. 1999). Others have proposed that correlation interferes with decoding the information represented by the firing rate of a population of neurons (Zohary et. al. 1994; Shadlen and Newsome 1998; Mazurek et al 2002).

It has been also thought that pair-wise correlations provide a good estimate of the total

amount of synchrony in a pool of neurons from which the recordings are obtained, and that correlations between pair of neuron reflect a high degree of synchronous firing within a larger assembly of neurons (Singer and Gray 1995; Engel et. al. 1992; Schneidman et. al. 2006). Moreover, pairwise correlations between neurons can also have a high temporal precision in the range of a few millisecond (Eckhorn et. al. 1988; Gray-Singer 1989; Roelfsema 1997; Alonso et. al. 1996; Abeles et. al. 1993). And from a different point of view, Von der Malsburg (1981) suggested that assemblies of neurons might convey additional information by firing in synchrony, since synchrony could be instrumental in forming relationships between the members of such assemblies.

Thus, throughout the years the matter of how the coding of sensory information is affected by spike correlations across neurons has been fraught with dissension, and the debate has become polarized into two different postures co-existent in the neuroscientific community. One of the postures, supported by many authors (Nirenberg et. al. 2001; Oram et. al. 1998; Petersen 2001; Levine et. al. 2002; Panzeri et. al. 2002a; Panzeri et. al. 2002b, Averbeck et. al. 2003; Averbeck and Lee 2003; Averbeck and Lee 2004; Golledge et. al. 2003), is that correlations are not important or play a minor role, whereas others have proposed that they are important in the coding of sensory information (Eckhorn et. al. 1988, Gray-Singer 1989; Gray et. al. 1989; Meister 1996; Vaadia et. al. 1995; De Charms et. al. 1996; Dan et. al. 1998; Steinmetz et. al. 2000).

This dissension can be traced to different methods used to asses the role of synchronized spike firing. For instance, one of the most used methods consisted in looking for stimulus-dependent changes in cross-correlograms (Eckhorn et. al. 1988; Gray-Singer 1989, Gray et. al. 1989; Vaadia et. al. 1995; De Charms et. al. 1996). However, the firing rate can alter the shape of cross-correlograms making difficult to separate information carried by firing rates from information carried by correlations. Moreover, cross-correlograms account only for near synchronous spikes. This is, they do not account for correlations which occur on a longer time scale and among patterns of spikes.

Information Theory measures the statistical significance of how neural responses vary with different stimuli. This is, it determines how much information about stimulus parameter values is contained in neural responses. Information Theory measures provide a much more quantitative and sensitive approach to correlations than methods that can only account for

near synchronized spikes. Numerous studies have explored the importance of the correlated responses for visual coding and perception, often by comparing the information conveyed by pairs of simultaneously recorded neurons with the sum of information provided by the respective individual cells (synergy/redundancy).

Unfortunately, information theoretic studies have provided disparate answers. For instance, retinal ganglion cells have been found to encode synergistically (Meister 1996), roughly independently (Nirenberg et. al. 2001), or redundantly (Puchalla et. al. 2005). In the lateral geniculate nucleus, (Dan et. al. 1998) reported synergistic effects. In cortex, most studies have concluded that neurons provide roughly independent information, with some evidence for weak synergy in V1 (Reich et. al. 2001; Golledge et. al. 2003; Kayser et. al. 2004), motor cortex (Averbeck and Lee 2003; Oram et. al. 2001), and somatosensory cortex (Petersen 2001). Given that cortical responses are strongly correlated (Zohary et. al. 1994; Bair et. al. 2001; Reich et. al. 2001) and that this correlation is stimulus dependent (Kohn and Smith 2005; Samonds and Bonds 2005) it is surprising that the information provided by cortical neurons is nearly independent.

Pairwise responses typically provide slightly more information, so that encoding is weakly synergistic. However, the simple comparison between pairwise and summed individual responses conflates several forms of correlations, making it impossible to judge the relative importance of synchronous spiking, basic tuning properties, and stimulus (in)dependent correlation. But, two Information measures have appeared in the literature. One of them, mentioned in paragraph before, aimed at quantifying the role of correlation by measuring synergy/redundancy (Brenner et. al. 2000; Liu et. al. 2001; Machens et. al. 2001, Schneidman et. al. 2003), whereas the other is provided by the information breakdown method (Pola et. al. 2003; Pola et. al. 2005; Montani et. al. 2007b). This measure can be used to understand how information about correlations affect the transformation from stimulus to response.

The results we present in this chapter are part of a second work performed in collaboration with Kohn and Smith (Montani et. al. 2007b). We applied an information theoretic approach for studying the role of correlation in the neuronal code, using the responses of pairs of neurons to drifting sinusoidal gratings of different orientations and contrasts, recorded in the primary visual cortex of anesthetized macaque monkeys. Our approach allowed us

to break down the information provided by pairs of neurons into a number of components. More in detail, we investigated the role of correlation in stimulus encoding in primary visual cortex, with two important extensions over previous studies. First, we used an exact information theoretic method to quantify the information conveyed by different coding mechanisms (Pola et. al. 2003). Second, we have applied this approach to responses evoked in primary visual cortex by stimuli which vary in two distinct ways: drift direction and contrast (Kohn and Smith 2005).

We confirmed that coding is roughly independent despite the presence of substantial correlation, with weak synergy or redundancy arising for particular stimulus manipulations and time scales. We showed that this independence comes about because of a balance between the strong synergy provided by stimulus-dependent correlation and redundancy arising from the similarity in tuning of the neurons. This analysis reveals that although synchrony is prevalent and informative, the additional information it provides is frequently offset by the redundancy arising from the similar tuning properties of the two cells. Thus, coding is roughly independent with weak synergy or redundancy arising depending on the similarity in tuning and the temporal precision of the analysis. Our findings suggest that this would allow cortical circuits to enjoy the stability provided by having similarly tuned neurons without suffering the penalty of redundancy as the associated information transmission deficit is compensated for by stimulus dependent synchrony.

3.2 *Methods*

To characterize the neuronal responses by a given stimuli is indeed very difficult because of the complexity and variability of these responses. Neurons typically respond by producing complex spike sequences that reflect both the intrinsic dynamics of the neuron and the temporal characteristics of the stimulus. Isolating features of the response that encode changes in the stimulus can be difficult, especially if the time scale for these changes is of the same order as the average interval between spikes. Neuronal responses can vary from trial to trial even when the same stimulus is presented repeatedly. There are many potential sources of this variability including variable levels of arousal and attention, randomness associated with various biophysical processes that affect neuronal firing, and the effects of other cognitive processes taking place during a trial.

The complexity and trial-to-trial variability of action potential sequences make it unlikely that we can describe and predict the timing of each spike deterministically. Instead, a complete description of the stochastic relationship between a stimulus and a response would require us to know the probabilities corresponding to every sequence of spikes that can be evoked by the stimulus. That is, the neural responses and their relationship to the stimuli are completely characterized by the probability distribution of spikes times as function of the stimulus. The independent-spike code corresponds to the case in which the generation of each spike is independent of all other spikes in the train. In contrast, if the individual spikes do not encode independently of each other, we call the code a correlation code, because correlations between spikes times may carry additional information. In fact, information is likely to be carried by both individual spikes and through correlations, and some arbitrary dividing line must be established to characterize the code.

Part of the difficulty in understanding population coding is that neurons are noisy and the same pattern of activity never occur twice, even if the same stimulus is presented. Because of this noise, population coding is necessarily probabilistic. One of the prevailing view of neural coding is that the meaningful signal is contained in the mean rate of the action potential discharges of a neuron, and rate variability is just noise. This noise may be filtered out by averaging across time or neuronal populations, rate coding can performs robustly in the presence of noise, but it has limited information capacity. This is, noise in the brain is correlated and it is essential we gain a thorough understanding of the correlational structure in the brain and its possible impact in the population code. An alternative view of the neural code is summarized by the term temporal coding; the notion that the timing of individual spikes also carries relevant information. In principle, selective temporal mechanisms could exploit the high intrinsic precision of cortical neurons to increase the efficiency of neural coding.

How to account for the entire complexity levels present in the brain signals just by using a single theoretical approach ? Information theory is the most rigorous way to quantify neural code reliability and constitutes an aspect of probability theory which allows us to quantify the information transmitted by communication channels (Shannon 1948). One possible application could be to quantify how much information neuronal activity carry about external sensory stimuli. More importantly, the exact breakdown of Information into its coding mechanisms allows a precise quantification of all the modalities with which

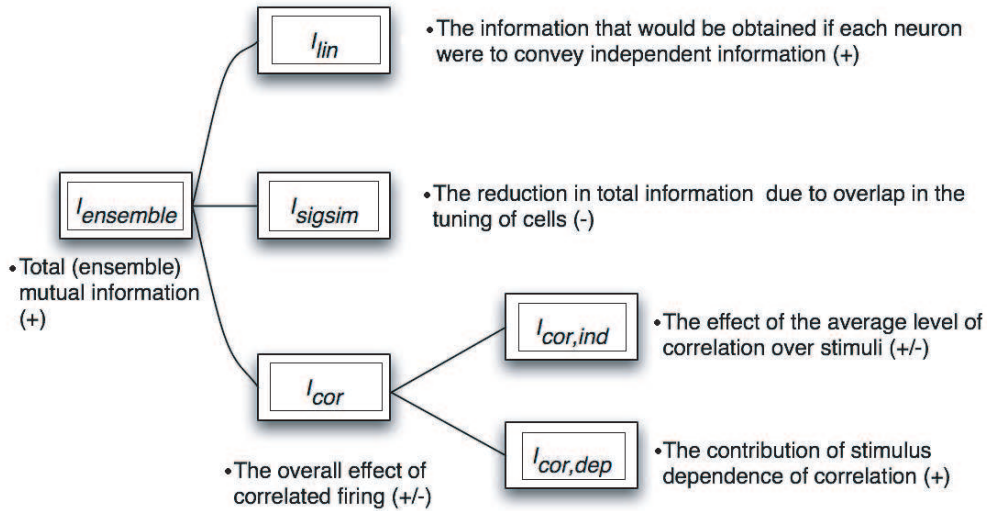


Fig. 3.1: Information component breakdown. The ensemble mutual information can be broken down into a linear component, the reduction of information due to the redundancy caused by overlap in tuning curves, and the contribution of correlated firing (I_{cor}). The noise correlation term can be further broken down to separate out the effect of the average level of correlation over all stimuli, and the stimulus-dependence of correlation – the latter term captures any effects due to coding by explicit modulation of correlation/synchronization.

correlations contribute to the neural code.

In this section we describe how we calculated the Shannon information transmitted by neuronal population activity (and a number of related quantities). Shannon mutual information quantifies the extent to which the responses are dependent upon the stimuli – it is a distance-like measure (the Kullback-Leibler divergence) between two probability distributions: the joint probability of responses and stimuli, $P(\mathbf{r}, \mathbf{s})$, and joint probability distribution that would apply if responses did not depend at all upon stimuli, $P(\mathbf{r})P(\mathbf{s})$. This dependence between responses and stimuli may take a number of forms – firing rate dependence, pairwise correlation dependence, etc. Information component breakdown methods (Figure 3.1) allow us to quantify the effect of such dependencies upon the mutual information and thus assess the different ways in which the correlations contribute to the neural code. If synergistic or redundant interactions between cells are observed, the information components may reveal

the mechanisms from which they arise.

The technical approach we adopt is a modification of a previously developed technique (Panzeri and Schultz 2001a; Schultz and Panzeri 2001; Panzeri et. al. 1999) in which a Taylor series expansion was used to break the Shannon information into its components. Pola et al (2003) generalised this approach by substituting correlation functions with probability functions, resulting in an exact information component breakdown. One disadvantage to the Pola approach is that the correlation components cannot be explicitly written in terms of entropies of probability distributions. While we do not see this as giving rise to problems of interpretation (but see Schneidman et al 2003), it does mean that advanced methods for entropy estimation cannot be used. Thus we have rewritten the correlational components as *approximate* entropies (i.e. an entropies plus additional terms which are very small and relatively immune to bias), allowing us to use a recently developed technique for minimizing the bias associated with estimating entropy from a limited number of experimental samples (Nemenman et. al. 2004). By using a Bayesian prior to generate a nearly uniform distribution of entropies, we thus correct for sample size dependent bias at its source and avoid potential artefacts that may occur when sampling is insufficient, as is typically the case in neurophysiological experiments.

We consider a time period of duration T unit time bins in which the activity of a given pair of cells is observed. The neural population response will be denoted by \mathbf{r} (drawn from a response space R) and a sensory stimulus from a given stimulus set S will be denoted by s . The mutual information transmitted by the population response about the whole set of stimuli (Shannon 1948; Cover and Thomas 1991) is written as

$$I(R; S) = H(R) - H(R|S), \quad (3.1)$$

where $H(R)$ and $H(R|S)$ are the total response entropy and the noise entropy respectively. They are defined as:

$$H(R) = - \sum_{\mathbf{r} \in R} P(\mathbf{r}) \log_2 P(\mathbf{r}), \quad (3.2)$$

$$H(R|S) = - \sum_{s \in S} P(s) \sum_{r \in R} P(\mathbf{r}|s) \log_2 P(\mathbf{r}|s), \quad (3.3)$$

where $P(r|s)$ is the probability of observing a given ensemble response vector r conditional upon the occurrence of stimulus s , and $P(r)$ is the average of $P(r|s)$ over all stimuli.

In order to understand the meaning of correlation one must define the probability of getting independent population responses as:

$$P_{ind}(\mathbf{r}|s) = \prod_{c=1}^C \prod_{t=1}^T P(r_{ct}|s), \quad (3.4)$$

and

$$P_{ind}(\mathbf{r}) = \langle P_{ind}(\mathbf{r}|s) \rangle_s, \quad (3.5)$$

where c is the label for each cell (up to $C=2$ cells in the pair for the analysis presented here, although the formalism is quite general in this respect), t indexes the time bin up to a maximum value of L corresponding to duration T , and the stimulus average $\langle x \rangle_s = \sum_{s=1}^S P(s)x$. The presence of noise correlation (correlation in the response variability for a fixed stimulus) or signal correlation (correlation in the tuning of, or signal conveyed by response variables) is indicated by $P_{ind}(\mathbf{r}|s) \neq P(\mathbf{r}|s)$ and $P(\mathbf{r}) \neq P_{ind}(\mathbf{r})$, respectively. Moreover, $P(s|\mathbf{r})$ is the true distribution of stimuli given responses and $P_{ind}(s|\mathbf{r})$ is the distribution one would derive in absence of knowledge of correlations. In practice, we obtained $P_{ind}(\mathbf{r}|s)$ numerically by multiplying the marginal probability distributions as apparent from 3.4.

The information component breakdown method allows us to write the total mutual information into a sum of components which are related to the different decoding mechanism (Panzeri and Schultz 2001a; Pola et. al. 2003)

$$I(R;S) = I_{lin} + I_{sig-sim} + I_{cor} \quad (3.6)$$

The first term of the information breakdown, I_{lin} , gives the total amount of information which would be conveyed if all the cells were independent:

$$I_{lin} = \sum_{c=1}^C \sum_{t=1}^T [H(R_{ct}) - H(R_{ct} | S)] \quad (3.7)$$

where

$$H(R_{ct} | S) = - \sum_{s \in S} P(s) \sum_{r_{ct}} P(r_{ct} | s) \log_2 P(r_{ct} | s), \quad (3.8)$$

and $H(R_{ct})$ is the averaged value across all the stimuli.

The signal similarity term $I_{sig-sim}$ quantifies the information loss arising from redundancy due to overlap in the tuning curves pertaining to response (cell,time) bins r_{ct} ("redundancy due to signal correlations")

$$I_{sig-sim} = H_{ind}(R) - \sum_{c=1}^C \sum_{t=1}^T H(R_{ct}), \quad (3.9)$$

where

$$H_{ind}(R) = - \sum_{\mathbf{r}} P_{ind}(\mathbf{r}) \log_2 P_{ind}(\mathbf{r}), \quad (3.10)$$

The third term, I_{cor} , quantifies the total amount of information due to the correlated activity on the overall neural coding:

$$I_{cor} = I(R; S) - H_{ind}(R) + \sum_{c=1}^C \sum_{t=1}^T H(R_{ct} | S). \quad (3.11)$$

This is, I_{cor} quantifies whether the presence "noise correlation" increase or decrease the information available in the neural responses.

So far, it is apparent that all of the terms can be written in terms of entropies of particular distributions. However, this correlation term can be further resolved into two components, a stimulus independent component $I_{cor-ind}$ and a stimulus dependent component $I_{cor-dep}$. This last term in the (Pola et. al. 2003) formalism is calculated as

$$I_{cor-dep} = I(R; S) - \chi + \sum_c H(R_c|S), \quad (3.12)$$

where

$$\chi = - \sum_{\mathbf{r}} P(\mathbf{r}) \log_2 P_{ind}(\mathbf{r}), \quad (3.13)$$

That is, the stimulus dependent correlation component is not made up entirely of entropies, and thus advanced entropy estimation techniques such as NSB cannot be applied. Moreover, χ can be substantially biased, which renders its calculation by previously available procedures difficult for all except very low-dimensional problems.

Formally speaking, the stimulus dependent correlation component can be defined as the Kullback-Leiber divergence between $P(s|\mathbf{r})$ and $P_{ind}(s|\mathbf{r})$, (Nirenberg et. al. 2001, Latham et. al 2005) – conceptually characterized by Nirenberg et al as the effect of correlations upon the decoding of stimuli:

$$I_{cor-dep} = D(P(s|\mathbf{r}) \| P_{ind}(s|\mathbf{r})) \equiv \sum_{\mathbf{r}} P(\mathbf{r}) \sum_s P(s|\mathbf{r}) \log_2 \frac{P(s|\mathbf{r})}{P_{ind}(s|\mathbf{r})} \quad (3.14)$$

In the following we rewrite the correlation stimulus dependent component from “first principles” using the Kullback-Leibler, for the case in which only pairwise correlations between neurons are considered. We note that this formalism can be easily extended to a larger number of cells.

$$I_{cor-dep} = D(P(s|r_1r_2) \| P_{ind}(s|r_1r_2)) \equiv \sum_{r_1r_2} \sum_s P(s)P(r_1r_2|s) \log_2 \frac{P(r_1r_2|s)}{P_{ind}(r_1r_2|s)} - \sum_{r_1r_2} P(r_1r_2) \log_2 \frac{P(r_1r_2)}{P_{ind}(r_1r_2)} \quad (3.15)$$

where

$$P_{ind}(r_1 r_2) = \sum_s P(s) P(r_1 | s) P(r_2 | s) \quad (3.16)$$

and

$$P(r_1 r_2) = \sum_s P(s) P(r_1 r_2 | s) \quad (3.17)$$

The second term in the Kullback-Leibler distance, $D_\Delta = \sum_{r_1 r_2} P(r_1 r_2) \log_2 \frac{P(r_1 r_2)}{P_{ind}(r_1 r_2)}$, does not change if we multiply and divide by exactly the same factor inside the logarithm.

$$D_\Delta = - \sum_{r_1 r_2} P(r_1 r_2) \log_2 \left(\frac{P(r_1 r_2) \langle P(r_1 | s) \rangle_s \langle P(r_2 | s) \rangle_s}{\langle P(r_1 | s) P(r_2 | s) \rangle_s \langle P(r_1 | s) \rangle_s \langle P(r_2 | s) \rangle_s} \right), \quad (3.18)$$

This is equivalent to saying

$$D_\Delta = \sum_{r_1 r_2} P(r_1 r_2) \log_2 \frac{P(r_1 r_2)}{\langle P(r_1 | s) \rangle_s \langle P(r_2 | s) \rangle_s} - \Delta = I(r_1; r_2) - \Delta \quad (3.19)$$

where $\Delta = \sum_{r_1 r_2} P(r_1 r_2) \log_2 \beta$

and,

$$\beta = \frac{\langle P(r_1 | s) \rangle_s \langle P(r_2 | s) \rangle_s}{\langle P(r_1 | s) P(r_2 | s) \rangle_s}, \quad (3.20)$$

the correlation stimulus dependent component can be rewritten as

$$I_{cor-dep} = \sum_{r_1 r_2} \sum_s P(s) P(r_1 r_2 | s) \log_2 \frac{P(r_1 r_2 | s)}{P_{ind}(r_1 r_2 | s)} - \sum_{r_1 r_2} P(r_1 r_2) \log_2 \frac{P(r_1 r_2)}{\langle P(r_1 | s) \rangle_s \langle P(r_2 | s) \rangle_s} - \Delta, \quad (3.21)$$

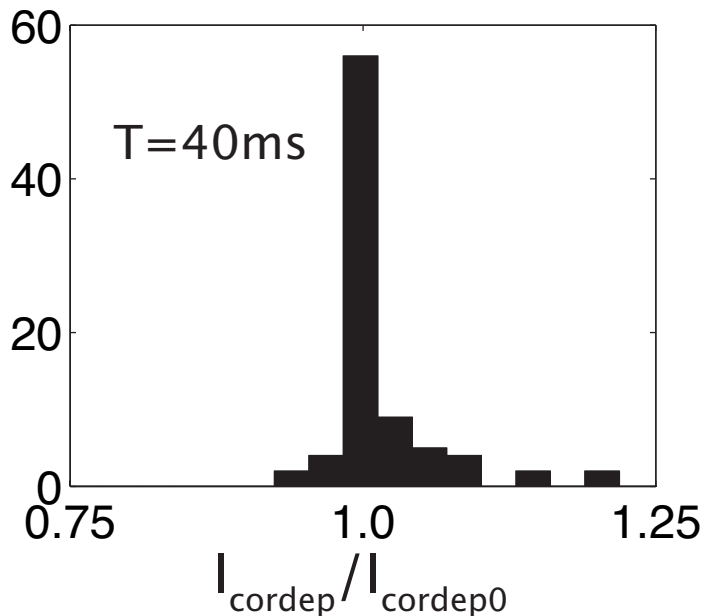


Fig. 3.2: The effect of Δ (at $T = 40$ ms for 102 pairs of neurons). $I_{cordep0}$ correspond to $\Delta = 0$.

The stimulus dependent correlation component has thus been expressed in terms of entropy quantities with the addition of a single term Δ ; the NSB estimation method can be applied to these quantities with the exception of Δ . The remaining non-entropy term (Δ) is essentially the stimulus-averaged response multiplied by a logarithmic function of the coefficient β summed over the whole space of responses. We are summing therefore in the space of responses quantities which have been averaged over the stimuli, and it is reasonable to expect a very low bias contribution from this term. Moreover, since β is the product of the stimulus-averaged response from each cell divided by the stimulus unconditional independent responses, it is reasonable to expect that it will always be close to one and therefore Δ will be close to zero. In practice, we included Δ in our calculations (without bias correction); the magnitude of Δ was always observed to be small.

Figure 3.2 shows an histogram of the ratio between the true value of I_{cordep} and that obtained by setting $\Delta=0$. We conclude from the histogram that the contribution from Δ will be reasonably small. In practice, we included Δ in our calculations (without bias correction).

Having expressed all of the quantities necessary to perform the information component analy-

sis in terms of entropies of particular (in some cases conditional) distributions, these entropies are computed by inserting the respective distributions into the NSB entropy estimation routine. We found that, for our dataset, this procedure resulted in substantially better estimation performance than we were able to achieve with techniques that we have used previously (Panzeri and Treves 1996). In addition, the NSB approach provides a convenient error estimate for the entropies, which can be propagated into error estimates for the information quantities. An alternative method to estimate $I_{cor-dep}$ has been also recently developed by Montemurro et. al. 2007.

We have expressed all information quantities in total information terms, measured in bits, as opposed to rates measured in bits/sec. In the context of the present study we believe that this leads to a clearer interpretation; a discussion of the relationship to information rate quantities will be presented later in this chapter.

3.3 *Experimental Procedures*

As we have mentioned in the previous chapter recordings were made by (Kohn and Smith 2005) in 10 cynomolgus (*Macaca fascicularis*), 1 bonnet (*M. radiata*) and 1 pig-tailed (*M. nemestrina*) adult male monkeys. All experimental procedures were approved by the New York University Animal Welfare Committee. This dataset has previously been described (Kohn and Smith 2005), as have the experimental procedures used in the laboratory (Cavanaugh et. al. 2002).

For the sake of completeness, we will mention again very briefly the experimental procedure in this chapter. Animals were premedicated with atropine (0.05 mg/kg) and diazepam (1.5 mg/kg) and anaesthetized initially with ketamine HCl (10 mg/kg). Anaesthesia during recording was maintained by intravenous infusion of sufentanil citrate (Sufenta; 4-8 $\mu\text{g}\cdot\text{kg}^{-1}\cdot\text{hr}^{-1}$). To minimize eye movements, vecuronium bromide was infused intravenously (Norcuron; 0.1 $\text{mg}\cdot\text{kg}^{-1}\cdot\text{hr}^{-1}$). Vital signs (EEG, ECG, end-tidal P_{CO_2} , temperature and lung pressure) were monitored continuously. The pupils were dilated with topical atropine and the corneas protected with gas-permeable contact lenses. Refraction was provided by supplementary lenses. Electrophysiological recordings were made using a seven-electrode array (Thomas Recording, Giessen, Germany). Spikes were detected using a hardware discrimi-

nator, and digitised with a temporal resolution of 0.25 ms. Most pairs of cells (90.5%) were recorded on separate electrodes. Use of an anaesthetised preparation for this experiment allowed many more trials to be collected than would otherwise be possible; this is particularly important for information theoretic analyses in which effective sampling is crucial. Use of sufentanil avoided some of the problems that are apparent with other anaesthetics such as halothane and isoflurane, including changes in contrast sensitivity (Movson et. al. 2003) and oscillations (Imas et. a. 2004).

3.3.1 *Visual Stimuli*

Stimuli were luminance modulated, drifting sine-wave gratings presented at a frame rate of 100 Hz. We measured, in order, the direction, spatial and temporal frequency, and size tuning for drifting sine-wave gratings. After characterising the stimulus preference for each cell independently, we measured correlation for responses evoked by stimuli of different directions and contrasts. The spatial and temporal frequency of these test stimuli were set between the preferred values of the two cells or at the value of the cell that responded less vigorously. Stimuli were presented between the receptive field (RF) centres of the cells and covered both RFs. All measurements were made using stimuli presented in a circular aperture to the dominant eye of the less responsive cell. A gray field of average luminance surrounded the stimuli.

Direction and contrast experiments were performed in separate blocks of trials. Within most (~90%) of these experiments, the presentation order of each direction or contrast was block randomized. In the direction experiments, we presented full-contrast gratings drifting in five distinct directions, spanning the range between evoking a weak response and driving both cells strongly. In the contrast experiments, we fixed the direction to that most effective at driving the pair of cells, and presented the stimulus at four contrasts, typically 1.56, 6.25, 25 and 100%. For cells with low contrast sensitivity, we adjusted the range of contrasts to extend from 12.5 to 100% in octave steps. Stimuli were presented for 2.56 sec with a 3 sec inter-stimulus interval during which we presented an isoluminant gray screen. Each stimulus was presented 30-200 times. However, for the purposes of the information calculations (see below), these stimuli were broken into individual cycles of the drifting grating, and thus a much greater number of experimental trials (480 to 3200, mean 1300) were available for the

purposes of information estimation.

3.3.2 Response characterisation

We characterised correlation using the (shift-predictor corrected) spike train cross-correlogram (CCG; (Perkel et. al. 1967) as described by (Kohn and Smith 2005), as well as by the use of information theory. For the purposes of the information calculations, we used response bins with fixed time window lengths T (which were integral fractions of the grating period τ , i.e. $T=\tau$, $T=\tau/2$, $T=\tau/4$ etc, where τ was the inverse of the stimulus temporal frequency used for the pair of cells – ranging from 80 ms to 320 ms). Response vectors r for each trial were calculated by counting spikes in these bins of length T ms; for codes comprising a pair of cells, the response vector had length two. The cardinality of the response vector was $(n_{smax,1}+1)(n_{smax,2}+1)$ where $n_{smax,i}$ is the maximum number of spikes (over all stimuli, for any trial) that was observed to be fired by cell i . For each window length T , we calculated the information quantities (as shown below) using all 480 to 3200 trials (cycles). When multiple windows could be extracted from a single cycle (e.g. 4 windows at $T=\tau/4$), the resulting information values from each window in the cycle were finally averaged together. Note that simple cells were cycle-modulated, so the results should be taken to be average information estimates, which should not affect conclusions with regard to the relative effect of correlations.

3.4 Results

We analyzed the activity of 147 pairs of single neurons in the primary visual cortex of anesthetized, paralyzed macaque monkeys (Kohn and Smith 2005). The neurons in each pair were typically complex cells separated by less than 500 microns that had a mean receptive field overlap of 75% and similar tuning properties: a mean difference of 37° in direction preference, 0.37 octaves in spatial frequency preference, and 0.36 octaves in temporal frequency preference. These neuronal pairs have previously been shown to manifest stimulus-dependent synchrony (Kohn and Smith 2005). In this chapter we present an information-theoretic analysis of the effect of this synchrony on neural coding of direction and contrast, making use of a modified version of the method of information components

(Panzeri and Schultz 2001a; Pola et. al. 2003; Montani et. al. 2007b). This approach allows us to provide new insights into mechanisms of sensory processing in the primary visual cortex by paying special attention on stimulus dependent correlation component. We report here on a subset of 102 pairs (for the orientation analysis) and 71 pairs (for the contrast analysis) of the original (Kohn and Smith 2005) dataset, chosen in order to satisfy convergence criteria for the entropy estimation procedure that we utilised (Nemenman et. al. 2004).

3.4.1 Direction coding: information adds linearly across cells

We examined the population coding of stimulus direction in primary visual cortex by quantifying simultaneously recorded pairwise responses as the number of spikes fired by each cell in the pair within a time window T (a “two letter word” response). We then calculated the total mutual information conveyed by the ensemble response about which stimulus direction gave rise to the response. We designated this $I_{ensemble}$ (Figure 3.1), and compared it with two other information measures: the sum of the mutual informations calculated from the individual neurons’ responses (i.e. the sum of two informations calculated from two “one letter words”, I_{sum}), and the mutual information calculated from a reduced code in which the spikes on each trial are pooled across cells (i.e. the information from a single “one letter word”, I_{pooled} , (Reich et. al. 2001). If the neurons’ responses are completely uncorrelated, then $I_{ensemble}$ should be equal to I_{sum} ; in the presence of correlations, $I_{ensemble}$ might exceed I_{sum} – which we would refer to as a *synergistic* interaction – or might be less than I_{sum} – which we would refer to as a *redundant* interaction. This commonly used definition of redundancy between a pair of information channels (cells) measures the extent to which they carry common information.

Figure 3.3 A shows a typical pair of cells (which we label pair A) with partially overlapping tuning curves (their direction preferences were 49 degrees apart). We presented five stimuli (solid circles in Figure 3.3 A) that drove each cell through a wide range of firing rates. The result, as can be seen in Figure 3.3C, is a substantial modulation in the height of the central peak of the cross-correlogram (CCG) of the neurons’ spike trains: at a particular orientation that drives both neurons moderately well, a fraction of spikes fired by each neuron tend to be synchronized with millisecond temporal precision (Kohn and Smith, 2005). For stimuli that do not drive both cells well, the extent of synchronization falls off sharply. This stimulus

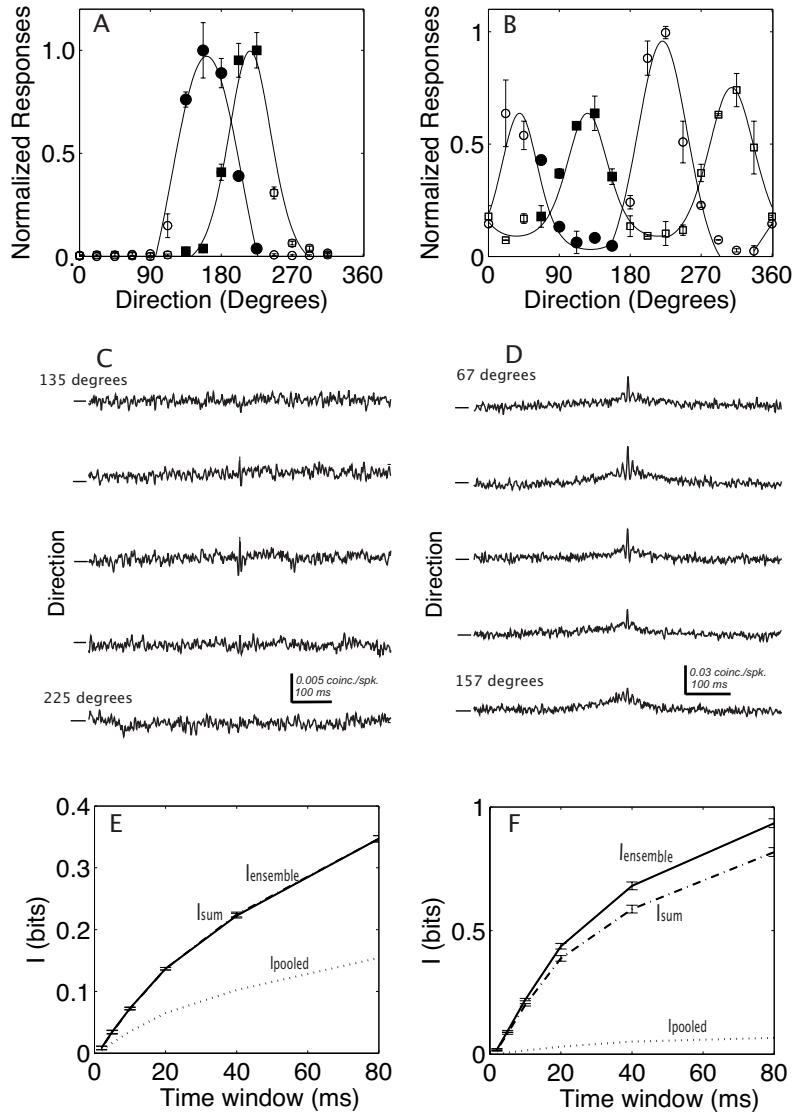


Fig. 3.3: Direction coding by two pairs of neurons. *A, B* Direction tuning curves for two pairs of neurons the first pair are both direction-selective, the second only slightly directionally biased (fitted using von Mises functions). *C, D* Cross-correlograms for each of the pairs above show that fine-timescale synchronization is induced for stimulus directions that drive both cells relatively well. The cross-correlation was measured for the five stimuli indicated by the filled circles in *A, B*. *E, F* Information analysis: the total information available from each pair of neurons ($I_{ensemble}$) is compared for different integration time windows T to the sum of the information values obtained from each constituent neuron alone (I_{sum}) and to the information from a pooled code in which the identity of the cell firing each action potential is ignored (I_{pooled}).

dependence of synchrony arises despite correcting for the basic rate dependence of the CCG (Kohn and Smith 2005); the origin of the stimulus-dependence in the cross-correlogram is discussed later in this chapter.

The synchronized firing illustrated above is an example of correlation: the timing of spikes in the two neurons is not independent. Does the substantial synchronization apparent in this example lead to a synergistic or redundant encoding of stimulus direction? In 3.3E it can be seen that the answer for this pair is neither. In this case, there appears to be a balance of contributions such that the overall effect of the correlation is neither synergistic nor redundant. The ensemble information ($I_{ensemble}$) is exactly equal to the sum of the single cell information values (I_{sum}), for a wide range of time windows.

A second example pair with more widely separated direction tuning curves (difference in direction preference of 87 degrees), is shown in 3.3B (which we label pair B). The height of the central peak of the CCG is again sensitive to stimulus direction (3.3D), but in this case the resulting interaction is synergistic : the ensemble mutual information is larger than the sum regardless of the time window over which spikes are counted (3.3F).

The picture over the entire population is one of a small amount of synergy: with a time window of 5 ms, the ensemble code does on average 2.4% better than the sum of single cell contributions (see Figure 3.4A,B). To compute the degree of synergy in the population for a range of time windows T , we calculated a synergy index (which we call the synergy fraction) as $(I_{ensemble} - I_{sum}) / I_{ensemble}$: values greater than zero indicates synergistic coding, values less than zero indicate redundancy. The synergistic effect of ensemble coding is more substantial at shorter time windows, where the fine temporal precision at which the spikes may synchronize has a significant effect – the maximum effect we observed was 13.7% at 2 ms (for technical reasons related to convergence of the numerical integral involved in the entropy computation, the smallest time window we were able to use), tailing off sharply at around 10 ms, where the synergy fraction is close to zero (Figure 3.4B). Thus, being very precise about spike timing leads to synergy rather than information independence (Schneidman et. al. 2003). The short time scale over which synergy is present agrees well with the time scale of synchrony in the population: the mean full width at half maximum of the CCG peaks was 9 ms. At longer time windows ($T \geq 20$ ms), the information became comparable in size to the stimulus entropy ($\log_2 5$ bits), and thus ceiling effects may reduce

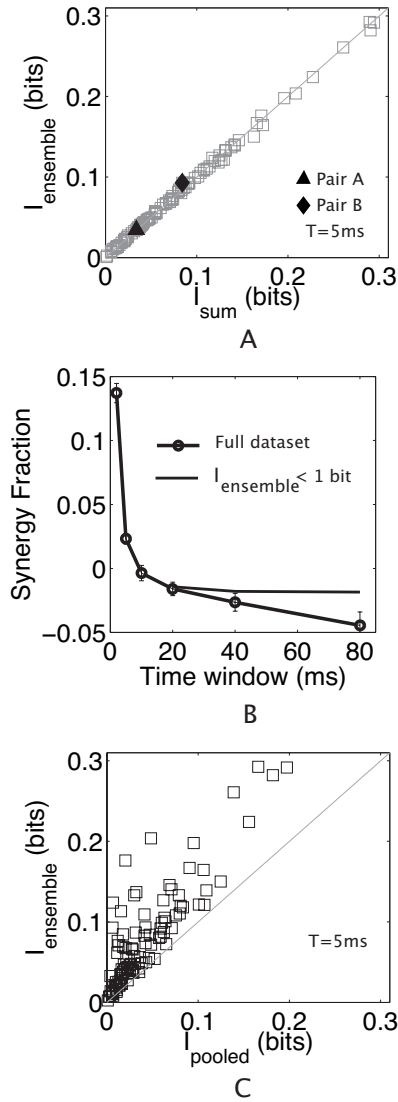


Fig. 3.4: Information adds relatively linearly across cells. *A* The total (ensemble) information available for each pair is plotted against the sum of the information available individually from each cell constituting the pair. The time window used for counting spikes was 5 ms. Pairs marked A and B correspond to the pairs illustrated in Figure 2*A, B*. *B* The synergy fraction (defined as $1 - I_{sum}/I_{ensemble}$ and indicating the fraction of information beyond that expected if the cells are independent) is plotted against the time window used for counting spikes. The lines show the average (\pm s.e.m.) over the entire dataset, and over only those pairs showing ensemble information lower than 1 bit (this latter curve excluding potential artefactual redundancy effects). *C* Pooling spikes across cells destroys a substantial amount of information in almost all cases indicating that the pattern of spikes across cells is informative.

the raw information values somewhat. We corrected for this by removing pairs from the population that presented a higher information amount than 1 bits at a given time window, an arbitrary but conservative threshold. It is apparent that in the absence of ceiling effects, the trend for long time windows is for the synergy fraction to asymptote to a slightly negative value, indicating that the mutual information adds across the neurons as if they were roughly independent.

In contrast to I_{sum} , the information available from the pooled code (I_{pooled}) is severely curtailed: destroying the identity of which cell fired a spike substantially reduces the information transmitted (in agreement with Reich et al., 2001). This was apparent in both example pairs A and B (Figures 3.2 E and F), and is true for every pair analysed (Figure 3.3C). The mean amount of information lost due to destroying cell identity was 46.33% of the ensemble information at $T = 5$ ms, and 46% at $T = 40$ ms (see also Reich et al., 2001).

3.4.2 *The role of correlations in direction coding: a balance of redundant and synergistic effects*

In the previous section we found that correlations between neurons lead to a weakly synergistic code for direction on fine timescales. In a sense, this is surprising because the pairs often displayed substantial synchronization whose strength was strongly dependent on the direction of the stimulus (Figure 2C,D; (Kohn and Smith 2005), suggesting that this synchrony should convey substantial information. On the other hand, the synchrony arises from common input to a pair of cells and was prevalent in our dataset precisely because the neurons had similar receptive field properties. The similarity in tuning properties means that the firing rate provides redundant information and raises the issue of how this information compares to that provided by correlated firing.

To examine the relative information conveyed by different aspects of the response, we separated the total mutual information into components reflecting the contributions of individual coding mechanisms (Figure 3.1). The linear component— I_{lin} —represents the information that would be obtained if each neuron were to convey independent information. This is equal to I_{sum} , which we calculated in the previous section by a different approach. $I_{sig-sim}$ represents the reduction in total information conveyed due to one source of redundancy: the overlap in the tuning of the cells. These first two components depend only on the firing

rates of the individual neurons, rather than the correlated or synchronized firing between neurons. The I_{cor} term captures the consequences of this correlated firing and can be separated further into stimulus-dependent ($I_{cor-dep}$) and stimulus-independent ($I_{cor-ind}$) parts. The effect of $I_{cor-dep}$, if non-zero, is always positive, but the effect of $I_{cor-ind}$ can be either positive or negative (*synergistic* or *redundant*), depending on the sign and magnitude of the overlap in tuning curves (see Panzeri et. al. 1999 for details). Breaking the information into its respective components allows us identify *how* synergy or redundancy arises.

Figure 3.5A shows the breakdown into components of the mutual information for pair A. In this case, the ensemble information is exactly equal to the linear component, indicating that there is (overall) no information provided by the correlation (consistent with the analysis of Figure 3.3E). This is true despite the presence of stimulus-dependent synchrony in this pair (Figure 3.3C). The reason for this lies in redundant contributions from the stimulus independent correlation ($I_{cor-ind}$) and the overlap in the tuning of the two cells, $I_{sig-sim}$, which offset exactly the information provided by the stimulus-dependent synchrony ($I_{cor-dep}$). Pair B, which showed a stronger synchronization effect, also showed a stronger contribution of the correlational components of the information. In this case, the stimulus-dependent correlation component $I_{cor-dep}$ was sufficiently large to outweigh redundant effects due to the average level of correlation ($I_{cor-ind}$) and the similarity in tuning ($I_{sig-sim}$), leading to an overall synergistic effect of correlation (Figure 3.5B).

For pair A (a fairly typical pair of cells), synchronization affected information content, but the stimulus-dependence of the synchronization served to precisely balance the redundancy due to overlapping tuning. The value of I_{cordep} (called ΔI by (Nirenberg et. al. 2001, derived using a different approach) has been argued to indicate the importance of correlations for decoding (Latham et. al 2005): I_{cordep} can be written as the Kullback-Leibler divergence between $P(s|\mathbf{r})$, the probability that a stimulus s elicited ensemble response \mathbf{r} , and $P_{ind}(s|\mathbf{r})$, such a probability distribution constructed without knowledge of the correlations. If correlations are not important for decoding which stimulus gave rise to the response, then these probability distributions should be identical, and I_{cordep} zero; as correlations increase in importance for decoding, I_{cordep} should also increase. For pair A, the value of I_{cordep} was relative small (10% of the ensemble information at $T=5$ ms). For pair B, the explicit information content in the stimulus dependence of correlations outweighed redundant effects and led to a more substantive value for I_{cordep} (18.5% at $T=5$ ms). For time windows of 5 ms, the

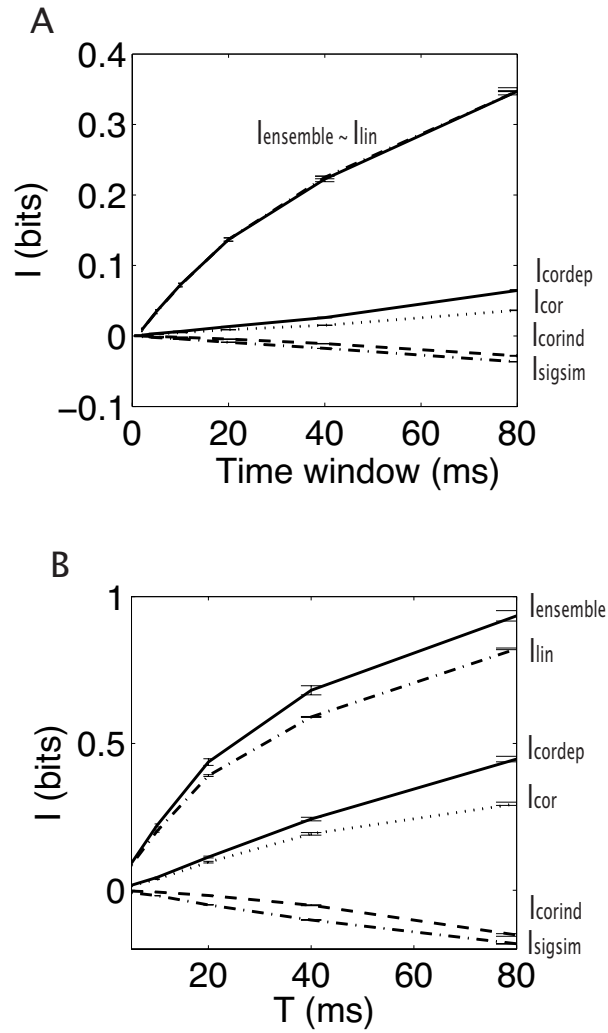


Figure 4

Fig. 3.5: Information component analysis for the example pairs, showing how the balance between a synergistic contribution due to orientation dependent synchronization ($I_{cor-dep}$), and redundant contributions from tuning overlap (I_{sigsim}) and the average level of correlation ($I_{cor-ind}$), give rise to the overall level of synergy or redundancy. The information components I_{lin} , I_{sigsim} and I_{cor} add together to give the total information $I_{ensemble}$. Panels A, B correspond to the same pairs of cells described in Figure 3.3 A, B.

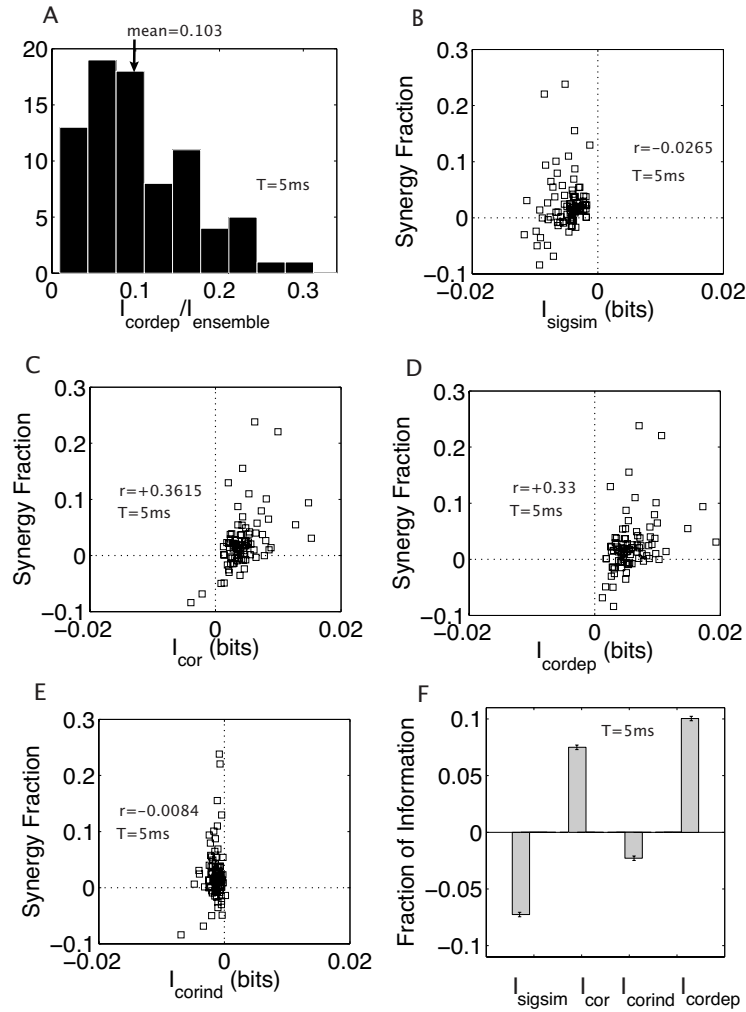


Fig. 3.6: Information components across the entire population of 102 pairs (direction coding). **A** Histogram of the relative contribution of I_{cordep} to the total information for a time window of 5 ms. **B** I_{sigsim} , reflecting the redundant contribution due to the overlap in tuning curves, is generally non-zero but is not strongly correlated with the overall amount of synergy or redundancy. **C** Correlational effects captured by I_{cor} are more strongly related to the extent of synergy in the coding. **D** The stimulus-dependent correlational component is strongly related to the extent of synergistic coding, whereas (**E**) the average level of correlation is unrelated. **F** A bar chart capturing the average value of each information component (expressed as a fraction of the total information, $I_{ensemble}$) over the entire dataset. Error bars indicate standard error of the mean ($N=102$).

mean value of I_{cordep} over the population was 10.3 (Figure 3.6 A). For longer time windows ($T = 40$ ms), the mean value of I_{cordep} was also about 10 %.

Which of the information components were responsible for the small amount of synergy that was observed? We examined this point by comparing the fraction of synergistic information $(I_{ensemble} - I_{sum})/I_{ensemble}$ to the information components on a pair-by-pair basis. For $T = 5$ ms it can be seen that the redundancies added by the signal-similarity term $I_{sigstim}$ (Figure 3.6B) are mostly canceled by synergistic contributions of the total correlation component I_{cor} (Figure 3.6C). I_{cor} is significantly related to the synergy fraction (correlation coefficient $r=+0.36$, significant to $p=0.0005$ by transforming the correlation to generate the t statistic), and contributes mostly synergistically (Figure 3.6C). The component breakdown of I_{cor} reveals that I_{cordep} (Figure 3.6D) is most predictive of the extent to which the pairs of neurons interact synergistically ($r=+0.33$; $p=0.001$); in contrast, I_{corind} is unrelated to the synergy fraction ($r= -0.008$, $p=0.94$; Figure 3.6E). The average values of each of the components over the entire population of pairs is shown in Figure 3.6F, for a time window of 5 ms, and in Figure 3.7A for a range of time windows.

Notice that the correlation coefficient r is the zeroth lag of the normalized covariance function, and the p -values test the hypothesis of no correlation. The p -value is computed by transforming the correlation to create a t statistic. If p less than 0.05, then the correlation r is significant.

In summary, it is the balance between I_{cordep} , on the one hand, and $I_{sigstim}$ and I_{corind} , on the other, that largely determines the degree of synergy. For time windows lower than 10 ms, the preservation of temporally precise spike synchrony results in correlational information which is a relatively large fraction of the total information $I_{ensemble}$ (Figure 3.7A). At time windows longer than 10 ms the synergy contribution from I_{cordep} is significantly curtailed, and effectively cancelled by the signal similarity term, $I_{sigstim}$, and also by I_{corind} , which provides a greater redundant contribution as the time window increases (Figure 6A). This is in agreement with the study of (Kohn and Smith 2005), where an orientation sensitive component of the response correlation was found to dominate for short time scales, and an orientation insensitive component for longer time scales.

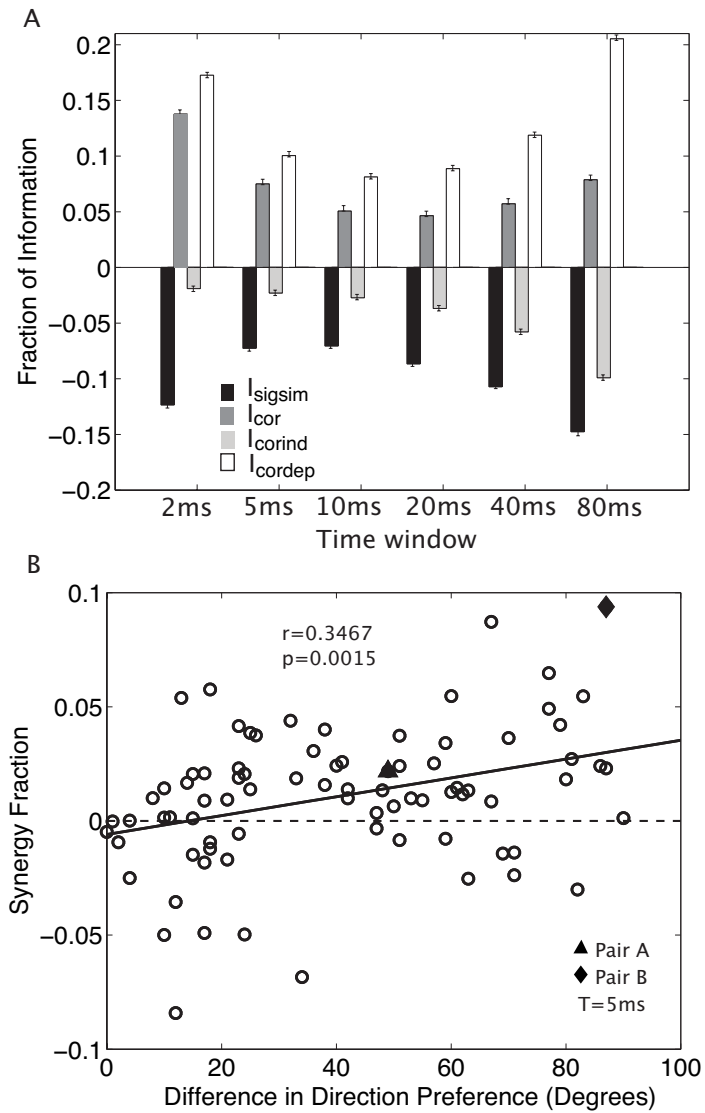


Fig. 3.7: A The relative effects of the information component are timescale-dependent. Bar charts show the average fraction of the information accounted for by the different components for time windows ranging from 2 to 80 ms: while the redundant contribution of $I_{cor-ind}$ grows with time window, the effects of the other components follow a ‘U’ or inverted ‘U’ curve. *B* Wide separation in direction preference leads to synergy. Time windows $T = 5ms$. Direction coding is redundant for pairs of neurons with similar tuning (negative synergy fraction).

3.4.3 Greater separation in direction preference leads to synergy

One important difference between the two examples is that for pair A the tuning preferences are closer together than for pair B, while pair B showed a stronger synergistic relationship than did pair A. As shown in Figure 3.7B for a time window of 5 ms, this is indicative of a general relationship: pairs with a greater separation in their preferred direction were more likely to interact synergistically, and those with preferred directions close together were more likely to carry redundant information. Linear summation of information across cells—when the synergy fraction is zero—occurred for neurons whose preferred directions were around 14 degrees apart (linear fit, Figure 3.7B; $r=0.35$, $p=0.0015$) for a time window of 5 ms. Neurons with widely separated tuning curves thus carry complementary information, even when correlations are taken into account, whereas neurons with similar direction tuning curves tend to carry redundant information.

The finding that synergy is strongest for pairs with dissimilar tuning may appear surprising because correlated firing, and sharp synchrony in particular, are strongest between nearby neurons that have similar tuning (Nelson et. al. 1992; Lee et. al. 1998; De Angelis et. al. 1999; Nowak et. al. 1999; Bair et. al. 2001; Kohn and Smith 2005). Our analysis reveals, however, that synergy is strongest between pairs of neurons for which correlation would be expected to be relatively weak. This is because although nearby neurons are particularly strongly correlated, this correlation arises from strong common input that presumably also gives rise to strongly overlapping tuning curves. The redundancy that arises from having similar tuning outweighs the information provided by correlation. For pairs with different preferences, even weak correlation can lead to synergistic coding since the tuning of the cells is less redundant. However, correlations do not necessarily lead to synergy. Weak correlations can lead to synergy or redundancy, depending on the similarity in tuning and relative magnitudes of I_{cordep} and I_{corind} . Moreover, we did not find any relationship between the Synergy Fraction and the high of the CCGs peaks. Attempting to relate the strength of stimulus-dependent synchrony to synergistic coding is thus perilous. When similarity in tuning and stimulus-independent correlation are taken into account, it is not necessarily the case that stronger synchrony leads to more synergistic coding.

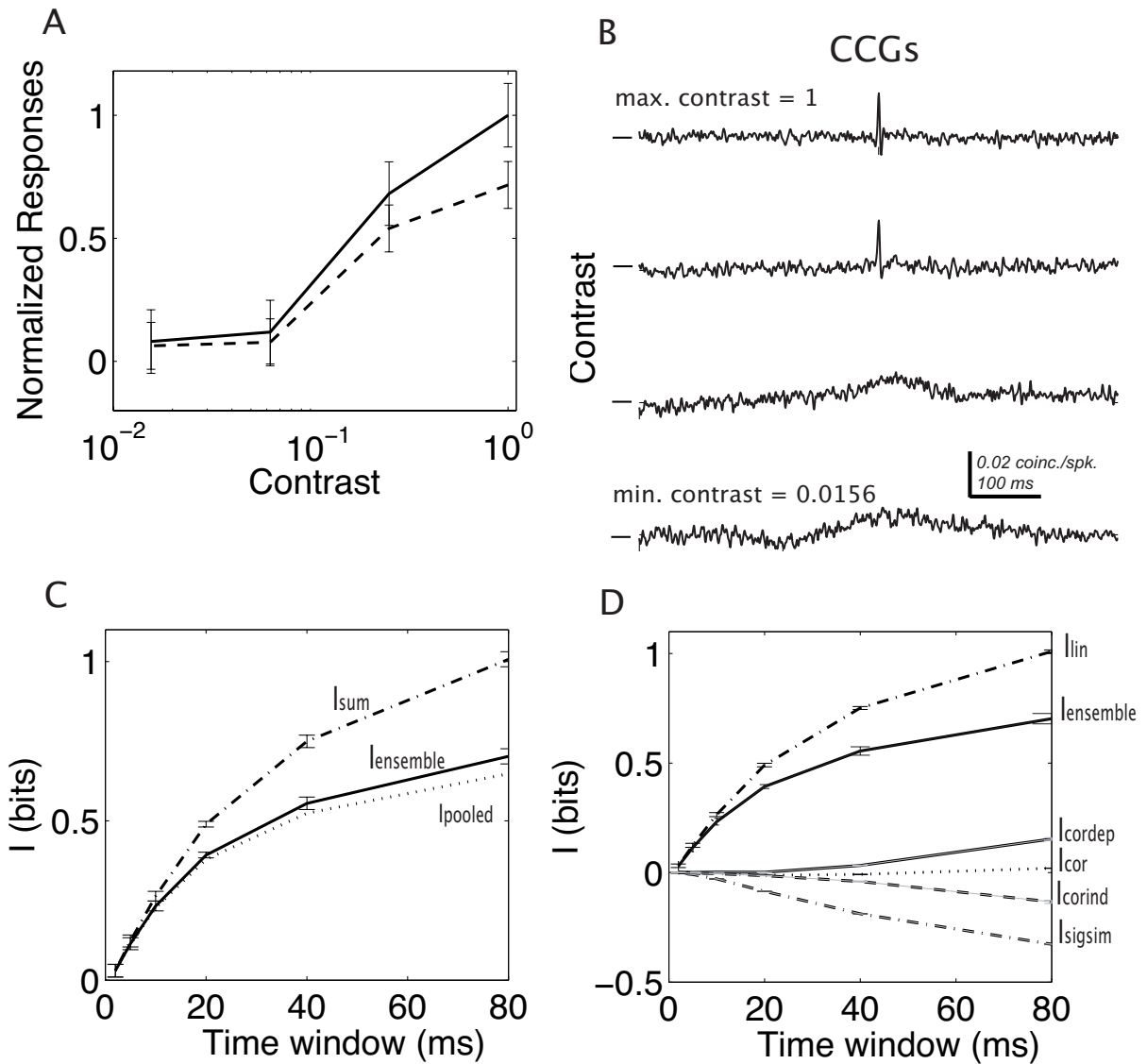


Fig. 3.8: Contrast coding. *A* Contrast tuning for a typical pair of cells (normalized to the maximal response of one of the cells). *B* Cross-correlograms show a decrease in the precision of spiking synchrony as contrast decreases. *C* The ensemble information is lower than the sum of that available from each individual cell contrast is coded redundantly by this pair of neurons. *D* Information components – the overall effect of I_{cor} is for this example minimal; the redundant effect can be seen to stem from $I_{sigstim}$, reflecting the strong overlap in contrast tuning.

3.4.4 *Contrast coding is redundant*

According to (Shannon 1948) redundancy is what wastes channel capacity. He defined redundancy as the difference between the entropy of the ensemble of the messages actually transmitted and the maximum entropy of the ensemble that the channel could transmit. A communication channel can only transmit information at rates up to a finite limit called its capacity, but the messages actually transmitted often contain less than this amount of information; the difference is the redundancy of the messages. The importance here is that any form of regularity in the messages is a form of redundancy, and since information and capacity are quantitatively defined, so is redundancy, and we have a measure for the quantity of environmental regularities.

Anatomical evidence in the brain shows that there are many more neurons at higher levels of the brain than at lower levels, which suggests that Shannon redundancy does not decrease, but instead increases. In the cortex it seems more likely that channel capacity increases rather than decreases. The two optic nerves of humans contain axons just over $2 \cdot 10^6$ retinal ganglion cells, whereas in V1 alone there are probably about 10^9 neurons. Information capacity at higher levels is likely to be greater than that of the representation in the retina or in the optic nerve. Following this reasoning, Shannon redundancy must increase, not decrease because information cannot be created.

A selective code is a code where some information is retained and some information is deliberately discarded. Selective codes do occur in nature, this is, a full reconstruction output-input is not possible. On the other hand, a redundancy-reducing code is a code where no information need to be lost. It has been hypothesized that mammalian sensory systems are efficient because they reduce the redundancy of natural sensory input. One way in which it might do this is by reducing the redundancy of the representation at successive stages of processing. This is called redundancy-reduction hypothesis (Attneave 1954; Barlow 1959). An animal must identify what is redundant in the sensory messages it perceives. This can tell it about structure and statistical regularity in its environment that are important for its survival. Some information about that would be conveyed by its genes, but sensory redundancy knowledge stems from its own experience.

What would be the typical result in a redundancy-reducing code? One could expect that a typical result of this kind of code would be to produce a distributed representation of

the sensory input with a high activity ratio, in which many neurons are active simultaneously, and with high and similar frequencies. However, such high activity-ratio distributed representations are inconvenient and highly inefficient from the statistical point of view (Gardner-Medwin and Barlow 2001). High-activity ratio distributed representations, which would be the product of redundancy reducing codes, could lead to inaccurate estimates of frequencies, and the resulting statistical inefficiency would make unreliable the learning. This would have disastrous consequences for survival.

In the previous sections, we have used information theory to study the role of correlations in the coding of stimulus direction in primary visual cortex. However, correlations are also modulated by stimulus *contrast* (Kohn and Smith 2005): whereas direction determines the height of the central peak of the CCG, the width of the central peak is primarily sensitive to stimulus contrast. This can be seen in the example in Figure 3.8 – a pair of neurons with relatively similar contrast tuning curves (Figure 3.8A), which show a broadening of the width of the CCG as contrast is reduced (Figure 3.8B). The different effect of altering stimulus direction and contrast on correlation provides an important test of whether there is a general role for correlation in stimulus coding, or whether the importance of correlation depends on the particular stimulus attribute in question.

In the example of Figure 3.8, the ensemble information about contrast is substantially less than the sum of the information available from each cell independently, regardless of the window of analysis (Figure 3.8C). Thus the coding of contrast is redundant. This can be explained by the fact that the contrast tuning functions of the neurons are similar, the values of stimulus dependent correlation component are smaller for contrast, and that there is a significant level of stimulus-independent correlation (e.g. substantial synchrony that is present at all contrast levels). Figure 3.8D shows that the major contributor in the coding of contrast is the large redundant $I_{sig\,sim}$ component of the information and that the effects of the average level of correlation ($I_{cor-ind}$) and the stimulus dependence of correlation ($I_{cor-dep}$) cancel each other.

The intuition provided by this example pair applies generally across the dataset. For the whole population at a time window of 5 ms, there was an average 3% redundancy. This redundancy arose despite the fact that correlation was contrast dependent: the average contribution of the stimulus dependent correlation component $I_{cor\,dep}$ is 6.3% of the total

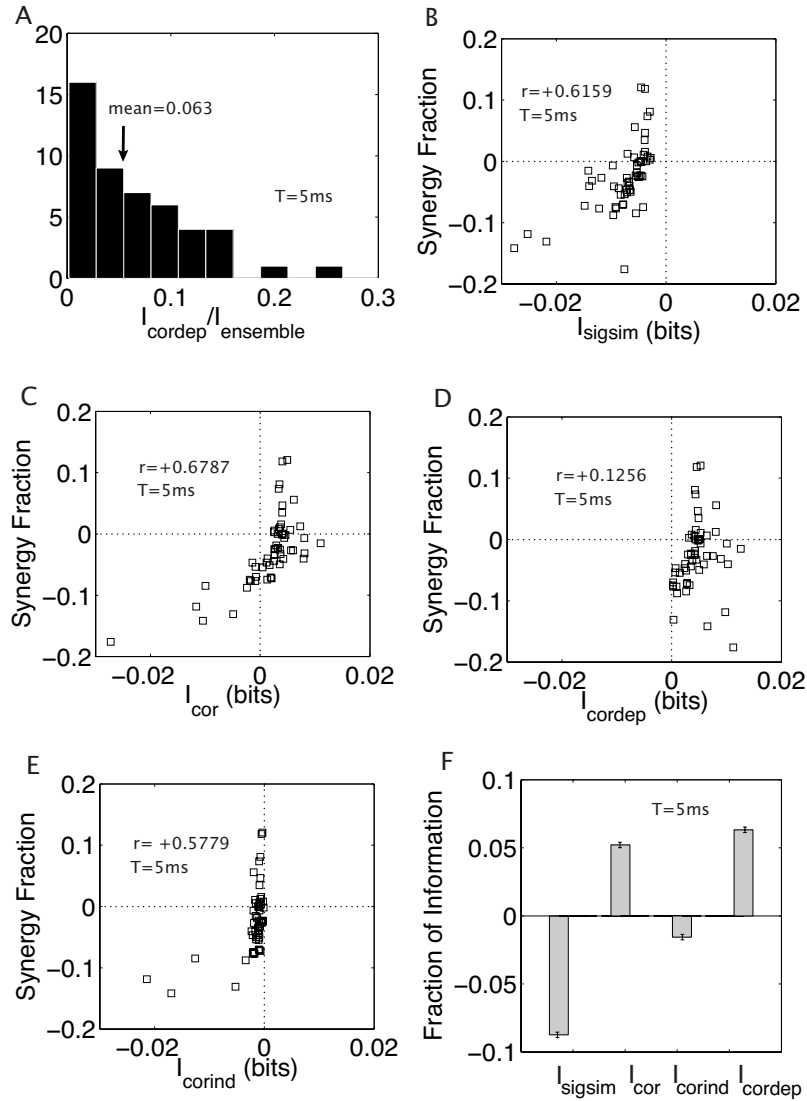


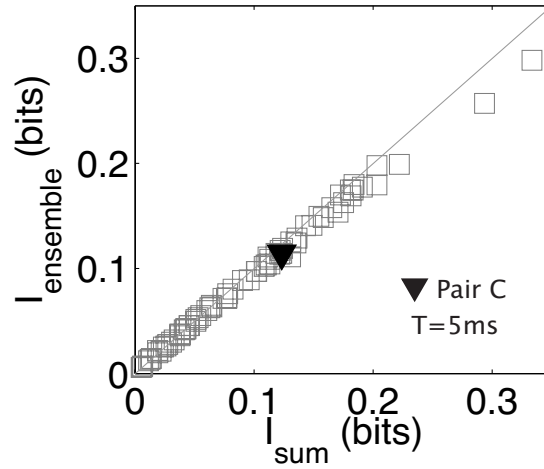
Fig. 3.9: Contrast coding across the population of 71 pairs of cells for which contrast data were available. *A* Histogram of the relative contribution of I_{cordep} to the total information for a time window of 5 ms. *B* The relationship between I_{sigsim} , the component reflecting the contribution due to the overlap in tuning curves, and the extent of redundancy as indicated by the negative synergy fraction. *C, D, E* The relationship between the magnitude of each of the correlation components of the information, and the overall extent of synergy, on a pair by pair basis across the entire dataset. *F* A histogram showing the average fraction of information captured by each component across the dataset.

information (Figure 3.9D). While the overall level of correlation (I_{cor} , Figure 3.9C) covaries significantly across the dataset with synergy fraction, I_{cordep} does not (Figure 8D). Much of the correspondence between I_{cor} and synergy/redundancy is accounted for by I_{corind} , which is strongly related to the synergy fraction ($r= +0.58$, $p=1 \times 10^{-5}$; Figure 3.9E). However, notice that this effect is driven by the three outliers in the lower left of Figure 3.9E and if these points are removed the analysis of I_{corind} will lead to results which are more in line with the one obtained for the orientation coding. The effect of the correlation components for contrast is relatively modest: Figure 3.9B,F shows that it is $I_{sigstim}$ that most strongly predicts the level of redundancy ($r=+0.62$, $p=1 \times 10^{-5}$) – indicating that the redundancy substantially arises from the high degree of similarity of all contrast tuning curves (the differing nature of the role of $I_{sigstim}$ in contrast and direction coding is apparent from comparison of Figures 3.6B and 3.9B). I_{cordep} does nevertheless have an effect on the coding regime, in that its lower value for the contrast dataset than the orientation dataset means that for contrast, the redundant effects are not compensated for (comparison of Figures 3.6F, 3.9F). These results are in general affected by the time window used to count spikes. The information is maximal (and redundancy lowest) at $T=2$ ms, a timescale which corresponds to a strong effect of fine timescale synchronization. As the time window is increased, and the effect of spike locking is averaged out, the redundancy increases, reaching a maximal value at 80 ms.

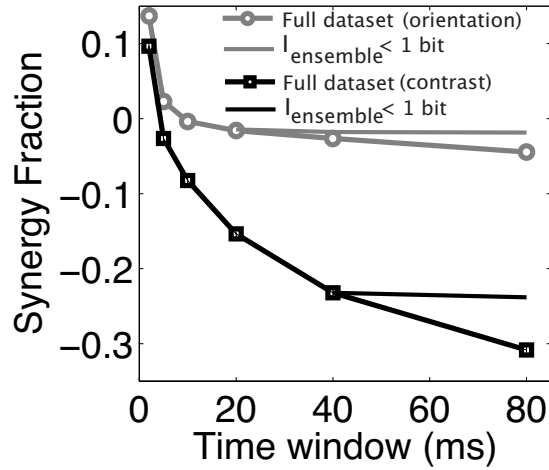
The relative uniformity of the redundancy for the contrast dataset is apparent from Figure 3.10A. Figure 3.10B summarizes the results over the population for the coding of contrast compared to direction coding. The pairs are weakly redundant at 5 ms – however by 40 ms time windows, this has turned into strong redundancy (synergy fraction equal to -0.235 (0.005)). Our findings show that the coding for contrast is more redundant than for direction, regardless of the window of analysis and despite the presence of significant correlation. This is consistent with the general picture that pairs of cells with similar tuning (typically the case for monotonic contrast tuning functions and true for a subset of the direction tuning data) have high correlation but that the coding is largely redundant.

3.4.5 Transfer and autocorrelation functions

Through the last two chapters of this thesis we have used an Information Theoretical approach for discussing the role of correlations between pair of neurons in V1. Another method



A



B

Fig. 3.10: Redundancy is observed across the entire dataset for contrast coding. *A* Even at $T = 5$ ms, redundancy was observed (points below diagonal). The pair marked ‘C’ is that referred to in Figure 3.8. *B* The degree of redundancy in the coding of contrast quickly becomes substantial as the time window is increased. The results for contrast coding are indicated by squares and a black line; the results for direction coding (from Figure 3.4 b) by the grey line and circles.

commonly used for this purpose is the cross correlation. The cross correlation is equal to the transfer function between the pair of neurons convolved with the autocorrelation function of one of the neurons (Papulis and Unnikrishna Pillai 2002),

$$CCG(r_1, r_2, \tau) \propto \sum_t A(r_1, t, \tau) \cdot T(r_1, r_2, t, \tau) \quad (3.22)$$

where r_1, r_2 denote the response (number of spikes in bin) of cell 1 and 2 respectively, and the summation is over time bins t . A and T are respectively the integrands (summands in the discrete notation used here) of the autocorrelation and transfer functions,

$$ACG(r, \tau) = \sum_t A(r, t, \tau) = \frac{\sum_t (r(t) - \langle r(t') \rangle_{t'}) (r(t + \tau) - \langle r(t') \rangle_{t'})}{\sum_{t'} (r(t') - \langle r(t'') \rangle_{t''})^2} \quad (3.23)$$

and

$$TF(r_1, r_2, \tau) = \sum_t T(r_1, r_2, t, \tau) = \sum_t \frac{r_2(t + \tau) - \langle r_2(t') \rangle_{t'}}{r_1(t + \tau) - \langle r_1(t') \rangle_{t'}} \quad (3.24)$$

The cross-correlation can also similarly be written as the sum over a summand C

$$CCG(r_1, r_2, \tau) = \sum_t C(r_1, r_2, t, \tau) = \frac{\sum_t (r_1(t) - \langle r_1(t') \rangle_{t'}) (r_2(t + \tau) - \langle r_2(t') \rangle_{t'})}{\sqrt{\sum_t (r_1(t) - \langle r_1(t') \rangle_{t'})^2} \sqrt{\sum_t (r_2(t) - \langle r_2(t') \rangle_{t'})^2}} \quad (3.25)$$

The transfer and the autocorrelation functions were calculated for finite bins (typically of 5 ms duration) using Matlab (Mathworks, Natick, MA, USA) functions *tf* and *xcorr*.

In order to gain a better understanding of how stimulus dependence might affect the transfer and autocorrelation functions, and to relate this to the information measure of correlations I_{cordep} , we will discuss the behaviour of these functions for a few representative pairs of cells in our data set.

Figure 3.11 shows the transfer and autocorrelation functions for two different stimuli (this pair of cells correspond to the one labelled as Pair A). Figure 3.11: A, C and E shows the

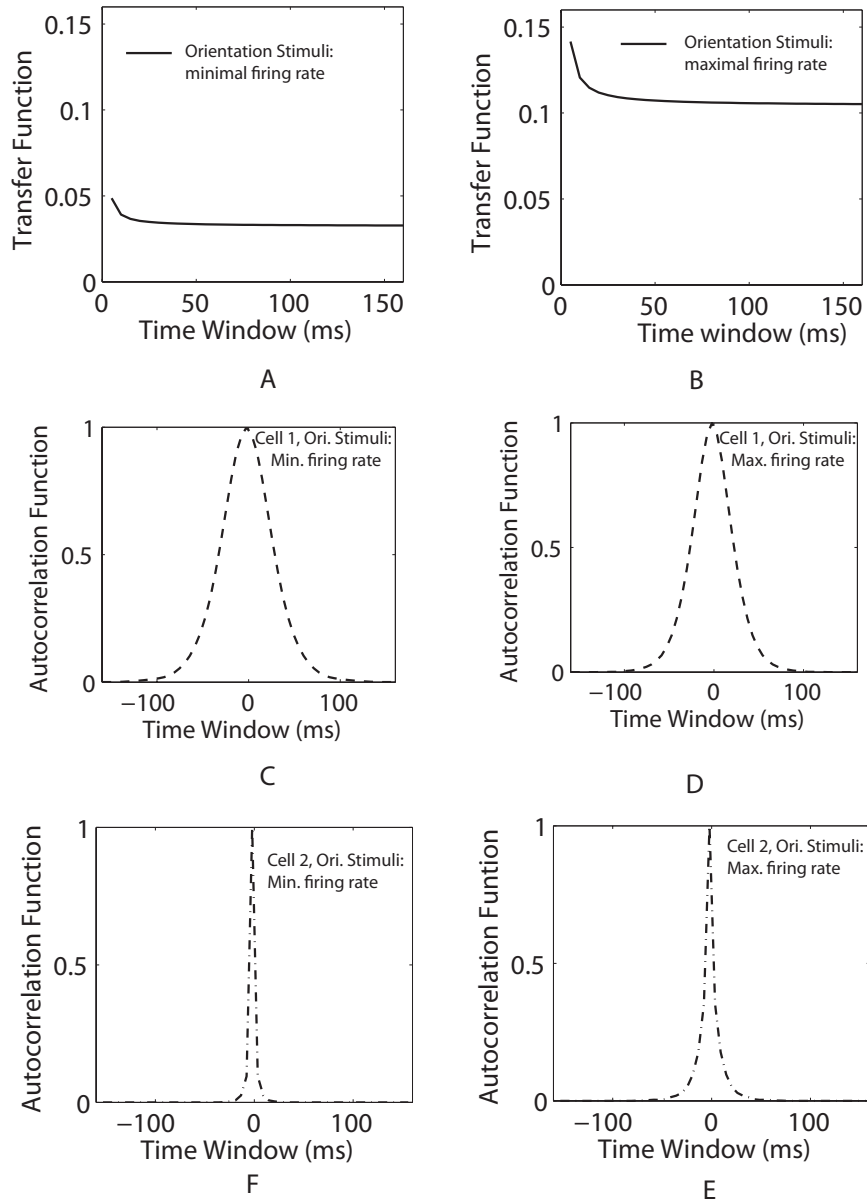
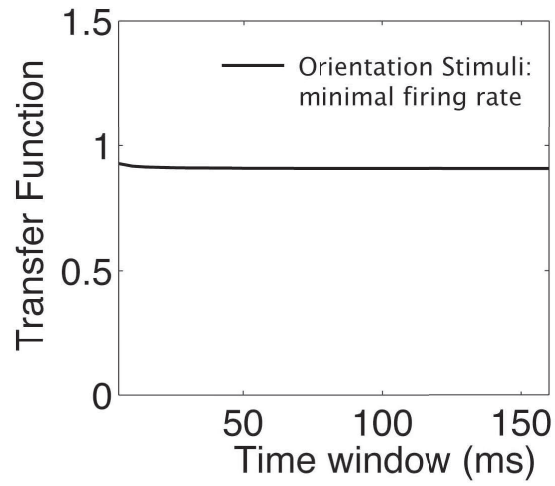


Fig. 3.11: A, B, Transfer function between pair of cells for two different stimuli orientation. C, D Autocorrelation functions for cell 1 for the two different preferred orientation. E, F Autocorrelation functions for cell 2 for two different preferred orientation (Pair A, time window fixed at 160 ms).

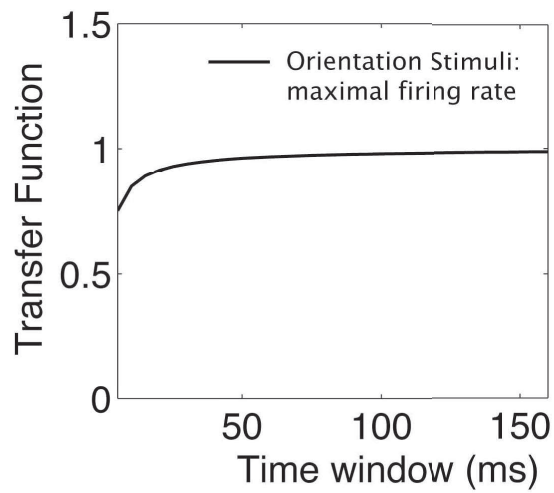
transfer and autocorrelation functions for the stimulus for which the average firing rate is minimal (135 degrees orientation). Figure B, D and F show the transfer and autocorrelation function at the preferred orientation in which the firing rate is maximal (171 degrees). Note that the transfer and the autocorrelation functions are dependent on the stimulus orientation (this can be appreciated in the changes of the width in the autocorrelation function between Figure 3.11:F and E). Transfer functions are essentially transformed by a scale factor. However, both autocorrelation functions change width if the stimulus orientation is changed. For this particular pair of cells (Pair A) the stimulus dependent correlation component I_{cordep} was typically 10 % of the ensemble information.

The results shown in 3.11 are representative of how the transfer and autocorrelation functions behaved in our data set. However, for pairs of cells where I_{cordep} was relatively small (see Figure 3.6D) the stimulus dependence of the transfer function was remarkably lower as shown in Figure 3.12, A and B. These figures shows the transfer function for a given pair of cells, with the smallest I_{cordep} that can be appreciated in Figure 3.6D, for two different set of stimuli (A and B correspond to the orientations with minimal and maximal firing rate respectively). On the other hand, Figure 3.13 A and B shows that the width of the autocorrelation functions is still slightly sensitive to the stimulus changes in orientation. For this particular pair of cells I_{cordep} was typically about 3% of the ensemble information.

Hence, even if the cross covariance and the stimulus dependent correlation component I_{cordep} are both good measures of correlation, a one to one relationship cannot be established between them. The cross covariance may show stimulus dependence through the transfer and the autocorrelation functions, or through only one of them. Moreover, in cases where the stimulus dependence in the transfer function is small, the cross covariance may still show stimulus dependence through the autocorrelation functions. We showed in particular two pairs of cells, one with relatively high and one with relatively low I_{cordep} . As might be expected if the effects are "real", the transfer function shows greater stimulus dependence in the case where I_{cordep} is larger; with small I_{cordep} , there was less dependence of the transfer function on the stimuli. However, there were dependences of the autocorrelation on the stimuli, so the picture is by no means simple.

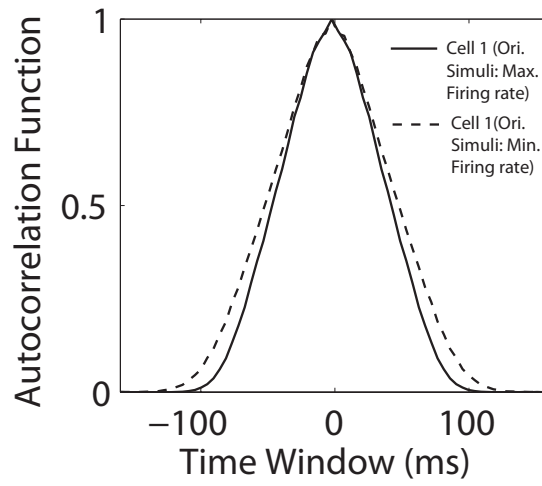


A



B

Fig. 3.12: A, Transfer function between pair of cells for the minimum, and B for the maximum firing rate (pair of cells with the smallest I_{cordep} value which can be found in Figure 3.6D, time window fixed at 160 ms).



A

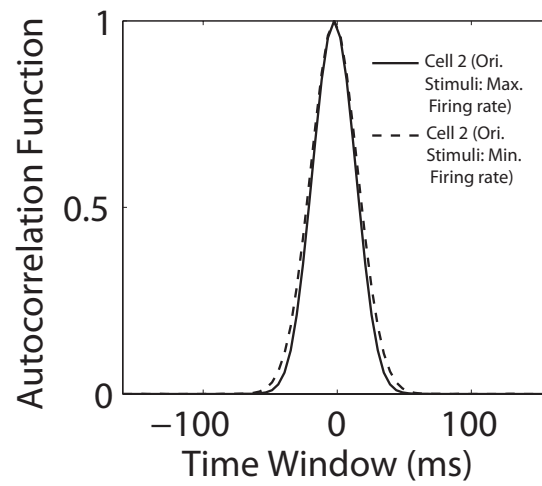


Fig. 3.13: A, B Autocorrelation functions for two different preferred orientation (pair of cells with the smallest I_{cordep} value which can be found in Figure 3.6D , time window fixed at 160 ms)

3.4.6 Information rate

Mutual information quantifies how faithfully the responses measured over some defined time period represent the stimuli. If we know exactly when and for how long the necessary information is present in a set of neuronal spike trains, then calculating the mutual information from this time period is exactly what we should do. In the absence of this knowledge (but armed with some general idea), a safe option is to compute the mutual information over a range of timescales.

Many authors wish to calculate a quantity representing the average information performance (typically as a rate in bits/sec) over some long time period (Borst and Theunissen 1999). Since on relatively short timescales, responses from different timescales are not independent, the mutual information values calculated from one time window and the following cannot be simply added: thus for short timescales, the information rate cannot be obtained simply by dividing the information by the time window (bin) in which it is calculated. A better estimate of the information rate might be obtained by calculating the information from both the first and the second time bins (we could say with a wordlength $L = 2$); a better still from three bins ($L = 3$), and so on.

$$cI_{rate}(R; S) = \lim_{L \rightarrow \infty} H(r_{i+1}, \dots, r_{i+L})/L - \lim_{L \rightarrow \infty} H(r_{i+1}, \dots, r_{i+L} | S)/L \quad (3.26)$$

$$= \lim_{L \rightarrow \infty} I(r_{i+1}, \dots, r_{i+L}; S)/L \quad (3.27)$$

$$(3.28)$$

and has units of bits per second.

In Figure 3.14, we show the calculation of the information rate for the same typical pairs of cells that we have been considering in the manuscript, by plotting the information at wordlength L divided by the total time window considered. The asymptote defines the information rate; the data has been fit with the function $y = 1/xa + c$ for illustrative purposes. The figure illustrates the use of this approach for determining the asymptotic information rate in a neural system.

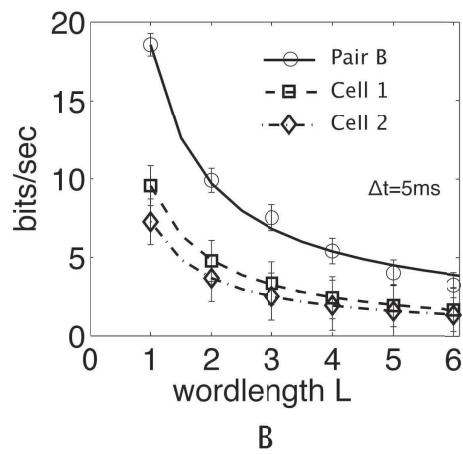
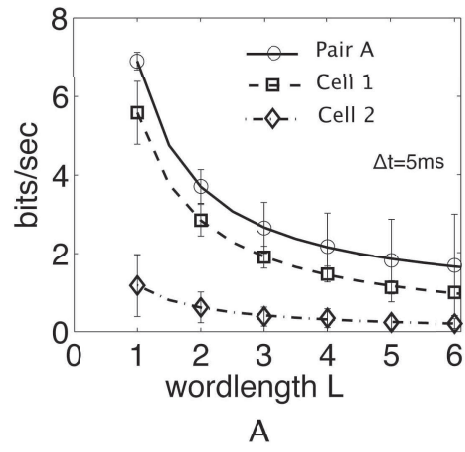


Fig. 3.14: Calculating asymptotic information rates. A, B. Information rate estimates at different word lengths for Pair A and for individual neurons, with bin widths $t=5\text{ms}$. The information rate is the limit of these curves as L approaches infinity.

3.5 Discussion

We have found that for direction coding the information available by being precise about spike timing for pairs of neurons in V1 adds super-linearly. But as the timescale becomes more coarse, information about direction adds slightly sub-linearly across pairs of cells in agreement with a previous information theoretic study of V1 cells (Reich et. al. 2001). We have revealed the origin of these effects by our information component analysis, which shows a redundant (negative) contribution to the information due to the overlap in tuning and to the average level of correlation (i.e. stimulus independent correlation). However, these components are balanced on average by a contribution from stimulus-dependent synchrony.

It is usually accepted that visual scene contains features such as edges and homogenous color patches, which give rise to statistical dependencies between neighboring regions of the visual image (Field 1987). To reduce redundancy, the visual system might use these features as a basis for representing visual input (Barlow 2001). The mammalian visual system is believed to efficiently encode natural visual information. One way in which it might do this is by reducing the redundancy of the representation at successive stages of processing (Attneave 1954; Barlow 1959).

Our results have showed that synergy was stronger (and redundancy weaker) for pairs of neurons with dissimilar tuning curves. Pairs of neurons with overlapping spatial receptive fields but dissimilar orientation tuning will provide a strong joint response to features such as corners and T-junctions in a visual scene (Das and Gilbert 1999); by comparison, those pairs with similar orientation tuning will be jointly driven best by lines and edges. Our results suggest that the pairwise coding of lines and edges is essentially independent, due to the effects of tuning-related redundancy, whereas the coding of features such as corners should be more synergistic. Analogously, the coding for changes in contrast is strongly redundant, due to the greater inherent similarity of the contrast tuning curves of the neurons in a pair.

To overcome the statistical inefficiency of high activity ratio distributed representations, which are the typical product of redundancy reduction code, one needs representations with minimum overlap. This is, representations with the minimum number of elements active in both inputs in pair of cells that need to be distinguished. However, our finding suggest that stimulus dependent correlations can help the neural code to overcome this problem. The

fact that the synchronization depends on the stimulus direction is critically important for coding: it serves to reduce the redundancy caused by cells having similar tuning. In our experiments we used direction stimuli that were relatively coarsely spaced (typically 22.5 degree increments). Another study used finer increments of orientation (Samonds et. al. 2003) and found the degree of fine timescale spike synchronization to be exquisitely dependent upon stimulus orientation. Our study might therefore under-estimate the contribution of stimulus-dependent synchrony to the neural population code for direction/orientation.

Contrast response functions of pairs of neurons tend to be fairly similar, and synchrony at lower contrasts is less temporally precise. For both contrast and direction coding, the redundant contributions are dominated by the similarity in tuning, although the redundancy is stronger for contrast. The average level of correlation plays a small redundant effect in both cases. The synergistic contribution of the stimulus dependence of correlations is also lower on average for contrast than for direction coding. Overall, this results in a coding regime more similar to the traditional intuition, in which correlations tend to result in redundancy, and thus limit the number of neurons whose outputs could usefully be combined to represent the stimulus variable. Importantly, the results of our analysis warn strongly against making general statements about the role of correlations in neural coding – as demonstrated here, the effect of correlations can be quite sensitive to both the timescale and the nature of the stimulus parameter that is being studied.

These principles underlying the neural coding of stimulus orientation and contrast were revealed by performing, for the first time, an information component breakdown of V1 neuronal responses. In doing so, it was crucial to use an effective sampling procedure (Nemenman et. al. 2004), to avoid the results being contaminated by residual bias. The sampling approach we took is described in detail in Chapter 4. The information component breakdown rendered transparent the interplay of synergistic and redundant interactions giving rise to the overall result of weakly synergistic coding at short timescales, and independent orientation (and strongly redundant contrast) coding at longer timescales. The information components, first derived for short time windows in (Panzeri et. al. 1999), and extended to arbitrary timescales by (Pola et. al. 2003), relate to terms that have been measured by others (see Schneidman et. al. 2003 for a review). In particular, the stimulus-dependent correlation component, I_{cordep} , is exactly equal to the quantity ΔI computed by (Nirenberg et. al. 2001; Nirenberg and Lathan 2003).

(Schneidman et. al. 2003) raised the importance of the distinction between different kinds of independence in neural coding. A first type of independence (which we will call Type I) is activity or response independence, which might apply if spike trains were truly uncorrelated, i.e. $p(r_1, r_2) = p(r_1)p(r_2)$. A second kind is conditional independence, which might apply if correlated activity could be explained purely by overlap in receptive field properties. This Type II independence notion accounts for the oftmade distinction between “signal” and “noise” correlations – only the former involve Type II dependence. Type III independence is *informational independence*, and applies to the situation when information adds linearly across cells, possibly despite the presence of activity and/or conditional dependencies. This latter case describes the situation for our direction dataset at long timescales, and is a fair description of the situation at short timescales given the weak synergy we observe. However, it is important to note that even a small amount of pairwise informational dependence can have a relatively large effect on the population code for direction (Shlens et. al. 2006; Schneidman et. al. 2006; Averbeck et. al. 2006), even if only pairwise correlations are present. Such an effect can be expected to be even larger if the pairwise correlations are themselves only the second order signature of higher order correlations. Thus deviations from informational independence of the order of 10% may well be of substantial importance.

The primary goal of the current study was to address how synchronisation of spike trains affects the neural coding of drifting gratings of different orientations and contrasts. This leads to an obvious question: what is synchronisation for? A number of theories have been proposed, including temporal binding (Singer and Gray 1995), fine orientation discrimination (Samonds et. al. 2003; Samonds et. al. 2004) and contour integration (Samonds et. al. 2006). Our results suggest a new role for stimulus-dependent synchronization: to create a coding regime that allows sensory information to be pooled across a neuronal population in a linear (i.e. informationally independent) or even super-linear way despite the presence of redundancy in the signals conveyed by individual cells (i.e. their similarity in tuning). This may be an important role, particularly if the redundancy is a necessary feature of cortical circuitry rather than an imperfection. Because redundancy can lead to improved robustness through fault-tolerance, it may well be desirable. By balancing this redundancy with stimulus-dependent synchronization, the brain could take advantage of both the robustness provided by redundancy and the accuracy due to pooling allowed by informational indepen-

dence.

We find that destroying the identity of which neuron fired each action potential results in a substantial loss in information about stimulus direction. This provokes the question: how could downstream neurons decode and make use of the positive information contribution provided by the stimulus-dependent synchronization? Simple linear readout schemes such as the population vector (Georgopoulos et. al. 1986) can not: a nonlinear readout algorithm is required, such as the nonlinear population vector (Shamir and Sompolinsky 2004). This does not address how such a readout should be implemented, however, and the implementation constraints are particularly severe if one considers that the information should be usable within a single neuronal layer, as opposed to a multi-layer network. An integrate-and-fire operation would effectively pool input spikes regardless of origin, thus being subject to the (Zohary et. al. 1994) limitations on combining information from correlated input neurons. Nonlinear dendritic summation (Hausser and Mel 2003) would thus appear to be a necessary feature for the biophysical implementation of a decoder capable of making use of the additional information contribution.

3.5.1 *An useful Mechanism for surviving*

Discovering the statistical structure of sensory messages is important. The best way to encode information depends enormously on the use that is made of it. If the aim were just to transmit information from one location of the brain to another then redundancy-reducing codes economizing channel capacity would be what only matters. But the brain is not just only a communication system, and we need to survey cases where compression is the best way to exploit statistical structure.

Our findings suggest a new role for stimulus-dependent synchronization: to create a coding regime that allows sensory information to be pooled across a neuronal population in a linear or even super-linear way despite the presence of redundancy in the signals conveyed by individual cells. This is, the neural code should convert hidden redundancy into a manifest, explicit, immediately recognized form, rather than reduce it or eliminate it.

Knowledge of the properties of signals that are behaviorally important for the animal can be used to improve the signal/noise ratio for their detection by matching characteristics of the



Fig. 3.15: Detecting changes in the orientation of tiger stripes (“orientation stimuli”) is vital for the surviving of a primate.

detector with those properties. As much as possible this preserves the stimulus energy and excludes other signal that would contribute with noise. This is important for birds detecting songs of their own species, and similarly for crickets, bats and electric fish.

A similar principle should be applicable from our findings to mammals. In the millisecond that the primary visual cortex of a superior primate processes the movement of a tiger in the forest, the synergy provided for the stimulus dependent synchronization by detecting the change in the orientation of the stripes (Figure 3.15) will be vital for its surviving. The animal must identify what is redundant in the sensory messages from the forest, because statistical regularities in its environment will be also essential for its survival. Redundancy provided by contrast stimuli, by a given visual stimuli in the forest, will help to improve robustness through fault-tolerance. By balancing this redundancy with stimulus-dependent synchronization, the brain could take advantage of both the robustness provided by redundancy and the accuracy due to pooling allowed by informational independence.

3.5.2 Hypercolumns and the physiological origin of synchronization

The hypercolumn is a form of macrocolumn specific to the visual cortex (Hubel and Weisel 1977). The visual cortex contains highly specific types of columns called orientation and ocular

dominance columns, as well as hypercolumns, the merging of more than one macrocolumn. The macrocolumn is a larger unit that consists of many minicolumns. The 'minicolumns' are highly repetitive and complex local network that contains within them the elements for redundancy. Cells in the column are excited by incoming stimuli with only small latency differences. However, different species reveal different types of columns in different regions of the brain.

Cortical neurons with similar stimulus selectivity are generally organized in columns that span the whole cortical depth (Mountcastle 1997). Panzeri et. al 2003 have found that the differences in the response properties of neurons located within the same column are not essential for representing salient stimulus features. This is, the columnar organization could act as a framework to facilitate pooling with minimal information loss. But, across-column pooling leads to information loss. Pooling can be an effective strategy for decoding stimulus location when restricted to individual cortical columns: all the information conveyed about principal whisker stimulation is preserved by the operation of within the column pooling. Moreover, they have shown that if a neuronal population is localized within a column, then each neuron in the population carried similar messages and their activity could be "averaged" together without any information loss. If the neurons were located in different somatosensory columns, then each neuron provided independent and unique information, so that "averaging" neurons on this spatial scale would lead to a huge information loss. Thus, cells in rat somatosensory cortex may convey information about the site of the whisker stimulation precisely by taking advantage of the column in which they are located. These findings suggest that columnar organization of barrel cortex serves to facilitate decoding of the location of the stimulated whisker (Panzeri et. al 2003).

(Hubener et. al. 1997) suggested that rather than to envisage the visual cortex as containing identical modules, it should be viewed as being composed of mosaics of functional domains with different properties arranged non-randomly. It has been proposed that the visual system reveals a columnar organization for an array of tasks, in what is referred to as multiple columnar systems (Hubener et. al. 1997). It is also reasonable to expect that spike activities between excitatory cells in the same column exhibit strong synchronization and sharp orientation selectivity. A study on feedforward inhibition in mouse barrel cortex closely links excitation and inhibition to the function of a column (Porter et. al. 2001). After an initial volley of excitation, input from the thalamus excites inhibitory inter-neurons, which then

fire on short latency. In this particular experiment it has been also found that thalamo-cortical excitation and inhibition work in synchrony, utilizing the most important sensory information while suppressing weaker or distracting inputs.

Our findings show how synchrony between single pairs of nearby neurons in primary visual cortex (V1) of macaque monkeys can be affected by very basic stimulus manipulations as orientation and contrast. Destroying the identity of which neuron fired each action potential resulted in a substantial loss in information. To overcome the statistical inefficiency of high activity ratio distributed representations, there are needed representations with minimum overlap. The neural code should convert therefore hidden redundancy into an obvious, clear and exact, straightaway recognized form, rather than reduce it or exclude it. Our findings indicate that stimulus dependent correlations can create a coding regime that allows sensory information to be pooled across a neuronal population in a linear or even super-linear way despite the presence of redundancy in the signals conveyed by individual cells (by cells having similar tuning) (Montani et. al. 2007b).

Understanding better how columns work depends much on the knowledge of the functioning of local inhibitory circuits. In chapter V we will present a computational model to study how simple focal abnormalities in GABAergic modulators affect information transmission in a population of neurons.

4. TOWARDS AN ALTERNATIVE MEASURE OF SPIKE CORRELATIONS

To evaluate how reliably one can decide if a given response on the population coding of sensory information comes from the full distribution, or from the product of independent distributions from each cell, we used recorded responses of pairs of single neurons in primary visual cortex of macaque monkey (V1) to stimuli of varying orientation (Kohn and Smith 2005). In this chapter we consider the Jensen-Shannon Divergence (JSD) as a distance measure of neuronal spike correlations and we discuss the advantages of this measure in comparison to KL. We applied this Divergence for fixed stimuli as a measure of discrimination between correlated and independent firing of pairs of cells in the primary visual cortex. The Nemenman-Shafee-Bialek estimator was used in our entropy estimation in order to remove all possible bias deviation from our calculations. We found that the relative Jensen-Shannon Divergence (measured in relation to case in which all cell fired completely independently) decreases with respect to the difference in orientation preference between the receptive field from each pair of cells. Our finding indicates that the Jensen-Shannon Divergence can be used for characterizing the effective circuitry network in a population of neurons.

4.1 *Introduction*

In their pioneering work Gauss and Riemann pointed out that one of the bases of geometry is the concept of distance between points in a given space (differentiable manifold, in modern terminology). According to their conceptions, the distance function (metric) determines all the geometrical properties of the space. More specifically, in mathematics, a metric space is a set where a notion of distance between elements of the set is defined. The metric space which most closely corresponds to our intuitive understanding of space is the 3-dimensional

Euclidean space. The Euclidean metric of this space defines the distance between two points as the length of the straight line connecting them. Topological spaces are mathematical structures that allow the formalization of concepts such as convergence, connectedness and continuity (Dugundji 1966; Kelley 1975). The conventional definition of a metric over a topological space specifies how separated two given points are. An alternative to the formal definition of a topological metric can also be applied to collections of more than two elements, i.e, to probability distributions (Amari and Nagaoka 2000; Wolpert 2004).

Distance functions are used in natural sciences as measures of content of a given shape or structure. They are useful tools for quantitative evaluation of the degree of similarity, shape content and symmetry with respect to an "ideal referent shape". Moreover, distance measures also play a fundamental role in statistical sciences. One of the important issues in applications of statistics and probability is finding appropriate probabilistic metrics of distance or affinity between probability distributions. In the previous chapter we used Kullback-Leiber divergence for characterizing stimulus dependency correlations in an ensemble of neurons (Nirenberg and Latham 2003; Pola et. al. 2003; Montani et. al. 2007b). Indeed, a number of divergence/information measures have been proposed as measures of discrimination or distributional similarity between probability distributions. Different measures such as Kullback-Leibler divergence, Jensen-Shannon distance (Rosso et. al. 2004; Rosso et. al. 2006), variation distance (Goldstein and Reinert 2006), Hellinger distance (Ouagnina 2003), chi square divergence (Broniatowski and Leorato 2006), Bhattacharyya (Choi and Lee 2003) distance have been applied in a variety of disciplines .

However, in probability theory and statistics, Jensen-Shannon distance is one of the most popular methods of measuring the similarity between two probability distributions. Jensen Shannon Divergence is a symmetrized and smoothed version of the all important divergence measure of Information Theory. It is a universal measure that provides interesting interpretations of information transmission (Grosse et. al. 2002). In this chapter we will use Jensen-Shannon distance as a discrimination measure between pairs of correlated cells in the primary visual cortex.

The importance of identifying appropriate measures of correlations and independence and quantifying their relation to the stimulus has been pointed out by (Schneidman et. al. 2003). To evaluate how reliably one can decide if a given response on the population coding of

sensory information comes from the full distribution, or from the product of independent distributions from each cell, we used recorded responses of pairs of single neurons in primary visual cortex of macaque monkey (V1) to stimuli of varying orientation which were presented in the previous chapter (Kohn and Smith 2005).

The results presented in this chapter were published in the American Institute of Physics Conference Proceedings (Montani et. al. 2007c).

4.2 Methods

Let's consider that a discrete distribution with probability function P_i represent data, observations, or a precisely calculated probability distribution. Suppose a second discrete distribution with probability function Q_i represents a theory, a model, another set of observations, or even an approximation of P_i . The KL divergence of P from Q is defined as,

$$D_{KL}(P||Q) \equiv \sum_{i=1}^n P_i \log_2 \left\{ \frac{P_i}{Q_i} \right\} , \quad (4.1)$$

The Kullback-Leibler divergence is a divergence measure between the two probability densities. It is a convex function of P_i , is always nonnegative, and equals zero only if $P_i = Q_i$. But, notice that the Kullback-Leibler divergence is not a distance metric since it is not symmetric and does not satisfy the triangle inequality (Grosse et. al. 2002). This kind of argument can be applied to any distance measures which account for the quotient or the difference between two probability densities P and Q .

Let's remember that Shannon entropy is defined as,

$$H(P) = - \sum_i P_i \log_2(P_i), \quad (4.2)$$

and consider a mixture of probability distributions,

$$P_{mix} = \sum_i \beta_i P_i, \quad (4.3)$$

where the coefficients are non negative and sum to 1. Introducing eq.(4.3) in the entropy function we can rewrite

$$H\left(\sum_i \beta_i P_i\right) = \sum_i \beta_i H(P_i) + \sum_i \beta_i D_{KL}(P_i \| P_{mix}), \quad (4.4)$$

and the concavity of the entropy function

$$H\left(\sum_i \beta_i P_i\right) \geq \sum_i \beta_i H(P_i). \quad (4.5)$$

is confirmed. Hence, it follows $D_{KL}(P \| Q) \geq 0$.

Notice that eq(4.4) can be rewritten as

$$H\left(\sum_i \beta_i P_i\right) - \sum_i \beta_i H(P_i) = \sum_i \beta_i D_{KL}(P_i \| P_{mix}), \quad (4.6)$$

and the left hand of eq(4.6) equation is the Jensen Shannon Divergence related to the mixture $\sum_i \beta_i P_i$. We define therefore the *general JSD* as (Lin 1991; Topsøe 2000),

$$JSD\left(\sum_i \beta_i P_i\right) = \sum_i \beta_i D_{KL}(P_i \| P_{mix}). \quad (4.7)$$

In the following we are going to discuss an interpretation of this quantity. Let's assume that an observer did not know how to discriminate between two probability distribution P and Q he/she would take advantage therefore of doing an average over $D_{KL}(P_\beta \| Q)$.

According to the compensation identity which is an identity of important significance in optimization problems (Matz and Duhamel 2004),

$$\sum_i \beta_i D_{KL}(P_i \| Q) = \sum_i \beta_i D_{KL}(P_i \| P_{mix}) + D_{KL}(P_{mix} \| Q) \quad (4.8)$$

and the minimum likelihood estimate correspond to $P_{mix} = Q$ and $\sum_i \beta_i D_{KL}(P_i \| P_{mix})$ is the corresponding minimum value, and therefore this quantity may be interpreted as the "minimum redundancy" (Topsoe 2000). Moreover, for any fixed Q

$$D_{KL} \left(\sum_i \beta_i P_i \| Q \right) \leq \sum_i \beta_i D_{KL}(P_i \| Q) \quad (4.9)$$

which proves that this quantity is a convex function.

In particular, by choosing $JSD(\frac{P}{2} + \frac{Q}{2})$ we reduce eq(4.7) to the Jensen Shannon distance between two distributions P and Q ,

$$D_{JSD}(P \| Q) = \frac{1}{2} D_{KL}(P \| G) + \frac{1}{2} D_{KL}(Q \| G) \quad (4.10)$$

where $G = \frac{P}{2} + \frac{Q}{2}$, and D_{KL} is the Kullback-Leibler divergence between the two distributions. Notice that eq.(4.10) can be directly related to the J -divergence (Johnson and Sinanovic 2001).

The JS is a distance measure between probability distributions and was introduced by Rao (1987)(Rao 1987) and Lin (1991) (Lin 1991) as a symmetrized and smoothed version of the Kulback-Leibler divergence. Kullback-Leibler divergence $D_{KL}(P \| G)$ can be considered as the inefficiency assuming that the true distribution is G when it is really P . JS can be interpreted therefore as the minimum inefficiency distance where P and Q correspond to two independent distributions (Endres and Schindelin 2003). We are assuming that P and Q are two discrete probability distributions. However, the extension to the continuous case is straightforward.

For completeness we will gather the mathematical properties of the Jensen Shannon distance in the following paragraphs.

(1) JSD is positive defined

$$D_{JSD}(P \| Q) \geq 0 \quad (4.11)$$

notice, JSD is equal to zero if and only if $P = Q$.

(2) JSD is symmetric in its arguments, i.e.,

$$D_{JSD}(P \| Q) = D_{JSD}(Q \| P). \quad (4.12)$$

(3) JSD is always well defined (Endres and Schindelin 2003).

(4) Its square root verifies the triangular inequality,

$$\sqrt{D_{JSD}(P\|Q)} \leq \sqrt{D_{JSD}(P\|G)} + \sqrt{D_{JSD}(G\|Q)}. \quad (4.13)$$

and JSD is the square of a metric that is equivalent to the Hellinger metric (Majtey et. al. 2005).

(5) \sqrt{JSD} is true metric for the probability distribution space (Endres and Schindelin 2003).

(6) JSD can also be interpreted as the capacity of a noisy information channel with two inputs giving the output distributions P and Q .

(7) JSD can be generalized to quantify the divergence between an arbitrary number of points.

J. Lin proposed a generalization of JSD as a distance for several probability distributions. In fact, let $P_1(x), \dots, P_N(x)$ be a set of probability distributions and let π_1, \dots, π_N be a collection of non-negative numbers such that $\sum_i \pi_i = 1$. Then the JSD of the probability distributions $P_i(x)$ with $i = 1, \dots, N$ is defined by

$$\mathcal{D}^{(\pi_1, \dots, \pi_N)}[P_1, \dots, P_N] = H \left[\sum_{i=1}^N \pi_i P_i \right] - \sum_{i=1}^N \pi_i H[P_i]. \quad (4.14)$$

A remarkable feature of this generalized JSD is that it is possible to assign different weight to each probability distribution P_i .

(8) It is a natural link between Information Theory and Geometry. Mutual Information is equal the JSD in the case in which we are considering just two stimuli.

Unlike other divergence measures, the JSD does not require the condition of absolute continuity for the probability distributions involved. JS distance it is always well defined and bounded and its square root is a true metric for the probability distributions space (is symmetric, and it verifies the triangle inequality) (Endres and Schindelin 2003). Moreover, Jensen Shannon Distance is a symmetrized and smoothed version of the Kullback-Leibler divergence the most used divergence measure of Information Theory (Pola et. al. 2003; Nirenberg and Latham 2003; Montani et. al. 2007b). In general, the measure of discriminability between two stimuli s_1 and s_2 is the JSD between $P(r|s_1)$ and $P(r|s_2)$.

The Jensen-Shannon divergence can be considered as a measure distance between the corresponding probability distribution function associated with each spikes fired observed patterns. The Jensen-Shannon divergence measures how reliably one can decide if a given

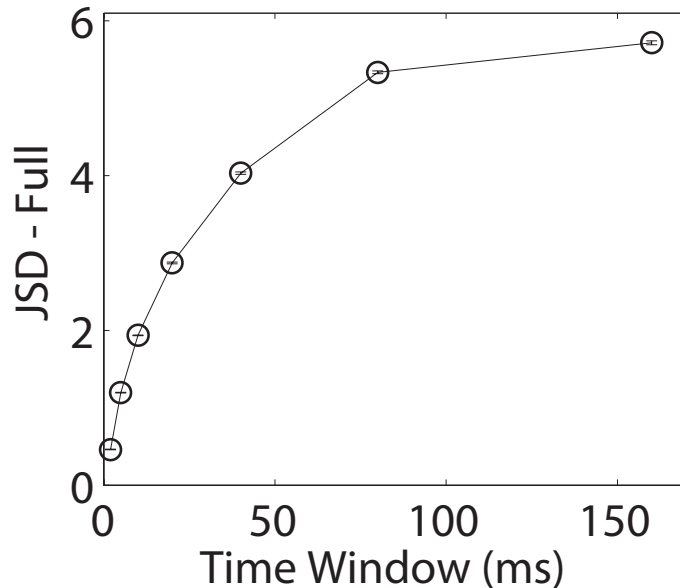


Fig. 4.1: For a typical pair of cells in V1 the JSD was calculated taken into account the full stimuli orientation dependency at seven different time windows (named as JSD Full).

response comes from the full distribution, $p(r_1 r_2)$, or the product of independent distributions, $p(r_1) \cdot p(r_2)$. In the present chapter we use the Jensen-Shannon Divergence for fixed stimuli as a measure of discrimination between pairs of correlated cells in the primary visual cortex of anesthetized macaque monkeys (Kohn and Smith 2005). Our findings indicates that the Jensen-Shannon Divergence may be used for characterizing the circuitry network in a population of neurons (Montani et. al. 2007c).

4.3 Results

We use the Jensen-Shannon divergence (JSD) taking $G = \frac{P+Q}{2}$ as (Rosso et. al. 2004; Rosso et. al. 2006),

$$JSD(P\|Q) = \frac{1}{2} \left[D_{KL} \left(P \parallel \frac{P+Q}{2} \right) + D_{KL} \left(Q \parallel \frac{P+Q}{2} \right) \right], \quad (4.15)$$

where D_{KL} is the Kullback-Leibler divergence between the two distributions.

The JSD allows us to decide how reliably one can decide if a given response comes from two different distributions. However, unlike the Kullback-Leibler divergence, it is symmetric,

always well defined and bounded. In particular if we choose $P \equiv P(r|s)$, the probability of getting response vector r conditional upon the occurrence of stimulus s , and $Q \equiv P_{ind}(r|s)$, the probability of getting independent population responses,

$$\begin{aligned}
JSD(P||Q) &= \frac{1}{2} \sum_{r_1, r_2} \sum_s P(s) P(r_1 r_2 | s) \log_2 P(r_1 r_2 | s) - \frac{1}{2} \sum_{r_1, r_2} P(r_1 r_2) \log_2 P(r_1 r_2) \\
&+ \frac{1}{2} \sum_{r_1, r_2} \sum_s P(s) P_{ind}(r_1 r_2 | s) \log_2 P_{ind}(r_1 r_2 | s) - \frac{1}{2} \sum_{r_1, r_2} P_{ind}(r_1 r_2) \log_2 P_{ind}(r_1 r_2) \\
&+ \sum_{r_1, r_2} \sum_s P(s) P_{mix-all}(r_1 r_2 | s) \log_2 P_{mix-all}(r_1 r_2 | s) \\
&- \sum_{r_1, r_2} P_{mix-all}(r_1 r_2) \log_2 P_{mix-all}(r_1 r_2). \tag{4.16}
\end{aligned}$$

where $P(r_1 r_2) = \sum_s P(s) P(r_1 r_2 | s)$ and $P_{ind}(r) = \sum_s P(s) P(r_1 | s) P(r_2 | s)$ are the average of $P(r|s)$ and $P_{ind}(r|s)$ over all the possible stimuli ($P(s) = \frac{1}{S}$).

We named $P_{mix-all}(r_1 r_2 | s) = \frac{P_{ind}(r_1 r_2 | s) + P(r_1 r_2 | s)}{2}$, and $P_{mix-all}(r_1 r_2) = \frac{P_{ind}(r_1 r_2) + P(r_1 r_2)}{2}$. By fixing the stimuli we can use the Jensen-Shannon divergence to measure how reliably one can decide if a given response comes from $P(r_1 r_2 | s_{fix})$, or $P_{ind}(r_1 r_2 | s_{fix})$. Comparing the JSD for pairs of correlated $P(r|s)$ and uncorrelated $P_{ind}(r|s)$ cells at a fixed stimuli, one can ask how much information one can gain about the effective network between cells.

Notice that eq.(4.16) is completely made up of Shannon entropies. Hence, having exactly expressed all of the quantities necessary to perform estimation of the Jensen-Shannon distance in terms of entropies of particular (in some cases conditional) distributions, these (six) entropies contributions are computed by inserting the respective distributions into the NSB entropy estimation routine. Thus, we can exactly apply the NSB entropy estimator without any kind of additional approach, which also constitutes a significant advantage with respect to the use of the KL divergence.

The concept of resistor average distance was defined in a similar framework by Johnson (Johnson and Sinanovic 2001). This was later used by Samonds et. al. 2003, who named "KL distance" to one half of the resistor average distance defined by Johnson and Sinanovic 2001. The resistor average is symmetric and one half of the resistor average provides a close approximation of the Chernoff distance (Johnson and Sinanovic 2001). It equals the harmonic sum (half of the harmonic mean) of the component KL distances.

This is, the resistor average and JSD are not exactly the same distant measures, and they

may well lead to different conclusions. The procedure used by Samonds et. al. 2003 to estimate the bias and to provide confidence to the measures was the bootstrap method. JSD is more closely related to the intuitive concept of "geometric mean" (see eq (4.7)). More importantly, notice that we can estimate JSD using the NSB entropy estimator without any kind of additional approach.

In order to evaluate how reliably one can decide if a given response on the population coding of sensory information comes from the full distribution, $P(r_1 r_2 | s_{fix})$, or from the product of independent distributions from each cell, $P_{ind}(r_1 r_2 | s_{fix})$, we used recorded responses of 42 pairs of single neurons in primary visual cortex of macaque monkey (V1) to stimuli of varying orientation. The experimental methods can be found in (Kohn and Smith 2005). They collected data from single pairs of cells in primary visual cortex. For each neuron, they first determined the preferred orientation and direction. This was done quantitatively by measuring the responses to sinusoidal gratings drifting in different directions (Kohn and Smith 2005), centered on the receptive field as determined by initial mapping (Kohn and Smith 2005).

Figure 4.1 shows the Jensen-Shannon divergence for one single pair of cells in V1 (Kohn and Smith 2005) using the NSB entropy estimator (Nemenman et. al. 2004) at different time windows. The Jensen Shannon divergence was calculated taking the full orientation dependency on both probabilities distributions. Plateau like behavior can be appreciated in the Jensen-Shannon as time window becomes bigger.

In Figure 4.2 we present the Jensen-Shannon Fraction for 42 pairs of single neurons V1 at fixed stimuli orientation as function of the difference in orientation preferences from the tuning curves obtained by each pair of cells (time window fixed at 5 ms). We define the Jensen-Shannon fraction as the minimum JS divergence obtained by fixing the stimuli in a given set $S = s_1, s_2, \dots, s_i$ divided by its maximum in an ensemble of neurons $JSD - Fraction = \frac{JSD(P,Q)_{min-s}}{JSD(P,Q)_{max-s}}$. Pairs of cells with similar preferred orientations present a higher JSD-Fraction than those that showed less similarities. This result is in agreement with the fact that cells which share similar preferred orientations are more likely to share a higher quantity of common inputs than those that present less similarities. Hence, those cells are more likely to present spikes with a higher degree of synchrony. By estimating the different JSD Fractions, we might be able to reconstruct the effective network in a population of neurons. Our finding suggests therefore that the Jensen-Shannon Divergence could

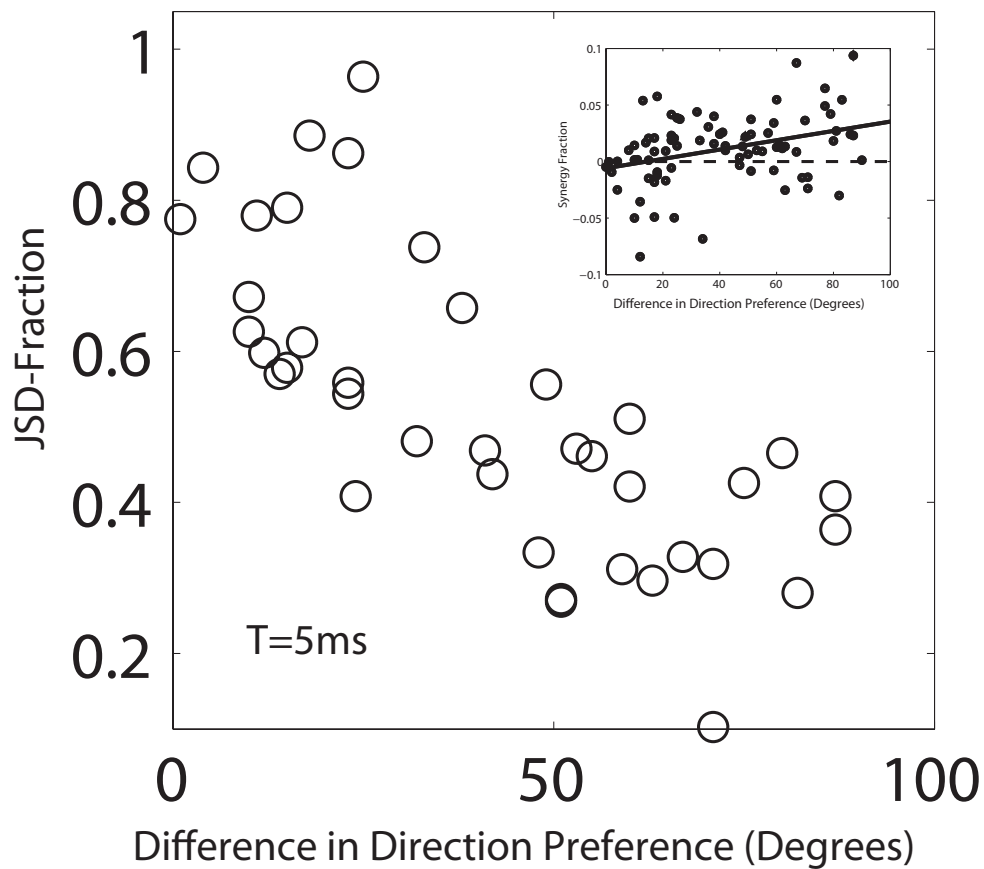


Fig. 4.2: $T = 5 \text{ ms}$, The relative Jensen-Shannon Divergence as a discrimination measure of correlations normalized with respect to its maximum value for this data set. In the upper part of this Figure the Synergy-Fraction is also plotted as function of Difference in Orientation Preference. Notice that cells with similar preferred orientation are more likely to share a higher quantity of common inputs than those that present less similarities.

be used for characterizing the effective circuitry network in a population of neurons.

4.4 Discussion

The present chapter describes the use of the Jensen-Shannon divergence (JSD) to characterize neuronal spike correlations as an alternative quantitative scheme to Kullback-Leibler divergence (KLD). Jensen-Shannon divergence (JSD) is a natural link between Information Theory and Geometry. Mutual Information is equal the JSD in the case in which we are considering just two stimuli. Unlike the Kullback-Leibler divergence (KLD), Jensen-Shannon divergence (JSD) is always well defined and bounded and its square root is a true metric for the probability distributions space (is symmetric, and it verifies the triangle inequality).

The Jensen Shannon Divergence is completely made up of Shannon entropies and therefore the NSB entropy estimator can be exactly applied. This constitutes a significant advantage to avoid bias deviations with respect to another measure of spike correlations which are based in the KL divergence.

We performed NSB method on a relative Jensen-Shannon Divergence for pairs of cells in V1 with stimuli dependence in orientation, considering the relevant timescale for sensory information. By fixing the stimuli we use the Jensen-Shannon divergence to measure how reliably one can decide if a given response comes from the full distribution or the probability of getting independent population responses.

As we discussed in chapter III, in the case of pairs of cells with different orientation preferences, even weak correlation can lead to synergistic coding since the tuning of the cells is less redundant. The temporal correlation comes about from strong common input that presumably also gives rise to strongly overlapping tuning curves. The redundancy that comes about from having similar tuning outweighs the information provided by correlation.

Our findings show that pairs of cells in V1 with similar preferred orientations present a higher relative JS divergence Fraction than those which have less similarities. The use of a relative Jensen-Shannon Divergence at a fixed stimuli provides us with a measure of how much information one can gain about the effective network between cells. We plan to investigate

further these features in a future analysis using a simultaneous multi-recording data set of many neurons.

5. THE ACCURACY OF A NEURAL POPULATION CODE AFTER FOCAL ISCHAEMIA

The underlying origins of synchronized firing between cortical neurons are still under discussion. Inter-cellular communication through chemically mediated synaptic transmission is considered a major contributor to the formation of neuronal synchrony. GABAergic inhibitory neurons may be involved in the generation of oscillatory activity in the cortex and its synchronization. Specifically, reduction of GABAergic inhibition may favour cortical plasticity producing functional recovery following focal brain lesions. Research into neurotransmitter systems is therefore of paramount importance to understand the origins of synchronized spiking. However, it is necessary to understand first how simple focal abnormalities in GABAergic modulators can affect the information transmission in an impaired brain tissue. We present a computational and analytical model of a topographically mapped population code which includes a focal lesion as well as a process for receptive field enlargement (plasticity). The model simulates the recovery processes in the brain, and allows us to investigate mechanisms which increase the ability of the cortex to restore lost brain functions. We have estimated the Fisher Information carried by the topographic map before and after stroke. Our finding shows that by tuning the receptive field plasticity to a certain value, the information transfer through the cortex after the stroke can be optimized.

5.1 *Introduction*

Excitatory neurons in the sensory areas (visual, auditory, and somatosensory) of the brain respond only to stimuli in restricted regions of the sensory field, referred as their receptive fields. However, due to the distributed organization of sensory systems, the representation of sensory objects requires integration of responses across different cortical regions. The reason

is that even basic features of an object are processed in parallel in different, specialized areas of the cortex. The integration should be complemented by mechanisms permitting binding of signals across different sensory modalities, since many objects encountered in the world are multisensory and possess, in various combinations, visual, auditory, haptic, and olfactory properties.

Gamma-aminobutyric acid (usually abbreviated to GABA) is an inhibitory neurotransmitter found in the nervous systems of widely divergent species. It is the most important inhibitory neurotransmitter in the central nervous system and also in the retina. In vertebrates, GABA acts at inhibitory synapses in the brain. GABA acts by binding to specific transmembrane receptors in the plasma membrane of both pre and postsynaptic neurons. This binding causes the opening of ion channels to allow either the flow of negatively-charged chloride ions into the cell or positively-charged potassium ions out of the cell. This will typically result in a negative change in the transmembrane potential, usually causing hyperpolarization. Neurons that produce GABA as their output are called GABAergic neurons, and have major inhibitory actions at receptors in the cerebral cortex of an vertebrate. GABAergic neurons have a major functions in the cortex. They are critically involved in mechanisms of reward, reinforcement and emotional arousal, and can induce recovery of sensorimotor function in the traumatically injured brain. Inter-celular communication through chemically mediated synaptic transmission is considered significant contributor to the formation of synchronized spike firing. The interneural network of GABAergic neurons connected by chemical synapses is a candidate for the generator of synchronized oscillations in the hippocampus (Fukuda et. al. 2000).

On the other hand, glutamate is the most abundant fast excitatory neurotransmitter in the mammalian nervous system. At chemical synapses, glutamate is stored in vesicles. Nerve impulses trigger release of glutamate from the pre-synaptic cell. In the opposing post-synaptic cell, glutamate receptors, such as the NMDA receptor (ionotropic receptor for glutamate), bind glutamate and are activated. Because of its role in synaptic plasticity, it is believed that glutamic acid is involved in cognitive functions like learning and memory in the brain. Glutamate transporters are found in neuronal and glial membranes. They rapidly remove glutamate from the extracellular space. In brain injury or disease, they can work in reverse and excess glutamate can accumulate outside cells. This process causes calcium ions to enter cells via NMDA receptor channels, leading to neuronal damage and eventual cell

death.

Investigations involving humans combining noninvasive recording techniques such as EEG and MEG with advanced methods of time series analysis have revealed that neural synchrony is associated with cognitive functions that require large-scale integration of distributed neural activity. Examples are attention-dependent stimulus selection, multi-modal integration, working memory, selective routing of activity, and conscious processing of stimuli (for a review see Singer 1999, Schnitzler and Gross 2005 and Varela et. al. 2001). Studies performed using novel methods of time series analysis have been developed for the examination of oscillatory brain activity and its synchronization. Spike trains synchrony is related to feature binding, learning and memory (Singer 1999; Borisyuk et. al. 2000a; Borisyuk et. al. 2001). Synchronization of oscillatory responses in the β and γ band is involved in a variety of cognitive functions, such as perceptual grouping, attention-dependent stimulus selection, routing of signals across distributed cortical networks, sensory-motor integration, working memory, and perceptual awareness.

The generation and synchronization of cortical β - and γ -oscillations involves several neurotransmitter systems. GABAergic neurons play a central role in the generation of high-frequency oscillations and their local synchronization, whereas glutamatergic connections appear to control their strength, duration, and long-range synchronization (Traub et al. 2004) and (Wang and Buzsaki 1996). Abnormalities in dopaminergic and serotonergic neurotransmitters are thought to play a central role in the pathophysiology of schizophrenia. But, unusual behavior in GABAergic inhibitory neurons (Lewis et al 2005) and NMDA-receptor dysregulation (Moghaddam 2003) has been also found in patients with schizophrenia. This is, dopaminergic dysfunctions can affect neural synchronization in schizophrenia via dopaminergic action on GABAergic interneurons (Seamans and Yang 2004). Recent evidence indicates a close relation between impaired neural synchrony in schizophrenia and cognitive deficits (Uhlhaas et al. 2006). In addition to chemical synaptic transmission, direct electrotonic coupling through gap junctions between inhibitory neurons may also contribute to the temporal patterning of population activity and, in particular, to the precise synchronization of oscillatory activity (Draguhn et al. 1998; Fukuda et al. 2006 ; Hormuzdi et al. 2001; Nase et al. 2003; Traub et al. 2001).

Several authors have recently proposed that cortical networks in autism may be character-

ized by an absence of a biological equilibrium between excitation and inhibition, which leads to hyperexcitability and unstable cortical networks (Hussman 2001) and (Rubenstein 2003). This hypothesis is consistent with abnormalities in GABAergic and glutamatergic transmitter systems. Indications for reduced GABAergic inhibition have been derived from the evidence that autism is associated with mutations of genes encoding subunits of the GABA receptor (DiCicco-Bloom et al. 2006). Anatomically, there is evidence for both hyper- as well as hypoconnectivity in autism. Abnormal glutamatergic neurotransmission is supported by polymorphisms in genes that encode both metabotropic and ionotropic glutamate receptors (Carlsson 1998) and (Polleux and Lauder 2004).

Epilepsy has been assumed to result from abnormal, hyper-synchronous neural activity. Clinical studies suggest that convulsive epilepsy is often associated with an absence of biological equilibrium between excitatory and inhibitory neurotransmitter systems, causing enhanced excitability. GABAergic interneurons play a critical role in maintaining this balance (Levitt, 2005) and accordingly, convulsive seizures can be suppressed or reduced by enhancing GABAergic transmission (Snead, 1992). As synchronization increases the impact of neural activity in target structures, enhanced GABAergic transmission may, in certain cases, facilitate seizures by inducing synchronous population discharges that then spread very effectively across neighboring networks. In the case of absence seizures which may occur in several forms of epilepsy, GABA-mediated hyperpolarization is essential for the development of the synchronized, low-frequency oscillations. They depend on low-threshold Ca^{2+} channels that are only activated when the membrane potential drops substantially below the average resting level (e.g., (McCormick and Williamson 1989; Huguenard and Prince 1994; Ulrich and Huguenard 1996). However, abnormalities in GABAergic transmission alone may not be sufficient for epileptogenesis in the mature cortex (Khalilov et al. 2005) and, gap junctions may play an important role in the synchronization and propagation of epileptic activity Carlen et al. 2000; Traub et al. 2001.

The role of temporal coordination abnormalities in neuronal synchronization and cognitive dysfunctions is of considerable clinical relevance to a better understanding of brain disorders. Certain brain disorders, such as schizophrenia, epilepsy, autism, Alzheimer's disease, and Parkinson's are associated with abnormal neural synchronization. Moreover, abnormalities in GABAergic inhibitory neurons may be involved in the generation of oscillatory activity and its synchronization (Traub et al. 2004; Wang and Buzsaki 1996). Reduction

of GABAergic inhibition may favor cortical plasticity producing functional recovery following focal brain lesions (Zihl and von Cramon 1985; Suzuki et. al. 2000; Frost et. al. 2003; Reinecke et. al. 2003; Xerri et. al. 1998; Schweigart and Eysel 2002; Rema and Ebner 2003; Nudo and Milliken 1996; Jablonka and Kossut 2006). Research into neurotransmitter systems is of paramount importance not only to understand the underlying origins of synchronized spikes, but also to develop further knowledge of the pathophysiological mechanisms underlying these neuropsychiatric disorders. A better understanding of sensory system information and processing by comparison between impaired and normal brain tissues will be of ultimate help in the understanding cognitive dysfunctions. It is very important to understand therefore how simple focal abnormalities in GABAergic modulators can affect the information transmission in the impaired brain tissue.

Several observations have shown that following stroke, the levels of γ -aminobutyric acid (GABAergic) inhibition in neighboring brain areas drops and others have shown that a reduction of GABAergic inhibition may favor cortical plasticity (Sober et. al. 1997; Carmichael 2003; Frahm et. al. 2004; Schiene et. al. 1999; Eysel and Schweigart 1999). From these findings it has been hypothesized that the brain supports recovery from lesion by decreasing GABAergic inhibition and thereby facilitating plasticity and reorganization of the cortical representation in surrounding areas. The reorganization of neural activity that follows after stroke is very important in producing functional recovery.

Insufficient blood transport to neurons in the brain due to blocked or ruptured blood vessels (stroke) can lead to damage or death of cells, causing functional impairment. Intact neurons surrounding a stroke-like lesion have been shown to adapt to the damage by expanding their sensory receptive fields in the direction towards the lesion, thereby restoring information processing capacity within the cortex. The expansion of the receptive fields can then be explained by the disinhibition caused by reduction in GABAergic modulators. Changes in levels of GABA only affect the inhibitory parts of receptive fields but leave the excitatory parts unaffected. This disrupted balance between excitation and inhibition causes the receptive field to expand asymmetrically from its original position towards the lesion.

5.2 *Topographic mapping of the cortex*

Disturbance of the cerebral blood supply due to blockage or rupture of blood vessels leads to neuronal damage or cell death, resulting in functional brain impairment (stroke). Many who survive a stroke do so with disability. Moreover, there are no effective treatments presently available (McCulloch J. and Dewar D.), and the brain processes that follow transient ischaemic episodes are still poorly understood (Carmichael 2003). This is true not only of the neurochemical cascades initiated by stroke, but also of the functional reorganization that occurs as the brain attempts to adapt to the injury and make optimal use of its reduced computational resources. A mathematical understanding of the principles by which the brain manages its information processing circuitry after injury may help in the development of therapeutic strategies. It may also help us to build machines which make use of this remarkable fault-tolerant aspect of the brain's computing architecture. In this chapter we present a first step towards understanding.

After a lesion in a sensory area of the cortex, neurons in the region of tissue surrounding the lesion tend to show hyper-excitability and enlarged receptive fields (Eysel and Schweigart 1999; Schweigart and Eysel 2002; Fujioka et al. 2004). This functional plasticity is apparent also in the recovery of motor function after stroke-induced impairment (Nudo et. al. 1996, Steinberg and Augustine 1997). Several physiological mechanisms are known to be involved in brain plasticity following a stroke. These include synaptic plasticity (Mittmann 2001), axonal sprouting (Dancause et. al. 2005), synaptogenesis (Stroemer et.al. 1998), neurogenesis (Felling 2003) and disinhibition / peri-infarct hyper-excitability (Sober et. al. 1997; Fujioka et al. 2004). Of these, disinhibition is perhaps the simplest mechanism, and we will thus use it as the basis of the current investigation. Underlying this model of post-stroke plasticity is the observation that after stroke, the level of GABA-ergic inhibition in cortex nearby to the lesion is reduced (Neumann-Haefelin et. al. 1995; Luhmann et. al. 1995; Schiene et. al. 1999; Frahm et. al. 2004). The disinhibition model alone, without rewiring, has been shown to account for many of the features of receptive field changes underlying behavioral recovery (Sober et. al. 1997).

Studying the consequences of stroke in a sensory part of the cortex allows us to examine the effects of stroke on the information processing capabilities of the cortical circuit, due to the topographic mapping of sensory information onto the surface of the cortex, as indicated

by retinotopic and columnar organization. A remarkable feature of sensory cortices in the brain is that the sensory world can be mapped topographically onto the cortical surface. This means that neighboring points in the sensory field evoke activity in neighboring regions of the cortex. Since receptive fields overlap, each point is monitored by a population of neighboring cells, rather than a single cell, and when a point is stimulated the population of neurons whose receptive fields include that particular site are excited.

Thus we are afforded a tool with which to extract principles that will also be relevant to association areas of cortex, but cannot be studied directly due to the more complex (or at least less well understood) representation of information. We will take advantage of this topographic feature of sensory cortex to develop and solve, under particular assumptions a mathematical model of functional recovery after cortical damage. We will use the theoretical approach that has been developed for the study of neuronal population coding (Seung and Sompolinsky 1993; Abbott and Dayan 1999; Deneve et. al. 1999). In this approach, Fisher information is used to measure the accuracy of the population code in representing a sensory variable - typically the orientation of a stimulus. We extend this approach to the calculation of Fisher topographic information - accuracy of representation of the (x, y) retinotopic position of a visual stimulus.

In this chapter, we present a computational model of a topographically mapped population code which includes a focal lesion as well as a process for receptive field enlargement (plasticity). The model simulates the recovery processes in the brain, and allows us to investigate mechanisms which increase the ability of the cortex to restore lost brain functions. Changes in the degree of plasticity of the receptive fields of the neurons, which could potentially be influenced to enhance information transfer through the cortex after stroke, were incorporated into the model. This allowed the exploration of effects resulting from changes in the concentration of this parameter on the level of functional restoration. Neurons close to the damaged region expand their receptive field more than those neurons further away in the cortex.

We developed model of the effect of focal ischaemia on the performance of a neuronal population code, in order to study physiological parameters that could be influenced as to enhance recovery from stroke. Our findings show that recovery of the accuracy of the population code is optimal at a specific amount of receptive field plasticity. This plasticity can be in-

fluenced by changing the level of γ -aminobutyric acid (GABA-ergic) inhibition in the areas surrounding the damaged tissue.

We use Fisher Information in order to calculate how much information a neural response carries about the stimuli. We estimate the Fisher Information carried by the topographic map before and after the stroke. We find that by tuning the receptive field plasticity to a certain value, the information transfer through the cortex after stroke can be optimized.

In this chapter we present the equations for Fisher information under three conditions: prior to stroke, immediately after the lesion and with functional recovery. The equations we derive are valid for a general receptive field model comprising the addition of an excitatory and an inhibitory component: this (with different parameters) captures both centre-surround Gaussian receptive fields and oriented cortical simple-cell like receptive fields. We present the results here for the former case. We find that there is a single optimal plasticity level for maximum recovery of function by the neuronal population code.

5.3 *Methods: A mathematical model of functional reorganization*

We assume a population of N neurons with receptive fields tiled evenly across two-dimensional visual space. We consider a model with periodic boundary conditions, i.e. a toroidal visual space. We want a receptive field model which can capture both center-surround and V1 simple-cell type receptive field structure, without too much change in the underlying mathematics. A key aspect of the receptive field model for this study is that the receptive fields must be established by the sum of an excitatory and an inhibitory component, which may then be passed through a transfer function representing the static spiking nonlinearity. This is in order that the core feature of the disinhibition plasticity model - separable effects on excitation and inhibition - can be implemented. The actual size of the receptive field is thus determined by the balance of excitation and inhibition - by shifting the balance it can be increased or decreased. In particular, this means that selective release from inhibition related to distance from a damage site will cause a relative shift towards excitation in the balance, and thus the net receptive field will appear to grow towards the lesion site (see Fig. 1). The receptive field is thus defined as

$$f_i(x, y, \theta) = f_i^{ex}(x, y, \theta) + f_i^{in}(x, y, \theta) \quad (5.1)$$

which defines the *average* response of neuron i to a stimulus centered at (x, y) and with orientation θ . f_i^{ex} and f_i^{in} are the excitatory and inhibitory components of the net synaptic current respectively, which we will refer to as the excitation and inhibition fields. Although we are defining a two-dimensional space of neurons, we use i as a label without loss of generality - to each i is associated a receptive field centered in visual space defined by x_{i0} and y_{i0} .

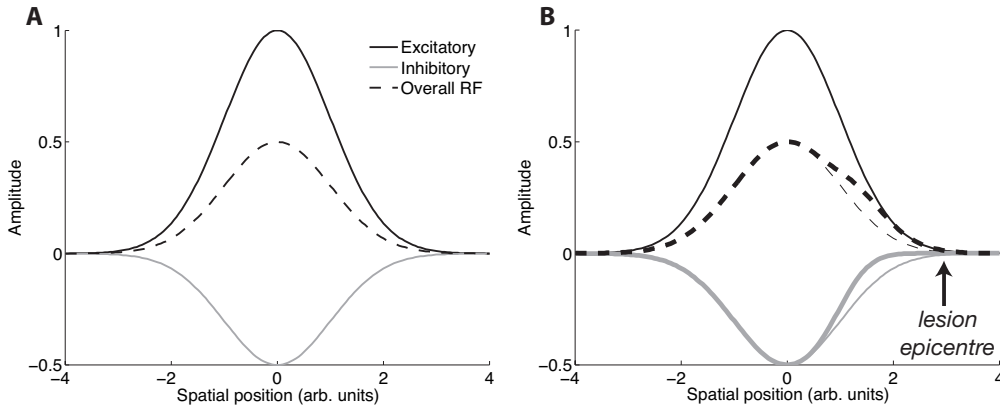


Fig. 5.1: Illustration of the mechanism for receptive field enlargement following a lesion. **A** The overall receptive field is formed from the sum of separate excitatory and inhibitory contributions - this is crucial for the mechanism to work. **B** With a lesion at the position indicated, the inhibitory component is reduced by a factor $1 - \exp(-d^\alpha/\gamma)$, where d is the distance from the lesion. This leads to disinhibition on one side of the receptive field, and consequently enlargement towards the lesion of the overall receptive field. For the example shown, $\gamma = 10$ and $\alpha = 4$.

At any given time (or experimental trial), the neuron will fire at instantaneous rate r_i , which is normally distributed about f_i with variance σ_n^2

$$P[\mathbf{r}|x, y, \theta] = \frac{1}{\sqrt{2\pi\sigma_n^2}} \exp\left[-\frac{(r_i - f_i(x, y, \theta))^2}{2\sigma_n^2}\right]. \quad (5.2)$$

We now consider the form that excitation field should take. The Gabor function (Gabor 1946) is a common choice for modelling the simple cell receptive field (Marcelja 1980). However, for the current purpose it is inconvenient: it provides a form for the overall shape of the receptive field that does not naturally break into excitatory and inhibitory contributions. This means

that it is difficult to incorporate a separate effect of plasticity on the GABAergic contribution to the receptive field. It has also been found that other functions, such as the difference of offset Gaussians, provide a better fit for both psychophysical data (Stork and Wilson 1990) and for the spatial contrast sensitivity functions of simple cells in monkey visual cortex (Hawken and Parker 1987). As the spatially offset difference of Gaussians (DOG-s) model also has the property of breaking naturally into separate excitatory and inhibitory contributions, we have more than enough reason to use it in the present study.

We thus define the excitation input field of each neuron as

$$f_i^{ex}(x, y, \theta) = \exp \left\{ -\frac{(x' - x_{i0}^{ex})^2 + \beta(y' - y_{i0}^{ex})^2}{2\sigma_{ex}^2} \right\} \quad (5.3)$$

where x_{i0}^{ex}, y_{i0}^{ex} indicate the center of neuron i 's excitation field in visual space, σ_{ex} controls envelope spread and $x' = x \cos \theta_i + y \sin \theta_i$, $y' = -x \sin \theta_i + y \cos \theta_i$ implements the orientation preference θ_i of the neuron. The spatial frequency preference of the neuron is given by ν_i , its phase preference by ψ_i and ellipticity by β . For the remainder of the chapter we will take $\psi = 0$ and $\beta = 1$ for all i .

To avoid complicating the model too much at this stage, we will consider the inhibitory components of the receptive fields to be non-oriented. This is supported by recent evidence from two-photon imaging of inhibitory interneurons in the GAD67-GFP (Δ neo) mouse, in which GABAergic neurons were found not to be orientation tuned (Sohya et. al. 2007). There is however some support for an orientation-tuned inhibitory component from whole-cell patch-clamp recordings in the cat (Anderson et. al. 2000). Inclusion of orientation-tuned inhibition would be possible in a future study. The inhibition field is thus

$$f_i^{in}(x, y, \theta) = -\exp \left\{ -\frac{(x - x_{i0}^{in})^2 + (y - y_{i0}^{in})^2}{2\sigma_{in}^2} \right\}. \quad (5.4)$$

where σ_{in} controls the spread of the inhibition field, and x_{i0}^{in}, y_{i0}^{in} its spatial location. x, y feature in this equation instead of x', y' , due to the lack of orientation tuning here. For simplicity we will consider in this paper only the numerical results for the situation where the spatial offset is zero, i.e. $x_{i0}^{ex} = x_{i0}^{in}$, $y_{i0}^{ex} = y_{i0}^{in}$.

This general receptive field model, illustrated in Figure 5.1, can thus represent, with appropriately chosen parameters, the receptive fields of retinal ganglion cells, lateral geniculate neurons, V1 simple cells and non-oriented cortical neurons. The latter case could also be applied to cortical receptive fields for other stimulus modalities.

5.3.1 The disinhibition model of post-lesion plasticity

A lesion is induced in the model by destroying a specific number of neurons in the population and zero-ing out their receptive fields. The damaged neurons are thus unable to respond to any incoming stimuli and do not contribute to the information transferred about the applied stimuli by the population across the cortex. The size of the lesion determines the number of damaged neurons and can be tuned to explore the effects of various sizes on the cortex. We define a region \mathcal{L} , in which the neurons are damaged, and thus not firing. Equation 5.1 thus becomes

$$f_i(x, y, \theta) = \begin{cases} f_i^{ex}(x, y, \theta) + f_i^{in}(x, y, \theta) & i \notin \mathcal{L} \\ 0 & i \in \mathcal{L} \end{cases}. \quad (5.5)$$

The affected neurons will thus not contribute to the population code.

After the lesion, we allow receptive field plasticity to occur. Note that we make a distinction in terms between receptive field plasticity (as used in the adult brain plasticity literature, see e.g. (Calford and Tweedale 1988)) and synaptic plasticity. Synaptic plasticity is in all likelihood one of the mechanisms contributing towards receptive field plasticity, but it is not a mechanism we consider explicitly in this model in its current form.

The essential element of the plasticity model is that release from inhibition should occur proportionally to proximity to the lesion. The precise form of this functional relationship is at present entirely unconstrained by the experimental data. We plan to perform experiments in the future to measure this relationship, but for the meantime hypothesize for the sake of progress that it is exponential. We also do not consider the dynamics of plasticity in the present model, but assume that this exponential relationship is reached at steady state. Thus Equation 5.6 becomes after plasticity

$$f_i^{in}(x, y, \theta) = - \exp \left\{ - \frac{(x - x_{i0}^{in})^2 + (y - y_{i0}^{in})^2}{2\sigma_{in}^2} \right\} \left[1 - \exp \left(\frac{-d_{\mathcal{L}}^{\alpha}(x, y)}{\gamma} \right) \right]. \quad (5.6)$$

where $d_{\mathcal{L}}(x, y)$ is the Euclidean distance of point (x, y) from the boundary of the lesioned region \mathcal{L} , the exponent α governs the shape of the falloff of disinhibition from the lesioned region, and γ determines the magnitude of the disinhibition that occurs.

5.3.2 A simulation of nonlinear neuronal responses

Before we introduce the mathematical formalism, a simple simulation will be performed to verify that it behaves as expected. Neuronal responses are complex and variable thus describing the relationship between stimulus and response is a difficult task. The model described in this section generates a neuronal population response to input stimuli. A simple neuronal model can estimate firing rates as instantaneous functions of the corresponding applied stimulus by assuming that contributions from different locations within the visual field sum linearly. That is, the spatial input stimulus, $s(x, y)$, is weighted linearly by the receptive field of each neuron, $f_n(x, y)$. The linear response of each neuron n to the input stimulus is thus generated by:

$$r_{linear}(x, y)_n = \sum_{x=1}^{size_x} \sum_{y=1}^{size_y} f_n(x, y) \cdot s(x, y) \quad (5.7)$$

$size_x$ and $size_y$ determine the height and width of the spatially mapped visual field respectively. By adding to the model a threshold-gain function, T , which is appropriately bounded from above and below the firing rate will be never be negative or unrealistically large.

White noise, w_n , is added to the system to incorporate the fact that a neuron does not always respond in the same way to a repeatedly applied stimulus. Thus, the actual response of each neuron n to a spatial stimulus s in the model is:

$$r_{nonlinear}(x, y)_n = T(r_{linear}(x, y)_n + w_n) \quad (5.8)$$

For the simulations that will be shown, the transfer function T was

$$T(r_{linear} + w_n) = g[r_{linear} + w_n - r_0]_+ \quad (5.9)$$

whereas the analytical results which we will present have currently been obtained for the simple case

$$T(r_{linear} + w_n) = r_{linear} + w_n. \quad (5.10)$$

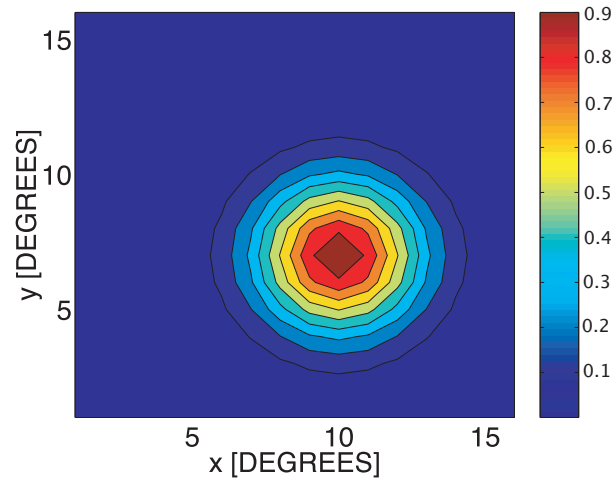


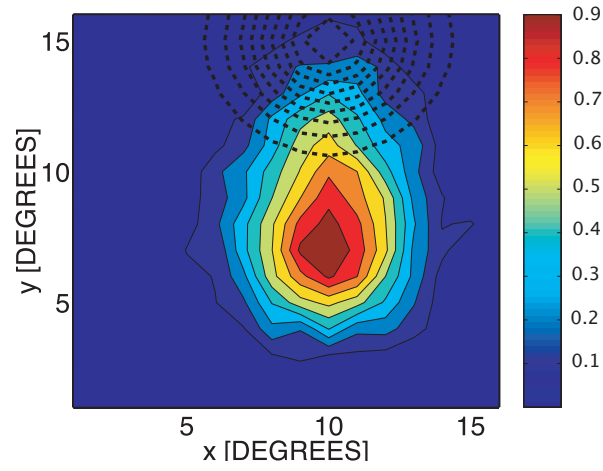
Fig. 5.2: A contour plot of the mapped receptive field of a single neuron, in the population before the a stroke lesion is induced The x- and y- coordinates represent degrees of visual field (Montani 2007d ; Einarsdottir and Montani and Schultz)

In the above, r_0 is the threshold value that the sum ($r_{linear} + w_n$) must reach before firing starts. Above threshold level, the firing rate is a linear function of r_{linear} and g is the gain.

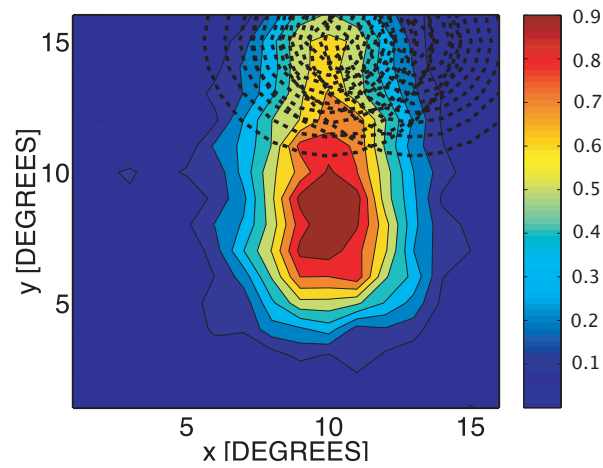
Figure 5.2 shows a contour plot of a receptive field of a single neuron in the neural population. The peak of the receptive field, $(x_0, y_0)_n$ is dependent of the position of the neuron within the cortex because its receptive field are mapped across it. In each trial, a white noise is applied to the population and the response of each neuron is recorded and used to calculate the points of the receptive field.

Figure 5.3 shows how the size of a damage influences the enlargement of receptive field. The damage in Figure 5.3B covers a larger area of neurons than the damage in Figure 5.3A and therefore influences a greater drop in inhibition. The plasticity levels are increased, dependent on the drop in GABA and for these simulations, $\gamma = 0.02$ refers to the plasticity level in the cortex following a small lesion shown in Figure 5.3 A and $\gamma = 0.1$ is the plasticity value induced by the larger lesion shown in Figure 5.3B.

Figure 5.4 shows the relationship between the expansion of receptive fields and the distance of neurons to the lesion. The expansion of each receptive field is represented as the deviation, in percentage, from the original base width, pre-lesion. The distance d_n from the damage is presented in arbitrary model units and is defined to be the shortest distance between neuron



A



B

Fig. 5.3: Receptive field adaptation following stroke-like lesion of different sizes, obtained by computer simulation. The damage is represented with black dotted lines. The intact neuron responds to the lesion by expanding its receptive field towards the damaged area (Montani 2007d ; Einarsdottir and Montani and Schultz).

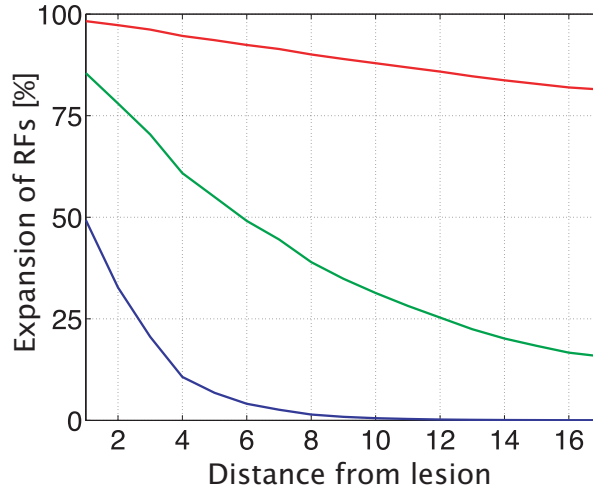


Fig. 5.4: Expansion in the receptive field versus the distance between the damage and the neurons is shown for different values of plasticity γ , which are dependent on the size of the damage. The blue line refers to $\gamma = 0.02$, green line to $\gamma = 0.1$ and the red line to $\gamma = 0.81$. Expansion is defined as the change in percentage between the base width of the receptive field pre- and post lesion (Montani 2007d ; Einarsdottir and Montani and Schultz).

n and each cell within the damaged area.

5.4 Results

5.4.1 Fisher topographic information

The Fisher information for the accuracy with which the variable x can be decoded from response r_i is given by

$$I(x) = - \int dr_i P(r_i|x) \frac{\partial^2 \log P(r_i|x)}{\partial x^2}. \quad (5.11)$$

The Cramer-Rao bound tells us that the mean-squared error of any decoder must be greater than or equal to $1/I(x)$. The Fisher information thus provides a good way to characterize the performance of a neural population code (Seung and Sompolinsky 1993; Abbott and Dayan 1999). In two dimensions, it is relatively straightforward to see that the following simple general-

ization of the usual quantity holds:

$$I(x, y) = - \int dr_i P(r_i|xy) \frac{\partial^2 \log P(r_i|xy)}{\partial x \partial y}. \quad (5.12)$$

This is of course the Fisher information provided by one neuron, and it is a function of spatial position. We will consider the situation where each neuron codes independently, and thus the population Fisher information is simply additive across neurons. We will also assume that all parts of retinotopic space are equally important, and thus we will consider the average Fisher information over space, which is $I = - \left\langle \sum_{i=1}^N \int_0^R dr_i P(r_i|xy) \frac{\partial^2 \log P(r_i|xy)}{\partial x \partial y} \right\rangle_{x,y}$ where R is the maximum response observed.

5.4.2 Fisher information for a lesioned retinotopic code

Taking derivatives of $\log P$ from Equation 5.4 and inserting them into the above equation, with the assumed noise model the expression for Fisher information becomes

$$I(x, y) = \sum_i \frac{1}{\sigma_n^2} \frac{\partial f_i}{\partial x} \frac{\partial f_i}{\partial y} \quad (5.13)$$

Now, the receptive field breaks into excitatory and inhibitory components, i.e.

$$\frac{\partial f}{\partial x} \frac{\partial f}{\partial y} = \frac{\partial}{\partial x} (f^{ex} + f^{in}) \frac{\partial}{\partial y} (f^{ex} + f^{in}). \quad (5.14)$$

and the Fisher information $I(x, y)$ can thus be written as the sum of excitatory, inhibitory and interaction terms:

$$I(x, y) = I_{ex} + I_{ex,in} + I_{in,ex} + I_{in} \quad (5.15)$$

where

$$I_{ex} = \frac{1}{\sigma_n^2} \sum_i (f_i^{ex})^2 \frac{(x - x_{i0})(y - y_{i0})\beta}{\sigma_{ex}^4} \quad (5.16)$$

$$\begin{aligned}
I_{in} = \frac{1}{\sigma_n^2} \sum_i \beta(f_i^{in})^2 & \left\{ \frac{(x - x_{i0})(y - y_{i0})(1 - e^{-d^\alpha/\gamma})^2}{\sigma_{in}^4} \right. \\
& - \frac{\alpha (x - x_{i0})(y - y_{iL})(1 - e^{-d^\alpha/\gamma})e^{-d^\alpha/\gamma}}{2 \sigma_{in}^2 d^{2-\alpha}\gamma} \\
& - \frac{\alpha (x - x_{iL})(y - y_{i0})(1 - e^{-d^\alpha/\gamma})e^{-d^\alpha/\gamma}}{2 \sigma_{in}^2 d^{2-\alpha}\gamma} \\
& \left. + \frac{e^{-2d^\alpha/\gamma}}{d^{2(2-\alpha)}\gamma^2} (x - x_{iL})(y - y_{iL}) \frac{\alpha^2}{4d^{2(2-\alpha)}} \right\} \quad (5.17)
\end{aligned}$$

$$\begin{aligned}
I_{ex,in} = \frac{1}{\sigma_n^2} \sum_i (f_i^{ex} f_i^{in}) & \left\{ \frac{(x - x_{i0})(y - y_{i0})\beta}{\sigma_{ex}^2} \left[\frac{(1 - e^{-d^\alpha/\gamma})}{\sigma_{in}^2} \right] \right\} + \\
& \frac{1}{\sigma_n^2} \sum_i (f_i^{ex} f_i^{in}) \left\{ \frac{(x - x_{iL})(y - y_{i0})}{d^{2-\alpha}\sigma_{ex}^2} \beta \frac{\alpha}{2} e^{-d^\alpha/\gamma} \right\} \quad (5.18)
\end{aligned}$$

$$\begin{aligned}
I_{in,ex} = \frac{1}{\sigma_n^2} \sum_i (f_i^{ex} f_i^{in}) & \left\{ \frac{(x - x_{i0})(y - y_{i0})\beta}{\sigma_{ex}^2} \left[\frac{(1 - e^{-d^\alpha/\gamma})}{\sigma_{in}^2} \right] \right\} + \\
& \frac{1}{\sigma_n^2} \sum_i (f_i^{ex} f_i^{in}) \left\{ \frac{(x - x_{i0})(y - y_{iL})}{d^{2\alpha}\sigma_{ex}^2} \beta \frac{\alpha}{2} e^{-d^\alpha/\gamma} \right\} \quad (5.19)
\end{aligned}$$

and x_L, y_L are the locations (in visual space) of the nearest lesioned area to neuron i . The spread of the excitation/inhibition field is controlled by σ_{ex} and σ_{in} , respectively. The noise deviation is given by σ_n .

I_{ex} and I_{in} are the excitatory and inhibitory contributions respectively. But, I_{in-ex} and $I_{in,ex}$ correspond to a mixed contributions made up of excitatory and inhibitory elements. Equations 5.17, 5.16, 5.20 and 5.19 were implemented in Figure 5.5 and 5.6 in order to illustrate the effects of the plasticity γ on the Fisher Information components. Following stroke-like damage the information surrounding the damaged area is increased. Notice that this increase is mostly due to the excitatory component I_{ex} .

Figure 5.7 Fisher Information as a function of the degree of plasticity γ for the analytical approach. Figure 5.8 show the Fisher Information as a function of the degree of plasticity γ using our simulation of nonlinear neuronal responses on eq. 5.15. In both cases the information transfer post stroke is dependent on the plasticity, γ .

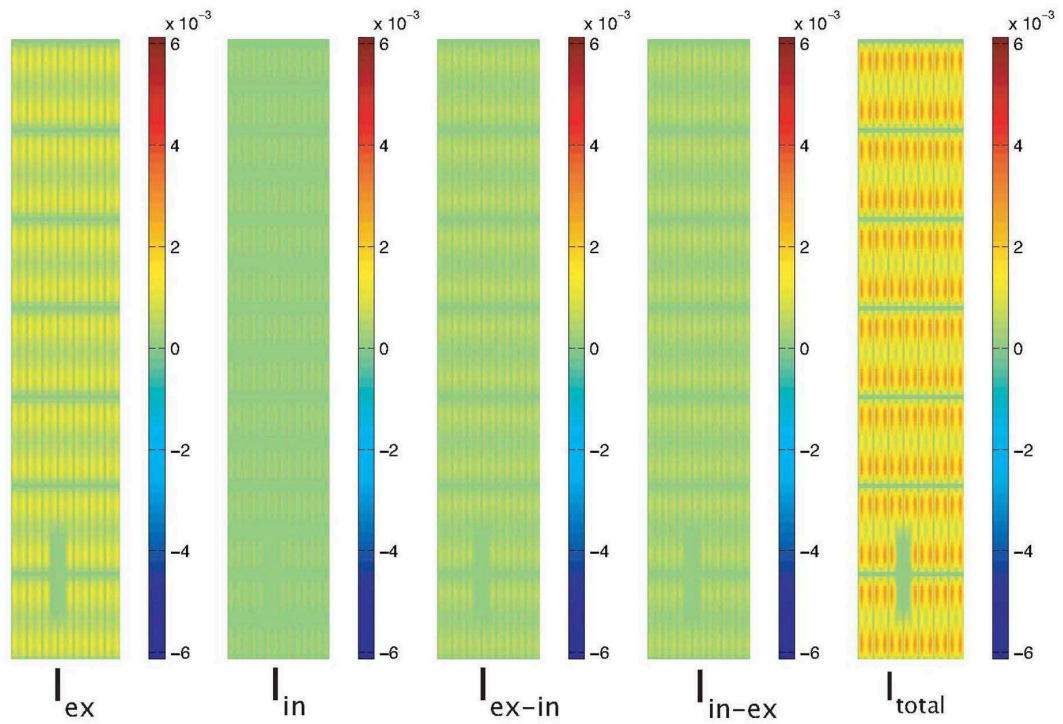


Fig. 5.5: Fisher Information components in the 2-D topographic map before the stroke. The different values of the Fisher information are displayed as a color map for different values of x and y . Notice that the changes in colors, inside each individual neuron, are due to the finite size effect of the lattice. For the example shown, $\gamma = 0, \sigma_n = 1, \sigma_{ex} = 2$ and $\sigma_{in} = 1$.

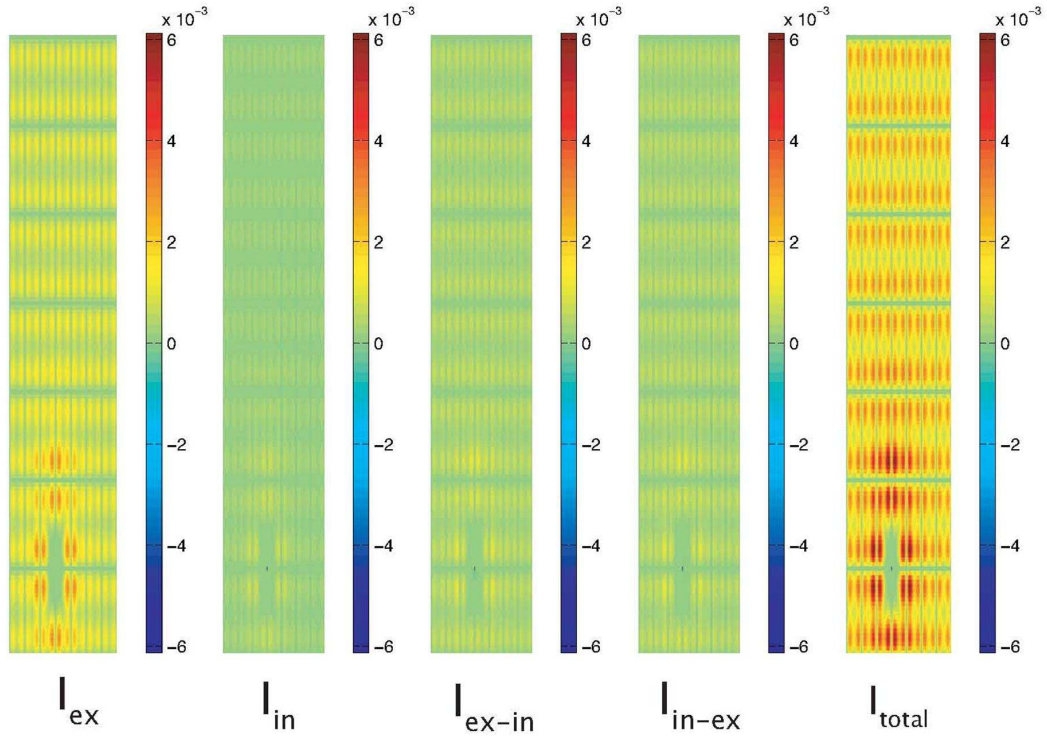


Fig. 5.6: Fisher Information components in the 2-D topographic map before the stroke. The different values of the Fisher information are displayed as a color map for different values of x and y . Notice that the changes in colors, inside each individual neuron, are due to the finite size effect of the lattice. For the example shown, $\gamma = 10, \sigma_n = 1, \sigma_{ex} = 2$ and $\sigma_{in} = 1$. Following stroke-like damage the information surrounding the damaged area is increased mostly due to an increase in the excitatory component I_{ex} .

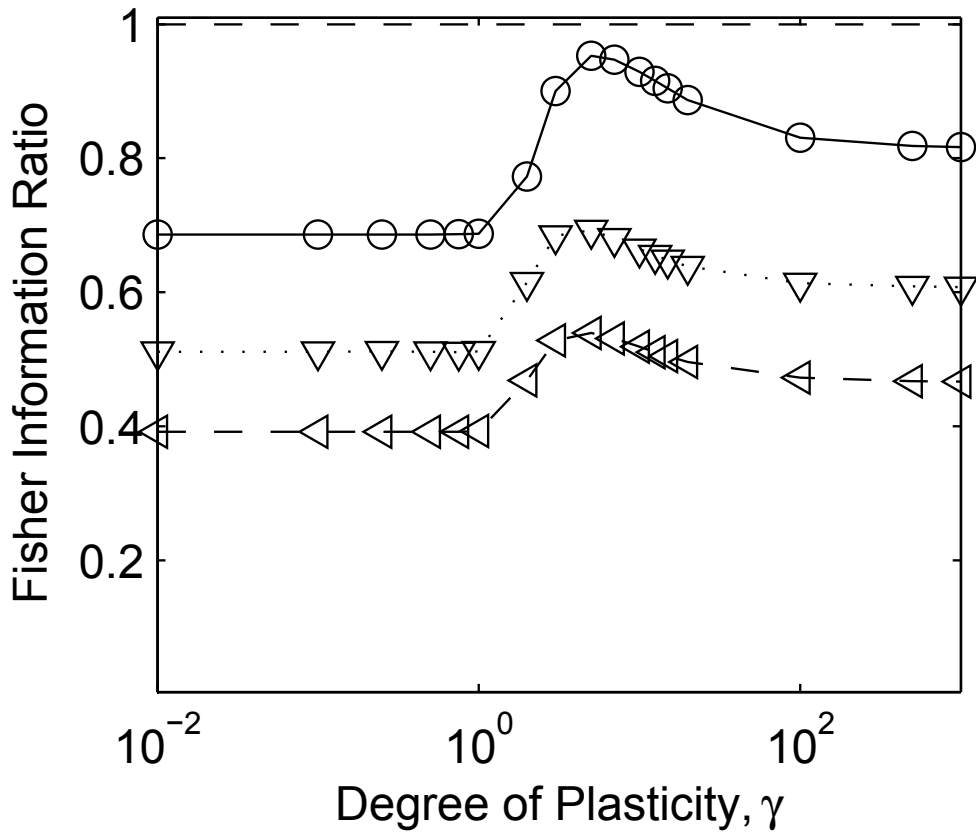


Fig. 5.7: Analytical results for Fisher Information as a function of the degree of plasticity γ . Solid black line indicates coding accuracy when the damage covers 3 % of the neurons in the population, the dotted line refers to 30 % damage and the dashed refers to 50 % damage. The population includes 64 neurons with a side length of visual space, i.e. distance before it starts repeating, equal to 40 and $\sigma_{ex} = 2$ and $\sigma_{in} = 1$).

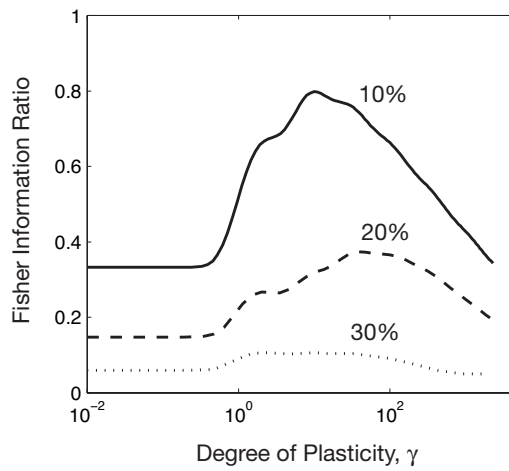


Fig. 5.8: Fisher Information as a function of the degree of plasticity γ using our simulation of nonlinear neuronal responses on the analytical expression (eq. 5.15). The black solid line indicates coding accuracy when the damage covers 10 % of the neurons in the population, the dashed line refers to 30 % damage and the dotted line refers to 70 % damage. The population includes 225 neurons with original receptive field spread $\sigma = 2$. The curves are normalised to the Fisher information prior to the stroke. The left asymptote corresponds to the performance after stroke, but prior to functional recovery.

Our findings in Figure 5.7 and 5.8 show that following a stroke-like damage, the information transfer drops from its original value because neurons within the damaged area do not convey information about the applied stimuli. When the plasticity level is raised, the neurons surrounding the damage start to expand their receptive fields in order to take up lost functions, and the information transfer increases. However, when γ is raised even further and the expansion increases, overlap of the receptive fields becomes too large and information is lost again. This is due to the fact that infinitely large receptive field do not provide any information about applied stimuli because every stimulus pattern is weighted in the same way and no discrimination is accomplished. Large overlapping receptive fields are therefore not specific enough to give information about the input. There is therefore a certain value, γ^0 which optimizes the performance of the cortex. Figure 5.7 and 5.8 shows the Fisher Information for three different sizes of damages. Bigger lesion led to more information loss and less recovery with increasing γ . The analytical formulation has particular advantages, in that it allows the effects to be broken down into excitatory, inhibitory, and interaction terms. The purely computational approach of course may be applied to a wider range of models.

5.5 Discussion

The current theoretical model describes how intact neurons surrounding a stroke-like cortical lesion adapt to the damage and to the resulting functional impairment. The neurons experience a dis-inhibition in their receptive fields and therefore their total receptive field expands in the direction of the lesion. The amount of enlargement apparent in each neuron is determined by two factors: the distance of the neuron in question from the damage and the size of the damage. Neurons close to the damage expand their receptive field more than neurons further away (Montani 2007d ; Einarsdottir and Montani and Schultz). In our approach, Fisher information is used to measure the accuracy of the population code in representing a sensory variable. We have simplified out the dependency on orientation of a stimulus, however, the model can be extended to include the orientation dependency just by replacing the Gaussian (DOG-s) model by Gabor functions (Gabor 1946).

Our findings shows that after a lesion, the accuracy of coding by the population, as measured by the Fisher information, drops by an amount which depends upon the size of the lesion.

If plasticity mechanisms result in an enlargement of receptive fields in the direction of the lesion (as predicted by the simple disinhibition model of plasticity), then some recovery of Fisher information is obtained as the neurons in the intact region begin to represent the spatial information previously represented by the damaged tissue. If plasticity is too large, however, then receptive fields become too big, and essentially become uninformative about the spatial location of a stimulus. There is thus a clear optimum level of plasticity for compensating for the effect of the lesion to the maximal extent possible. This phenomenon appears to be quite robust, and relevant to reasonable physiological parameters. Our findings suggest that by tuning the receptive field plasticity levels to certain value, the information transfer through the cortex post stroke can be optimized. This may be of interest both for understanding the effects of potential therapeutic interventions in stroke, as well as for developing engineering principles for incorporating brain-like redundancy into machines.

However, the parameters in the current study were chosen in order to illustrate the operation of the model. There is currently little available quantitative physiological data concerning the exact shape of receptive field enlargement following stroke. However, the experiments required to do so are quite feasible, and we plan to carry them out using a photothrombosis model stroke in the rodent preparation. We note that while the disinhibition model has been assumed here, as a first step, our mathematical approach could be used with relatively minor changes to compute the Fisher information associated with any parameterized change in receptive field shape following the lesion, including those for instance generated by synaptic plasticity and sprouting processes which are difficult to model explicitly using our approach. An understanding of the precise shape changes following stroke will help us to assess the effect of novel pharmacological therapeutic interventions that may be piloted in rodent preparations. An understanding of the operating principles by which they occur will also be important for the engineering of devices such as sensory arrays which make use of fault-tolerant algorithms with brain-like recovery of function properties.

6. AN ANALYTICAL APPROACH TO THE PDF AND FISHER INFORMATION CONSIDERING HIGHER-ORDER CORRELATIONS IN A POPULATION OF NEURONS

A widespread distribution of neuronal activity can generate higher-order stochastic interactions. In this case, pair-wise correlations do not uniquely determine synchronizing spikes firing in a population of neurons and higher order interactions across neurons can not be disregarded. In this chapter we present a new statistical approach, using the information geometry framework to analyze the probability distribution function (PDF) of spike firing patterns by considering higher order correlations in a neuronal pool. This allows us to study the limit of a large population of neurons and to introduce a deformation parameter associated to the higher order correlations in the PDF. We present also an analytical estimation of the Fisher information which allows us to evaluate the implications of higher order correlations between spikes on information transmission in a population of neurons.

6.1 *Introduction*

Probabilities are daily used in real world applications, often without any understanding of their mathematical foundations and of the meaning attached to them. Statistical Mechanics, more than other discipline in physics, has been beset with problems of methodology and presentation. Even philosophers have argued over the meaning of probabilities, in particular when are applied to single events. However, mathematicians sidestepped this issue long time ago by stripping away any physical interpretation and treating probability as a measure accompanied by a set of rules. Nowadays mathematicians are at the forefront of developing new statistical methodologies and performing cutting edge research of ultimate help to solve statistical problems. The conundrums of many scientific disciplines have important aspects

of probabilistic science at its heart.

The idea of combining statistic and differential geometry was introduced by Amari in the early eighties (Amari 1980; Amari 1982). However, the major scientific journals were reluctant at that time to accept this new idea. The attempt made by Curado and Tsallis in 1991 (Curado and Tsallis 1994) of dealing with a generalized statistics encouraged Amari and Nagaoka to revive their results on information geometry (for a review of their work see Amari and Nagaoka 2000). Probability distributions are indeed fundamental elements over which fields such as statistic, stochastic processes, and Information Theory are developed (Amari and Nagaoka 2000, Amari 1992 and Amari 1997). Information geometry itself provides a new analytical tool within the field of statistical mechanics, which has emerged from investigating the geometrical structures of a manifold of probability distributions. Strictly speaking, information geometry is the geometric study of statistical estimations. To consider statistical estimations from the differential geometry point of view has allowed several previous open problems to be solved; information theory has already established itself within the field of statistical mechanics. In the field of information theory, stochastic process, and systems, information geometry allows the investigation of previously unexplored possibilities (Amari and Nagaoka 2000).

Information-geometric measures can be used to analyze neural firing patterns including not only the second-order, but also taking into account higher-order correlations across neurons (Amari 2001; Nakahara and Amari 2002; Bothe et. al. 2000; Tanaka 2000; Ikeda et. al. 2004; Wu et. al. 2004)). A widespread distribution of neuronal activity can generate higher-order stochastic interactions (Amari et al. 2003). The aim of this chapter is to evaluate the significance of these higher order correlations, in the case that correlations can not be reduced to pairwise correlations in a population code. More specifically, we estimate analytically the widespread PDF and Fisher Information in the limit of a large number of neurons by taking into account higher-order correlations across the neuronal pool.

The results presented in this chapter were obtained in collaboration with Stefano Panzeri and are being prepared for publication elsewhere (Montani and Panzeri 2007; in preparation).

6.2 Methods

A combination of a family of probability distributions has a natural hierarchical structure. In the Information Geometry framework, the neuronal firing is represented by a binary vector $X = (X_1, \dots, X_n)$, each X_i indicates that the i^{th} neuron is silent at a short time bin t_i if $X_i=0$. In contrast, if $X_i=1$ the i^{th} neuron is firing a spike. We denote $P=P(X)$ as the probability distribution of getting the X neurons firing. Each $P(X)$ is given by 2^n probabilities, $p_{i_1, \dots, i_n} = \text{Prob}\{X_1=i_1, \dots, X_n=i_n\}$, $i_k=0,1$, normalized by the condition $\sum_{i_1 \dots i_n} p_{i_1 \dots i_n} = 1$.

This probability distribution can be exactly expanded as (Nakahara and Amari 2002),

$$P(X) = \exp \left\{ \sum x_i \theta_i + \sum_{i < j} x_i x_j \theta_{ij} + \sum_{i < j < k} x_i x_j x_k \theta_{ijk} + \dots + \sum_{i < \dots < n} x_i \dots x_n \theta_{i \dots n} - \psi, \right\} \quad (6.1)$$

All the $\theta_{ijk \dots n}$, together have $2^n - 1$ components and form a coordinate system, called θ - *coordinates* which correspond to e-flat structure in S_n . (Nakahara and Amari 2002). The normalizing factor ψ correspond to $-\log_2 p(x_1=x_2=\dots=x_n=0)$.

The set of all probability distributions form a $2^n - 1$ dimensional manifold in S_n .

The distribution $P(X)$ can be decomposed into marginals

$$\eta_i = \text{Prob}\{x_i = 1\} = E\{x_i\}, \quad i = 1, \dots, n \quad (6.2)$$

$$\eta_{ij} = \text{Prob}\{x_i = 1; x_j = 1\}, \quad i < j \quad (6.3)$$

$$\eta_{ijk} = \text{Prob}\{x_i = 1; x_j = 1; x_k = 1\}, \quad i < j < k \quad (6.4)$$

$$\eta_{1 \dots n} = \text{Prob}\{x_1 = 1; x_2 = 1; x_3 = 1 \dots; x_n = 1\}, \quad (6.5)$$

which have a $2^n - 1$ components and define a m-flat structure in S_n . (Nakahara and Amari 2002).

$E_n(\theta)$ is defined as a manifold in which the marginals $\eta_i, \dots, \eta_{1 \dots n}$ can change freely but θ is fixed. This is, the manifold $E_n(\theta)$ spans all the geometrical directions in which the marginal changes but the correlations coordinate θ is fixed.

The θ -coordinates which are orthogonal to the marginals $\eta_1, \eta_2, \eta_{12} = \eta_1 \eta_2$ for the linear contribution are given by,

$$\theta_i = \log_2 \left\{ \frac{P_i}{P_0} \right\}; \quad (6.6)$$

where P_i is the probability $Prob\{X_i=1\}$ of the i^{th} neuron to be firing a spike, and P_0 is the probability of getting no responses $Prob\{X_i=0\}$.

The sub-manifold $E_1(0)$ consists of all the independent distributions. This can be achieved imposing the constraints

$$\theta_{ij} = \theta_{ijk} = \theta_{ijkl} = \dots = \theta_{i\dots n} = 0, \quad (6.7)$$

which leads to the distribution $P^{(1)}$

$$P^{(1)} = e^{\sum_i x_i \theta_i} \quad (6.8)$$

which is the distribution one would derive in the absence of knowledge of spike correlations under the maximum entropy principle. The normalizing factor is given by,

$$\psi = \log_2(P_0), \quad (6.9)$$

In the case of pairwise correlations the marginals are,

$$\eta_1 = P_{10} + P_{11} \quad (6.10)$$

and

$$\eta_2 = P_{01} + P_{11} \quad (6.11)$$

with

$$\eta_{12} = E[x_1 x_2] = p_{12}, \quad (6.12)$$

The coordinates orthogonal to the marginals are given by,

$$\theta_{ij} = \log_2 \left\{ \frac{P_{ij}P_0}{P_iP_j} \right\} \quad (6.13)$$

where P_{ij} denotes $Prob\{X_i=1, X_j=1\}$. The sub-manifold $E_2(0)$ is composed of all the distributions which take into account only pairwise interactions. This is, the condition

$$\theta_{ijk} = \theta_{ijkl} = \dots = \theta_{i\dots n} = 0, \quad (6.14)$$

leads to

$$P^{(2)} = e^{x_i\theta_i + x_ix_j\theta_{ij} - \psi} \quad (6.15)$$

which correspond to the distribution that takes into account spikes correlations up to second order.

In the case of a triplewise interaction the marginals are given by,

$$\eta_i = E[x_i] = Prob\{x_i = 1\}; (i = 1, 2, 3) \quad (6.16)$$

with

$$\eta_{ij} = E[x_ix_j] = Prob\{x_i = x_j = 1\}; (i = 1, 2, 3) \quad (6.17)$$

and

$$\eta_{123} = E[x_1x_2x_3] = Prob\{x_i = x_j = x_k = 1, \} (i = 1, 2, 3) \quad (6.18)$$

For triple-wise correlations the θ -coordinates which are orthogonal to the marginal contributions are given by,

$$\theta_{ijk} = \log_2 \left\{ \frac{P_{ijk} \prod_l P_l}{P_0 \prod_{l_1 l_2} P_{l_1} P_{l_2}} \right\} \quad (6.19)$$

where P_{ijk} denotes $Prob\{X_i=1, X_j=1, X_k=1\}$.

The sub-manifold $E_3(0)$ is composed of all the distributions up to triplewise order interactions. This is, the condition

$$\theta_{ijkl} = \dots = \theta_{i\dots n} = 0, \quad (6.20)$$

leads to

$$P^{(3)} = e^{x_i \theta_i + x_i x_j \theta_{ij} + x_i x_j x_k \theta_{ijk} - \psi} \quad (6.21)$$

which accounts for pairwise and triple-wise spike correlations.

In the case of fourth order correlations the orthogonal θ -coordinates to the “fourth order marginals” are,

$$\theta_{ijkl} = \log_2 \left\{ \frac{P_{ijkl} \prod_{l_1 l_2} P_{l_1 l_2} P_0}{\prod_{l_1 l_2} P_{l_1} P_{l_2} \prod_{l_3} P_{l_3}} \right\} \quad (6.22)$$

The distributions present before $P^{(1)}$, $P^{(2)}$, $P^{(3)}$, \dots $P^{(i)}$, with the constraint $\theta_{i\dots n} = 0$, correspond to stable distributions of the Boltzman machine in the neural network (Nakahara and Amari 2002). Each of them correspond to a probability distribution whose entropy is larger than (or equal to) that of all other members of a specified class of distributions. This is, they all satisfy the maximum entropy (Nakahara and Amari 2002).

6.3 Results

6.3.1 Pooling across neurons:

The amount of pairwise informational dependence can have a relatively large effect on the population code (Averbeck et. al. 2006). It is usually not difficult to incorporate pairwise correlations dependency in the probability distribution of the ensemble. In this way, it is also relatively easy to compare to the probability of the ensemble with probability distribution of getting independent population responses.

However, pairwise correlations across neurons do not always determine the probability distribution of synchronized postsynaptic events. Synchronous events in which a large proportions of neurons take place should exist even in the case of weak pairwise correlations. Unfortunately, pairwise correlations only provide an indirect measure of the probability distributions of higher order correlations. Even when pairwise correlations in an ensemble of neurons are fixed, the probability of measuring higher order events may be undetermined. This gives an idea that to estimate higher order dependencies among a decomposition of a number of stochastic variables is a difficult task.

Information geometry allows us to decompose quantitatively stochastic dependency into an orthogonal sum of pairwise, triplewise, quadruplewise, and further higher order dependencies. This gives a new invariant decomposition of joint entropy, which is very important for extracting intrinsic interactions in firing patterns of an ensemble of neurons, and for estimating recurrent functional connectivity on the information coding.

A widespread distribution of neuronal activity can generate higher-order stochastic interactions across neurons that should not be disregarded. We use Information Geometry to analyze the probability distribution function (PDF) of spike firing patterns by taking into account higher order correlations in a neuronal pool. This allows us to consider the limit of a large population of neurons and to introduce a deformation parameter associated to the higher order correlations in the PDF. An analytical approach to the estimation of the Fisher information allows us to identify higher order correlations with a deformation parameter and to speculate about their possible role on information transmission (Montani and Panzeri 2007; to be submitted).

If we assume that a "target neuron" can not process separately spikes from different neurons, then the label of the neuron which fired each spike is lost. Hence, the pooling mechanism can be understood as a simple information processing strategy in the nervous system. Let's consider a neuronal pooling of just N neurons (let's say k firing and $N - k$ silent, $0 \leq k \leq N$). The probability of k neurons firing is,

$$P(k) = \binom{n}{k} \cdot e^{\left\{ \sum_{i=1}^k \binom{k}{i} \cdot \theta_i - \psi(\theta) \right\}} \quad (6.23)$$

which can equivalently be expressed as,

$$P(k) = \binom{n}{k} \cdot e^{\left\{ k \cdot \theta_1 + \sum_{i=2}^k \binom{k}{i} \cdot \theta_i - \psi(\theta) \right\}} \quad (6.24)$$

Notice that since we are considering a neuronal pool, a simple index $1 \leq i \leq k$ is included in θ coordinates which accounts for higher order contributions because all neurons are equal and thus all thetas of the same order are equal and independent of the index combination.

Taking the limit of $n \rightarrow \infty$, we can rewrite the probability distribution as

$$P(k) = e^{\left\{ \sum_{i=1}^k \binom{k}{i} \cdot \theta_i - \psi(\theta) + nH(r) \right\}} \quad (6.25)$$

where $r = \frac{k}{N}$ and $H(r) = -r \cdot \log(r) - (1 - r) \cdot \log(1 - r)$, and $e^{nH(r)}$ is the normalization factor which results from $\binom{n}{k}$ by taking the limit $n \rightarrow \infty$ (Stirling asymptotic formula for factorial Leung et. al. 1997).

(Amari et al. 2003) have proved that when the activity of the probability distribution is not concentrated, the interactions $\theta_2 \dots \theta_n$ scale as $\theta_i = O(\frac{1}{n^{i-1}})$, if $i \leq \frac{n}{2}$. Or, $\theta_i = O(\frac{1}{n^{n-i}})$, if $i > \frac{n}{2}$. Figure 6.1 shows a widespread distribution where the probability distribution present

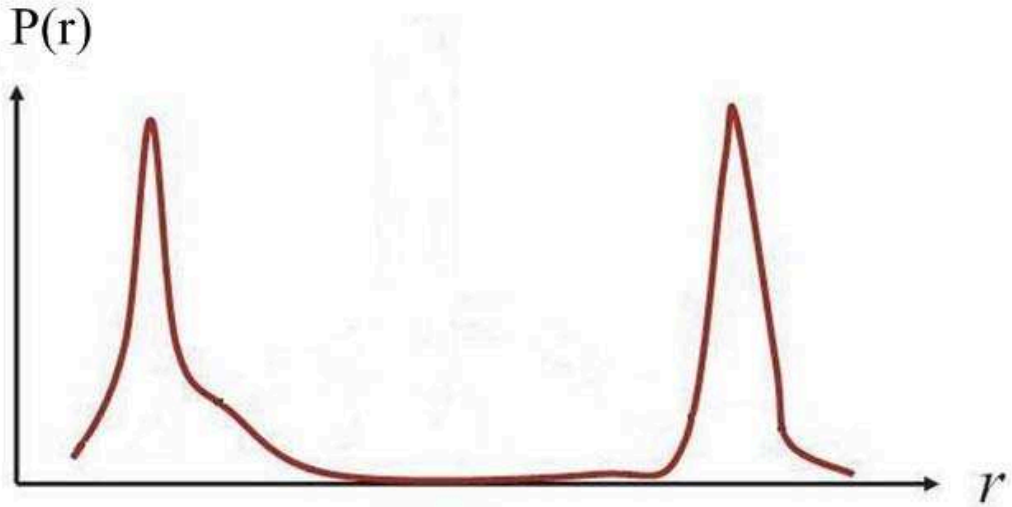


Fig. 6.1: Widespread probability distribution, $P(r)$, accounting for higher order correlations .

two peaks. The neurons fire synchronized at one time and are quiescent at other times. This behavior correspond to the case in which higher order correlations generate a widespread distribution of neuronal activity. The firing activity of the neurons is centered on its mean when all the neurons fire independently.

Let's consider for a moment repeated independent trials in a population of neurons. They are called Bernoulli trials if there are only two possible outcomes for each trial and their probabilities remain the same throughout the trials. Let's define $b(k; n, p)$ as the probability that N Bernoulli trials with probabilities p of having k neurons firing and $z = 1 - p$ in $N - k$ neurons silent,

$$b(k; n, p) = \binom{n}{k} p^k z^{n-k} \quad (6.26)$$

In the case in which many neurons (N) are recorded simultaneously several spikes k can be measured to fire in synchrony across the population. However, the number k of spikes being fired is not usually a large quantity when compared to the total number of neurons N .

In contrast to the bimodal distribution shown in Figure 6.1, neuronal spike firing is more often represented by unimodal Poisson distribution. More specifically, in the limit of N large

and p small a binomial distribution eq.(6.26) can be described by a Poisson distribution, which usually called as the "Poisson regime" (Feller 1950). This is, if we consider N to be sufficiently large and p small enough in order to ensure that $\lambda = N \cdot p$ is a finite quantity, the binomial distribution converges to the Poisson distribution with mean λ . In this case, the following identity holds

$$\frac{b(k; n, p)}{b(k-1; n, p)} = \frac{\lambda}{k} + O\left(\frac{1}{n}\right), \quad (6.27)$$

and from eq.(6.24) the quotient between $P(k)$ and $P(k-1)$ is

$$\frac{P(k)}{P(k-1)} = \left(\frac{n-k+1}{k}\right) e^{\left\{\theta_1 + \sum_{i=2}^{k-1} \frac{(k-1)}{i!(k-1-i)!} \cdot \left[\frac{k}{k-1} - 1\right] \theta_i + \theta_k\right\}}. \quad (6.28)$$

In the particular case of $k = 1$ we can write,

$$\frac{b(1; n, p)}{b(0; n, p)} = \frac{\lambda}{1} + O\left(\frac{1}{n}\right). \quad (6.29)$$

and the quotient between $P(1)$ and $P(0)$ is

$$\frac{P(1)}{P(0)} = n e^{\theta_1} \quad (6.30)$$

and since we choose $n \rightarrow \infty$ ($\lambda = n \cdot p$ where p is an small quantity),

$$\lambda \approx (n) \cdot e^{\theta_1} + O\left(\frac{1}{n}\right), \quad (6.31)$$

which can also be rewritten as,

$$\frac{\lambda}{n} \approx e^{\theta_1} + O\left(\frac{1}{n^2}\right). \quad (6.32)$$

This implies $\left(\frac{\lambda}{n}\right)^k \approx e^{k\theta_1}$, and the probability of having k neurons firing can be expressed as,

$$P(k) = \frac{n(n-1)\dots(n-(k+1)) \lambda^k}{(n)^k k!} e^{\left\{ \sum_{i=2}^k \binom{k}{i} \cdot \theta_i - \psi(\theta) \right\}}, \quad (6.33)$$

In the limit of $n \rightarrow \infty$, since $\lim_{n \rightarrow \infty} \frac{n(n-1)\dots(n-(k+1))}{(n)^k} = 1$,

$$P(k) \approx \frac{\lambda^k}{k!} e^{-\psi} e^{\left\{ \sum_{i=2}^k \binom{k}{i} \cdot \theta_i \right\}}, \quad (6.34)$$

Defining,

$$q(k) = e^{\left\{ \sum_{i=2}^k \binom{k}{i} \cdot \theta_i \right\}}, \quad (6.35)$$

and imposing (if $i \leq \frac{n}{2}$)

$$\binom{k}{i} \cdot \theta_i > \binom{k}{i+1} \cdot \theta_{i+1} \quad (6.36)$$

$\Rightarrow \frac{1}{k-i} \cdot \theta_i > \frac{1}{i+1} \cdot \theta_{i+1}$ we can choose the condition which will ensure a finite contribution from the higher order contributions. If $i > \frac{n}{2}$ a similar relation should hold $\binom{k}{i} \cdot \theta_i <$

$\binom{k}{i+1} \cdot \theta_{i+1}$ which leads to $\frac{1}{k-i} \cdot \theta_i < \frac{1}{i+1} \cdot \theta_{i+1}$.

Assuming $\theta_i \approx \frac{\bar{\theta}_i}{n^{i-1}}$, if $i \leq \frac{n}{2}$ ($\theta_i \approx \frac{\bar{\theta}_i}{n^{n-i}}$, if $i > \frac{n}{2}$) the condition of $q(k)$ being finite can be expressed as $\bar{\theta}_i > \left(\frac{k-i}{i+1}\right) \frac{\bar{\theta}_{i+1}}{n}$ ($\bar{\theta}_i < \left(\frac{k-i}{i+1}\right) n \bar{\theta}_{i+1}$, if $i > \frac{n}{2}$) and therefore under this constraints

$$q(k) = e^{\left\{ \sum_{i=2}^k \binom{k}{i} \cdot \theta_i \right\}}, \quad (6.37)$$

can be interpreted as a *finite deformation parameter* associated to higher order correlations.

This is,

$$P_q(k) \approx \frac{\lambda^k}{k!} e^{-\psi} e^{q(k)}, \quad (6.38)$$

where $q(k)$ is a deformation parameter in the Poisson distribution which accounts for higher order correlations. This quantity accomplishes the normalization condition $\int dk \cdot P_q(k) = 1$ when integrated over the entire space of responses. The PDF defined in the Information Geometry framework (Nakahara and Amari 2002; Amari et al. 2003) is normalized to one and therefore the approach we used to obtain eq.(6.38) is also normalized since we have taken the limit of large N for which the contribution in the term of the order $O(\frac{1}{N})$ can be disregarded ($\lambda \approx (n) \cdot e^{\theta_1} + O(\frac{1}{n})$).

If $k = 0$, assuming Bernoulli trials, the distribution $b(k;n,p)$ in the ‘*Poisson approximation*’ converges to $b(0;n,p) = e^{-\lambda} + O(\frac{1}{n})$. But, $\langle k \rangle = \frac{\partial \psi}{\partial \theta_1} \Rightarrow \langle k \rangle \sim \lambda$, which corresponds to the averaged responses over trials (notice that the derivative was taken with respect to θ_1). Hence, $P_q(k) \approx \frac{\langle k \rangle^k}{k!} e^{-\langle k \rangle} e^{q(k)}$ is what we will name in the following as ‘*q-deformed Poisson*’ distribution. The scheme developed above with the restriction imposed will be denoted the ‘*q-deformed Poisson regime*’.

Let’s consider a ‘*q-deformed Poisson*’ for observed pattern of activity k to a given stimulus with unknown orientation ξ ,

$$P_q(k|\xi) = \frac{f(\xi)^k e^{-f(\xi)} e^{q(k,\xi)}}{k!}, \quad (6.39)$$

where we named $\langle k \rangle = f(\xi)$ as the mean response over trials for a Poisson distribution. Notice that the bracket denotes $\langle \dots \rangle = \int dk \dots P_q(k|\xi)$.

We define *q-deformed mean response over trials* as

$$\langle k \rangle_{q(\xi)} = \int dk \cdot k \cdot P_q(k|\xi), \quad (6.40)$$

and the *q-deformed variance* as,

$$\langle \sigma^2 \rangle_{q(\xi)} = \int dk \cdot (k - f(\xi))^2 \cdot P_q(k|\xi). \quad (6.41)$$

In the case where “ $q(k, \xi)$ ” can be disregarded $P_q(k|\xi) \rightarrow P_P(k|\xi) = \frac{f(\xi)^k e^{-f(\xi)}}{k!}$, converges to a Poisson distribution, and $\langle \sigma^2 \rangle_{q(\xi)} \rightarrow \sigma^2$ converges to the *variance of a Poisson distribution* $\sigma^2 = f(\xi)$.

In the ‘ q -deformed Poisson regime’ we can estimate the Fisher Information as,

$$I = \left\langle \left\{ \frac{\partial \log P_q(k|\xi)}{\partial \xi} \right\}^2 \right\rangle_q, \quad (6.42)$$

and if the regularity condition

$$\int \frac{\partial^2 P_q(k|\xi)}{\partial \xi^2} = 0 \quad (6.43)$$

is accomplished the following identity holds

$$I = - \left\langle \frac{\partial^2 \log P_q(k|\xi)}{\partial \xi^2} \right\rangle_q. \quad (6.44)$$

Taking the logarithm of the deformed probability distribution,

$$\log P_q(k|\xi) = k \log f(\xi) - f(\xi) - (\log(k!) - \log(e^{q(k,\xi)})), \quad (6.45)$$

the first partial derivate with respect to ξ ,

$$\frac{\partial \log P_q(k|\xi)}{\partial \xi} = k \cdot \frac{f'(\xi)}{f(\xi)} - f'(\xi) + q'(\xi, k), \quad (6.46)$$

and its square can be expressed as,

$$\begin{aligned} \left[\frac{\partial \log P_q(k|\xi)}{\partial \xi} \right]^2 &= \frac{f'(\xi)^2}{f(\xi)^2} \left[(k - f(\xi)) + \frac{q'(\xi, k) f(\xi)}{f'(\xi)} \right]^2 \\ &= \frac{f'(\xi)^2}{f(\xi)^2} (k - f(\xi))^2 + (k - f(\xi)) \frac{2q'(k, \xi) f'(\xi)}{f(\xi)} + q'(k, \xi)^2. \end{aligned} \quad (6.47)$$

Notice that if “ $q'(k, \xi)$ is disregardable or $q(k, \xi) \equiv q(k)$ does not present stimulus dependency” the following identity holds $\left[\frac{\partial \log P_q(k|\xi)}{\partial \xi} \right]^2 = \frac{f'(\xi)^2}{f(\xi)^2} [(k - f(\xi))]^2$. This is exactly equal to the expression we would have obtained for $\left[\frac{\partial \log P_P(k|\xi)}{\partial \xi} \right]^2$ in the case of a Poisson distribution.

In response to a given stimulus with unknown orientation "ξ", the observed pattern of activity is represented by "k". What can we say about "ξ" given "k" by taking into account higher order correlations? Fisher Information reads,

$$I = \langle \sigma^2 \rangle_{q(\xi)} \cdot \frac{f'(\xi)^2}{f(\xi)^2} + \left\langle (k - f(\xi))q'(k, \xi) + \frac{q'(k, \xi)^2 f(\xi)}{2f'(\xi)} \right\rangle_q(\xi) \cdot \frac{2f'(\xi)}{f(\xi)}. \quad (6.48)$$

Fisher information is maximum where the slope is maximum. The effect of higher order correlations into Fisher information are essentially being determined by the quotient between *q deformed variance* $\langle \sigma^2 \rangle_{q(\xi)}$ and the square of the mean $\langle k \rangle = f(\xi)$ without any deformation plus additional contributions from the higher order correlation terms accounted in $q'(k, \xi)$.

In the case in which the "deformation parameter $q(k, \xi)$ is disregardable", considering that in this case the *q-deformed variance* over trial (see eq.6.41) is equal to the mean $f(\xi)$, $P_q \rightarrow P_P$ and,

$$I = \frac{f'(\xi)^2}{f(\xi)}, \quad (6.49)$$

this expression is reduced exactly to the case of the Fisher Information for a Poisson distribution.

Let's consider for a moment the case in which the neuronal activity is modelled as a Gaussian and the noise is assumed to be pairwise-correlated throughout the population (Shamir and Sompolinsky 2001; Shamir and Sompolinsky 2004). The pattern of activity k of the neurons to a given stimulus with unknown orientation ξ is distributed according to a Gaussian distribution,

$$P(k|\xi) = \frac{\exp\left\{\frac{1}{2\sigma_{Gauss}(\xi)}(k - f_{Gauss}(\xi))^2\right\}}{Z}. \quad (6.50)$$

where Z is the normalization factor, $f_{Gauss}(\xi)$ is the Gaussian tuning function and $\sigma_{Gauss}(\xi)$ accounts for pairwise correlations. Fisher Information for the neuronal pool in this case is given as (Shamir and Sompolinsky 2001),

$$I_g = I_{mean} + I_{corr}, \quad (6.51)$$

where

$$I_{mean} = \frac{f'_{Gauss}(\xi)^2}{\sigma_{Gauss}(\xi)} \quad (6.52)$$

and

$$I_{corr} = \frac{\sigma'_{Gauss}(\xi)^2}{2\sigma_{Gauss}(\xi)^2}. \quad (6.53)$$

Notice that the pairwise correlation factor with stimuli dependency in orientation, $\sigma_{Gauss}(\xi)$, and the derivative with respect to the stimuli $\sigma'_{Gauss}(\xi)$, are being included in I_{corr} . The expression above has been implicitly used in the neuro-physiological data analyzed in the previous chapters of this thesis, and correspond to the Fisher Information of the neuronal pooling limit accounting for pairwise correlations. If higher order correlations can be simple reduced to pairwise contributions, then eq.(6.48) has a structure which present a few similarities with respect to eq.(6.51). However, it is important to point out that the widespread probability distribution described in this chapter can not be reproduced using a "Gaussian readout" correlation model and an exact approach including higher order contributions in Information Geometry framework is needed.

6.4 Discussion

Neuronal populations can represent information in the higher order statistics of the responses. Experimental findings show that Information exist not only in the mean firing rates but also in higher order statistic of neuronal responses. In the case of a widespread distribution where the probability distribution presents two peaks, the neurons fire synchronized at one time and are quiescent at other times. This behavior correspond to the case in which higher order correlations generate a widespread distribution of neuronal activity, and the firing activity of the neurons is centered on its mean when all the neurons fire independently. In this particular case, pair-wise correlations do not uniquely determine synchronizing spike firing in a population of neurons.

Thus, higher order correlations across neurons should be taken into account. It is necessary therefore a formalism which allow us to account for a proper description of the Information in terms of higher-order correlations. We developed a new statistical approach, using the

information geometry framework, to account for higher order correlations in the probability distribution function of firing spike patterns of a neuronal pool. This approach allows us to calculate analytically the Fisher Information of the neural population by taking into account all the possible contributions from higher order correlations terms. Moreover, the probability distribution described in this chapter can not be simply reproduced using a "Gaussian readout" correlation model. Our exact formalism allows us to include higher order contributions and to reproduce the widespread distribution where the probability distribution presents two peaks.

It is well known that Fisher Information constitutes an useful measure of the accuracy of a population's code. However, depending on whether it is necessary or not to extract information about pair-wise or higher order correlations in the neural code, the "Gaussian readout" approach is not longer valid. The formalism presented above can be understood as an exact formalism to account for cases in which higher order correlations are a necessary feature to describe the firing spike patterns of a neuronal pool. *The deformation parameter* $q(\xi)$ controls the efficiency of the information encoded in the mean activity, $f(\xi)$ (first term of eq. (6.48)) and provides an additional source of information about the stimuli ξ (second term of eq. (6.48)). Moreover, the distributions function used to estimate Fisher Information correspond to stable distributions of the Boltzmann machine in the neural network (Nakahara and Amari 2002). Thus, the PDF correspond to a probability distribution whose entropy is larger than (or equal to) that of all other members of a specified class of distributions. This is, they all satisfy the maximum entropy (Nakahara and Amari 2002).

The results presented above will be extended in the close future to the general case in which the identity of the cells is taken into account. We are also currently developing a numerical simulation to compare the "Gaussian readout" correlation model with the exact approach developed in this chapter. This comparison will be presented in a paper which is about to be submitted (Montani and Panzeri; 2007)

7. CONCLUSIONS

The brain is basically composed of two types of cells, nerve cells known as neurons, and support cells. There are about one thousand billion neurons in a primate brain. One of the aims of neuroscience is to understand the mechanisms through which the information about sensory stimuli is processed in the brain. The relationship between the state of the word being perceived and neuronal activity is of paramount importance for understanding brain functions. Information Theory allow us to quantify how much information neuronal activity carries about external sensory stimuli. However, the brain is not just a communication system, and we need to survey cases where compression is a way to exploit the statistical structure of the stimuli. The best way to encode information depends enormously on how much compression is used. Discovering possible statistical structures of sensory messages can give new insights of the neural coding.

The spiking activity of nearby cortical neurons is not independent, and we need to understand how neurons work together to represent sensory information. Numerous studies have explored the importance of this correlated responsivity for visual coding and perception, often by comparing the information conveyed by pairs of simultaneously recorded neurons with the sum of information provided by the respective individual cells. The simple comparison between pairwise and summed individual responses conflates several forms of correlation, however, making it impossible to judge the relative importance of synchronous spiking, basic tuning properties, and stimulus (in)dependent correlation. We found that although synchrony is prevalent and informative, the additional information it provides is frequently offset by the redundancy arising from the similar tuning properties of the two cells. Thus, coding is roughly independent with weak synergy or redundancy arising depending on the similarity in tuning and the temporal precision of the analysis. Our findings suggest that this would allow cortical circuits to enjoy the stability provided by having similarly tuned neurons without suffering the penalty of redundancy as the associated information transmission

deficit is compensated for by stimulus dependent synchrony.

More specifically, we found that for direction coding the information available by having precise spike timing for pairs of neurons in V1 adds super-linearly. But at more coarse timescale, information about direction adds slightly sub-linearly across pairs of cells in agreement with a previous study of V1 cells by (Reich et. al. 2001), based on information theory. We have revealed the origin of these effects by our information component analysis, which shows a redundant (negative) contribution to the information due to the overlap in tuning and to the average level of correlation (i.e. stimulus independent correlation). However, these components are balanced on average by a contribution from stimulus-dependent synchrony.

It is usually accepted that visual scene contains features such as edges and homogenous color patches, which give rise to statistical dependencies between neighboring regions of the visual image (Field 1987). Knowledge of the properties of signals that are behaviorally important for the animal can be used to improve the signal/noise ratio for their detection by matching characteristics of the detector with those properties. As much as possible this preserves the stimulus energy and excludes other signal that would contribute with noise. To reduce redundancy, the visual system might use these features as a basis for representing visual input (Barlow 2001). Our results have showed that synergy was stronger (and redundancy weaker) for pairs of neurons with dissimilar tuning curves. Pairs of neurons with overlapping spatial receptive fields but dissimilar orientation tuning will provide a strong joint response to features such as corners and T-junctions in a visual scene (Das and Gilbert 1999); by comparison, those pairs with similar orientation tuning will be jointly driven best by lines and edges. Our results suggest that the pairwise coding of lines and edges is essentially independent, due to the effects of tuning-related redundancy, whereas the coding of features such as corners should be more synergistic. Analogous to this, the coding for changes in contrast is strongly redundant, due to the greater inherent similarity of the contrast tuning curves of the neurons in a pair.

To overcome the inefficiency of distributed representations with high activity ratio, which are the typical product of code to reduce redundancy, one needs representations with minimum overlap. This is, representations with the minimum number of elements active in inputs to the pair of cells that need to be distinguished. However, our findings suggest that stimulus dependent correlations can help the neural code to overcome this problem. The fact that the

synchronization depends on the stimulus direction is critical for coding: it serves to reduce the redundancy caused by cells having similar tuning.

Contrast response functions of pairs of neurons tend to be fairly similar, and synchrony at lower contrasts has less temporal precision. For both contrast and direction coding, the redundant contributions are dominated by similarity in tuning, although the redundancy is stronger for contrast. The average level of correlation plays a small redundant effect in both cases. The synergistic contribution of stimulus dependence of correlations is also lower on average for contrast than for direction coding. Overall, this results in a coding regime more similar to the traditional intuition, in which correlations tend to result in redundancy, and thus limit the number of neurons whose outputs could usefully be combined to represent the stimulus variable. Importantly, the results of our analysis warn strongly against making general statements about the role of correlations in neural coding. As demonstrated here, the effect of correlations can be quite sensitive to both the timescale and the nature of the stimulus parameter that is being studied.

Our results suggest a new role for stimulus-dependent synchronization: to create a coding regime that allows sensory information to be pooled across a neuronal population in a linear (i.e. informationally independent) or even super-linear way despite the presence of redundancy in the signals conveyed by individual cells (i.e. their similarity in tuning). This may be an important role, particularly if the redundancy is a necessary feature of cortical circuitry rather than an imperfection. Because redundancy can lead to improved robustness through fault-tolerance, it may well be desirable.

We find that destroying the identity of which neuron fired an action potential results in a substantial loss in information about stimulus direction. This provokes the question: how could downstream neurons decode and make use of the positive information contribution provided by the stimulus-dependent synchronization? Simple linear readout schemes such as the population vector (Georgopoulos et. al. 1986) can not decode this scheme. A nonlinear readout algorithm is required, like a nonlinear population vector (Shamir and Sompolinsky 2004). This does not address how such a readout should be implemented, however, and the implementation constraints are particularly severe if one considers that the information should be usable within a single neuronal layer, as opposed to a multi-layer network. An integrate-and-fire operation would effectively pool input spikes regardless of origin, thus being subject to the

limitations on combining information from correlated input neurons (Zohary et. al. 1994). Nonlinear dendritic summation (Hausser and Mel 2003) would thus appear to be a necessary feature for the biophysical implementation of a decoder capable of making use of the additional information contribution.

A similar principle should be applicable from our findings to primates. The animal must identify what is redundant in the sensory messages, because statistical regularities in its environment will be also essential for its survival. Redundancy provided by contrast in visual stimuli, will help to improve robustness through fault-tolerance. By balancing this redundancy with stimulus-dependent synchronization, the brain could take advantage of both the robustness provided by redundancy and the accuracy due to pooling allowed by informational independence.

We have discussed the advantages of the Jensen-Shannon measure in comparison to the Kullback-Leiber divergence. More specifically, we have investigated the Jensen-Shannon Divergence as a measure of distance between the corresponding probability distribution functions associated with each spikes fired observed patterns. We found that the relative Jensen-Shannon Divergence (measured in relation to the case in which all cells fired completely independently) decreases with respect to the difference in orientation preference between the receptive field from each pair of cells. Our finding indicates that the Jensen-Shannon Divergence can be used for characterizing the effective circuitry network in a population of neurons.

To understand first how simple focal abnormalities in GABAergic modulators can affect the information transmission in an impaired brain tissue we developed a computational and analytical model of a topographically mapped population code. The model includes a focal lesion as well as a process for receptive field enlargement (plasticity). It simulates the recovery processes in the brain, and allows us to investigate mechanisms which increase the ability of the cortex to restore lost brain functions. We estimated the Fisher Information carried by the topographic map before and after the stroke. Our finding shows that by tuning the receptive field plasticity to a certain value, the information transfer through the cortex after stroke can be optimized.

A widespread distribution of neuronal activity can generate higher-order stochastic interactions. If neurons fire synchronized at one time and are quiescent at other times, pair-wise

correlations do not uniquely determine synchronizing spiking in a population of neurons and higher order interactions across neurons cannot be disregarded. We present a new statistical approach, using the information geometry framework, for analyzing the probability density function (PDF) of spike firing patterns by considering higher order correlations in a neuronal pool. In chapter VI, we studied the limit of a large population of neurons and associated a deformation parameter to the higher order correlations in the PDF. We have also performed an analytical estimation of the Fisher information in order to evaluate the implications of higher order correlations between spikes on information transmission. Our formalism, leads to a new procedure to study higher order stochastic interactions. This will allow us, in the near future, to evaluate how different stimuli structures can influence the neural coding through higher order spike correlations.

Short-term plasticity with respect to spike train structure has been demonstrated in a variety of conditions (Dobrunz and Stevens 1999; Lisman 1997; Snider and Bonds 1998, Tsodyks et. al. 1997; Usrey et. al. 1998; Varela et. al. 1997). He developed a theory to provide a framework for many perceptual phenomena that remain unexplained. Von der Malsburg 1981 proposed that the temporal correlations between neurons could help to avoid a potential combinatorial problem in neural coding. Theories that propose the creation of "cardinal" cells to represent particular combinations of signals from lower-order neurons are implausible because the number of combinations to be coded exceeds the number of neurons available. In Von der Malsburg theory, which constitutes the original formulation of the binding theory, the activity of low-order neurons would be combined only when their spike activity was synchronized to within a few milliseconds to create a synchronously active cell assembly. Their elaborations are termed correlation theory or temporal binding theory, where perceptually related features are linked through correlated firing among subpopulations of cells. The original basis of the cell assembly theory was that relationships were formed between cells based on anatomical connections (Hayek 1952; Hebb 1949). However, acknowledging the dynamic and adaptive nature of the brain, Hayek (1952) proposed that the formation of cell assemblies might not require actual anatomical changes in synaptic connections. It could instead result from short-term enhancement of synaptic effectiveness (a form of plasticity) generated by changes in the temporal structure of spike trains (Von der Malsburg 1981).

But conceptual problems arise when the binding is considered as strictly intra-cortical (Eckhorn et. al. 1988; Gray-Singer 1989). Intra-cortical binding through oscillation essen-

tially solves the problem using circular logic. The cortex bind object features to identify the object, but to bind the features the cortex needs to know in advance that they are part of the same object.

It is important to consider the information coding as a multi-level process with several hierarchical levels where the dynamics and synchronization of the neural activity plays a fundamental role (Borisjuk et. al. 1997). The results presented in this Thesis do not bear on directly with the role of oscillation or synchrony in solving the binding problem. However, our findings are in agreement with the (Samonds et. al. 2004) suggestions that cortical synchrony starts with the visual stimulus and the retinal input. Spatial and temporal correlations in the visual scene cause synchronous activation of populations of retinal cells. This leads to matching cortical latencies, triggering synchronization. Transient synchrony occurs with either dynamic or novel stimuli (Kruse and Eckhorn 1996) propagating from retina to LGN to cortex (Castelo-Branco 1998; Neuenschwander et. al. 2002). Moreover, it is reasonable to interpret the pathway from the retina to the cortex as a non-linear network which accounts for fine temporal synchronization with stimulus dependence in the responses at the level of the cortical processing. This is, to build a sort of multistage temporal binding integration theory, which could account for all the features not included in the von der Malburg hypothesis.

The overall findings of this thesis warn about making any extensive statement about the role of neuronal spike correlations without considering the general case that includes higher order correlations, and suggest a need to reshape the current debate about the role of spike correlations across neurons.

APPENDIX

.1 Publications

The works previously presented in chapter II, III, IV and V have appeared in print.

- Montani F., Kohn A., Smith M.A., Schultz S.R. (2007), The role of correlations in direction and contrast coding in the primary visual cortex., *J Neurosci*, Vol: 27, Pages: 2338 - 2348, 1529-2401.
- Montani F., Kohn A., Smith M.A., Schultz S.R. (2007), How do stimulus-dependent correlations between V1 neurons affect neural coding?, *Neurocomputing*, Vol: 70, Pages: 1782 - 1787.
- Montani F., Rosso O. A. and Schultz S. R. (2007). Discrimination Measure of Correlations in a Population of Neurons by using the Jensen-Shannon Divergence. *AIP Conference Proceedings 913 XV Conference on Nonequilibrium Statistical Mechanics and Nonlinear Physics*, pp. 184-189.
- Einarsdottir H., Montani F. and Schultz S. R. (2007). A mathematical model of receptive field reorganization following stroke. *IEEE International Conference on Development and Learning*, in press.

Two preprints are about of being submitted.

- Montani F., Einarsdottir H., and Schultz S. R. (2007). The accuracy of a neural population code after focal ischaemia. To submitted to *Network*.
- Montani F. and Panzeri S. (2007). An analytical approach to the PDF and Fisher Information considering higher-order correlations in a population of neurons. To be submitted to *Neural Computation*.

BIBLIOGRAPHY

- [Abeles 1982] Abeles, M. (1982) Role of cortical neuron: integrator or coincidence detector. *Isr. J. Med. Sci.*, 18: 83-92.
- [Abeles et. al. 1993] Abeles M, Bergman H, Margalit E, Vaadia E. (1993) Spatiotemporal firing patterns in the frontal cortex of behaving monkeys. *J Neurophysiol.* 1993 Oct;70(4):1629-38.
- [Abbott and Dayan 1999] Abbott, L.F., and Dayan, P. (1999). The effect of correlated variability on the accuracy of a population code. *Neural Comput.* 11, 91-101 MIT Press.
- [Abeles 1982] Abeles, M. (1982) Role of cortical neuron: integrator or coincidence detector. *Isr. J. Med. Sci.*, 18: 83-92.
- [Aersten et. al. 1989] Aertsen, A.M.H.J, Gerstein, G.L., Habib, M.K, and Palm, G. (1989) Dynamics of neuronal firing correlation: modulation of 'effective connectivity'. *J. Neurophysiol.*, 61, 900-917.
- [Aiple and Krueger 1998] Aiple, F. and Krueger, J. (1998). Neuronal synchrony in monkey striate cortex: interocular signal flow and dependency on spikes rates. *Exp.. Brain Res.*, 72, 141-149.
- [Alais 1998] Alais D., Blake R. and Lee S. -H (1998), Visual features that vary together over time group together over space. *Nat. Neurosci.* 1 , 160-164.
- [Alonso at. al. 1996] Alonso, J.M., Ursey, W.M. and Reid, R.C. (1996). Precisely correlated firing in cells of the lateral geniculate nucleus. *Nature*, 383, 815-819.
- [Alonso et. al. 1998] Alonso, J.M., and Martinez, L.M. (1998). Functional connectivity between simple cells and complex cells in cat striate cortex. *Nat. Neurosci.*, 1, 395-403.

- [Amari 1980] Amari, S. (1980) Theory of information spaces—a geometrical foundation of statistic, POST RAAG, Report 106.
- [Amari 1982] Amari, S. (1982) Differential Geometry of curved exponential families—curvature and information loss, *The Annals of Statistics*,10,357-385.
- [Amari 1992] Amari, S (1992), Information Geometry of Boltzmann Machines, *IEEE Transactions of Neuronal Networks*,3,2,260–271,1992
- [Amari 1997] Amari, S. (1997), Information Geometry, *Contemporary Mathematics*, 203,81–95,1997, American Mathematical Society.
- [Amari and Nagaoka 2000] Amari, S. and Nagaoka, H. (2000), *Methods of Information Geometry*, Translation of Mathematical Monographs, 191,OXFORD University Press.
- [Amari 2001] Amari, S. (2001), Information Geometry on Hierarchy of Probability Distributions, *IEEE Transactions on Information Theory*,47, 5, 1701–1711,
- [Amari et al. 2003] Amari S., Nakahara H., Wu S. and Sakai Y., Synchronous firing and higher-order interactions in neuron pool , *Neural Computation*,15, 127–142, 2003, Massachusetts Institute of Technology.
- [Andersen 1995] Andersen R. A. (1995), Encoding of intention and spatial location in the posterior parietal cortex. *Cereb. Cortex* 5, pp. 457-469.
- [Anderson et. al. 2000] Anderson, J.S. and Carandini, M. and Ferster, D. (2000),Orientation Tuning of Input Conductance, Excitation, and Inhibition in Cat Primary Visual Cortex, *Journal of Neurophysiology*, 84, 2, 909–926, Am Physiological Soc.
- [Attneave 1954] Attneave F Some informational aspects of visual perception. *Psychol Rev.* 1954,61(3):183-93.
- [Averbeck and Lee 2003] Averbeck, B.B., and Lee D. (2003). Neural Noise and movement-related codes in the macaque supplement area. *J Neurosci*.
- [Averbeck et. al. 2003] Averbeck BB, Crowe DA, Chafee MV, Georgopoulos AP (2003). Neural activity in prefrontal cortex during copying geometrical shapes. II. Decoding shape segments from neural ensembles. *Exp Brain Res.*;150(2):142-53.

- [Averbeck and Lee 2004] Averbeck BB, Lee D. Related Articles, Links Coding and transmission of information by neural ensembles. *Trends Neurosci.* 2004 Apr;27(4):225-30. Review.
- [Averbeck et. al. 2006] Averbeck, B.B., Lathan P.E. and Pouget A. (2006). Neural correlations, population coding and computation. *Nature Reviews Neurosci.* 7, 358-366.
- [Azouz and Gray 1999] Azouz, R. and Gray, C.M. (1999) Cellular mechanisms contributing to response variability of cortical neurons in vivo. *J. Neurosci.*, 19, 2209-2223.
- [Bair and Koch 1996] Bair W, Koch C (1996). Temporal precision of spike trains in extrastriate cortex of the behaving macaque monkey. *Neural Comput.* ;8(6):1185-202.
- [Bair 1997] Bair, W., Cavanaugh, J., and Movshon, J. (1997). Reconstructing stimulus velocity from neuronal responses in area MT. *NIPS*, 10:34-40.
- [Bair et. al. 2001] Bair, W., Zohary E., and Newsome, W.T. (2001). Correlated firing in macaque visual area MT: time scales and relationship to behavior. *J. Neurosci.* 21,1676-1697.
- [Barlow 1959] Barlow, H. B. (1959). Sensory mechanisms, the reduction of redundancy, and intelligence. In *The mechanisation of thought processes*, 535-539. H.M.S.O., London.
- [Barlow 2001] Barlow H. (2001). Sensory mechanisms, the reduction of redundancy, and intelligence. *Network.*12(3):241-53.
- [Ben-Yishai et. al. 1995] Ben-Yishai R, Lev Bar-Or R, Sompolinsky H (1995) Theory of orientation tuning in visual cortex. *Proc Natl Acad Sci USA* 92: 3844-3848.
- [Bennett et. al. 2004] Bennett MV, Zukin RS. (2004) Electrical coupling and neuronal synchronization in the mammalian brain. *Neuron.*;41(4):495-511.
- [Borisjuk et. al. 1990] Borisjuk GN, Borisjuk RM, Kirillov AB, Kryukov VI, and Singer W. (1990). Modelling of oscillatory activity of neuron assemblies of the visual cortex. In: *Proc. of Inter. Joint. Conf. on Neural Networks-90*, San Diego,2:431-434.
- [Borisjuk et. al. 1997] Borisjuk RM, Borisjuk GN (1997). Information coding on the basis of synchronization of neural activity. *BioSystems* 40, 3-10.

- [Borisyuk et. al. 2000a] Borisyuk R., Denham M., Kazanovich Y., Vinogradova O (2000). An oscillatory neural network model of sparse distributed memory and novelty detection. *BioSystems* 58, 265-272.
- [Borisyuk et. al. 2000b] Borisyuk G.N., Borisyuk R.M., Kazanovich Y.B. (2000). Temporal structure of neural activity and models of information processing in the brain. Chapter in *Time and the Brain*, ed. R. Miller, Harwood Acad Publ., pp.331-349
- [Borisyuk et. al. 2001] Borisyuk R., Denham M., Hoppensteadt F., Kazanovich Y. (2001), Vinogradova O. (2001) Oscillatory model of novelty detection. *Network - Comput in Neural Syst*, 12: 1-20.
- [Borst and Theunissen 1999] Borst A, Theunissen FE (1999) Information theory and neural coding. *Nature Neuroscience* 2: 947-957
- [Bothe et. al. 2000] Bothe, S. M., Spekreijse, H. and Roelfsema, P.R. (2000) The Effects of Pair-wise and Higher-order correlations on the Firing rate of a Postsynaptic Neuron, *Neural Computation*, 12, 153-159, Massachusetts Institute of Technology.
- [Brenner et. al. 2000] Brenner N, Strong SP, Koberle R, Bialek W, de Ruyter van Steveninck RR. Synergy in a neural code. *Neural Comput.* 2000 Jul;12(7):1531-52.
- [Broniatowski and Leorato 2006] Broniatowski, M. and Leorato, S. (2006) An estimation method for the Neyman chi-square divergence with application to test of χ^2 , *Journal of Multivariate Analysis*, Volume 97, 6, 1409-1436.
- [Bryant et. al. 1973] Bryant, J., Marcos, A.R. and Segundo, G.H. (1973) Correlations of neuronal spike discharges produced by monosynaptic connections and by common inputs *J Neurophysiol*, Mar 1973; 36: 205 - 225.
- [Buracas et. al. 1998] Buracas GT, Zador AM, DeWeese MR, Albright TD. Efficient discrimination of temporal patterns by motion-sensitive neurons in primate visual cortex. *Neuron*. 1998 May;20(5):959-69.
- [Buzsaki et. al. 1996] Buzsaki G, Penttonen M, Nadasdy Z, Bragin A. (1996) Pattern and inhibition-dependent invasion of pyramidal cell dendrites by fast spikes in the hippocampus in vivo. *Proc Natl Acad Sci U S A*. Sep 3;93(18):9921-5.

- [Carlen et al. 2000] Carlen P.L., Skinner F., Zhang L., Naus C., Kushnir M., and Perez Velazquez J.L., The role of gap junctions in seizures, *Brain Res. Brain Res. Rev.* 32 (2000), 235-241.
- [Calford and Tweedale 1988] Calford, M.B. and Tweedale, R. (1988), Immediate and chronic changes in responses of somatosensory cortex in adult flying-fox after digit amputation, *Nature*, 332, 6163, 446-448.
- [Carmichael 2003] Carmichael, S.T.(2003), Plasticity of Cortical Projections after Stroke, Carmichael, S.T., *The Neuroscientist*, 9, 1, 64.
- [Carlton 1969] Carlton, A. G. (1969). On the bias of information estimates. *Psychological Bulletin*, 71, 108-109.
- [Carlsson 1998] Carlsson M.L., Hypothesis: is infantile autism a hypoglutamatergic disorder? Relevance of glutamate - serotonin interactions for pharmacotherapy, *J. Neural Transm.* 105 (1998), 525-535.
- [Castelo-Branco 1998] Castelo-Branco, M., Neuenschwander, S. and Singer, W. (1998) Synchronization of visual responses between the cortex, lateral geniculate nucleus, and retina in the anesthetized cat. *J. neurosci.*, 18, 6395-6410.
- [Cavanaugh et. al. 2002] Cavanaugh, J.R., Bair, W. and Movshon, J.A. (2002). Nature and interaction of signals from the receptive field center and surround in macaque V1. *J Neurophysiol* 88:2530-2546.
- [Chacron 2006] Chacron M.J. (2006). Nonlinear Information Processing in a Model Sensory System *J Neurophysiol*, May 2006; 95: 2933 - 2946.
- [Choi and Lee 2003] Euisun Choi and Chulhee Lee (2003), Feature extraction based on the Bhattacharyya distance *Pattern Recognition*, Volume 36, 8, 1703-1709.
- [Christiakova 1998] M., Christiakova, M and Singer, W. (1998) Modifications of discharge patterns of neurocortical neurons by induced oscillations of the membrane potential. *Neuroscience*, 83: 15-25.

- [Churchland et. al 1994] Churchland P. S., Ramachandran V. S. and Sejnowski T. J, A critique of pure vision (1994). In: C. Koch and J.L. Davis, Editors, Large-Scale Neuronal Theories of the Brain, MIT Press, Cambridge, MA .
- [Cobb et. al. 1995] Cobb S.R., Buhl E. H., Halasy K., Paulsen O. and Somogyi P. (1995), Synchronization of neuronal activity in hippocampus by individual GABAergic interneurons. *Nature* 378, 75-78.
- [Cover and Thomas 1991] Cover TM, Thomas JA (1991) *Elements of Information Theory*: Books: Wiley Series in Telecommunications and Signal Processing.
- [Curado and Tsallis 1994] Curado, E.M.F. and Tsallis, C. (1991), Generalized statistical mechanics: connections with thermodynamics, *Journal of Physics A*, 24,L69–L72.
- [Dan et. al. 1998] Dan, Y., Alonso, J.-M., Usrey, W.M. and Reid, R.C. (1998). Coding of visual information by precisely correlated spikes in the lateral geniculate nucleus. *Nature Neurosci.* 1(6):501-507.
- [Dancause et. al. 2005] Dancause, N. and Barbay, S. and Frost, S.B. and Plautz, E.J. and Chen, D. and Zoubina, E.V. and Stowe, A.M. and Nudo, R.J. (2005), Extensive Cortical Rewiring after Brain Injury, *Journal of Neuroscience*, 25, 44, 10167–10179, *Soc Neuroscience*.
- [Darian-Smith et. al. 1973] Darian-Smith I, Johnson KO, Dykes R (1973) Cold fiber population innervating palmar and digital skin of the monkey: responses to cooling pulses. *J Neurophysiol* 36:325346.
- [Das and Gilbert 1999] Das A., & Gilbert C. D.(1999), Topography of contextual modulations mediated by short-range interactions in primary visual cortex. *Nature* 399, 655-661.
- [De Angelis et. al. 1999] DeAngelis GC, Ghose GM, Ohzawa I, Freeman RD (1999) Functional micro-organization of primary visual cortex: receptive field analysis of nearby neurons. *J Neurosci* 19: 4046-4064.
- [De Charms et. al. 1996] De Charms, R.C., and Merzenich, M.M. (1996). Primary cortical representation of sounds by the coordination of action-potential timing. *Nature* 381, 610-613.

- [Deneve et. al. 1999] Deneve, S. and Latham, P.E. and Pouget, A. (1999), Reading population codes: a neural implementation of ideal observers, *Nature Neuroscience*, 2, 740–745.
- [De Oliveira et. al. 1997] De Oliveira, S.C., Thiele, A. and Hoffman, K.P. (1997). Synchronization of neural activity during stimulus expectation in a direction discrimination task. *J. Neurosci.* 17, 9248-60.
- [Desimone 1991] Desimone R., Face-selective cells in the temporal cortex of monkeys (1991). *J. Cogn. Neurosci.* 3 , 1-8.
- [De Oliveira et. al. 1997] De Oliveira, S.C., Thiele, A. and Hoffman, K.P. (1997). Synchronization of neural activity during stimulus expectation in a direction discrimination task. *J. Neurosci.* 17, 9248-60.
- [DiCicco-Bloom et al. 2006] DiCicco-Bloom E., Lord C., Zwaigenbaum L., Courchesne E., Dager S.R., Schmitz C., Schultz R.T, Crawley J. and Young L.J., The developmental neurobiology of autism spectrum disorder, *J. Neurosci.* 26 (2006), 68976906.
- [Dobrunz and Stevens 1999] Dobrunz LE and Stevens CF. Response of hippocampal synapses to natural stimulation patterns. *Neuron* 22: 157166, 1999.
- [Draguhn et al. 1998] Draguhn A., Traub R.D., Schmitz D. and Jefferys J.G., Electrical coupling underlies high-frequency oscillations in the hippocampus in vitro, *Nature* 394 (1998), 189192.
- [Dugundji 1966] Dugundji, J. (1966) *Topology*, Allyn and Bacon, Boston.
- [Eckhorn et. al. 1988] Eckhorn R, Bauer R, Jordan W, Brosch M, Kruse W, Munk M, Reitboeck HJ (1988) Coherent oscillations: a mechanism of feature linking in the visual cortex? Multiple electrode and correlation analyses in the cat. *Biol Cybern* 60:121130.
- [Edelman 1987] Edelman, G.M. (1987) *Neural Darwinism: the Theory of Neural Group Selection*. Basic Books, New York. Mitzdorf, U. (1985). Current source-density method and application in cat cerebral cortex: investigation of evoked potentials and EEG phenomena. *Physiol. Rev.* 65, 37-100.

- [Einarsdottir and Montani and Schultz] H. Einarsdottir, F. Montani and S. R. Schultz (2007). A mathematical model of receptive field reorganization following stroke. IEEE International Conference on Development and Learning, in press.
- [Endres and Schindelin 2003] D. Endres, J. Schindelin (2003), IEEE Trans. Inf. Theory , 49, 1858–1860.
- [Engel et. al. 1990] Engel, A.K., König, P., Gray, C. M. and Singer, W. (1990). Stimulus-dependent neuronal oscillations in cat visual cortex: inter-columnar interactions as determined by cross-correlation analysis. Biol. Cybern. 60:121-30.
- [Engel et. al. 1992] Engel AK, König P, Kreiter AK, Schillen TB, Singer W., Temporal coding in the visual cortex: new vistas on integration in the nervous system. Trends Neurosci. 1992 Jun;15(6):218-26.
- [Engel et. al. 1997] Engel, A. K., Roelfesma, P.R., Fries, P., Brecht, M. and Singer, W. (1997) Role of then temporal domain for response selection and perceptual binding. Cereb. Cortex.7: 571-582.
- [Eysel and Schweigart 1999] Eysel, U.T. and Schweigart, G.(1999), Increased Receptive Field Size in the Surround of Chronic Lesions in the Adult Cat Visual Cortex, Cerebral Cortex, 9, 2, 101–109.
- [Feller 1950] Feller, W (1950), An Introduction to Probability Theory and Its Applications, Vol. 1, 3rd Edition, John Wiley and Sons.
- [Felling 2003] R. J. Felling and S. W. Levison(2003), Enhanced neurogenesis following stroke, J. Neurosci., 73,277-283.
- [Field 1987] Field, D.J., (1987) Relations between the statistics of natural images and the response properties of cortical cells, J. Opt. Soc. Am. A 4 pp. 2379-2394.
- [Frahm et. al. 2004] Frahm C., and Haupt, C. and Witte OW (2004),GABA Neurons Survive Focal Ischemic Injury, Klin Neurophysiol, 35.
- [Friedman-Hill et. al. 2000] Friedman-Hill S, Maldonado PE, Gray CM (2000) Dynamics of striate cortical activity in the alert macaque: I. Incidence and stimulus dependence of gamma-band neuronal oscillations. Cereb Cortex 10: 1105-1116.[Abstract/Free Full Text]

- [Frien et. al. 2000] Frien A, Eckhorn R, Bauer R, Woelbern T, Gabriel A (2000) Fast oscillations display sharper orientation tuning than slower components of the same recordings in striate cortex of the awake monkey. *Eur J Neurosci* 12: 1453-1465.
- [Frost et. al. 2003] S. B. Frost, S. Barbay, K. M. Friel, E. J. Plautz and R. J. Nudo (2003) Reorganization of Remote Cortical Regions After Ischemic Brain Injury: A Potential Substrate for Stroke Recovery *J Neurophysiol.* 2003 Jun;89(6):3205-14.
- [Fukuda et. al. 2000] Fukuda T, Kosaka T. Gap junctions linking the dendritic network of GABAergic interneurons in the hippocampus. *J Neurosci.* 2000;20:1519-1528.
- [Fukuda et. al. 2000] Fukuda T, Kosaka T. Gap junctions linking the dendritic network of GABAergic interneurons in the hippocampus. *J Neurosci.* 2000;20:1519-1528.
- [Fukuda et al. 2006] Fukuda T., Kosaka T., Singer W. and Galuske R.A., Gap junctions among dendrites of cortical GABAergic neurons establish a dense and widespread inter-columnar network, *J. Neurosci.* 26 (2006), 3434-3443.
- [Fujioka et al. 2004] H. Fujioka and H. Kaneko and S. S. Suzuki and K. Mabuchi (2004), Hyperexcitability-associated rapid plasticity after a focal cerebral ischemia, *Stroke*, 35, e346-e348.
- [Gabor 1946] Gabor, D (1946), *Theory of Communication*, *J. Inst. Electr. Eng.*, 93, 429-57, Institution of Electrical Engineering.
- [Galarreta and Hestrin 1999] Galarreta M, Hestrin S (1999). A network of fast-spiking cells in the neocortex connected by electrical synapses. *Nature.* ;402(6757):72-5.
- [Gardner-Medwin and Barlow 2001] Gardner-Medwin AR, Barlow HB. The limits of counting accuracy in distributed neural representations. *Neural Comput.* 2001 Mar;13(3):477-504.
- [Gawne 1993] Gawne, T.J., Richmond, B.J., (1993). How independent are the messages carried by adjacent inferior temporal cortical neurons? *J. Neurosci.* 13, 2758-2771.
- [Gawne et. al. 1996] Gawne, T.J., Kjaer, T.W., Herz, J.A., and Richmond, B.J. (1996). Adjacent visual cortical complex cells share about 20% of their stimulus-related information. *Cerebr Cortex* 6 , 482-489.

- [Gerstein and Perkel 1969] Gerstein, G.L., Perkel D.H. (1969). Simultaneously recorded trains of action potentials: analysis and functional interpretation. *Science* 164 (881), 828-30.
- [Georgopoulos et. al. 1986] Georgopoulos, A.P., Schwartz, A.B. and Kettner, R.E. (1986). Neuronal population coding of movement direction. *Science* 243:1416-1419.
- [Georgopoulos 1990] Georgopoulos AP. Neural coding of the direction of reaching and a comparison with saccadic eye movements. *Cold Spring Harb Symp Quant Biol.* 1990;55:849-59.
- [Gibson et. al. 1999] Gibson JR, Beierlein M, Connors BW (1999). Two networks of electrically coupled inhibitory neurons in neocortex. *Nature.* 402(6757):75-9.
- [Goldstein and Reinert 2006] Goldstein, L. and Reinert, G (2006), Total Variation Distance for Poisson Subset Numbers. *Annals of Combinatorics*, Volume 10, Number 3, 333-341.
- [Golledge et. al. 2003] Golledge HD, Panzeri S, Zheng F, Pola G, Scannell JW, Giannikopoulos DV, Mason RJ, Tove MJ, Young MP (2003). Correlations, feature-binding and population coding in primary visual cortex. *Neuroreport.* May 23;14(7):1045-50.
- [Green and Swets 1966] Green, D.M., Swets J.A. (1966) *Signal Detection Theory and Psychophysics*. New York: Wiley.
- [Gochin et. al. 1991] Gochin, P.M, Miller, E.K., Gross, C.G. and Gerstein, G.L. (1991). Functional interactions among neurons in inferior temporal cortex of the awake macaque. *Exp. Brain res.*, 84, 505-516.
- [Golledge et. al. 2003] Golledge H.D., Panzeri S., Zheng F., Pola G., Scannell J.W., Giannikopoulos D.V., Mason R.J., Tovee M.J., Young M.P. (2003). Correlations, feature-binding and population coding in primary visual cortex. *Neuroreport* 14(7):1045-50.
- [Gray-Singer 1989] Gray, C.M. and Singer, W. (1989). Stimulus specific neuronal oscillations in orientation columns in cat visual cortex. *Proc. Natl. Acad. Sci. USA*, 86, 1698-1702.
- [Gray et. al. 1989] Gray, CM, Koenig, P., Engel, A.K. and Singer, W. (1989). Oscillatory responses in cat visual cortex exhibit inter-columnar synchronization which reflects global stimulus properties. *Nature*, 388, 334-337.

- [Gray et. al. 1997] Gray CM, Viana Di Prisco G (1997) Stimulus dependent neuronal oscillations and local synchronization in striate cortex of the alert cat. *J Neurosci* 17: 3239-3253.
- [Gray 1999] Gray, C.M. (1999). The temporal correlation hypothesis of visual feature integration: still alive and well. *Neuron* 24(1):31-47.
- [Grosse et. al. 2002] I. Grosse, P. Bernaola-Galvan, P. Carpena, R.R. Roldan, J.L. Oliver, H.E. Stanley, *Phys. Rev. E* 65 (2002) 041905.
- [Hata et. al. 1998] Hata, Y., Tsumoto, T., Sato, H., Hagihara, K. and Tamura, H. (1998). Inhibition contributes to orientation selectivity in visual cortex of cat. *Nature*, 335, 815-817.
- [Hayek 1952] Hayek FA. *The Sensory Order*. Chicago, IL: University of Chicago Press, 1952.
- [Hausser and Mel 2003] Häusser, M. and Mel, B. (2003). Dendrites: bug or feature? *Current Opinion in Neurobiology* 13:372-83.
- [Hebb 1949] Hebb DO. *The Organization of Behavior: A Neuropsychological Theory*. New York: Wiley, 1949.
- [Hubel et. al. 1962] Hubel,D.H. and Wiesel, T.N. (1962). Receptive fields, binocular interaction and functional architecture in the cat's visual cortex *J. Physiol. (London)* 160, 106-154.
- [Huguenard and Prince 1994] Huguenard J.R. and Prince D.A., Intrathalamic rhythmicity studied in vitro: nominal T-current modulation causes robust antioscillatory effects, *J. Neurosci.* 14 (1994), pp. 54855502.
- [Hussman 2001] Hussman J.P., Suppressed GABAergic inhibition as a common factor in suspected etiologies of autism, *J. Autism Dev. Disord.* 31 (2001), 247248.
- [Hawken and Parker 1987] Hawken, MJ and Parker, AJ (1987), Spatial Properties of Neurons in the Monkey Striate Cortex, *Proceedings of the Royal Society of London. Series B, Biological Sciences*, 231,1263,251–288, JSTOR.
- [Hormuzdi et al. 2001] S.G. Hormuzdi, I. Pais, F.E. LeBeau, S.K. Towers, A. Rozov, E.H. Buhl, M.A. Whittington and H. Monyer, Impaired electrical signaling disrupts gamma frequency oscillations in connexin 36-deficient mice, *Neuron* 31 (2001), 487495.

- [Hubel et. al. 1962] Hubel, D.H. and Wiesel, T.N. (1962). Receptive fields, binocular interaction and functional architecture in the cat's visual cortex *J. Physiol. (London)* 160, 106-154.
- [Hubel and Weisel 1977] Hubel and Wiesel, 1977. Ferrier lecture. Functional architecture of macaque monkey visual cortex. *Proc R Soc Lond B Biol Sci.* 1977 Jul 28;198(1130):1-59.
- [Hubener et. al. 1997] Hubener M, Shoham D, Grinvald A, Bonhoeffer T. Spatial relationships among three columnar systems in cat area 17. *J Neurosci*; 17: 927084.
- [Ikeda et. al. 2004] Ikeda, I and Tanaka T and Amari S (2004), Information Geometry of Mean Field Approximation, *Neural Computation*, 16, 1179-1810, Massachusetts Institute of Technology.
- [In 1926 Adrian and Zotterman] Adrian, E. D. and Zotterman, Y. (1926). Impulses from a single sensory cell end-organ. *J. Physiol. (London)* 61, 465-483.
- [Imas et. a. 2004] Imas, O.A., Ropella, K.M., Wood, J.D. and Hudetz, A.G. (2004). Haolthane augments event-related gamma oscillations in rat visual cortex. *Neuroscience* 123:269-78.
- [Jablonka and Kossut 2006] Jablonka, J., and Kossut, M. (2006). Focal stroke in the barrel cortex of rats enhances ipsilateral response to vibrissal input *Acta Neurobiol Exp.* , 66: 261-266
- [Johnson et. al. 1973] Johnson KO, Darian-Smith I, LaMotte C (1973) Peripheral neural determinants of temperature discrimination in man: a correlative study of responses to cooling skin. *J Neurophysiol* 36:347-370.
- [Johnson 1980] Johnson KO (1980) Sensory discrimination: neural processes preceding discrimination decision. *J Neurophysiol* 43:1793-1815.
- [Johnson and Sinanovic 2001] Johnson D and Sinanovic S (2001), Symmetrizing the Kullback-Leibler distance, Rice University, Tech. Rep.
- [Kayser et. al. 2004] Kayser, C., and Konig, P. (2004). Population coding of orientation in the visual cortex of alert cats – an information theoretic analysis. *Neuroreport* 15 (18), 2761-2764.

- [Khalilov et al. 2005] Khalilov I., Le Van Quyen M., Gozlan H. and Ben-Ari Y., Epileptogenic actions of GABA and fast oscillations in the developing hippocampus, *Neuron* 48 (2005), 787-796.
- [Kelley 1975] Kelley, J. L. (1975) *General topology*. New York, Van Nostrand.
- [Kennel et. al. 2005] Kennel M.B., Shlens, J., Abarbanel, H. D., Chichilnisky E. J. (2005). Estimating Entropy rates with Bayesian Confidence Intervals. *Neural Computation* 17, 1531-1576.
- [Kita et. al. 1990] Kita H, Kosaka T, Heizmann CW (1990). Parvalbumin-immunoreactive neurons in the rat neostriatum: a light and electron microscopic study. *Brain Res.* 1990 Dec 17;536(1-2):1-15.
- [Kohn and Smith 2005] Kohn, A., and Smith, M. A. (2005). Stimulus Dependence of Neuronal Correlation in Primary Visual Cortex of the Macaque, *The Journal of Neuroscience*, 25(14) , 3661-3673.
- [Kruse and Eckhorn 1996] Kruse W., Eckhorn R. (1996) Inhibition of sustained gamma oscillations (35-80 Hz) by fast transient responses in cat visual cortex. *Proc Natl Acad Sci U S A.*;93(12):6112-7.
- [Kreiter and Singer 1992] Kreiter, A. K., and W. Singer (1992) Oscillatory neuronal responses in the visual cortex of awake macaque monkey. *Eur. J. Neurosci.* 16, 2381-2496.
- [Kreiter and Singer 1996a] Kreiter, A.K., and Singer, W. (1996a) On the role of neural synchrony in the primate visual cortex. In: A. Aertsen and V. Braitenberg (Eds.), *Brain Theory - Biological Basis and Computational Principles*. Elsevier, Amsterdam, 201-227.
- [Kreiter and Singer 1996b] Kreiter, A.K., and Singer, W. (1996b). Stimulus-dependent synchronisation of neuronal responses in the visual cortex of the awake macaque monkey. *Journal of Neuroscience* 16, 2381-2396.
- [Kreiter et. al. 1996] Kreiter, A.K., and Singer, W. (1996). Stimulus-dependent synchronisation of neuronal responses in the visual cortex of the awake macaque monkey. *J. Neurosci* 16: 2381-2396.

- [Kreiter and Singer 1992] Kreiter, A. K., and W. Singer (1992) Oscillatory neuronal responses in the visual cortex of awake macaque monkey. *Eur. J. Neurosci.* 16: 2381-2496.
- [Kreiter et. al. 1996] Kreiter, A.K., and Singer, W. (1996). Stimulus-dependent synchronisation of neuronal responses in the visual cortex of the awake macaque monkey. *J. Neurosci* 16: 2381-2396.
- [Kayser and Koenig 2004] Kayser, C., and Konig, P. (2004). Population coding of orientation in the visual cortex of alert cats an information theoretic analysis. *NeuroReport* 15 (18), 2761-2764.
- [Kirkwood 1979] Kirkwood, P.A. (1979). On the use and interpretation of cross-correlation measurement in the mammalian central nervous system. *J. neurosci. Methods*, 1, 7152-7161.
- [Koenig et. al. 1994] Koenig, P., Engel, A.K. and Singer, W. (1996). Integrator or coincidence detector? The role of cortical neurons revisited. *Trends Neurosci.* 19, 130-137.
- [Kohn and Smith 2005] Kohn, A., and Smith, M. A. (2005). Stimulus Dependence of Neuronal Correlation in Primary Visual Cortex of the Macaque, *The Journal of Neuroscience*, 25(14) , 3661-3673.
- [Kreiter and Singer 1996b] Kreiter, A.K., Singer, W. (1996b). Stimulus-dependent synchronisation of neuronal responses in the visual cortex of the awake macaque monkey. *Journal of Neuroscience* 16, 2381-2396.
- [Lampl et. al. 1999] Lampl I, Reichova I, Ferster D (1999). Synchronous membrane potential fluctuations in neurons of the cat visual cortex. *Neuron.* Feb;22(2):361-74.
- [Landisman et al. 2002] Landisman CE, Long MA, Beierlein M, Deans MR, Paul DL, Connors BW (2002). Electrical synapses in the thalamic reticular nucleus. *J Neurosci.* 2002 Feb 1;22(3):1002-9.
- [Larkum et. al. 1999] Larkum, M.E., Zhu, J. J. and Sakmann, B. (1999) A new cellular mechanism for coupling inputs arriving at different cortical layers. *Nature*, 398, 338-341.
- [Latham et. al 2005] Latham, P.E., and Nirenberg, S. (2005). Synergy, Redundancy, and Independence in Population Codes, Revisited. *J. Neurosci* 25: 5195-5206.

- [Lebedev et al. 2000] Lebedev, M.A., Mirabella, G., Erchova, I., and Diamond, M.E., (2000). Experience-dependence plasticity of rat barrel cortex: redistribution of activity across barrel-columns. *Cereb. Cortex* 10, 23-31.
- [Lee et. al. 1998] Lee, D., Port, N.L., Kruse, W., and Georgopoulos, A.P. (1998). Variability and correlated noise in the discharge of neurons in motor and parietal areas of the primate cortex. *J. Neurosci.* 18: 1161-1170.
- [Lee and Blake 1999] Lee S.-H and Blake R. (1999), Visual form created solely from temporal structure. *Science* 284 , 1165-1168.
- [Leonards et. al. 1996] Leonards U., Singer W. and Fahle M. (1996), The influence of temporal phase differences on texture segmentation. *Vision Res.* 36 , pp. 2689-2697.
- [Leung et. al. 1997] Leung C.S, Chan L.W. (1997), Stability and Statistical Properties of Second-Order Bidirectional Associative Memory, *IEEE Transactions on Neural Networks*, 8, 2, 267-277.
- [Levine et. al. 2002] LevineMW, Castaldo K, KasapogluMB (2002) Firing coincidences between neighboring retinal ganglion cells: inside information or epiphenomenon? *Biosystems* 67:139 146.
- [Lewis et. al. 2003] Lewis, T., and Rinzel, J. (2003). Dynamics of spiking neurons connected by both inhibitory and electrical coupling. *J. Comput. Neurosci.*, 14, 283-309 .
- [Lewis et al 2005] Lewis D.A., Hashimoto T. and Volk D.W., Cortical inhibitory neurons and schizophrenia, *Nat. Rev. Neurosci.* 6 (2005), 312324.
- [Lin 1991] Lin, J. (1991) *IEEE Trans. Inf. Theory* 37 (1991) 145.
- [Lisman 1997] Lisman JE. Bursts as a unit of neural information: making unreliable synapses reliable. *Trends Neurosci* 20: 3843, 1997.
- [Liu et. al. 2001] Liu RC, Tzonev S, Rebrik S, Miller KD. Variability and information in a neural code of the cat lateral geniculate nucleus. *J Neurophysiol.* 2001 Dec;86(6):2789-806.
- [Luhmann et. al. 1995] Luhmann, H.J. and Mudrick-Donnon, LA and Mittmann, T. and Heinemann, U. Ischaemia-induced long-term hyperexcitability in rat neocortex, *Eur J Neurosci*,7,2,180-91,1995,Blackwell Synergy.

- [Ma 1981] Ma, S.K. (1981). Calculation of entropy from data of motion. *J Statistical Physics* 26:221-240.
- [Mainen and Sejnowski 1995] Mainen Z.F. and Sejnowski T.J. (1995). Reliability of spike timing in neocortical neurons. *Science*, 268, 1503-1506.
- [Makarenko and Llinas 1998] Makarenko V. and Llinas R (1998). Experimentally determined chaotic phase synchronization in a neuronal system. *PNAS*, 95, Issue 26, 15747-15752.
- [Marcelja 1980] Marcelja S. (1980), Mathematical description of the responses of simple cortical cells., *J Opt Soc Am*, 70, 11, 1297–300.
- [Machens et. al. 2001] Machens CK, Stemmler MB, Prinz P, Krahe R, Ronacher B, Herz AV. Representation of acoustic communication signals by insect auditory receptor neurons. *J Neurosci*. 2001 May 1;21(9):3215-27.
- [Majtey et. al. 2005] Majtey, A.P., Lamberti, W. and Prato, D.P. (2005), Jensen-Shannon divergence as a measure of distinguishability between mixed quantum states, *Phys. Rev. A* 72, 052310-5.
- [Maldonado 2000] Maldonado, P.E., Friedman-Hill, S. and Gray, C.M. (2000). Dynamics of striate cortical activity in the alert macaque: II. Fast time scale synchronization. *Cerebral Cortex* 10:1117-31.
- [Mastrorade1983] Mastrorade, D.N. (1983). Correlated firing of cat retinal ganglion cells: Spontaneously active input to x- and y-cells. *J Neurophysiol.* 49, 303-24.
- [Mangulis and Tang 1998] Mangulis, M. and Tang., C.-M. (1998) Temporal integration can readily switch between sublinear and supralinear summation. *J. Neurophysiol.*, 79: 2809-2814.
- [Mann-Metzer 1999] Mann-Metzer, P., and Yarom, Y. (1999). Electrical coupling interacts with intrinsic properties to generate synchronized activity in cerebellar networks of inhibitory interneurons. *J. Neurosci.*, 19, 3298-3306.
- [Mastrorade1983] Mastrorade, D.N. (1983). Correlated firing of cat retinal ganglion cells: Spontaneously active input to x- and y-cells. *J Neurophysiol.* 49, 303-24.

- [Matsumara et. al. 1996] Matsumara, M., Chen, D.F., Sawaguchi, T., Kubota, K. and Fetz, E.E. (1996) Synaptic interactions between primate precentral cortex neurons revealed by spike triggered averaging of intracellular potential in vivo. *J. neurosci.*, 16, 7757-7767.
- [Matz and Duhamel 2004] Matz, G. and Duhamel, P., Information geometric formulation and interpretation of accelerated Blahut-Arimoto-type algorithms, in *Proc. IEEE ITW-2004*, San Antonio (TX), pp. 66–70.
- [Mazurek et al 2002] Mazurek M.E. and Shadlen M.N. (2002). Limits to the temporal fidelity of cortical spike rate signals. *Nat Neurosci.* 5: 463-471.
- [McCormick and Williamson 1989] McCormick DA and Williamson A, Convergence and divergence of neurotransmitter action in human cerebral cortex, *Proc. Natl. Acad. Sci. USA* 86 (1989), 80988102.
- [McCulloch J. and Dewar D.] McCulloch J. and Dewar D. (2001), A radical approach to stroke therapy, *Proceedings of the National Academy of Sciences of the USA*, 98, 20, 10989-10991.
- [Meister et. al. 1995] Meister M, Lagnado L, Baylor DA (1995) Concerted signaling by retinal ganglion cells. *Science* 270:12071210.
- [Meister 1996] Meister, M. (1996). Multineuronal codes in retinal signaling. *PNAS* 93(2):609-14.
- [Michalski et. al. 1983] Michalski, A., Gerstein, G.L., Czarkowska, J. and Tarnecki, R., (1983). Interactions between cat striate cortex neurons. *Exp. Brain. Res.*, 51,97-107.
- [Mittmann 2001] T. Mittmann and U. T. Eysel(2001), Increased synaptic plasticity in the surround of visual cortex in rats, *NeuroReport*, 12, 15, 3341-3347.
- [Moghaddam 2003] B. Moghaddam, Bringing order to the glutamate chaos in schizophrenia, *Neuron* 40 (2003), 881884.
- [Molotchnikoff et. al. 1998] Molotchnikoff, S. and Shumikhina, S. (1998) Synchronization, gamma oscillations and spatial integration of line segments in the cat visual cortex. *Vis. Res.*, 36, 2037-2046.

- [Montani et. al. 2007a] F. Montani, A. Kohn, M. Smith and S. R. Schultz (2006), How do stimulus-dependent correlations between V1 neurons affect neural coding?, *Neurocomputing*, 2007, Vol: 70, Pages: 1782 - 1787.
- [Montani et. al. 2007b] Montani, F. , Kohn, A. Smith, M. A. and Schultz, S. R. (2007), The Role of Correlations in Direction and Contrast Coding in the Primary Visual Cortex *J. Neurosci.*, 27: 2338 - 2348.
- [Montani et. al. 2007c] Montani, F. ,Rosso, O. A., Schultz., S. R. (2007). Discrimination Measure of Correlation in a Population of Neurons Using the Jensen-Shannon Divergence, *AIP Conference Proceedings* 913, 184-189.
- [Montani 2007d] Montani F., Einarsdottir H., and Schultz S.R. (2007). A mathematical model of receptive field reorganization following stroke. *IEEE International Conference on Development and Learning*, Poster Presentation.
- [Mountcastle 1957] Mountcastle, V.B. (1957). Modality and topographic properties of single neurons of cat somatic sensory cortex *J. Neurophysiol.* 20, 408-434.
- [Montemurro et. al. 2007] Marcelo A. Montemurro, Riccardo Senatore and Stefano Panzeri (2007) Tight data-robust bounds to mutual information combining shuffling and model selection techniques. *Neural Computation* 19(11): 2913-2957.
- [Moore et. al. 1970] Moore, G.P. , Segundo, J.P., Perkel, D.H. and Levitan, H. (1970) Statistical signs of synaptic interaction in neurons. *Biophys. J.* 10, 876-900.
- [Mountcastle 1957] Mountcastle, V.B. (1957). Modality and topographic properties of single neurons of cat's somatic sensory cortex. *J. Neurophysiol.* 20, 408-34.
- [Mountcastle 1997] Mountcastle V.B. (1997). The columnar organization of the neocortex. *Brain* 1997; 120: 70122.
- [Movson et. al. 2003] Movshon, J.A., Albright, T.D., Stoner, G.R. Majaj, N. J. and Smith, M. A. (2003). Cortical responses to visual motion in alert and anesthetized monkeys. *Nature Neuroscience* 6:3.

- [Nakahara and Amari 2002] Nakahara, H. and Amari, S. (2002), Information-geometric measure for neural spikes , *Neural Computation*,14, 2269–2316, Massachusetts Institute of Technology.
- [Nase et al. 2003] Nase G., Singer W., Monyer H. and Engel A.K., Features of neuronal synchrony in mouse visual cortex, *J. Neurophysiol.* 90 (2003), 1115-1123.
- [Nelson et. al. 1992] Nelson JI, Salin PA, Munk MH-J, Bullier J (1992) Spatial and temporal coherence in cortico-cortical connections: a cross-correlation study in areas 17 and 18 in the cat. *Vis Neurosci* 9: 21-37.[ISI][Medline]
- [Nemenman et. al. 2002] Nemenman, I., Shafee, F. and Bialek, W. (2002). Entropy and inference, revisited. In T. G. Dietterich, S. Becker, and Z. Ghahramani, editors, *Adv. Neural Inf. Proc. Syst.* 14, Cambridge, MA, 2002. MIT Press.
- [Nemenman et. al. 2004] Nemenman, I., Bialek, W., and Steveninck, R., (2004). Entropy and information in neuronal spike trains: Progress on the sampling problem. *Phys. Rev. E* 69, 056111-6.
- [Neuenschwander et. al. 2002] Neuenschwander S, Castelo-Branco M, Baron J, Singer W (2002). Feed-forward synchronization: propagation of temporal patterns along the retinorecortical pathway. *Philos Trans R Soc Lond B Biol Sci.* ;357(1428):1869-76.
- [Neumann-Haefelin et. al. 1995] Neumann-Haefelin, T. and Hagemann, G. and Witte, OW (1995), Cellular correlates of neuronal hyperexcitability in the vicinity of photochemically induced cortical infarcts in rats in vitro.,*Neurosci Lett*, 193, 2, 101–4.
- [Nemenman] Nemenman, I. (2006) Inference of entropies of discrete random variables with unknown cardinalities, personal communication (unpublished manuscript).
- [Nirenberg et. al. 2001] Nirenberg, S., Carcieri, S.M., Jacobs, A.L. and Latham, P.E. (2001). Retinal ganglion cells act largely as independent encoders. *Nature* 411:698-701.
- [Nirenberg and Latham 2003] Nirenberg, S. and Latham, P.E. (2003) Decoding neuronal spike trains: how important are correlations? *Proc. Natl. Acad. Sci.* 100:7348-7353.
- [Nirenberg et. al. 2001] Nirenberg, S., Carcieri, S.M., Jacobs, A.L. and Latham, P.E. (2001). Retinal ganglion cells act largely as independent encoders. *Nature* 411:698-701.

- [Nirenberg and Lathan 2003] Nirenberg, S. and Latham, P.E. (2003) Decoding neuronal spike trains: how important are correlations? *Proc. Natl. Acad. Sci.* 100:7348-7353.
- [Nowak et. al. 1999] Nowak LG, Munk MHJ, James AC, Girard JP, Bullier J (1999) Cross-correlation study of the temporal interactions between areas V1 and V2 of the macaque monkey. *J Neurophysiol* 81: 1057-1074.
- [Nudo and Milliken 1996] Nudo RJ, Milliken GW (1996) Reorganization of movement representations in primary motor cortex following focal ischemic infarcts in adult squirrel monkeys. *J Neurophysiol* 75: 2144-2149.
- [Nudo et. al. 1996] Nudo, R.J. and Wise, B.M. and SiFuentes, F. and Milliken, G.W.(1996),Neural Substrates for the Effects of Rehabilitative Training on Motor Recovery After Ischemic Infarct, Nudo, R.J. and Wise, B.M. and SiFuentes, F. and Milliken, G.W.,*Science*,272,5269,1791.
- [Ouagnina 2003] Ouagnina, H. (2003), Hellinger distance estimation of nonlinear dynamical systems, *Statistics and Probability Letters* Volume 63, 2, 177-184.
- [Oram et. al. 1998] Oram MW, Hatsopoulos NG, Richmond BJ, Donoghue JP (2001) Excess synchrony in motor cortical neurons provides redundant direction information with that from coarse temporal measures. *J Neurophysiol* 86:1700 1716.
- [Oram et. al. 2001] Oram M.W., Hatsopoulos N.G., Richmond B.J., and Donoghue J.P. (2001) Excess synchrony in motor cortical neurons provides redundant direction information with that from coarse temporal measures. *J Neurophysiol.* 8
- [Palanca and DeAngelis 2005] Palanca and DeAngelis (2005). Does neuronal synchrony underlie visual feature grouping? *Neuron.* 2005 Apr 21;46(2):333-46.
- [Paninski 2003] Paninski, L. (2003) Estimation of entropy and mutual information. *Neural Computation* 15:1191-1254.
- [Panzeri and Treves 1996] Panzeri, S. and Treves, A. (1996). Analytical estimates of limited sampling biases in different information measures. *Network* 7:87-107.

- [Panzeri et. al. 1999] Panzeri, S., Schultz, S.R., Treves, A., and Rolls, E. T. (1999), Correlations and the encoding of information in the nervous system. *Proceedings of the Royal Society of London Series B: Biological Sciences*, 266, 1001-1012.
- [Panzeri and Schultz 2001a] Panzeri, S. and Schultz, S.R. (2001). A unified approach to the study of temporal, correlational and rate coding. *Neural Computation*, 13(6) , 1311-1349.
- [Panzeri et. al. 2001b] Panzeri, S., Petersen, S.R., Schultz, S.R., Lebedev, M., and Diamond, M. (2001). The role of spike timing the coding of stimulus location in rat somatosensory cortex.. *Neuron* 29:769-777.
- [Panzeri et. al. 2002a] Panzeri S., Pola G., Petroni F., Young M.P. and Peterson R.S. (2002). A critical assessment of different measures of the information carried by correlated neuronal firing. *Biosystems* 67 (1-3), 177-185.
- [Panzeri et. al. 2002b] Panzeri S, Golledge HDR, Zheng F, Pola G, Blanche TJ, Tovee MJ, Young MP (2002a) The role of correlated firing and synchrony in coding information about single and separate objects in cat V1. *Neurocomputing* 4446:579 584.
- [Panzeri et. al 2003] Panzeri S., Petroni F., Petersen R.S. and Diamond M.E.(2003). Decoding Neuronal Population Activity in Rat Somatosensory Cortex: Role of Columnar Organization, *Cerebral Cortex*, Vol. 13, No. 1, 45-52.
- [Papoulis and Unnikrishna Pillai 2002] Papoulis, A. and Unnikrishna Pillai, S. (2002). *Probability, Random Variables and Stochastic Process*, 4th edition, chap. 10, McGraw-Hill, Delhi.
- [Parker and Newsome 1998] Parker AJ, Newsome WT (1998) Sense and the single neuron: probing the physiology of perception. *Annu Rev Neurosci* 21:227-277
- [Perkel et. al. 1967] Perkel, D.H., Gerstein, G.L. and Moore, G.P. (1967). Neuronal spikes trains and stochastic point processes II. Simultaneous spikes trains. *Biophys. J.*, 7, 419-440.
- [Petersen 2001] Petersen, R.S., Panzeri, S. and Diamond, M.E. (2001). Population coding of stimulus location in rat somatosensory cortex. *Neuron* 32(3):503-14.
- [Pfeuty et. al. 2003] Pfeuty, B., Mato, G., Golomb, D., and Hansel, D. (2003). Electrical synapses and synchrony: The role of intrinsic currents. *J. Neurosci*, 23, 6280-6294.

- [Pfeuty et. al. 2005] Pfeuty B, Mato G, Golomb D, Hansel D (2005). The combined effects of inhibitory and electrical synapses in synchrony. *Neural Comput.* 2005 Mar;17(3):633-70.
- [Pola et. al. 2003] Pola, G., Thiele, A., Hoffmann, K-P., and Panzeri, S. (2003). An exact method to quantify the information transmitted by different mechanisms of correlational coding. *Network Computation in Neural Systems* 14, 35-60.
- [Pola et. al. 2005] Pola G, Petersen RS, Thiele A, Young MP, Panzeri S. [2005]. Data-robust tight lower bounds to the information carried by spike times of a neuronal population. *Neural Comput.* 2005 Sep;17(9):1962-2005.
- [Polleux and Lauder 2004] Polleux F. and Lauder J.M., Toward a developmental neurobiology of autism, *Ment. Retard. Dev. Disabil. Res. Rev.* 10 (2004), 303317.
- [Porter et. al. 2001] Porter JT, Johnson CK, Agmon A (2001). Diverse types of interneurons generate thalamus-evoked feedforward inhibition in the mouse barrel cortex. *J Neurosci.*; 21: 2699710.
- [Prut et. al. 1998] Prut, Y., Vaadia, E., Bergman, H., Haalman, I., Slovlin, H. and Abeles, M. (1998) Spatiotemporal structure of cortical activity : properties and behavioral relevance. *J. Neurophysiol.* 79, 2857-2874.
- [Puchalla et. al. 2005] Puchalla, J.L., Schneidman, E., Harris, R.A. and Berry, M.J. (2005). Redundancy in the population code of the retina. *Neuron* 46(3):493-504.
- [Purpura et. al. 1994] Purpura K. P., Victor J.D., and Katz E (1994). Striate Cortex Extracts Higher-Order Spatial Correlations from Visual Textures. *PNAS* 91: 8482-8486.
- [Rao 1987] Rao, C. (1987) *IMS-Lectures Notes*, 10, 217.
- [Reich et. al. 2001] Reich, D.S., Mechler, F., Victor, J.D. (2001). Independent and Redundant Information in Nearby Cortical Neurons. *Science* 294, 2566-2568.
- [Reike et. al. 1998] F. Rieke, D. Warland, R. R. de Ruyter van Steveninck and W. Bialek (1998). *Spikes: exploring the neural code*. MIT Press, Cambridge, USA.
- [Reinecke et. al. 2003] Reinecke S, Dinse HR, Reinke H, Witte, O.W. Induction of bilateral plasticity in sensory cortical maps by small unilateral cortical infarcts in rats. *Eur J Neurosci.* 2003 Feb;17(3):623-7.

- [Rema and Ebner 2003] Rema V, Ebner FF (2003) Lesions of mature barrel field cortex interfere with sensory processing and plasticity in connected areas of the contralateral hemisphere. *J Neurosci* 23: 10378-10387. [Erratum in: *J Neurosci* 23: following 11269.]
- [Richmond and Gawne 1998] Richmond, B.J., and Gawne, T.J. (1998). The relationship between neuronal codes and cortical organization. In: H.B. Eichenbaum and J.L Davis (Eds.), *neuronal Ensembles, Strategies for Recording and decoding*. Wiley, New York, pp. 57-79.
- [Riehle et. al. 1997] Riehle A, Grun S, Diesmann M, Aertsen A (1997). Spike synchronization and rate modulation differentially involved in motor cortical function. *Science*. 1997 Dec 12;278(5345):1950-3.
- [Roddey et. al. 2000] Roddey JC, Girish B, and Miller JP. Assessing the performance of neural encoding models in the presence of noise. *J Comp Neurosci* 8: 95112, 2000.
- [Roelfsema 1997] Roelfsema, P.R., Engel, A.K., Koenig, P., and Singer, W. (1997). Visuo-motor integration is associated with zero time-lag synchronization among cortical areas. *Nature*, 385, 157-161.
- [Roelfsema 1998] Roelfsema, P.R. (1998) Solution to the binding problem. *Z. Naturforsch.*, 53, 691-715.
- [Roelfsema et. al. 2004] Roelfsema, P R, Lamme, V A F and Spekreijse, H. (2004) Synchrony and covariation of firing primary visual cortex during contour grouping. *Nat. Neurosci.* 7:982-991.
- [Rolls et. al. 1997a] Rolls ET, Treves A, Tovee MJ, Panzeri S (1997a). Information in the neuronal representation of individual stimuli in the primate temporal visual cortex. *J Comput Neurosci*. 1997 Nov;4(4):309-33.
- [Rolls 1997b] Rolls ET, Treves A, Tovee MJ (1997b). The representational capacity of the distributed encoding of information provided by populations of neurons in primate temporal visual cortex. *Exp Brain Res*. 1997 Mar;114(1):149-62.

- [Rosso et. al. 2004] P.W. Lamberti, M. T. Martin, A. Plastino and O. A. Rosso, *Physica A* **334**, 119–131 (2004).
- [Rosso et. al. 2006] O. A. Rosso, M. T. Martin, A. Figliola, K. Keller and A. Plastino, *J. Neuroscience Meth.* **153**, 163–182 (2006).
- [Rubenstein 2003] Rubenstein J.L and Merzenich M.M., Model of autism: increased ratio of excitation/inhibition in key neural systems, *Genes Brain Behav.* 2 (2003), 255267.
- [Rust et. al. 2002] N. Rust, S. R. Schultz and J. A. Movshon (2002). A reciprocal relationship between reliability and responsiveness in developing cortical neurons. *Journal of Neuroscience* 22:10519-10523.
- [Sakurai 1996] Sakurai Y (1996) Population coding by cell assemblies: what it really is in the brain. *Neurosci Res* 26:1-16.
- [Sakurai 1999] Sakurai Y (1999) How do cell assemblies encode information in the brain? *Neurosci Biobehav Rev.* 1999;23(6):785-96.
- [Samengo 2002] Samengo, I. (2002). Estimating probabilities from experimental frequencies. *Phys. Rev. E* 65:046124.
- [Samonds et. al. 2003] Samonds, J. M., Allison, J. D., Brown, H. A. and Bonds, A. B. (2003). Cooperation between area 17 neuron pairs enhances fine discrimination of orientation. *J Neurosci* 23:2416-2425.
- [Samonds et. al. 2004] Samonds, J. M., Allison, J. D., Brown, H. A. and Bonds, A. B. (2004). Cooperative synchronized assemblies enhance orientation discrimination. *PNAS* 101:6722-6727.
- [Samonds and Bonds 2005] Samonds, J. M., and Bonds, A. B., Gamma oscillation maintains stimulus structure-dependent synchronization in cat visual cortex. *J. Neurophysiol* 93, 223236.
- [Samonds et. al. 2006] Samonds, J. M., Zhou, Z., Bernard, M.R. and Bonds, A. B. (2006). Synchronous activity in cat visual cortex encodes collinear and cocircular contours. *J. Neurophysiol* 95, 2602-2616.

- [Schiene et. al. 1999] Schiene, K. and Staiger, JF and Bruehl, C. and Witte, OW (1999), Enlargement of cortical vibrissa representation in the surround of an ischemic cortical lesion., J Neurol Sci, 162,1, 6–13.
- [Schneidman et. al. 2003] Schneidman, E., Bialek, W., Berry, M.J. (2003). Synergy, redundancy, and independence in population codes. J Neuroscience 23 , 11539-11553.
- [Schneidman et. al. 2006] Schneidman, E., Berry, M.J., Segev, R. and Bialek, W. (2006). Weak pairwise correlations imply strongly correlated network states in a neural population. Nature 440:1007-1012.
- [Schnitzler and Gross 2005] Schnitzler A. and J. Gross, Normal and pathological oscillatory communication in the brain, Nat. Rev. Neurosci. 6 (2005), pp. 285296.
- [Schultz and Panzeri 2001] Schultz, S. R., and Panzeri, S. (2001). Temporal correlations and neural spike train entropy. Physical Review Letters 86: 5823-5826.
- [Schultz S.R 2006] Schultz S.R (2006), Signal-to-Noise Ratio in Neuroscience, Scholarpedia.
- [Schweigart and Eysel 2002] Schweigart, G. and Eysel, U.T.(2002), Activity-dependent receptive field changes in the surround of adult cat visual cortex lesions, European Journal of Neuroscience, 15, 10, 1585–1596, Blackwell Synergy.
- [Seamans and Yang 2004] Seamans J.K. and Yang C. R., The principal features and mechanisms of dopamine modulation in the prefrontal cortex, Prog. Neurobiol. 74 (2004), 158.
- [Seung and Sompolinsky 1993] Seung, HS and Sompolinsky, H.(1993) ,Simple Models for Reading Neuronal Population Codes, Proceedings of the National Academy of Sciences, 90, 22,10749–10753, National Acad Sciences.
- [Shadlen and Newsome 1994] Shadlen MN, Newsome WT (1994). Noise, neural codes and cortical organization. Curr Opin Neurobiol.;4(4):569-79.
- [Shadlen et. al. 1996] Shadlen MN, Britten KH, Newsome WT, Movshon JA (1996) A computational analysis of the relationship between neuronal and behavioral responses to visual motion. J Neurosci 16:14861510.

- [Shadlen and Newsome 1998] Shadlen, M.N., Newsome, W.T. (1998). The variable discharge of cortical neurons: implications for connectivity, computation and information coding. *J. Neurosci* 18: 3870-3896.
- [Shadlen and Movshon 1999] Shadlen MN, Movshon JA (1999). Synchrony unbound: a critical evaluation of the temporal binding hypothesis. *Neuron*;24(1):67-77, 111-25.
- [Shamir and Sompolinsky 2001] Shamir, M. and Sompolinsky, H. (2001). Correlation codes in Neuronal Populations. *NIPS 2001*, 277-284.
- [Shamir and Sompolinsky 2004] Shamir, M. and Sompolinsky, H. (2004). Nonlinear population codes. *Neural Computation* 16:1105-1136.
- [Shannon 1948] Shannon, C.E. (1948). A mathematical theory of communication AT and T Bell Labs Tech. J. 27 379-423.
- [Shlens et. al. 2006] Shlens, J. Field, G. Gauthier, J, Grivich, M., Petrusca, D. Sher, A., Litke A. and Chichilnisky E.J. (2006). The structure of multi-neuron firing patterns in primate retina. *J. Neurosci.* 26:8254-66.
- [Singer 1990a] Singer, W. (1990a). Search for coherence; a basic principle of cortical self organization. *Conc. Neurosci.*, 1(1), 1-26.
- [Singer 1993] Singer, W. (1993). Neuronal representations, assemblies and temporal coherence. In: T.P. Hicks, S. molotchnikoff and T. Ono (Eds.), *Progress in brain research*, Vol. 95. Elsevier, Amsterdam, 461-474.
- [Singer and Gray 1995] Singer, W. and Gray, C.M. (1995). Visual feature integration and the temporal correlation hypothesis. *Annu Rev Neurosci* 18:555-586.
- [Series et. al. 2004] Series P, Latham PE, Pouget A (2004) Tuning curve sharpening for orientation selectivity: coding efficiency and the impact of correlations. *Nat Neurosci* 7: 1129-1135.
- [Singer 1990b] Singer, W. (1990b). The formation of cooperative cell assemblies in the visual cortex. *J. Exp. Biol.*, 153, 177-197.

- [Singer and Gray 1995] Singer, W. and Gray, C. M. (1995) Visual feature integration and the temporal correlation hypothesis. *Annu. Rev. Neurosci.* 18, 555-586.
- [Singer 1999] Singer, 1999 W. Singer, Neuronal synchrony: A versatile code of the definition of relations?, *Neuron* 24 (1999), 4965.
- [Snider and Bonds 1998] Snider RK and Bonds AB. Classification of non-stationary neural signals. *J Neurosci Methods* 84: 155166, 1998.
- [Snippe and Koenderink 1992] Snippe HP, Koenderink JJ. (1992) *J Neurophysiol.* 49, 303-24. Information in channel-coded systems: correlated receivers. *Biol Cybern.*;67(2):183-90.
- [Sober et. al. 1997] Sober, S.J., Stark, Yamasaki, D.S., and Lytton, W.W. (1997). Receptive Field after strokelike cortical ablation: A role for activation dynamics. *Journal of Neurophysiology*, 78:3438-3443.
- [Softky 1994] Softky, W. (1994). Sub-millisecond coincidence detection in active dendritic trees. *Neuroscience*, 58(1), 13-41.
- [Sohya et. al. 2007] Sohya, K. and Kameyama, K. and Yanagawa, Y. and Obata, K. and Tsumoto, T.(2007),GABAergic Neurons Are Less Selective to Stimulus Orientation than Excitatory Neurons in Layer II/III of Visual Cortex, as Revealed by In Vivo Functional Ca²⁺ Imaging in Transgenic Mice, *Journal of Neuroscience*, 27, 8, 2145,2007, Soc Neuroscience.
- [Stork and Wilson 1990] Stork, D.G. and Wilson, H.R.(1990),Do Gabor functions provide appropriate descriptions of visual cortical receptive fields?, *Journal of the Optical Society of America A*, 7, 8, 13621373, OSA.
- [Steinberg and Augustine 1997] Steinberg, BA and Augustine, JR (1997),Behavioral, anatomical, and physiological aspects of recovery of motor function following stroke.,*Brain Res Brain Res Rev*, 25, 1, 125–32.
- [Stroemer et.al. 1998] Stroemer, R.P. and Kent, T.A. and Hulsebosch, C.E.(1998) Enhanced Neocortical Neural Sprouting, Synaptogenesis, and Behavioral Recovery With D-Amphetamine Therapy After Neocortical Infarction in Rats, *Stroke*, 29, 2381–2395, Am Heart Assoc.

- [Steinmetz et. al. 2000] Steinmetz PN, Roy A, Fitzgerald PJ, Hsiao SS, Johnson KO, Niebur E (2000) Attention modulates synchronized neuronal firing in primate somatosensory cortex. *Nature* 404:187190.
- [Stevens and Zador 1998] Stevens, C.F. and Zador, A.M. (1998) Input synchrony and the irregular firing of cortical neurons. *Nat. Neurosci.* 1, 210-217.
- [Strong et. al. 1998a] Strong, S.P., Koberle, R., de Ruyter van Steveninck, R.R. and Bialek, W. (1998). Entropy and information in neural spike trains. *Physical Review Letters* 80:197-200.
- [Strong et. al. 1998b] Strong SP, de Ruyter van Steveninck RR, Bialek W, Koberle R (1998). On the application of information theory to neural spike trains. *Pac Symp Biocomput.* 1998;:621-32.
- [Surmier and Weinberg 1985] Surmier, D.J. and Weinberg, R.J. (1985). The relationship between cross-correlation measures and underlying synaptic events. *Brain Res.*, 331, 180-184.
- [Suzuki et. al. 2000] Suzuki R.; Kontinen V.K.; Matthews E.; Williams E.; Dickenson A.H. (2000) Enlargement of the Receptive Field Size to Low Intensity Mechanical Stimulation in the Rat Spinal Nerve Ligation Model of Neuropathy 163 (2), 408-413(6).
- [Tanaka 2000] Tanaka, T (2000), *Information Geometry of Mean Field Approximation, Neural Computation*, 1952-1968, Massachusetts Institute of Technology.
- [Tolhurst 1989] Tolhurst, D.J. (1989). The amount of information transmitted about contrast by neurons in cat's visual cortex. *Vis Neurosci* 2, 409-413.
- [Toyama et. al. 1981a] Toyama, K., Kimura, M. and Tanaka, K. (1981a). Cross correlation analysis of interneuronal connectivity in cat visual cortex. *J. Neurophysiol.*, 46(2), 191-201.
- [Toyama et. al. 1981b] Toyama, K., Kimura, M. and Tanaka, K. (1981b). Organization of cat visual cortex as investigated by cross-correlation technique. *J. Neurophysiol.*, 46(2), 202-214.
- [Traub et al. 2001] Traub R.D., Whittington M.A., Buhl E.H., LeBeau F.E., Bibbig A., Boyd S., Cross H. and Baldeweg T., A possible role for gap junctions in generation of very

- fast EEG oscillations preceding the onset of, and perhaps initiating, seizures, *Epilepsia* 42 (2001), 153170.
- [Ts'o et. al. 1986] Ts'o, D.Y., Gilbert, C.D. and Weisel, T.N. (1986). Relationships between horizontal interactions and functional architecture in cat striate cortex as revealed by cross-correlation analysis. *J. Neurosci.*,6(4), 1160-1170.
- [Ts'o and Gilbert 1988] Ts'o, D.Y., Gilbert, C.D. (1988). The organization of chromatic and spatial interactions in the primate striate cortex. *J. Neurosci.*, 8 , 1712-1727.
- [Tsodyks et. al. 1997] Tsodyks MV and Markham H. The neural code between neocortical pyramidal neurons depends on neurotransmitter release probability. *Proc Natl Acad Sci USA* 94: 719723, 1997.
- [Thomas and Cover] Thomas M. Cover, Joy A. Thomas (1991). *Elements of Information Theory*. John Wiley and Sons, New York.
- [Tolhurst 1989] Tolhurst D J, (1989) "The amount of information transmitted about contrast by neurons in the cat's visual cortex" *Visual Neuroscience* 2, 409-413
- [Topsoe 2000] Topsoe, E. (2000), Some Inequalities for Information Divergence and related measures of discrimination, *IEEE Trans. Inform. Theory.*, Vol 46, 1602-1609.
- [Traub et al. 2001] Traub RD, M.A. Whittington, E.H. Buhl, F.E. LeBeau, A. Bibbig, S. Boyd, H. Cross and T. Baldeweg, A possible role for gap junctions in generation of very fast EEG oscillations preceding the onset of, and perhaps initiating, seizures, *Epilepsia* 42 (2001), 153170.
- [Traub et al. 2004] R.D. Traub, A. Bibbig, F.E.N. LeBeau, E.H. Buhl and M.A. Whittington, Cellular mechanisms of neuronal population oscillations in the hippocampus in vitro, *Annu. Rev. Neurosci.* 27 (2004), 247278.
- [Treisman and Gelade 1980] Treisman and Gelade (1980). A feature-integration theory of attention. *Cognit Psychol.* 1980 Jan;12(1):97-136.
- [Tsodyks et. al. 1993] Tsodyks M, Mitkov I, and Somplinsky H. Pattern of synchrony in inhomogeneous networks of oscillators with pulse interactions. *Phys Rev Lett* 71: 12801283, 1993.

- [Uhlhaas et al. 2006] Uhlhaas P.J., Linden D.E.J, Singer W., Haenschel C., Lindner M., Maurer K. and Rodriguez E., Dysfunctional long-range coordination of neural activity during Gestalt perception in schizophrenia, *J. Neurosci.* 26 (2006), 81688175.
- [Uhlhaas and Singer 2006] Uhlhaas PJ, Singer W. (2006). Neural synchrony in brain disorders: relevance for cognitive dysfunctions and pathophysiology. *Neuron*. Oct 5;52(1):155-68.
- [Ulrich and Huguenard 1996] Ulrich D. and Huguenard J.R., Gamma-aminobutyric acid type B receptor-dependent burst-firing in thalamic neurons: a dynamic clamp study, *Proc. Natl. Acad. Sci. USA* 93 (1996), 1324513249.
- [Usher and Donnelly 1998] Usher M. and Donnelly N (1998)., Visual synchrony affects binding and segmentation in perception. *Nature* 394 , pp. 179-182.
- [Usrey et. al. 1998] Usrey WM, Reppas JB, and Reid RC. Paired-spike interactions and synaptic efficacy of retinal inputs to the thalamus. *Nature* 395: 384387, 1998
- [Usrey and Reid 1999] Usrey WM, Reid RC (1999). Synchronous activity in the visual system. *Annu Rev Physiol.* 1999;61:435-56.
- [Vaadia et. al. 1995] Vaadia E., Abeles M, Bergman H, Prut Y, Slovin H, Aertsen A. (1995) Dynamics of neuronal interactions in monkey cortex in relation to behavioural events. *Nature* 373, 515-518.
- [Van der Schaaf A. and van Hateren 1996] Van der Schaaf A. and van Hateren J.H. (1996), Modelling the power spectra of natural images-statistics and information, *Vision Res.* 36 , pp. 2759-2770.
- [Varela et. al. 1997] Varela JA, Sen K, Gibson J, Fost J, Abbott LF, and Nelson SB. A quantitative description of short-term plasticity at excitatory synapses in layer 2/3 of rat primary visual cortex. *J Neurosci* 17: 79267940, 1997.
- [Varela et. al. 2001] Varela F., Lachaux J. P., Rodriguez E. and Martinerie J., The brainweb: phase synchronization and large-scale integration, *Nat. Rev. Neurosci.* 2 (2001), 229239.

- [Venance et. al. 2000] Venance, L., Rozov, A., Blatow, M., Burnashev, N., Feldmeyer, D., and Monyer, H. (2000). Connexin expression in electrically coupled postnatal rat brain neurons. *Proc. Natl. Acad. Sci.*, 97, 10260-10265.
- [Volgushev 1998] Volgushev, M.A. (1998). Interactions of neurons in the orientational column of the cat visual cortex. *Sensornye Sistemy* 1, 263-271.
- [Volgushev et.al. 1998] Volgushev, M., Christiakova, M and Singer, W. (1998) Modifications of discharge patterns of neurocortical neurons by induced oscillations of the membrane potential. *Neuroscience*, 83: 15-25.
- [Von der Malsburg 1981] Von der Malsburg, C. (1981). The correlation theory of brain function. *Int. Rep.-Max. -Plank-Inst. Biophys. Chem., Goettingen*, 81-2, 1-40.
- [Von der Malsburg and Schneider 1986] Von der Malsburg, C. and Schneider, W. (1986). A neural cocktail-party processor. *Boil. Cybern.*, 54, 29-40.
- [Wang and Buzsaki 1996] Wang X.J. and Buzsaki G., Gamma oscillation by synaptic inhibition in a hippocampal interneuronal network model, *J. Neurosci.* 16 (1996), 64026413.
- [Werner and Mountcastle 1965] Werner G, Mountcastle VB (1965) Neural activity in mechanoreceptive cutaneous afferents: stimulus-response. *J Neurophysiol* 28:359-397.
- [Wickens 2001] Wickens T.D(2001) *Elementary Signal Detection Theory*, Oxford University Press.
- [Wolpert and Wolf 1995] Wolpert, D.H. and Wolf, D.R. (1995). Estimating functions of probability distributions from a finite set of samples. *Physical Review E* 52:6841-54.
- [Wolpert 2004] Wolpert, D. H. (2004), Metrics for more than two points at once, arXiv:nlin/0404032v1.
- [Wu et. al. 2004] , Wu S., Amari S. and Nakahara H. (2004), Information processing in a neuron ensemble with the multiplicative correlation structure, *Neural Networks*, 17, 2, 205-214, Elsevier.
- [Xerri et. al. 1998] Xerri C, Merzenich MM, Peterson BE, Jenkins W. (1998) Plasticity of primary somatosensory cortex paralleling sensorimotor skill recovery from stroke in adult monkeys. *J Neurophysiol.* 79(4):2119-48.

[Zihl and von Cramon 1985] Zihl J, von Cramon D. Visual field recovery from scotoma in patients with postgeniculate damage. A review of 55 cases. *Brain*. 1985, 108, 335-65.

[Zohary et. al. 1994] Zohary, E., Shadlen, M.N., and Newsome, W.T. (1994) Correlated neuronal discharge rate and its implications for psychophysical performance. *Nature* 370 , 140-143.